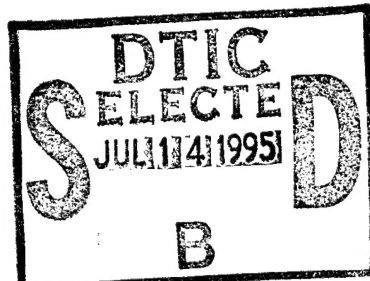


DOT/FAA/CT-94/116

FAA Technical Center  
Atlantic City International Airport,  
N.J. 08405

# Vertical Drop Test of a Narrow-Body Fuselage Section with Overhead Stowage Bins and Auxiliary Fuel Tank on Board



April 1995

Final Report

This document is available to the U.S. public  
through the National Technical Information  
Service, Springfield, Virginia 22161.



U.S. Department of Transportation  
Federal Aviation Administration

19950707 054

DTIC QUALITY INSPECTED 5

NOTICE

This document is disseminated under the sponsorship of the U. S. Department of Transportation in the interest of information exchange. The United States Government assumes no liability for the contents or use thereof.

The United States Government does not endorse products or manufacturers. Trade or manufacturers' names appear herein solely because they are considered essential to the objective of this report.

**Technical Report Documentation Page**

1. Report No.  DOT/FAA/CT-94/116	2. Government Accession No.	3. Recipient's Catalog No.	
4. Title and Subtitle  VERTICAL DROP TEST OF A NARROW-BODY FUSELAGE SECTION WITH OVERHEAD STOWAGE BINS AND AUXILIARY FUEL TANK SYSTEM ON BOARD		5. Report Date April 1995	
7. Author(s) Logue, Thomas V.; McGuire, Robert J.; Reinhardt, John W.; Vu, Dr. Tong V.		6. Performing Organization Code AAR-431	
9. Performing Organization Name and Address Federal Aviation Administration Technical Center Atlantic City International Airport, NJ 08405		8. Performing Organization Report No.	
12. Sponsoring Agency Name and Address U.S. Department of Transportation Federal Aviation Administration Technical Center Atlantic City International Airport, NJ 08405		10. Work Unit No. (TRAIS)	
		11. Contract or Grant No.	
15. Supplementary Notes  FAA Technical Center Program Manager: Gary Frings		13. Type of Report and Period Covered  Final Report October 1993-September 1994	
16. Abstract  In October 1993 the FAA Technical Center conducted a vertical drop test of a narrow-body fuselage section. This test was structured to determine the impact response characteristics of some typical items of mass found aboard transport airplanes to assess the adequacy of the design standards and regulatory requirements for those components.  A primary objective of this test was to determine the dynamic response characteristics of the onboard overhead stowage bins and auxiliary fuel tank system, as well as the fuselage section itself, when subjected to a potentially survivable impact. The dynamic impact environment and the resultant response of the onboard overhead stowage bins and auxiliary fuel tank system were characterized. The structural support reactions for those onboard items of mass were measured and compared to predicted values which were based on static analyses and tests.  The test was intentionally structured to impose a dynamic load condition in excess of the current design and certification requirements for the onboard items of mass so that the dynamic fracture loads and modes of fracture for those components could also be determined and evaluated.			
17. Key Words  Overhead stowage bins, auxiliary fuel tank, acceleration, dynamic testing, vertical velocity change		18. Distribution Statement  This document is available to the public through the National Technical Information Service, Springfield, Virginia 22161	
19. Security Classif. (of this report)  Unclassified	20. Security Classif. (of this page)  Unclassified	21. No. of Pages 146	22. Price

## ACKNOWLEDGMENTS

The authors wish to acknowledge the assistance and technical guidance provided by Mr. Stephen J. Soltis, the Federal Aviation Administration's National Resource Specialist for Crash Dynamics, during the course of this project. His considerable knowledge of this subject area and his willingness to help during the conduct and reporting phases is greatly appreciated.

Accession For	
NTIS GRA&I	<input checked="" type="checkbox"/>
DTIC TAB	<input type="checkbox"/>
Unannounced	<input type="checkbox"/>
Justification	
By _____	
Distribution	
Availability Codes	
Distr	Avail and/or Special
A-1	

## TABLE OF CONTENTS

	Page
EXECUTIVE SUMMARY	xi
BACKGROUND	1
TEST OBJECTIVES	1
DESCRIPTION OF TEST FACILITY AND TEST ARTICLE	2
Test Facility	2
Test Article	4
INSTRUMENTATION	11
General	11
Fuselage	12
Overhead Stowage Bins	16
Boeing Links	17
C&D Attachments	17
Auxiliary Fuel Tank and Cradle	18
Test Dummies	24
Platform Load Cells	24
Cameras	24
DATA ACQUISITION SYSTEM	26
Data Acquisition System	26
Work Station	29
OVERHEAD STOWAGE BIN CALIBRATIONS	29
Calibration Procedures	29
Boeing Bin	29
Calibration 1	29
Calibration 2	31
C&D Bin	31
Calibration Analysis and Results	32
Boeing Stowage Bin Static Load Computations	35
C&D Stowage Bin Static Load Computations	40
Upper Brackets	40
Lower Fittings	41
TEST INITIATION	49
RESULTS AND DISCUSSION	50
Fuselage Structure	50
Boeing Stowage Bin	50
C&D Stowage Bin	51
Auxiliary Fuel Tank System	51
DATA ANALYSIS	52
Film Analysis	52
Data Reduction	54
Fuselage Structure	54
Auxiliary Fuel Tank	56
Platform	58

Anthropomorphic Dummies	59
Overhead Stowage Bins	59
Boeing Bin	59
C&D Bin	64
Summary of Accelerations	68
PHOTOGRAPHIC DOCUMENTATION	70
CONCLUSIONS	92
REFERENCES	94
APPENDIX A	95

## LIST OF FIGURES

Figure	Page
1 Drop Test Facility	3
2 Test Section, Side View	4
3 Test Section, Top View Seat Numbers	5
4 330-Gallon, Double Wall, Cylindrical Auxiliary Fuel Tank	8
5 Test Section Cross Section	9
6 Fuselage Mounted Sensors	13
7 Boeing Overhead Stowage Bin	16
8 Boeing Link: Sensor Location and Diagram	19
9 C&D Overhead Stowage Bin	20
10 C&D Upper Brackets: Sensor Locations	21
11 C&D Lower Fittings: Sensor Locations	22
12 Auxiliary Fuel Tank Cradle: Instrumentation Locations	23
13 Camera Locations	25
14 Boeing Overhead Stowage Bin: Loading Distribution	30
15 Boeing Link Installation Angle	31
16 Sensitivity Coefficient vs. Bolt Location	32
17 Bolt Location Identifiers (Upper Bracket)	33
18 Upper Bracket Installation Angles	33
19 C&D Overhead Stowage Bin: Loading Distribution	34
20 Lower Fitting Installation Angles	43
21 Fuselage Deformations	56
22 Platform Total Load	58
23 Boeing Link 17B Load Comparison	62
24 Boeing Link 18B Load Comparison	62
25 Boeing Link 25B Load Comparison	63
26 Boeing Link 28B Load Comparison	63
27 Forward Upper Bracket Load Comparison	66
28 Middle Upper Bracket Load Comparison	66
29 Rear Upper Bracket Load Comparison	67
30 C&D Bin Total Vertical Load	67
31 Accelerometer Locations and $G_{max}$ Values of the Fuselage	68
32 Accelerometer Locations and $G_{max}$ Values of the Overhead Stowage Bin Compartments and the Auxiliary Fuel Tank	69
33 Front View of Drop Test Facility	71
34 Side View of Test Article, Prior to Impact	71
35 Front View of Test Article After Impact	72
36 Overall View of Boeing Bin	72
37 Boeing Links 25B and 17B, Pretest	73
38 Boeing Links 25B and 17B, Posttest	73
39 Boeing Links 28B and 18B, Pretest	74
40 Boeing Links 28B and 18B, Posttest	74
41 Boeing Link 31B, Pretest	75

42	Boeing Link 31B, Posttest	75
43	Boeing Bin Broken Forward Hinge, Posttest	76
44	Boeing Bin Broken Aft Hinge, Posttest	76
45	PSU Unit After Separation, Posttest	77
46	C&D Bin Overall View, Pretest	77
47	C&D Bin Overall View, Posttest	78
48	C&D Bin Upper Forward Bracket, Posttest	78
49	C&D Bin Lower Forward Area, Posttest	79
50	C&D Bin Upper Center Section, Posttest	79
51	C&D Bin Aft Overall View, Posttest	80
52	C&D Bin Aft Upper Bracket, Posttest	80
53	C&D Bin Upper Aft Bin, Posttest	81
54	Auxiliary Fuel Tank Front Overall View, Pretest	81
55	Auxiliary Fuel Tank Front Overall View, Posttest	82
56	Auxiliary Fuel Tank Underside View, Posttest	82
57	Auxiliary Fuel Tank Inside, Posttest	83
58	Auxiliary Fuel Tank Drainage Hole, Posttest	83
59	Auxiliary Fuel Tank Drainage Hole Close Up, Posttest	84
60	Auxiliary Fuel Tank Drainage Hole Connector, Posttest	84
61	Auxiliary Fuel Tank Drainage Hose Connector, Posttest	85
62	Auxiliary Fuel Tank Drainage Hole Connectors Inside View, Posttest	85
63	Front Quarter View of Lower Fuselage Section, Posttest	86
64	Underside of Fuselage Section, Aft to Forward, Posttest	86
65	Forward Right Side Lower Fuselage Section, Posttest	87
66	Forward Left Side Lower Fuselage Section, Posttest	87
67	Lower Fuselage Section, Left Side BS 1140, Posttest	88
68	Lower Fuselage Section, Left Side BS 1180, Posttest	88
69	Underside Fuselage Floor Section Left-Side BS 1180, Posttest	89
70	Fuselage Interior Right Quarter View, Posttest	89
71	Fuselage Interior Left Quarter View, Posttest	90
72	Fuselage Interior Seats 16-18, Posttest	90
73	Fuselage Interior Rear View, Posttest	91

## LIST OF TABLES

	Table	Page
1	Seats and Occupants	6
2	Test Article Weight	10
3	Instrumentation	11
4	Sensor Locations	14
5	Data Acquisition System Configuration and Calibration	27
6	Sensitivity Coefficients of the Boeing Links	35
7	Boeing Bin Static Calibration: Analysis 1	37
8	Boeing Bin Static Calibration: Analysis 2	37
9	Boeing Bin Static Calibration: Analysis 3	38
10	Boeing Bin Static Calibration: Analysis 4	38
11	Boeing Bin Static Calibration: Analysis 5	39
12	Boeing Bin Static Calibration: Analysis 6	39
13	Influence Coefficients of the Boeing Bin Links	40
14	Sensitivity Coefficients of the C&D Lower Fittings	42
15	C&D Static Calibration: Analysis 1	45
16	C&D Static Calibration: Analysis 2	46
17	C&D Static Calibration: Analysis 3	47
18	C&D Static Calibration: Analysis 4	48
19	Influence Coefficients of C&D Overhead Stowage Bin Attachments	49
20	Lower Fuselage Crush Measurements	50
21	Camera Speeds	53
22	Time Reference Events	53
23	Fuselage Accelerations During Initial Impact	55
24	Fuselage Accelerations During Primary Impact	55
25	Tank Accelerations	57
26	Maximum Strains on the Tank Supports	57
27	Boeing Bin Accelerations	60
28	Boeing Links' Maximum Measured Loads	61
29	C&D Bin Accelerations	64
30	C&D Bin Upper Brackets Maximum Measured Loads	65
31	C&D Bin Lower Fittings Maximum Measured Loads	65

## EXECUTIVE SUMMARY

In October 1993 the FAA Technical Center conducted a vertical drop test of a narrow-body fuselage section. This test was structured to determine the impact response characteristics of some typical items of mass installed aboard transport airplanes to assess the adequacy of the design standards and regulatory requirements for those components.

A primary objective of the test was to determine the dynamic response characteristics of the onboard overhead stowage bins and auxiliary fuel tank system, as well as the fuselage section itself, when subjected to a potentially survivable impact. The dynamic impact environment and the resultant response of the onboard overhead stowage bins and auxiliary fuel tank system were characterized. The structural support reactions for those onboard items of mass were measured and compared to predicted values which were based on static analyses and tests.

The test was intentionally structured to impose a dynamic load condition in excess of the current design and certification requirements for the onboard items of mass so that the dynamic fracture loads and modes of fracture for those components could also be determined and evaluated. For the test, overhead bins from the Boeing company and C&D Interiors were tested, as well as a double-wall, cylindrical, auxiliary fuel tank configuration.

The vertical impact velocity for the drop test was 30 feet per second which resulted in a test section average deceleration of 36G<sub>max</sub>. This is considered to be a severe but survivable impact. This caused from 4 to 20 inches of crush to the lower tapered fuselage section. There was no loss of habitable space in the cabin area.

Both overhead stowage bins experienced various degrees of attachment fractures. The Boeing bin maintained its structural integrity and remained attached to the structure. The C&D bin experienced separations between the lower surface and vertical bulkheads. Both bins suffered fractures of their hinges and door locking mechanisms resulting in the spilling of their contents. The Personal Services Units (PSU) attached to the underside of the Boeing bins detached almost immediately upon impact.

The auxiliary fuel tank system remained firmly attached to its mounting system during and after the test. There was minimal distress to the cabin floor to which it was attached. The simulated fuel leaked slowly out of the tank after the test. The discharge line attached to the bottom of the tank was forced upward, rupturing the welds around the discharge line in both the inner and outer tank walls.

The G levels measured in this test were probably higher than normal due to the influence of the auxiliary fuel tank. However, such a configuration may typically be found in service.

## BACKGROUND

This vertical impact test is one of a series of fuselage section and full-scale airplane tests conducted in support of the Federal Aviation Administration's (FAA) ongoing Aircraft Safety Research Plan (Reference 1). Such tests included the Full-Scale Transport Airplane Controlled Impact Demonstration (Reference 2) which included an instrumented overhead stowage bin experiment (Reference 3) and a number of transport airplane fuselage section longitudinal impact tests with seats (Reference 4), an auxiliary fuel tank (Reference 5), and overhead stowage bins on board (Reference 6).

Cabin safety is an element of the FAA's Aircraft Safety Research Plan. Previous cabin safety research efforts have led to the definition of the survivable crash environment, the development of crash dynamic analytical modeling methodologies, and improved design standards and regulatory requirements for aircraft seats and aircraft interiors. This test was structured to determine the impact response characteristics of some typical items of mass installed on board a transport airplane to assess the adequacy of the design standards and regulatory requirements for those components.

## TEST OBJECTIVES

The primary objective of the test was to determine the dynamic response characteristics of the onboard overhead stowage bins and auxiliary fuel tank system, as well as the fuselage section itself, when subjected to a potentially survivable impact. The dynamic impact environment and the resultant response of the onboard overhead stowage bins and auxiliary fuel tank system were characterized. The structural support reactions for those onboard items of mass were measured and compared to predicted values based on static analyses and tests.

Additional test objectives included:

- Obtain test data to validate analytical predictions.
- Evaluate the impact response characteristics of interior overhead bins and double-wall auxiliary fuel tank systems.
- Identify failure modes, if possible, for interior overhead bins and double-wall auxiliary fuel tank systems under dynamic impact conditions.

The test was intentionally structured to simulate a severe, but survivable, crash. Therefore, this test imposed a dynamic load condition in excess of the current design and certification requirements for the onboard items of mass.

## DESCRIPTION OF TEST FACILITY AND TEST ARTICLE

### TEST FACILITY.

The Technical Center drop test facility (figure 1) is comprised of two 50-foot vertical steel towers connected at the tops by a horizontal platform. An electrically powered winch, mounted on the platform, is used to raise or lower the test article and is controlled from the base of one of the tower legs. The lifting capacity of the winch is rated at 13,600 pounds. Attached to the winch is a reeved hoisting cable which is used to raise the test article. A sheave block assembly hanging from the free end of the reeved cable is engaged to a solenoid operated release hook. The release hook is connected to the airframe by a cable/turnbuckle assembly with hooks bolted to the fuselage section at four locations. Located below the winch cable assembly and between the tower legs is a 15- by 36-foot wooden platform which rests upon I-beams and is supported by 12 independent load cells.

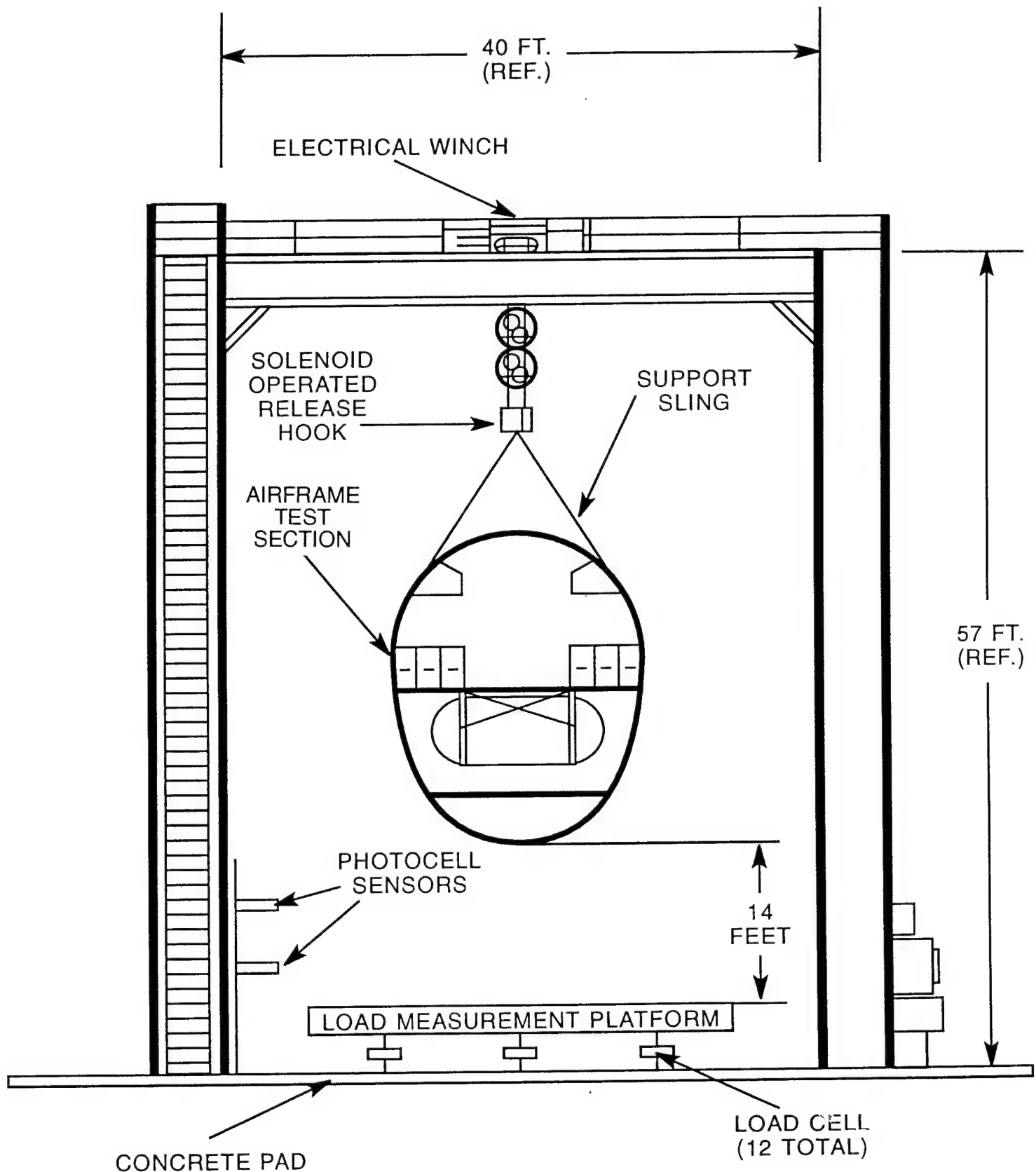


FIGURE 1. DROP TEST FACILITY

## TEST ARTICLE

The test article was a ten-foot tapered section of a Boeing 707 cut from body station (BS) 1120 to 1240 (figure 2). The section was equipped with seats, overhead bins, and an auxiliary fuel tank system. The outer floor beams at each end of the section were reinforced to minimize the open end effects, i.e., to simulate the reaction that would be seen if an entire aircraft fuselage was tested.

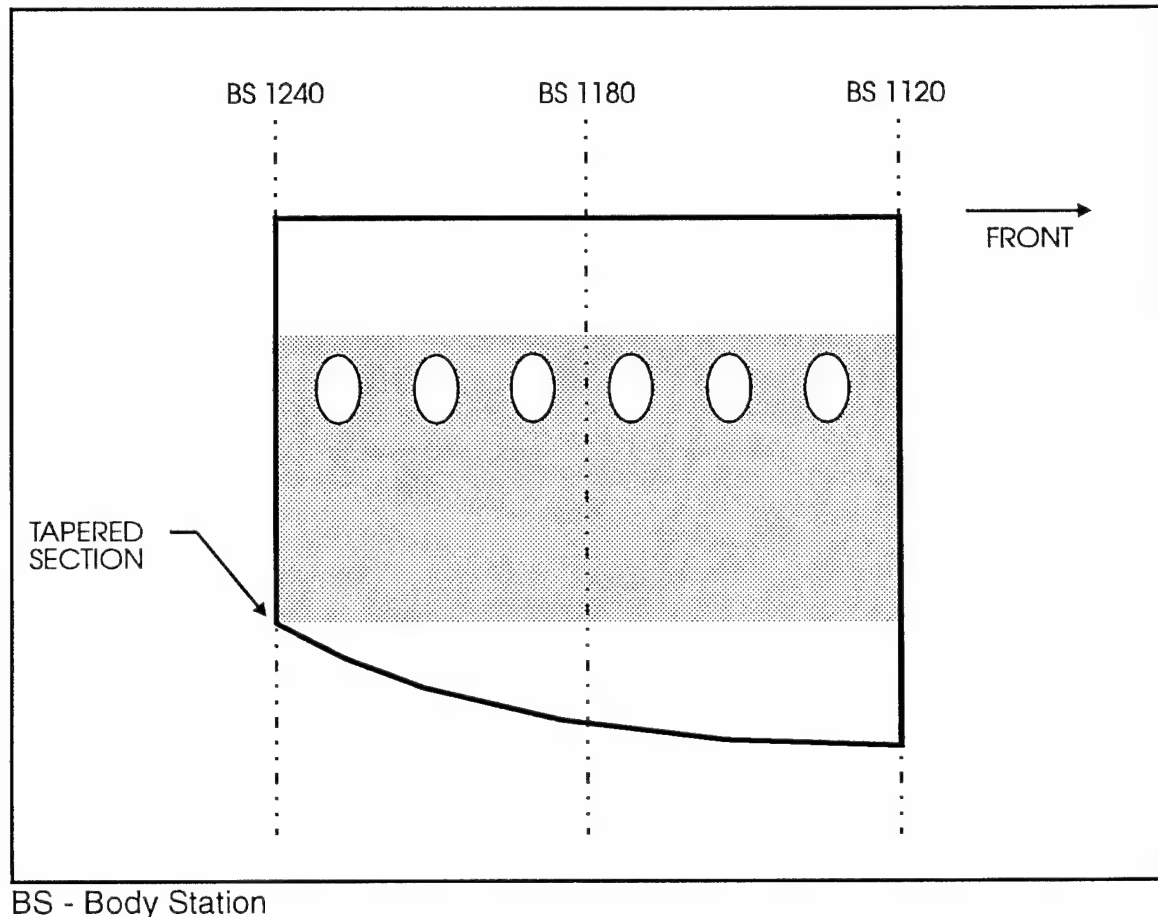


FIGURE 2. TEST SECTION, SIDE VIEW

The test article contained six floor-mounted, triple passenger seats placed in three rows. For the purpose of this report the seats were numbered one through eighteen (figure 3). All seats were "9g rated seats," and contained an anthropomorphic dummy or other type of ballast (table 1). The seats and dummies were utilized to achieve the desired test section weight and were not of primary interest in the test.

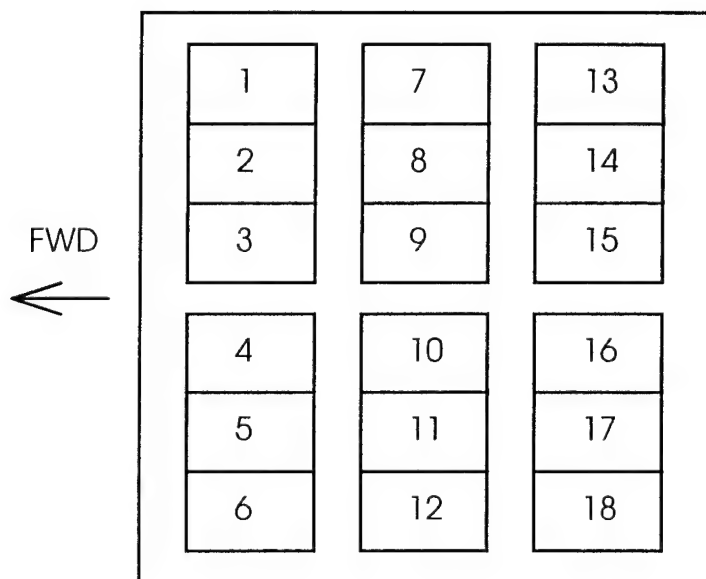


FIGURE 3. TEST SECTION, TOP VIEW SEAT NUMBERS

TABLE 1. SEATS AND OCCUPANTS

SEAT NUMBER	SEAT WEIGHT	OCCUPANT	OCCUPANT WEIGHT	INSTRUMENTATION
1	95 lbs	Standard	158 lbs	None
2		Standard	158 lbs	None
3		Standard	158 lbs	None
4	99 lbs	Standard	158 lbs	None
5		Standard	158 lbs	None
6		Standard	158 lbs	None
7	64 lbs	Standard	158 lbs	None
8		Instrumented	165 lbs	Pelvic Accel.(z), Load Cell
9		Standard	158 lbs	None
10	64 lbs	Self-Contained	172 lbs	Pelvic Triaxial Accel., Load Cell
11		Instrumented	165 lbs	Pelvic Accel.(z), Load Cell
12		Standard	158 lbs	None
13	95 lbs	Anthropomorphic	165 lbs	None
14		Wood Block	165 lbs	None
15		Anthropomorphic	165 lbs	None
16	99 lbs	Anthropomorphic	165 lbs	None
17		Standard	158 lbs	None
18		Anthropomorphic	165 lbs	None

The standard dummies were mannequins, with no instrumentation, placed in the seats to simulate the weight of an actual occupant. The anthropomorphic dummies are of the Hybrid II type, manufactured to represent the 50 percentile male adult passenger. Two of these dummies were instrumented with vertical accelerometers and load cells in their pelvic area. The self-contained dummy was an anthropomorphic dummy equipped with its own data acquisition system and power supply. A more detailed description of the instrumentation is discussed in the instrumentation section of this report. The final type of ballast used was a torso shaped wood block placed in seat number 14. All the dummies and ballast were strapped firmly into their seats with restraint systems.

The auxiliary fuel tank system was a 330-gallon, double-walled, cylindrical tank (figures 4, 54, and 57). The tank was mounted to the underside of the fuselage floor (figure 5), between BS 1140 and BS 1180. The installation included reinforcement of 5 bays' floor beams from BS 1140 to BS 1240. The reinforcement consisted of adding intercostals between traverse floor beams in each bay and longitudinal stops at the cradle tracks. The tank contained 247.5 gallons of water to simulate the weight of a full tank of fuel and was pressurized to 2.5 psi.

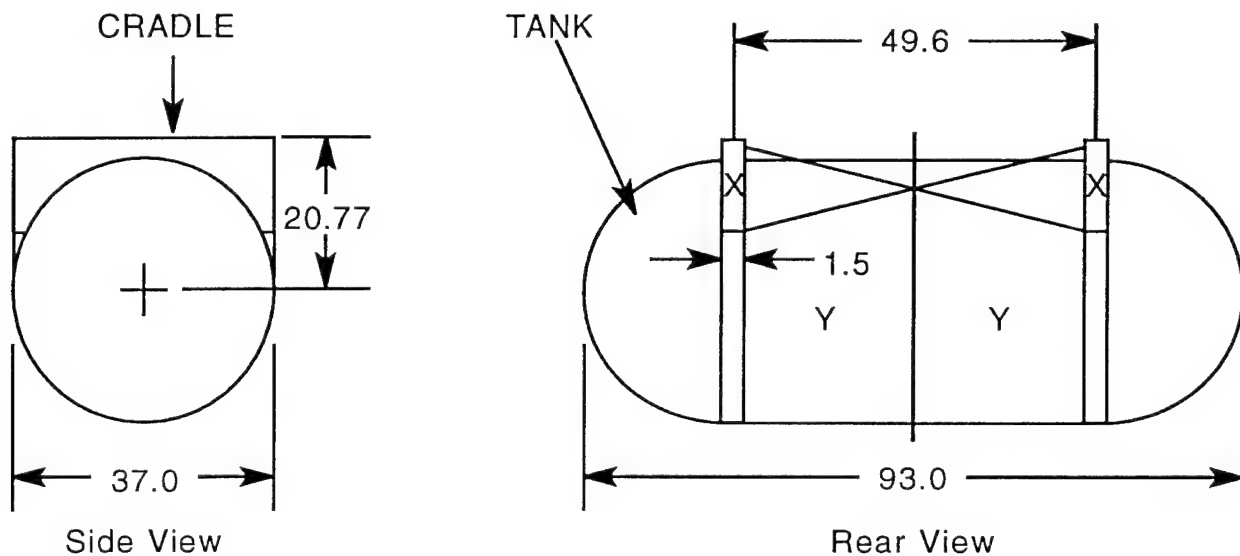
A 60-inch Boeing overhead stowage bin was mounted on the left side of the fuselage. A 20-inch Boeing overhead stowage bin was mounted in front of the 60-inch bin, and another 20-inch bin was mounted behind the 60-inch bin. Two Personal Service Units (PSU) were attached under the Boeing bin. The bin was instrumented with accelerometers and the support links were instrumented with strain gages, both of which are discussed in the instrumentation section.

On the right side of the fuselage, a 113-inch C&D stowage bin was mounted. This bin also was instrumented with accelerometers and its support attachments were strain gaged. Details of the instrumentation appear in the instrumentation section.

The test article also had three onboard cameras which are discussed in the instrumentation section.

The total weight of the test article was 8097 pounds. The individual item weights are presented in table 2.

ALL MEASUREMENTS IN INCHES



WEIGHTS

OTHER	94
TANK	242
FUEL	2055*
CRADLE ASSY	54
	2445 LB

OTHER WEIGHTS

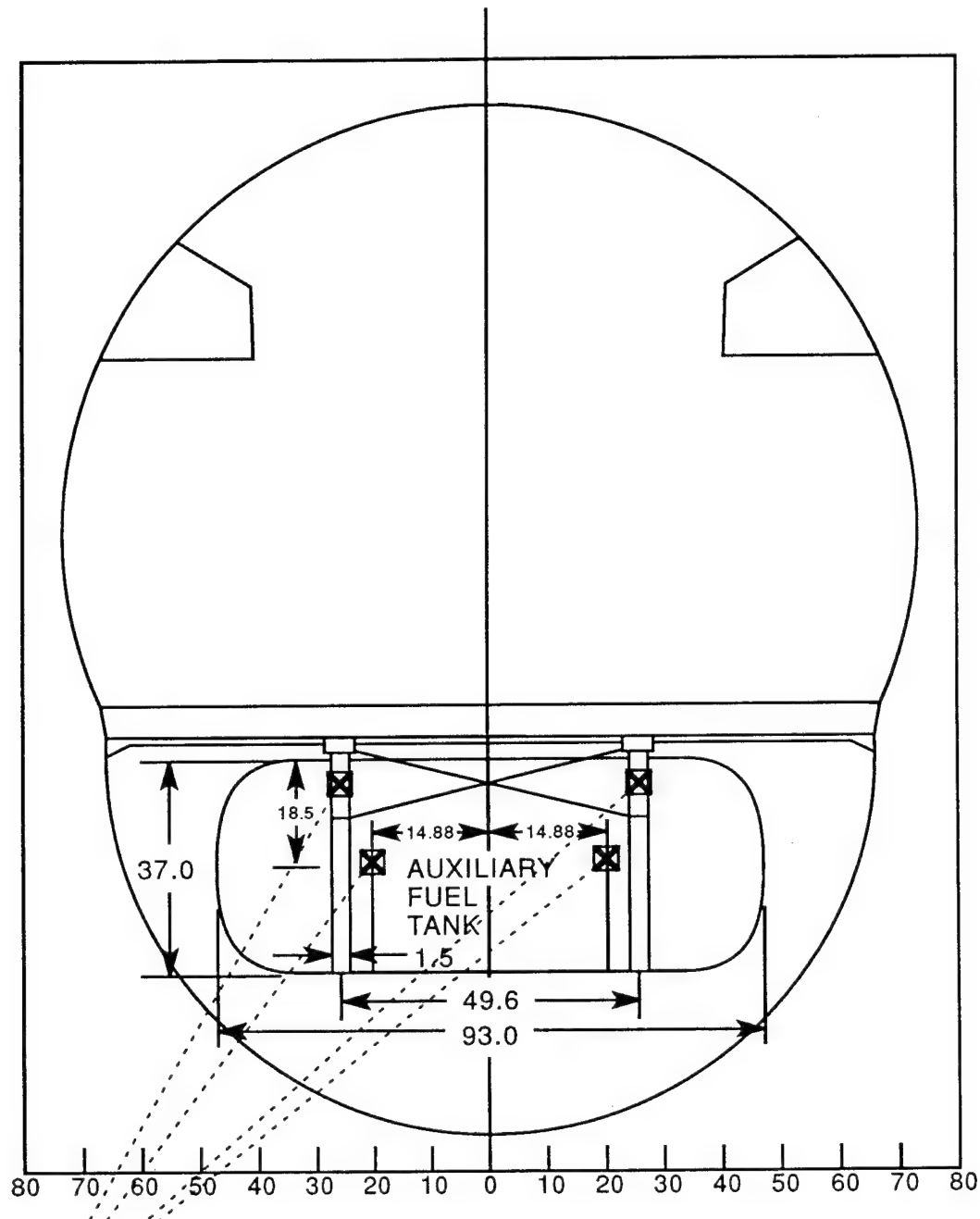
FUEL LINES	17
INTERCOSTAL	52
MISC	25
	94 LB

\* BASED ON 75 PERCENT FULL WITH WATER  
(8.3 LB/GALLON)

X = VERTICAL ACCELEROMETERS ON FRONT  
AND REAR

Y = VERTICAL ACCELEROMETERS ON REAR  
AND VERTICAL AND LONGITUDINAL  
ACCELEROMETERS ON FRONT

FIGURE 4. 330-GALLON, DOUBLE WALL, CYLINDRICAL AUXILIARY FUEL TANK



UNITS IN INCHES

FIGURE 5. TEST SECTION CROSS SECTION

TABLE 2. TEST ARTICLE WEIGHT

	Item	Number	Weight	Total	
DUMMIES	Standard	10	158	1580	
	Anthropomorphic	6	165	990	
	Wood	1	165	165	
	Self-Contained	1	172	172	
				SUB	2907
FUSELAGE	Power/lights	1	31	31	
	Airframe	1	1522	1522	
				SUB	1553
AUX. FUEL TANK					
	Intercostals	1	94	94	
	Cradle	1	54	54	
	Tank	1	242	242	
	Fuel lines	1	10	10	
		1	7	7	
		1	7	7	
	Water	1	2055	2055	
				SUB	2469
OVERHEAD BINS					
	C&D	1	66	66	
	Simulated Luggage	1	213	213	
	Boeing	1	46	46	
	Simulated Luggage	1	214	214	
	Personal Service Unit	2	15.5	31	
				SUB	570
CAMERAS	High Speed	2	28	56	
	High Speed	1	26	26	
				SUB	82
SEATS	Right Hand, Forward	1	99	99	
	Left Hand, Forward	1	95	95	
	Right Hand, Center	1	64	64	
	Left Hand, Center	1	64	64	
	Right Hand, Aft	1	99	99	
	Left Hand, Aft	1	95	95	
				SUB	516
<b>TOTAL</b>					<b>8097</b>

## INSTRUMENTATION

### GENERAL.

The instrumentation used in the test included accelerometers, strain gages, displacement transducers (string potentiometers), pelvic load cells, and platform load cells. The instrumentation complied with SAE J211, Instrumentation for Impact Tests (Reference 8).

The accelerometers used were an undamped, medium g-level piezoresistive type designed specifically for crash test studies. The median sensitivity was 2 mv/g, with 10 vdc applied excitation. Prior to the test, compensation for signal offset due to thermal effects was provided. Shunt calibrations were performed on the accelerometers and strain gage bridges to insure correct sensitivity. Pretest strain gage calibrations were conducted on all individual supports for the overhead stowage bins as were total calibrations of the bins mounted in place in the fuselage.

Two displacement transducers fore and aft of the auxiliary fuel tank had a range of +/-10 inches and a sensitivity of 47.3 mv/v/in. The two displacement transducers mounted from ceiling to floor had a range of +/-20 inches, with an extension cable for the desired length. The median sensitivity for the upper transducers was 22.7 mv/v/in with 10 vdc applied excitation.

Table 3 shows the type and number of the instruments associated with the test.

TABLE 3. INSTRUMENTATION

	Accelerometer			Strain Gage	Load Cell	String Pot.	Total
	Long.	Lat.	Vert.				
Fuselage	4	4	10	-	-	4	22
Dummies	-	-	2	-	2	-	4
Fuel Tank	2	-	4	-	-	-	6
Fuel Tank Cradle	-	-	4	12	-	-	16
Boeing Bin	1	1	2	7	-	-	11
C&D Bin	1	1	3	12	-	-	17
Velocity	-	-	1	-	-	-	1
Platform	-	-	1	-	12	-	13
Spare	-	-	-	-	-	-	2
						TOTAL	92

## FUSELAGE.

As shown in figure 6, there were a total of 18 accelerometers located on the aircraft structure. Referring to the floor as  $Z=0$  and center of the front view of the fuselage as  $Y=0$ , table 4 indicates the channel number and the  $X$ -,  $Y$ -, and  $Z$ -coordinates of the accelerometers on the fuselage, as well as all the other instrumentation used in the test. The majority of the accelerometers were concentrated about BS1180, the midsection of the aircraft specimen. This area was selected because it was the approximate location of the auxiliary tank, instrumented dummies, and midsection of the overhead stowage bins. The other accelerometers were located at strategic points about the structure to assist in the test analysis. Two displacement transducers were mounted on the aircraft ceiling at BS1180, with the cable end attached to the cabin floor. Their purpose was to indicate any deformation of the floor due to the auxiliary fuel tank impacting the underside of the floor. There were also two displacement transducers mounted on the underside of the floor, with the cable attached to the bottom of the aircraft structure. These were mounted fore and aft of the auxiliary fuel tank to determine the amount of crushing of the aircraft structure. These data will be used in an FAA-sponsored program to analytically simulate testing. The accelerometers measuring structural data were recorded on channels 301-403, the transducers measuring the floor deformations were recorded on channels 429 and 430, and the transducers measuring the aircraft crushing were recorded on channels 413 and 414.

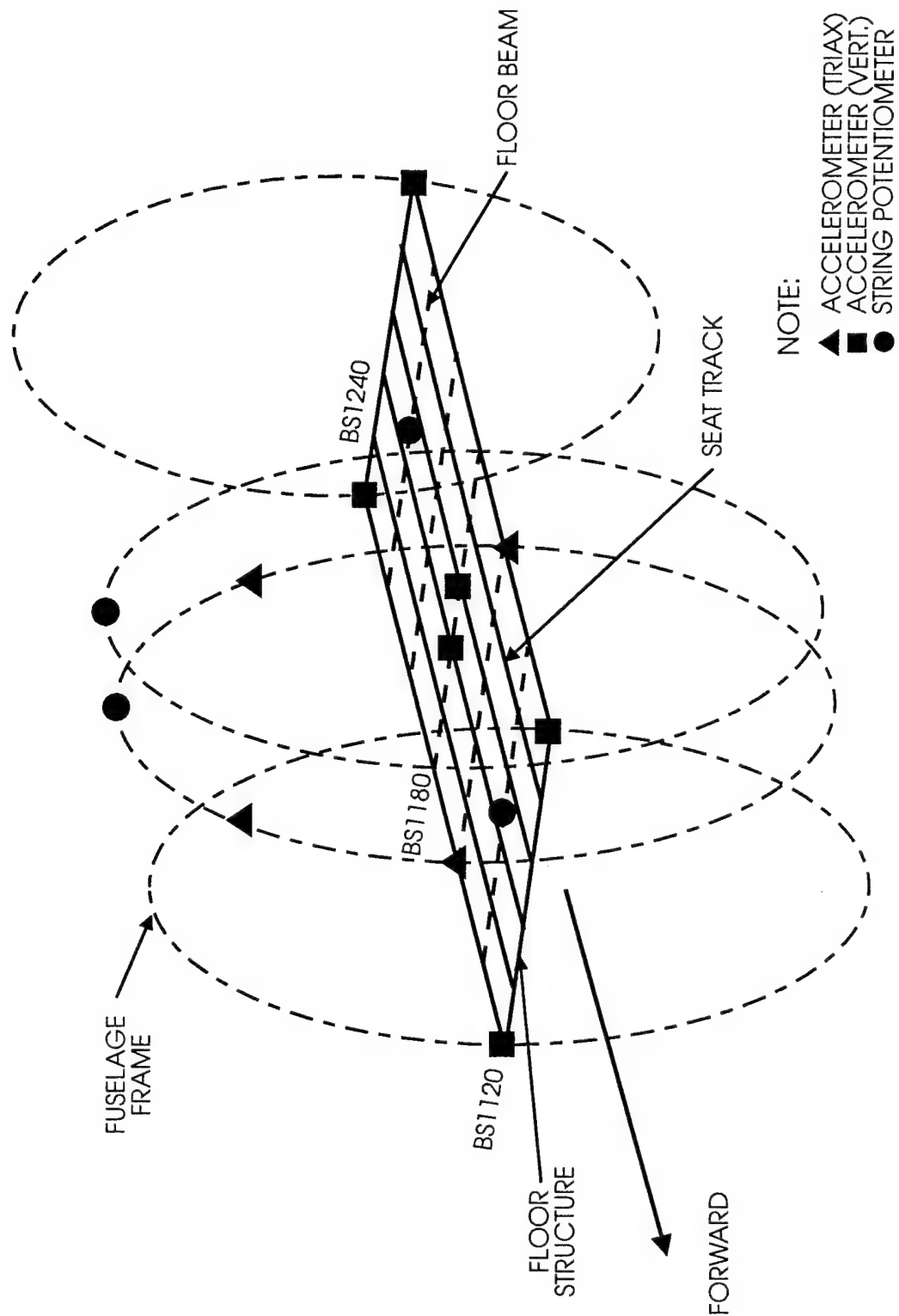


FIGURE 6. FUSELAGE MOUNTED SENSORS

TABLE 4. SENSOR LOCATIONS

CHANNEL NUMBER	SENSOR LOCATION			COMMENTS
	FUSELAGE STATION (X)	BUTT LINE (Y)	WATER LINE (Z)	
101	1190	-25	-24	Aft Port Cradle (strain gauges)
102	1190	-25	-16	Aft Port Cradle (strain gauges)
103	1186	-25	-11	Aft Port Cradle (strain gauges)
104	1190	25	-24	Aft Starboard Cradle (strain gauges)
105	1190	25	-16	Aft Starboard Cradle (strain gauges)
106	1186	25	-11	Aft Starboard Cradle (strain gauges)
107	1154	-25	-24	Forward Port Cradle (strain gauges)
108	1154	-25	-16	Forward Port Cradle (strain gauges)
109	1158	-25	-11	Forward Port Cradle (strain gauges)
110	1154	25	-24	Forward Starboard Cradle (strain gauges)
111	1154	25	-24	Forward Starboard Cradle (strain gauges)
112	1158	25	-11	Forward Starboard Cradle (strain gauges)
113	1200	-	-	Boeing Overhead Bin (strain gauges)
114	1160	-	-	Boeing Overhead Bin (strain gauges)
115	1152	-	-	Boeing Overhead Bin (strain gauges)
201	1212	-	-	Boeing Overhead Bin (strain gauges)
202	1152	-	-	Boeing Overhead Bin (strain gauges)
203	1212	-	-	Boeing Overhead Bin (strain gauges)
204	1160-1180	-	-	Boeing Overhead Bin (strain gauges)
205	1134	-	-	C&D Interiors Inc. Overhead Bin (strain gauges)
206	1134	-	-	C&D Interiors Inc. Overhead Bin (strain gauges)
207	1189	-	-	C&D Interiors Inc. Overhead Bin (strain gauges)
208	1189	-	-	C&D Interiors Inc. Overhead Bin (strain gauges)
209	1245	-	-	C&D Interiors Inc. Overhead Bin (strain gauges)
210	1245	-	-	C&D Interiors Inc. Overhead Bin (strain gauges)
211	1135	-	-	C&D Interiors Inc. Overhead Bin (strain gauges)
212	1135	-	-	C&D Interiors Inc. Overhead Bin (strain gauges)
213	1211	-	-	C&D Interiors Inc. Overhead Bin (strain gauges)
214	1211	-	-	C&D Interiors Inc. Overhead Bin (strain gauges)
215	1206	-	-	C&D Interiors Inc. Overhead Bin (strain gauges)
216	1206	-	-	C&D Interiors Inc. Overhead Bin (strain gauges)
217	1185	-35	23	ATD's Load Cell
218	1185	35	23	ATD's Load Cell
219	-	-	-	Load Cell, Under Platform
220	-	-	-	Load Cell, Under Platform
221	-	-	-	Load Cell, Under Platform
222	-	-	-	Load Cell, Under Platform
223	-	-	-	Load Cell, Under Platform
224	-	-	-	Load Cell, Under Platform
225	-	-	-	Load Cell, Under Platform
226	-	-	-	Load Cell, Under Platform
227	-	-	-	Load Cell, Under Platform
228	-	-	-	Load Cell, Under Platform
229	-	-	-	Load Cell, Under Platform
230	-	-	-	Load Cell, Under Platform

TABLE 4. SENSOR LOCATIONS (CONTINUED)

CHANNEL NUMBER	SENSOR LOCATION			COMMENTS
	FUSELAGE STATION (X)	BUTT LINE (Y)	WATER LINE (Z)	
301	1240	68	2	Accelerometer mounted on aircraft structure. ID# AA67. Axis -Z
302	1240	-68	2	Accelerometer mounted on aircraft structure. ID# AA74. Axis Z
303	1170	-25	0	Accelerometer mounted on aircraft structure. ID# CJ46. Axis -Z
304	1180	68	2	Accelerometer mounted on aircraft structure. ID# A89K. Axis Z
305	1180	68	2	Accelerometer mounted on aircraft structure. ID# AA77. Axis Y
306	1180	68	2	Accelerometer mounted on aircraft structure. ID# AA58. Axis X
307	1180	68	68	Accelerometer mounted on aircraft structure. ID# DE71. Axis -Z
308	1180	68	68	Accelerometer mounted on aircraft structure. ID# AA89. Axis Y
309	1180	68	68	Accelerometer mounted on aircraft structure. ID# AA57. Axis X
310	1120	68	2	Accelerometer mounted on aircraft structure. ID# AA56. Axis -Z
311	1120	-68	2	Accelerometer mounted on aircraft structure. ID# AA73. Axis -Z
312	1170	25	0	Accelerometer mounted on aircraft structure. ID# AA27. Axis -Z
313	1180	-68	68	Accelerometer mounted on aircraft structure. ID# DE93. Axis -Z
314	1180	-68	68	Accelerometer mounted on aircraft structure. ID# DE92. Axis Y
315	1180	-68	68	Accelerometer mounted on aircraft structure. ID# AA49. Axis X
401	1180	-68	2	Accelerometer mounted on aircraft structure. ID# A79J. Axis -Z
402	1180	-68	2	Accelerometer mounted on aircraft structure. ID# A81F. Axis Y
403	1180	-68	2	Accelerometer mounted on aircraft structure. ID#
404	1198	21	-27	Accelerometer mounted on aux. fuel tank. ID#
405	1198	21	-27	Accelerometer mounted on aux. fuel tank. ID#
406	1200	23	-16	Accelerometer mounted on aux. fuel tank. ID# AA59. Axis Z
407	1200	-23	-16	Accelerometer mounted on aux. fuel tank. ID# A90F. Axis -Z
408	1160	21	-27	Accelerometer mounted on aux. fuel tank. ID# CV29. Axis -Z
409	1160	21	-27	Accelerometer mounted on aux. fuel tank. ID# CX80. Axis X
410	1160	-21	-27	Accelerometer mounted on aux. fuel tank. ID# CR31. Axis Z
411	1160	-21	-27	Accelerometer mounted on aux. fuel tank. ID# AA86. Axis X
412	1150	23	-16	Accelerometer mounted on aux. fuel tank. ID# AA98. Axis Z
413	1140	0	-10	String potentiometer
414	1220	0	-10	String potentiometer
415	1150	-23	-16	Accelerometer mounted on aux. fuel tank. ID# AA24. Axis -Z
416	1180	-60	68	Accelerometer mounted on C&D bin. ID# GK19. Axis -Z
417	1180	-60	68	Accelerometer mounted on C&D bin. ID# A53F. Axis -Y
418	1180	-60	68	Accelerometer mounted on C&D bin. ID# A32F. Axis X
419	1120	-60	68	Accelerometer mounted on C&D bin. ID# CV70. Axis -Z
420	1240	-60	68	Accelerometer mounted on C&D bin. ID# A77J. Axis -Z
421	1120	60	68	Accelerometer mounted on Boeing bin. ID# DB59. Axis -Z
422	1180	60	68	Accelerometer mounted on Boeing bin. ID# A71F. Axis -Z
423	1180	60	68	Accelerometer mounted on Boeing bin. ID# FY04. Axis -Y
424	1180	60	68	Accelerometer mounted on Boeing bin. ID# A95G. Axis X
425	1185	-35	23	ATD'S accelerometer. ID# AA72. Axis Z
426	-	-	-	Accelerometer underneath platform. ID# AA54. Axis Z
427	-	-	-	Velocity trap
428	1185	35	23	ATD'S accelerometer. ID# AA85. Axis Z
429	1177	15.25	90	String potentiometer
430	1177	15.25	90	String potentiometer
431				Load cell, under platform

## OVERHEAD STOWAGE BINS.

The Boeing overhead stowage bin (figure 7) had strain gages bonded to its support links, as shown in figure 8. The C&D overhead stowage bin (figure 9) had strain gages attached to its upper brackets and lower fittings, as shown in figures 10 and 11, respectively. Figures 7 and 9 show the layout of the fixtures on the Boeing and C&D bins, respectively. There were 7 channels recorded in full-bridge configuration for the Boeing bin, and 12 channels were recorded for axial and bending loads for the C&D bin (refer to table 3).

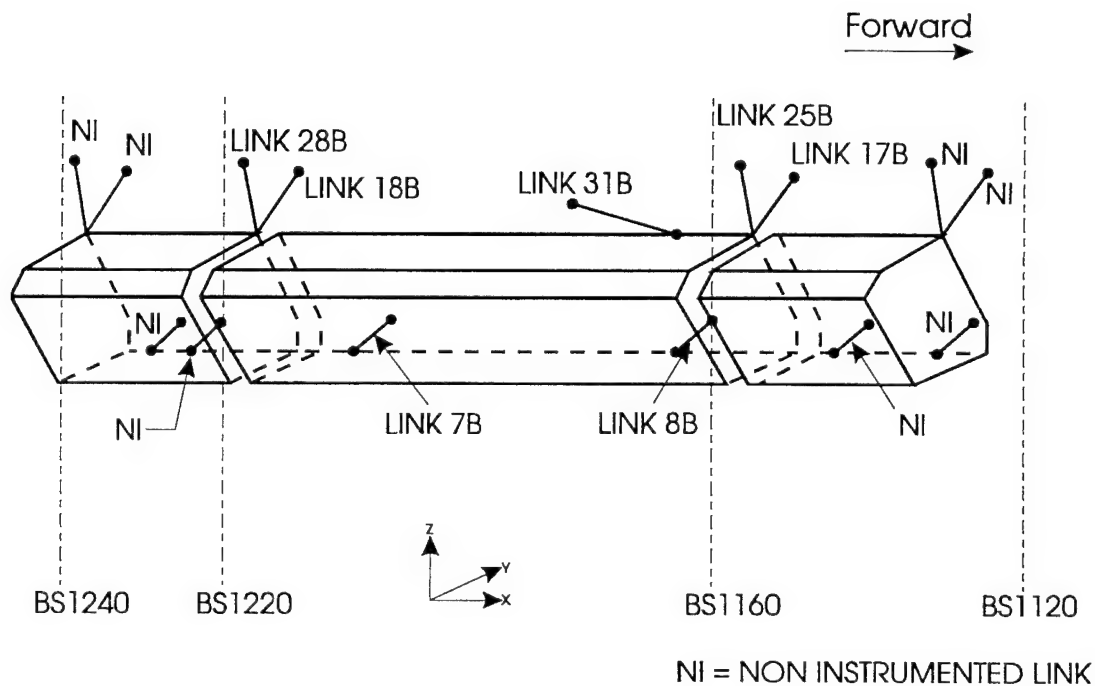


FIGURE 7. BOEING OVERHEAD STOWAGE BIN

BOEING LINKS. There were a total of seven instrumented links, with three different lengths: 2.375, 3.25, and 12.25 inches. The links with lengths of 2.375 and 3.5 inches were primarily designed to react against vertical and lateral loading while the 12.25-inch link was designed to counteract the longitudinal forces during static or dynamic loading of the bins.

Figure 8 illustrates the strain gage locations and bridge configuration on the 3.25-inch-long link. The sensors were placed in the center section of the link, aligned parallel to the longitudinal axis ( $z_L$ ) of the link, and configured as full Wheatstone bridges. Two sets of two strain gages were placed  $180^\circ$  apart from each other. The strain gage specifications were as follows:

- a. Gage Type: CEA-13-062UT-350
- b. Resistance:  $350.0 \pm 0.4\%$  Ohms
- c. Gage Factor:  $2.130 \pm 0.5\%$
- d. Transverse Sensitivity:  $1.5 \pm 0.2\%$

The same locations and configuration were used with the other two link sizes.

C&D ATTACHMENTS. There were six C&D overhead stowage bin attachments calibrated. These attachments had two different kinds of geometry as shown in figures 10A and 11A. Three brackets supported the upper section of the bin, and three fittings supported the lower section of the bin.

The upper brackets (figure 10) were instrumented to measure bending and axial loading. The bending bridge was configured as a quarter Wheatstone bridge, with three wire leads, (figure 10B). Its specifications were as follows:

- a. Gage Type: CEA-13-062UW-350
- b. Resistance:  $350.0 \pm 0.3\%$  Ohms
- c. Gage Factor:  $2.165 \pm 0.5\%$
- d. Transverse Sensitivity:  $0.9 \pm 0.2\%$

The axial sensitive strain gages were placed 0.25 inch below the bolt slot (center) and 0.75 inch from the front edge (figure 10A). The gages' axes were parallel and concentric to the assumed  $z_u$ -axis. There were two gages on either side of the bracket flange. They were configured as a full Wheatstone bridge (figure 10C). Their specifications were as follows:

- a. Gage Type: CEA-13-062UW-350
- b. Resistance:  $350.0 \pm 0.3\%$  Ohms
- c. Gage Factor:  $2.165 \pm 0.5\%$
- d. Transverse Sensitivity:  $0.9 \pm 0.2\%$

The C&D lower fittings (figure 11) were also instrumented to measure bending and axial loading. The bending strain gages were placed on the top surface of the complex fitting flange (figure 11A). It was configured as a half Wheatstone bridge (figure 11B). Their specifications were as follows:

- a. Gage Type: CEA-13-062UT-350
- b. Resistance: 350.0 +/-0.4% Ohms
- c. Gage Factor: 2.130 +/-0.5%
- d. Transverse Sensitivity: 1.5 +/-0.2%

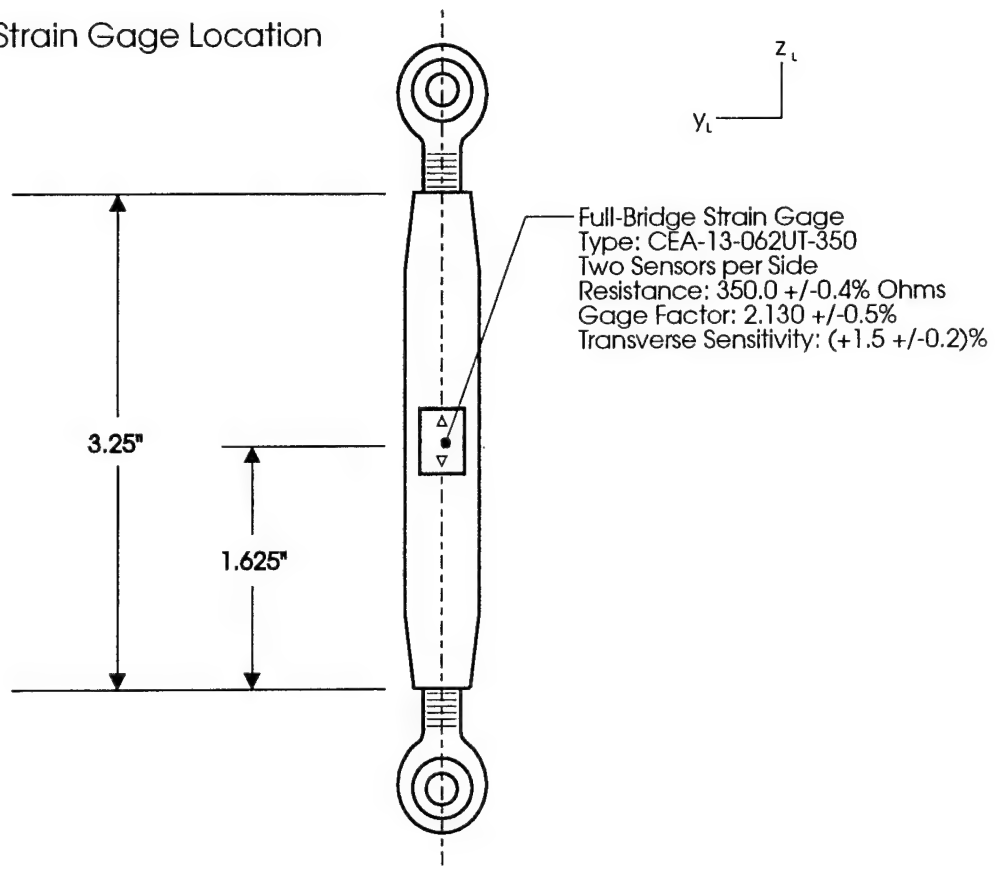
The axial sensitive strain gages were also placed on the flange, but on its sides (figure 11A). The gages' primary axes were parallel to the assumed y'-axis. There were two gages on either side of the fitting flange. They were configured as full Wheatstone bridges (figure 11C). The gages' specifications were as follows:

- a. Gage Type: CEA-13-062UT-350
- b. Resistance: 350.0 +/-0.4% Ohms
- c. Gage Factor: 2.130 +/-0.5%
- d. Transverse Sensitivity: 1.5 +/-0.2%

#### AUXILIARY FUEL TANK AND CRADLE.

The auxiliary fuel tank's four upper cradle corners were strain gaged on the vertical and diagonal supports, along with the support strap, as shown in figure 12, for a total of 12 channels. All data were recorded on channels 101 to 112. Four accelerometers were attached to the cradle and recorded data in the Z-direction. Six accelerometers were attached to the tank, with four recording in the Z-direction and two in the X-direction.

A. Strain Gage Location



B. Full-Bridge Diagram (Axial)

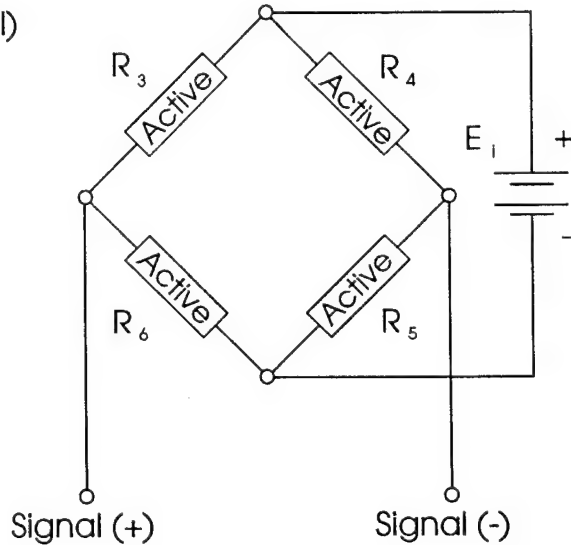


FIGURE 8. BOEING LINK: SENSOR LOCATION AND DIAGRAM

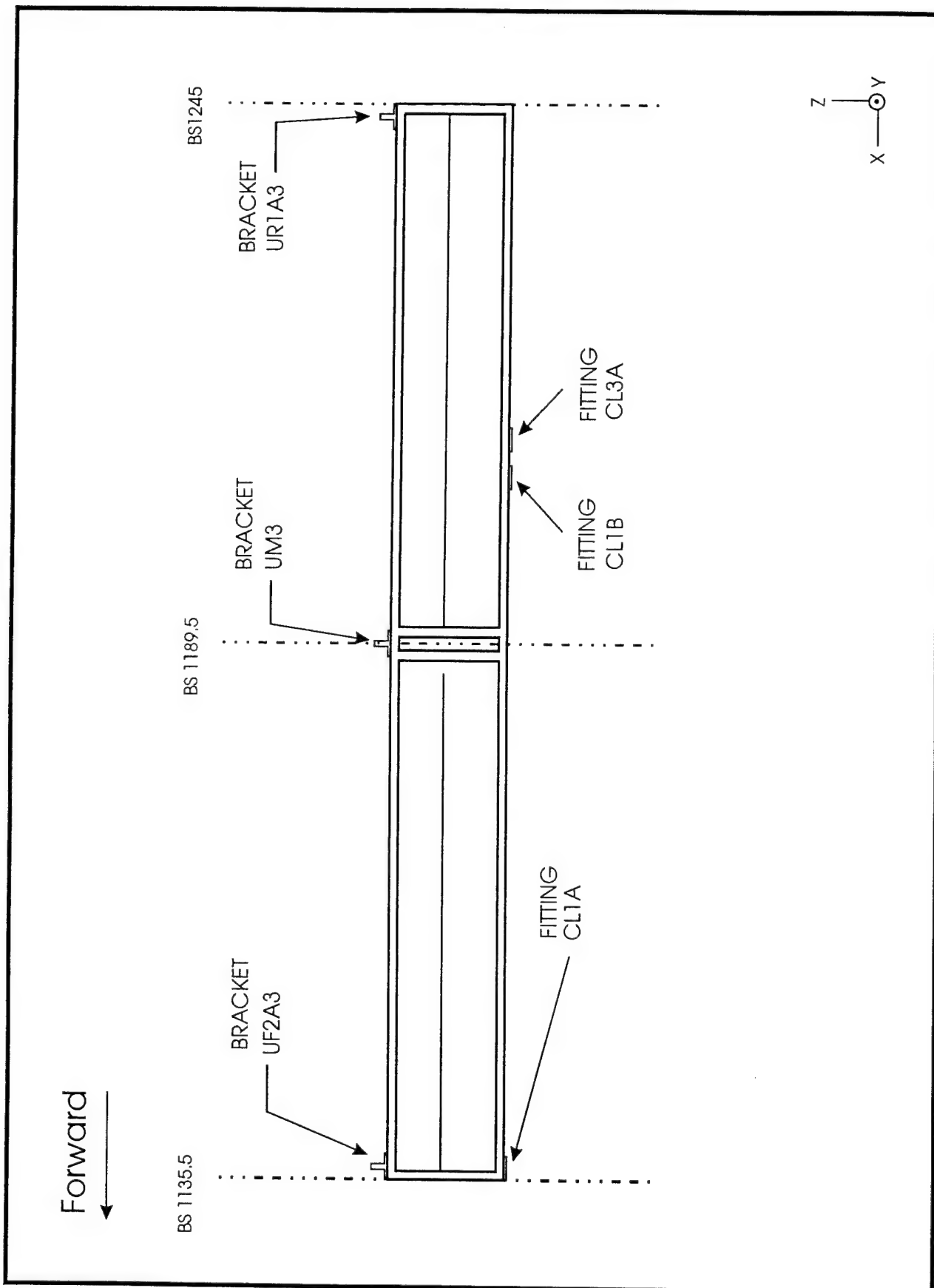


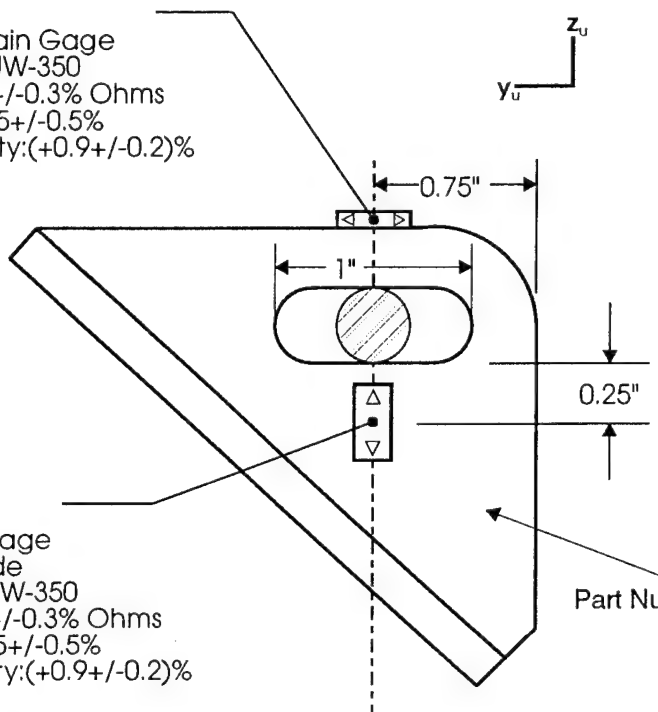
FIGURE 9. C&D OVERHEAD STOWAGE BIN

### A. Strain Gage Location

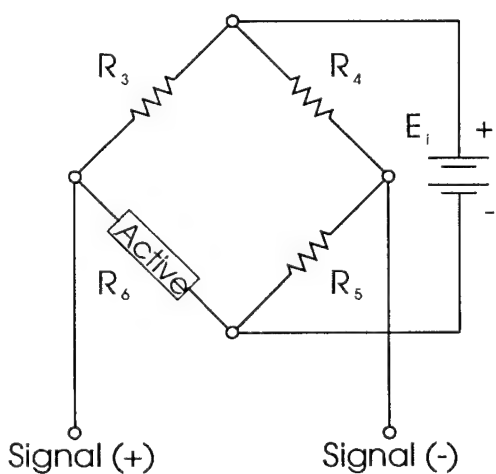
Bending Bridge  
 Quarter-Bridge Strain Gage  
 Type: CEA-13-062UW-350  
 Resistance:  $350.0 \pm 0.3\%$  Ohms  
 Gage Factor:  $2.165 \pm 0.5\%$   
 Transverse Sensitivity:  $(+0.9 \pm 0.2)\%$

Axial Bridge  
 Full-Bridge Strain Gage  
 Two Sensors per Side  
 Type: CEA-13-062UW-350  
 Resistance:  $350.0 \pm 0.3\%$  Ohms  
 Gage Factor:  $2.165 \pm 0.5\%$   
 Transverse Sensitivity:  $(+0.9 \pm 0.2)\%$

Part Number: 3351080



### B. Quarter-Bridge Diagram (Bending)



### C. Full-Bridge Diagram (Axial)

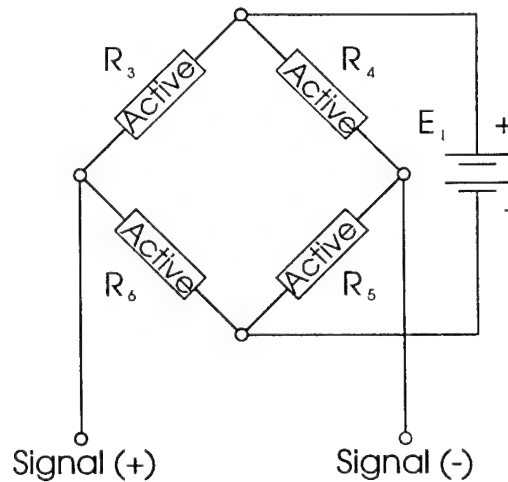
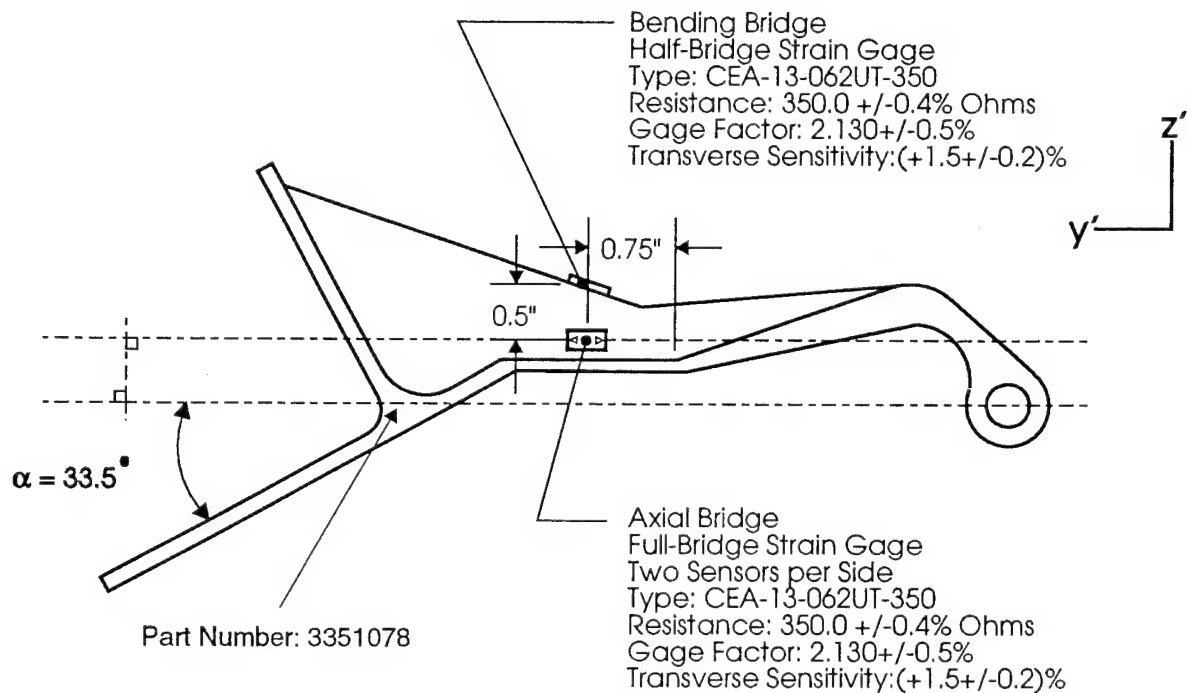
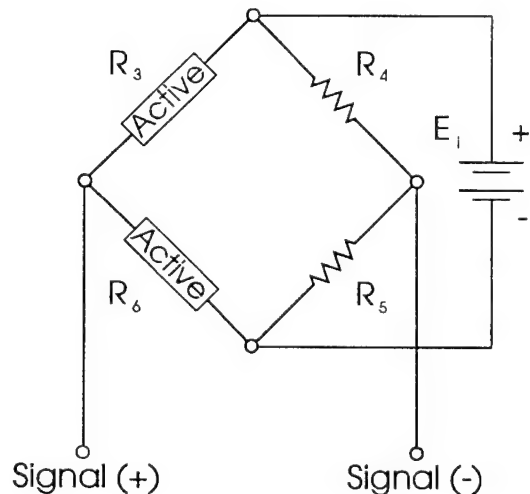


FIGURE 10. C&D UPPER BRACKETS: SENSOR LOCATIONS

### A. Strain Gage Location



### B. Half-Bridge Diagram (Bending)



### C. Full-Bridge Diagram (Axial)

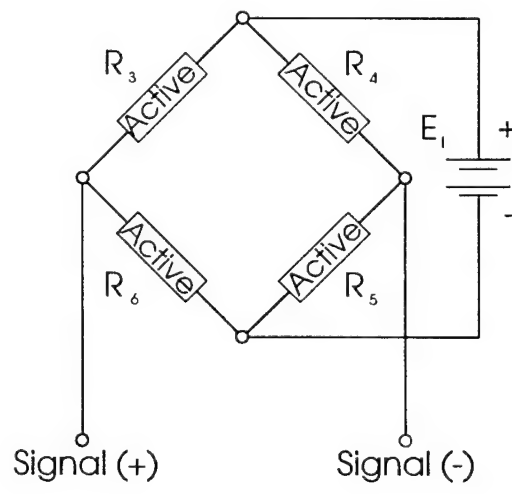


FIGURE 11. C&D LOWER FITTINGS: SENSOR LOCATIONS

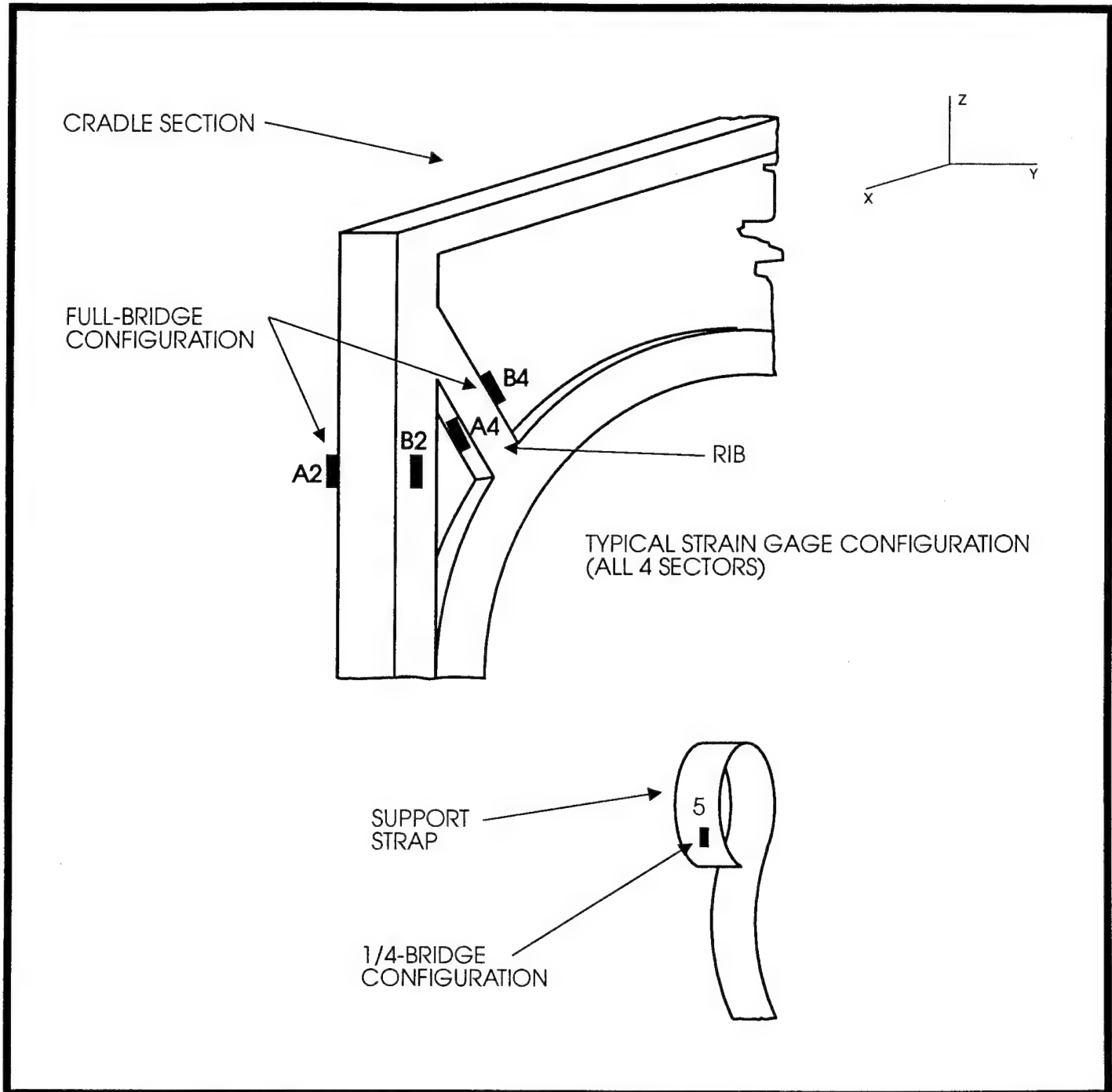


FIGURE 12. AUXILIARY FUEL TANK CRADLE: INSTRUMENTATION LOCATIONS

### TEST DUMMIES.

There were two instrumented dummies located at BS 1180, seats 8 and 11 (figure 3), each of which contained one pelvic load cell and one pelvic accelerometer. These test dummies were 50th percentile, Hybrid II anthropomorphic dummies. These instruments recorded the lower lumbar load and acceleration during the impact. Load cell data were recorded on channels 217 and 218, and accelerometer data were recorded on channels 425 and 428. The pelvic load cell sensitivity was 8.43 mv at 5000 lbs capacity, with 10 vdc applied excitation, or 577 lbs/mv.

### PLATFORM LOAD CELLS.

There were three rows of four load cells under the impact platform. A hydraulic jack was located on the top of each load cell, and all were activated at the same time with a central pump. As the platform was raised off the ground, pressure was put on the load cells. The tare was zeroed by the computer system, and the platform was ready for the impact. Each load cell capacity was 0-50000 lbs, with a full-scale output of 3 mv at 10 vdc excitation. The load cells were recorded individually on channels 219 - 221, 223-230 and 431. The platform load cell data were used to verify the impact loads and determine their distribution. The platform load cells measured the reactive forces generated during the drop of the test section.

### CAMERAS.

Twelve high-speed cameras were used to record the test; see figure 13 for camera locations. Camera 1 was operated at a nominal speed of 1000 frames/second while the other 11 were operated at a nominal speed of 500 frames/second. Actual film speeds are given in the Data Analysis section of this report.

Cameras 1 and 2 provided a front view of the auxiliary fuel tank and an overall view, respectively. Camera 3 focused on the Boeing bin and camera 4 showed a front quarter view from the left side. Camera 5 showed a lower view of the right side of the fuselage. Camera 6 was an aft quarter view from the right side while camera 7 was an aft overall view. Camera 8 focused on the C&D bin from a forward left view. Camera 9 showed an aft view of the auxiliary fuel tank.

The remaining three cameras were mounted on the fuselage. Camera 10 provided a close-up view of the forward Boeing bin support links. Camera 11 showed a view of the fuselage floor along the center aisle. Camera 12 provided a close-up view of the center upper bracket of the C&D bin.

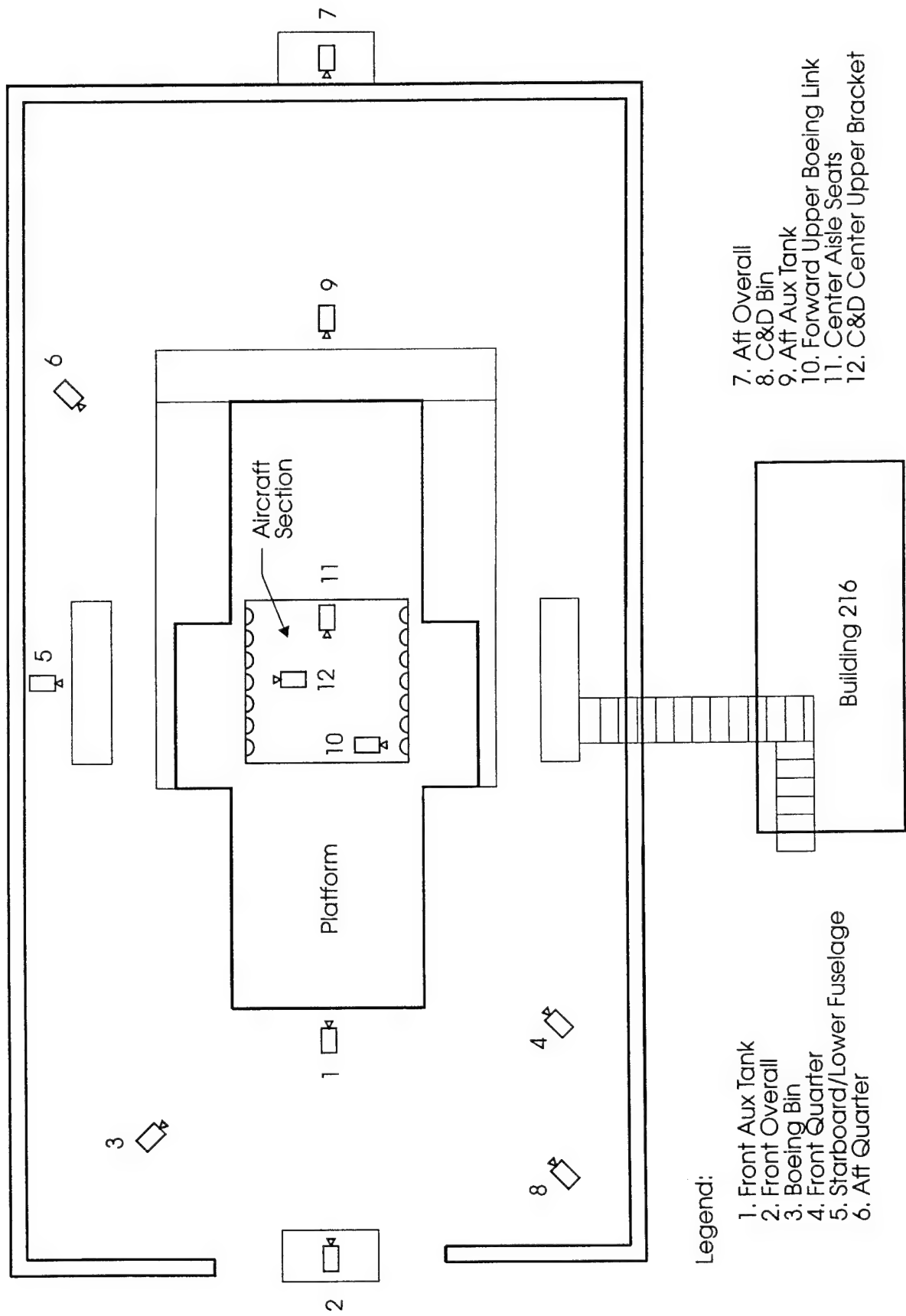


FIGURE 13. CAMERA LOCATIONS

## DATA ACQUISITION SYSTEM

### DATA ACQUISITION SYSTEM.

The system NEFF490 is a high-speed data acquisition system which sampled all 92 channels at 10,000 samples per second per channel. All data for each channel was stored in onboard memory (256K bytes) during the test. Data channels were prefiltered at 1000 Hz.

Each channel has a differential input amplifier with full scale inputs from 5 to 10 volts dc and a cutoff frequency of 1000 hertz. The analog to digital converter was a 12 bit converter with an accuracy of 0.1% of programmable full scale. The system supplies programmable bridge excitation voltages for all the instrumentation. Quasi-real-time Monitor Mode was used to display all of the systems channel data on the monitor screen at the same time.

Test data were transferred to an IBM compatible machine by an IEEE 488 interface for further analysis.

Before each test, the system used a program-initiated bridge auto-balance on all inputs to compensate for any variation in the zero state of the instruments. A shunt-resistance calibration was used to assure system reliability. This was accomplished by putting a known value of a precision resistor across the transducer and measuring the unbalance in engineering units. The data acquisition system software controlled all phases of the calibration process, including balance millivolt outputs, measuring sensitivity, shunt calibrations, and conversion coefficients for calculating engineering units. Calibration data are stored in the database for use in subsequent acquisition sessions. Table 5 shows all of the aforementioned pretest calibration data. For the auxiliary fuel tank readings (channels 101 to 112), low-level outputs from the strain gage bridges (due to the inability to put an adequately large vertical load on the tank) necessitated using the number "1" for the various calibration coefficients.

Due to the geometry of the C&D attachments, it was necessary to use both axial and bending strain gages to determine the loads. Therefore, a number "1" had to be used because more than one shunt calibration value had to be used for these channels (Ch 205-216). Number "1" means that the data collected was received in millivolts.

TABLE 5. DATA ACQUISITION SYSTEM CONFIGURATION AND CALIBRATION

CHANNEL NUMBER	FULL SCALE VALUE (MV)	SHUNT CALIBRATION READINGS	ENGINEERING UNIT CONVERSION	BALANCE OUTPUT (MV)	MEASURED SENSITIVITY
101	20	1 EU	-	0.000	10.69 MV/EU
102	20	1 EU	-	0.000	10.64 MV/EU
103	20	1 EU	-	-20.000	7.35 MV/EU
104	20	1 EU	-	0.000	10.69 MV/EU
105	20	1 EU	-	0.000	10.67 MV/EU
106	20	1 EU	-	0.000	10.69 MV/EU
107	20	1 EU	-	0.000	10.65 MV/EU
108	20	1 EU	-	0.000	10.66 MV/EU
109	20	1 EU	-	0.010	10.68 MV/EU
110	20	1 EU	-	0.000	10.66 MV/EU
111	20	1 EU	-	0.000	10.66 MV/EU
112	20	1 EU	-	0.000	10.66 MV/EU
113	40	475.67 LBS	LBS=-142.02+45.11*MV	3.027	0.0222 MV/LBS
114	40	410.85 LBS	LBS=-25.06+38.88*MV	0.566	0.0257 MV/LBS
115	40	601.83 LBS	LBS=-388.19+57.03*MV	6.660	0.0175 MV/LBS
201	40	474.83 LBS	LBS=-461.82+45.02*MV	10.332	0.0222 MV/LBS
202	40	605.52 LBS	LBS=-1173.40+57.53*MV	20.371	0.0174 MV/LBS
203	40	615.43 LBS	LBS=-551.28+58.44*MV	9.434	0.0171 MV/LBS
204	40	461.76 LBS	LBS=-522.37+43.77*MV	12.285	0.0228 MV/LBS
205	40	1 EU	-	0.000	-10.59 MV/LBS
206	10	1 EU	-	0.000	10.00 MV/LBS
207	20	1 EU	-	0.068	-10.59 MV/LBS
208	20	1 EU	-	0.000	10.55 MV/LBS
209	80	1 EU	-	0.000	-10.57 MV/LBS
210	10	1 EU	-	0.000	10.00 MV/LBS
211	20	1 EU	-	0.000	10.55 MV/LBS
212	80	1 EU	-	0.000	10.69 MV/LBS
213	20	1 EU	-	0.000	10.58 MV/LBS
214	80	1 EU	-	0.000	10.68 MV/LBS
215	20	1 EU	-	0.000	10.55 MV/LBS
216	80	1 EU	-	0.000	10.68 MV/LBS
217	10	5932.65 LBS	LBS=0.00+593.55*MV	0.005	0.0017 MV/LBS
218	10	5983.78 LBS	LBS=-10.54+599.73*MV	0.005	0.0017 MV/LBS
219	20	17799.52 LBS	LBS=1.64+1679.11*MV	0.000	0.0006 MV/LBS
220	20	17656.65 LBS	LBS=32.53+1665.63*MV	0.000	0.0006 MV/LBS
221	20	18107.14 LBS	LBS=3.33+1707.34*MV	0.000	0.0006 MV/LBS
222	20	NOT CONNECTED	-	-	-
223	20	17519.53 LBS	LBS=-53.72+1666.82*MV	0.000	0.0006 MV/LBS
224	20	17960.62 LBS	LBS=-17.90+1666.52*MV	0.010	0.0006 MV/LBS
225	20	17576.54 LBS	LBS=34.23+1669.30*MV	0.000	0.0006 MV/LBS
226	20	18032.23 LBS	LBS=3.26+1667.72*MV	0.000	0.0006 MV/LBS
227	20	17639.97 LBS	LBS=4.88+1666.36*MV	0.000	0.0006 MV/LBS
228	20	17600.92 LBS	LBS=6.51+1666.05*MV	0.000	0.0006 MV/LBS
229	20	17034.50 LBS	LBS=0.00+1664.44*MV	0.000	0.0006 MV/LBS
230	20	17649.00 LBS	LBS=22.79+1667.21*MV	0.000	0.0006 MV/LBS
301	40	73.77 G'S	G'S=0.48+4.75*MV	0.000	0.2106 MV/G'S
302	40	81.49 G'S	G'S=0.00+5.21*MV	0.000	0.1916 MV/G'S
303	40	81.56 G'S	G'S=-0.17+5.16*MV	0.000	0.1933 MV/G'S
304	40	84.58 G'S	G'S=-0.41+4.96*MV	0.000	0.2012 MV/G'S

TABLE 5 . DATA ACQUISITION SYSTEM CONFIGURATION AND CALIBRATION (CONTINUED)

CHANNEL NUMBER	FULL SCALE VALUE (MV)	SHUNT CALIBRATION READINGS	ENGINEERING UNIT CONVERSION	BALANCE OUTPUT (MV)	MEASURED SENSITIVITY
305	40	84.09 G'S	G'S=-0.01+5.38*MV	0.000	0.1857 MV/G'S
306	40	70.99 G'S	G'S=-0.64+4.54*MV	0.000	0.2196 MV/G'S
307	40	78.72 G'S	G'S=-0.47+5.08*MV	0.000	0.1968 MV/G'S
308	40	74.90 G'S	G'S=0.18+4.80*MV	0.000	0.2083 MV/G'S
309	40	73.02 G'S	G'S=-0.46+4.67*MV	0.000	0.2144 MV/G'S
310	40	71.97 G'S	G'S=-0.31+4.74*MV	0.000	0.2144 MV/G'S
311	40	70.53 G'S	G'S=-1.14+4.43*MV	0.000	0.2318 MV/G'S
312	40	97.87 G'S	G'S=0.04+5.11*MV	0.000	0.1952 MV/G'S
313	40	93.14 G'S	G'S=-0.18+5.07*MV	0.000	0.1971 MV/G'S
314	40	93.83 G'S	G'S=-0.65+5.99*MV	0.000	0.1672 MV/G'S
315	40	78.16 G'S	G'S=-0.06+4.74*MV	0.059	0.2114 MV/G'S
401	40	84.50 G'S	G'S=-0.49+5.10*MV	0.000	0.1965 MV/G'S
402	40	104.32 G'S	G'S=-0.45+5.02*MV	0.059	0.1993 MV/G'S
403	40	89.98 G'S	G'S=0.04+5.12*MV	0.020	0.1955 MV/G'S
404	40	101.77 G'S	G'S=-0.24+5.24*MV	0.000	0.1892 MV/G'S
405	40	80.57 G'S	G'S=-1.34+4.85*MV	0.000	0.2034 MV/G'S
406	40	70.90 G'S	G'S=-0.12+4.62*MV	0.000	0.2154 MV/G'S
407	40	77.80 G'S	G'S=-0.56+5.11*MV	0.000	0.1951 MV/G'S
408	40	88.11 G'S	G'S=-0.26+5.04*MV	0.000	0.1993 MV/G'S
409	40	91.32 G'S	G'S=0.07+6.16*MV	0.000	0.1632 MV/G'S
410	40	102.60 G'S	G'S=-0.06+5.13*MV	0.039	0.1961 MV/G'S
411	40	73.72 G'S	G'S=-0.12+4.61*MV	0.000	0.2191 MV/G'S
412	40	73.17 G'S	G'S=-0.41+4.80*MV	0.000	0.2119 MV/G'S
413	10240	NONE	INCH=-20.00+0.0044*MV	4465.000	-
414	10240	NONE	INCH=-20.00+0.0044*MV	4335.000	-
415	40	70.18 G'S	G'S=-0.23+4.25*MV	0.000	0.2356 MV/G'S
416	40	82.49 G'S	G'S=-1.00+5.00*MV	0.000	0.2013 MV/G'S
417	40	64.72 G'S	G'S=0.20+5.00*MV	0.020	0.2004 MV/G'S
418	40	63.16 G'S	G'S=-0.77+4.48*MV	0.215	0.2245 MV/G'S
419	40	81.49 G'S	G'S=0.19+4.86*MV	0.000	0.2155 MV/G'S
420	40	89.84 G'S	G'S=-0.24+5.08*MV	0.000	0.1970 MV/G'S
421	40	89.55 G'S	G'S=-0.10+5.12*MV	0.000	0.1932 MV/G'S
422	40	64.56 G'S	G'S=-0.42+5.03*MV	0.000	0.1978 MV/G'S
423	40	74.02 G'S	G'S=-1.02+6.23*MV	0.000	0.1598 MV/G'S
424	40	78.62 G'S	G'S=-0.55+5.03*MV	0.000	0.1978 MV/G'S
425	40	70.08 G'S	G'S=-0.04+4.49*MV	0.000	0.2217 MV/G'S
426	40	76.69 G'S	G'S=-0.14+5.12*MV	0.000	0.1941 MV/G'S
427	5120	NONE	SEC=0.00+1.00*MV	3407.500	-
428	40	67.50 LBS	LBS=-0.13+4.42*MV	0.000	0.2252 MV/LBS
429	10240	NONE	INCH=-10.00+.0021*MV	4720.000	-
430	10240	NONE	INCH=-10.00+.0021*MV	4810.000	-
431	20	18012.70 LBS	LBS=-115.33-1663.36*MV	0.000	-0.0006 MV/LBS

## WORK STATION.

The work stations used for data reduction were two IBM compatible NCR System 3230, with a 486 microprocessor chip having a clock speed of 33Mhz. Its hard disk capacity was 245 megabytes(MB), and its random access memory (RAM) was 4 MB. The system had a math coprocessor, one parallel port, two serial ports, a 3.5" floppy disk drive, and a 14" monitor. This work station was configured to run the NEFF 490 System software and to import data from the signal conditioners. DADISP software was used for data analyses.

## OVERHEAD STOWAGE BIN CALIBRATIONS

A total of four calibration tests were conducted on the overhead stowage bins. The objective of these tests was to verify and validate the output of the strain gages. Two calibrations were performed on each Boeing and C&D bin. These stowage compartments were installed onboard the aircraft prior to the calibrations. This same installation was used for the vertical drop test. Various strain gages configured as either quarter, half, or full Wheatstone bridges were bonded to the attachments in order to measure axial and bending load information. More information on the gages, their configuration, sensitivity coefficients, and full-scale values may be found in reference 7. All gages, nineteen total, were connected to the NEFF 490 data acquisition system.

The loads generated on these attachments were applied by means of ballast weight (bags of metal pellets). The weight of each bag was measured and recorded prior to this initial calibration phase.

## CALIBRATION PROCEDURES.

Two different types of overhead bins were subjected to similar calibration procedures. The following subsections describe, in some detail, the procedures used.

BOEING BIN. The objective of the first calibration was to find the reacting forces on the links when the center compartment of the bin was loaded and to determine static equilibrium utilizing the strain gages' output. Then, a second calibration was conducted to determine the influence of the small end compartments when loaded on the center compartment links. Figure 14 illustrates the basic design of the Boeing bin and applied load distribution used for these calibrations.

Calibration 1 - Before conducting the first bin calibration, the angle of each link was measured with respect to the top surface of the bin and the aircraft lateral axis (figure 15). Measured angles are recorded in tables 7 through 12. These

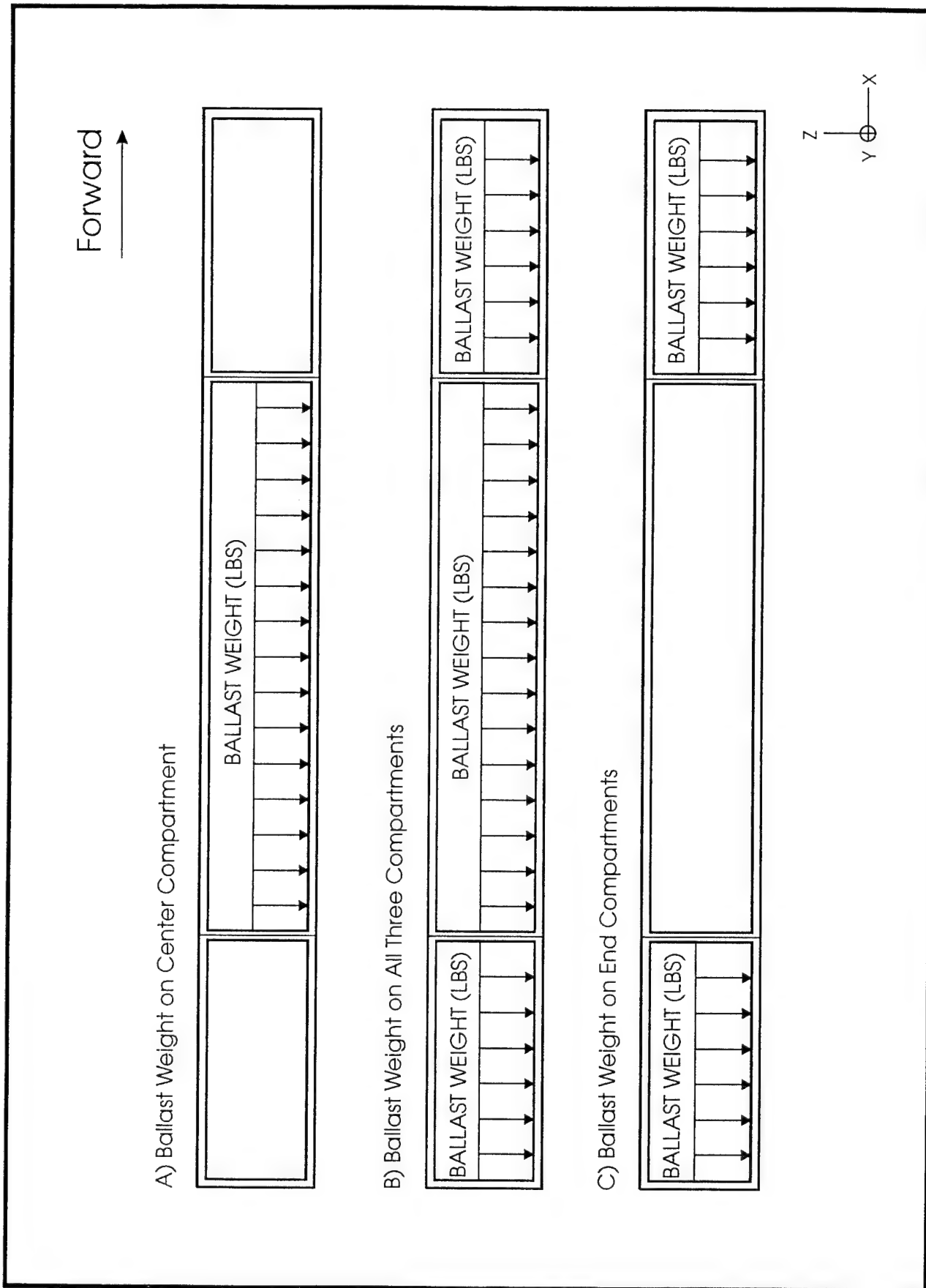


FIGURE 14. BOEING OVERHEAD STOWAGE BIN: LOADING DISTRIBUTION

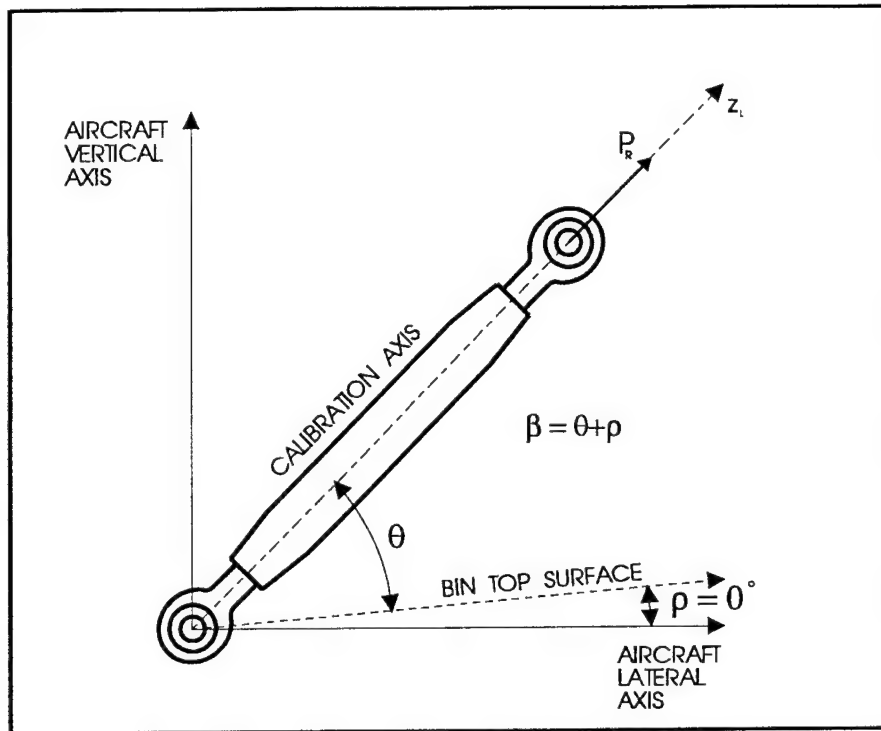


FIGURE 15. BOEING LINK INSTALLATION ANGLE

angles were needed for the verification calculations during post test analysis. After measuring the angles, the bin was incrementally loaded in the vertical Z-direction to a maximum force of 621 pounds using ballast weights. The link angles, when the bin was loaded, were recorded to be the same as in the pretest measurement. The center compartment was loaded first, as illustrated in figure 14A, to a maximum force of 414 pounds. After that, 50 pounds were added to each end compartment until reaching a total of 621 pounds (figure 14B). Data were collected at 0, 207, 311, 414, 517, 621, and again at 0 lbs.

Calibration 2 - Once the link installation angles were recorded, the end bin compartments were loaded in approximately 100-lb increments to a maximum weight of 406 pounds (203 pounds on the forward small end bin and 203 pounds on the aft small end bin, figure 14C). Data were collected at 0, 101, 202, 304, 406, and again at 0 lbs.

C&D BIN . Two calibrations were done on the C&D stowage bin when it was statically loaded to find the reaction forces of the bin attachments and to determine static equilibrium.

Before the calibrations were done, the exact location of the bolt, in the one-inch slot of the upper bracket, was determined (figure 17). In addition, the installation angles were measured. These measurements were repeated after each weight increment.

Previous attachments calibration (reference 7) indicated that the sensitivity coefficients of the bending strain gages bonded on the upper brackets were dependent on the location of the bolt in the slot (figure 16). At zero load, the forward bracket bolt was centered in the slot (location 4), and the middle and rear brackets bolts were at the end of the slot (location 7). Bolt location identifiers are presented in figure 17 and the C&D upper bracket's installation angles are shown in figure 18.

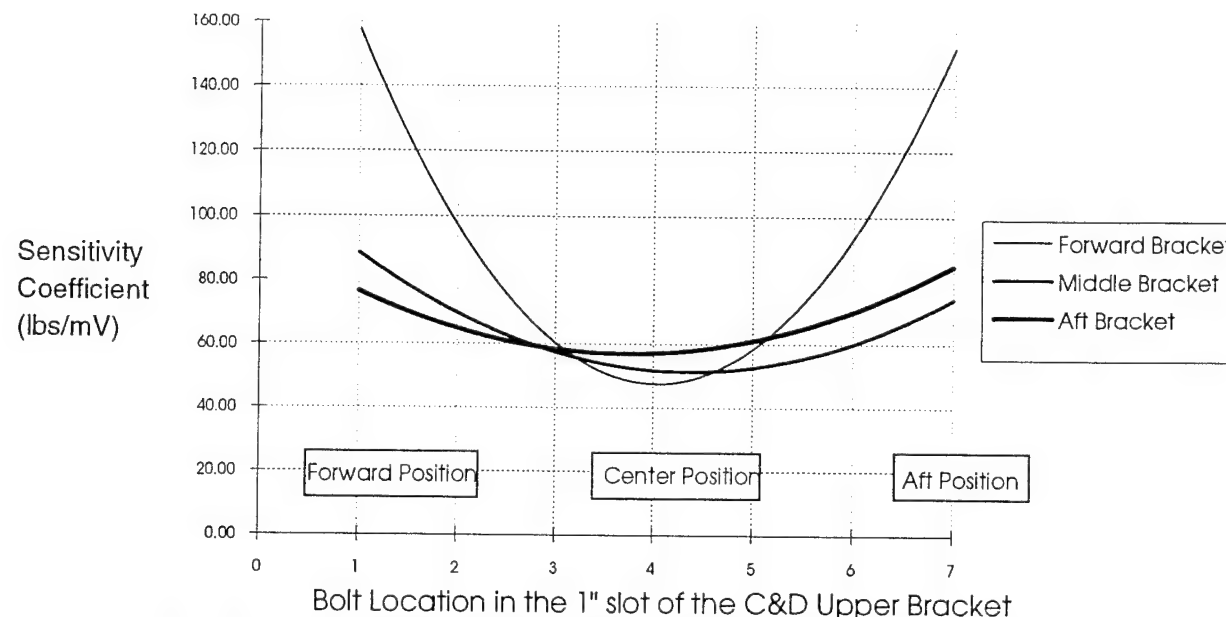


FIGURE 16. SENSITIVITY COEFFICIENT VS BOLT LOCATION

After recording the bolt locations and installation angles, the compartments were loaded vertically to a maximum load of 1017 lbs for the first calibration and 1018 lbs for the second calibration. Lead bags, added in 200 lbs increments, were placed as close to the bin floor center as possible and spread from the center to the front and back walls (figure 19). At maximum stowage compartment loading, the bolt locations and the installation angles were measured again. The same bolt locations were recorded during both calibrations; the forward bracket bolt was recorded at location 2.3, the middle bracket bolt was at location 6.6, and the rear bracket bolt at location 2.5.

#### CALIBRATION ANALYSIS AND RESULTS.

After the calibration data were collected, the expected loading on the strain gaged attachments was verified using static equilibrium (equations 1, 2, and 3)

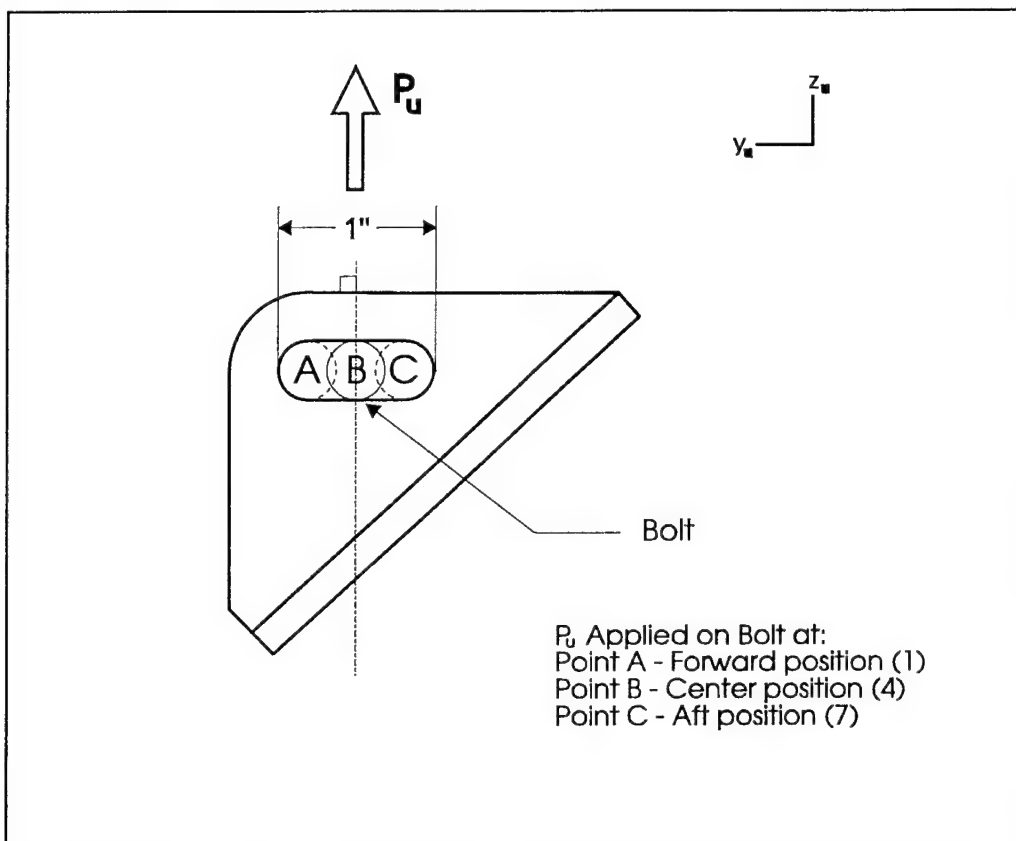


FIGURE 17 . BOLT LOCATION IDENTIFIERS (UPPER BRACKET)

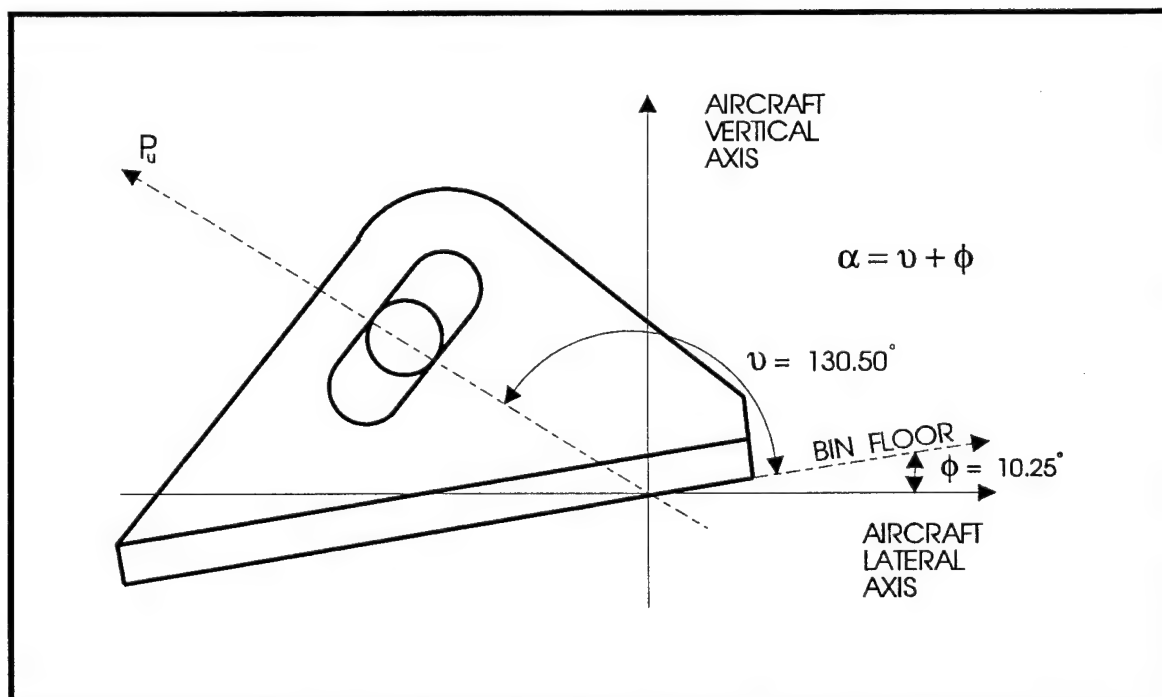


FIGURE 18. UPPER BRACKET INSTALLATION ANGLES

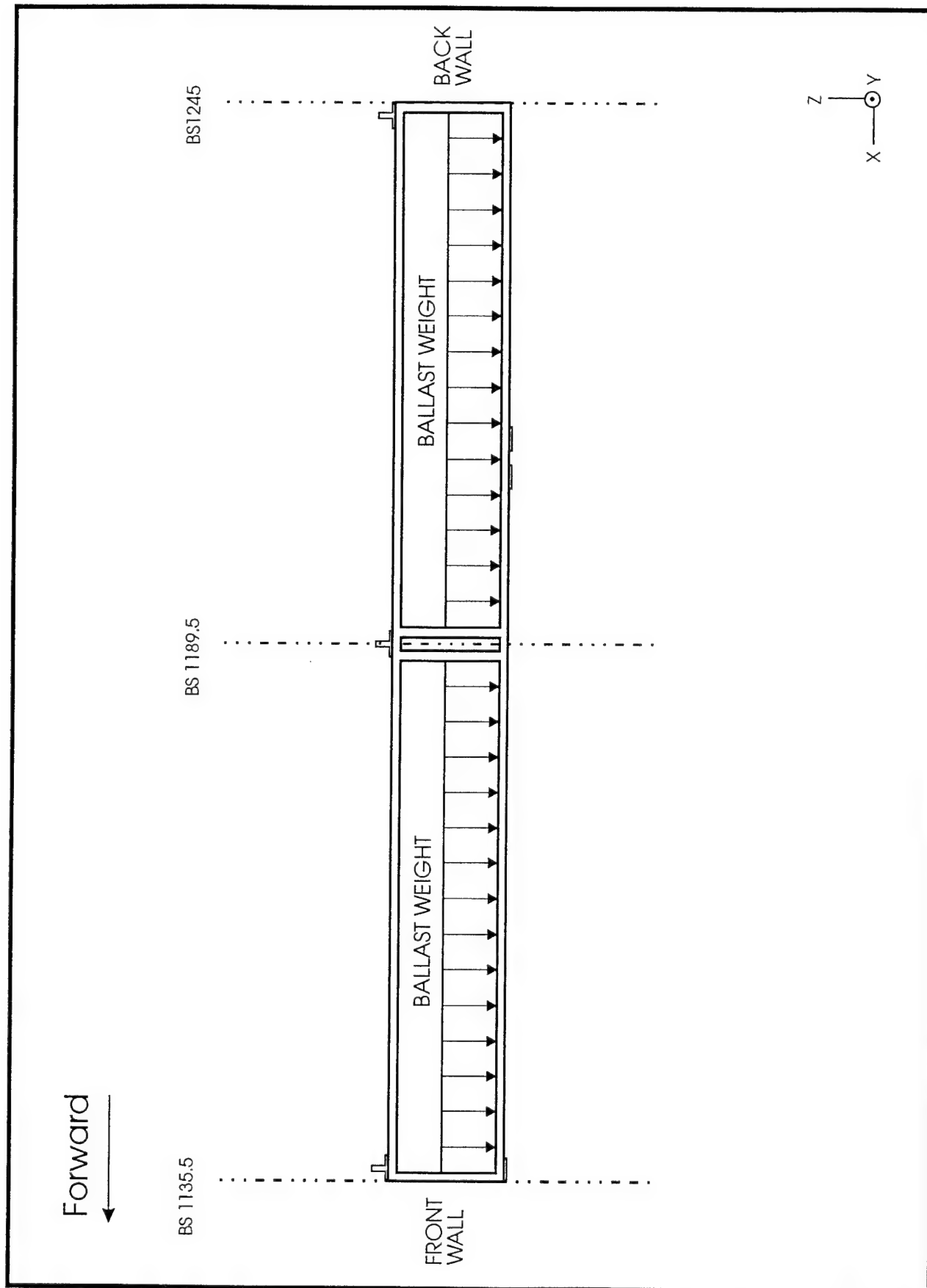


FIGURE 19. C&D OVERHEAD STOWAGE BIN: LOADING DISTRIBUTION

TABLE 6. SENSITIVITY COEFFICIENTS OF THE BOEING LINKS

ATTACHMENT IDENTIFICATION	CHANNEL NUMBER	SENSITIVITY COEFFICIENT "K" (lbs/mV)	OFFSET (lbs)
7B	113	45.13	-2.96
8B	114	38.98	3.64
17B	115	57.10	4.54
18B	201	45.05	5.42
25B	202	57.45	0.76
28B	203	58.39	-2.39
31B	204	43.81	-1.42

$$\sum P_x = 0 \quad (1)$$

$$\sum P_y = 0 \quad (2)$$

$$(\sum P_z) - W_b = 0 \quad (3)$$

where,

$P_x$  = The X-component of the resultant force on the attachment (lbs)

$P_y$  = The Y-component of the resultant force on the attachment (lbs)

$P_z$  = The Z-component of the resultant force on the attachment (lbs)

$W_b$  = Ballast weight (lbs)

BOEING STOWAGE BIN STATIC LOAD COMPUTATIONS. The resultant force of each link was calculated by multiplying the strain gages' electrical output by the corresponding sensitivity coefficient (see equation 4 and table 6). Then, the magnitudes of the X-, Y-, and Z-components of the resultant force were calculated using equations 5, 6, and 7.

$$P_R = e_0 K \quad (4)$$

$$P_x = 0 \quad (5)$$

$$P_y = P_R \cos(\beta) \quad (6)$$

$$P_z = P_R \sin(\beta) \quad (7)$$

where,

$P_R$  = Resultant force acting on the link (lbs)

$e_0$  = The electrical output of the strain gages (mV)

$K$  = The sensitivity coefficient (calibration factor, lbs/mV)  
 $\beta$  = The angle between the Y-axis (aircraft lateral axis) and calibration axis.

After all the resultant force components were calculated for all the links the static equilibrium of the bin was verified. Tables 7 through 12 list the results of these calculations for each loading case and show that the measured load is close to the applied load. Tables 7 through 9 and table 12 show that force equilibrium was achieved.

The effects of loading the end bins are shown in tables 10 and 11. These two tables show a force unbalance in the Z-direction due to the 100 pounds which were placed in the end bin compartments. These compartments had links that were not instrumented. Therefore, the measured reaction forces do not balance with the applied weight.

The summation of forces in the Y-direction shows some small unbalanced reactions. These may be attributed to the measured theta ( $\theta$ ) angles. These angles were only measured to the nearest degree, and a fraction of a degree will affect the calculations.

The influence of each link on overall bin loading was also determined. The influence coefficient,  $m$ , was calculated by determining the slope of the line representing ballast weight versus strain gage output. Equation 8 was used to determine the coefficients.

$$m = \frac{A_2 - A_1}{W_2 - W_1} \quad (8)$$

where,

$A$  = strain gage output value (mV)  
 $W$  = ballast weight (lbs)

Table 13 shows the vertical and the longitudinal influence coefficients of the links for the Boeing bins. Postcalibration inspection revealed that the bin was not damaged after applying the 621 pounds.

TABLE 7. BOEING BIN STATIC CALIBRATION: ANALYSIS 1

ATTACHMENT ID	SENSOR READING @ 0 LBS (mV)	SENSOR READING @ 207 LBS (mV)	SENSOR READING DELTA (mV)	CALIBRATION FACTOR (Reference 7)	RESULTANT LOAD (LBS)	BETA ANGLE (DEGREES)	VERTICAL (Z) LOAD COMPONENT LBS	LATERAL (Y) LOAD COMPONENT LBS
7B (CH113)	11.065	11.172	0.117	45.13	5.28	145.00	3.03	-4.32
8B (CH114)	0.48828	0.76179	0.27349	38.98	10.66	150.00	5.33	-9.23
17B (CH115)	5.5859	6.5039	0.918	45.05	41.36	126.50	33.25	-24.59
18B (CH201)	9.4141	10.215	0.8009	58.39	46.76	134.00	33.65	-32.48
25B (CH 202)	19.375	20.605	1.23	57.1	70.23	67.10	64.70	27.33
28B (CH203)	8.125	9.3945	1.2695	57.45	72.93	67.50	67.38	27.92
31B (CH204)	12.168	12.168	0	43.81	0.00	8.00	0.00	0.00
						<b>SUM</b>	<b>207.34</b>	<b>-15.37</b>

Tension is positive

TABLE 8. BOEING BIN STATIC CALIBRATION: ANALYSIS 2

ATTACHMENT ID	SENSOR READING @ 0 LBS (mV)	SENSOR READING @ 311 LBS (mV)	SENSOR READING DELTA (mV)	CALIBRATION FACTOR (Reference 7)	RESULTANT LOAD (LBS)	BETA ANGLE (DEGREES)	VERTICAL (Z) LOAD COMPONENT LBS	LATERAL (Y) LOAD COMPONENT LBS
7B (CH113)	11.065	11.211	0.156	45.13	7.04	145.00	4.04	-5.77
8B (CH114)	0.48828	0.683594	0.195314	38.98	7.61	150.00	3.81	-6.59
17B (CH115)	5.5859	7.1875	1.6016	45.05	72.15	126.50	58.01	-42.91
18B (CH201)	9.4141	10.586	1.1719	58.39	68.43	134.00	49.23	-47.53
25B (CH 202)	19.375	21.289	1.914	57.1	109.29	67.10	100.67	42.54
28B (CH203)	8.125	9.9414	1.8164	57.45	104.35	67.50	96.41	39.94
31B (CH204)	12.168	12.168	0	43.81	0.00	8.00	0.00	0.00
						<b>SUM</b>	<b>312.17</b>	<b>-20.32</b>

Tension is positive

TABLE 9. BOEING BIN STATIC CALIBRATION: ANALYSIS 3

ATTACHMENT ID	SENSOR READING @ 0 LBS (mV)	SENSOR READING @ 414 LBS (mV)	SENSOR READING DELTA (mV)	CALIBRATION FACTOR (Reference 7)	RESULTANT LOAD (LBS)	BETA ANGLE (DEGREES)	VERTICAL (Z) LOAD COMPONENT LBS	LATERAL (Y) LOAD COMPONENT LBS
7B (CH113)	11.055	11.23	0.175	45.13	7.90	145.00	4.53	-6.47
8B (CH114)	0.48828	0.820313	0.332033	38.98	12.94	150.00	6.47	-11.21
17B (CH115)	5.5859	7.539063	1.953163	45.05	87.99	126.50	70.74	-52.33
18B (CH201)	9.4141	10.977	1.5629	58.39	91.26	134.00	65.66	-63.38
25B (CH202)	19.375	21.973	2.598	57.1	148.35	67.10	136.65	57.74
28B (CH203)	8.125	10.723	2.598	57.45	149.26	67.50	137.89	57.13
31B (CH204)	12.168	12.168	0	43.81	0.00	8.00	-	-
							<b>SUM</b>	<b>421.94</b>
								<b>-18.52</b>

Tension is positive

TABLE 10. BOEING BIN STATIC CALIBRATION: ANALYSIS 4

ATTACHMENT ID	SENSOR READING @ 0 LBS (mV)	SENSOR READING @ 517 LBS* (mV)	SENSOR READING DELTA (mV)	CALIBRATION FACTOR (Reference 7)	RESULTANT LOAD (LBS)	BETA ANGLE (DEGREES)	VERTICAL (Z) LOAD COMPONENT LBS	LATERAL (Y) LOAD COMPONENT LBS
7B (CH113)	11.055	11.23	0.175	45.13	7.90	145.00	4.53	-6.47
8B (CH114)	0.48828	0.8984	0.41012	38.98	15.99	150.00	8.00	-13.84
17B (CH115)	5.5859	7.6757	2.0898	45.05	94.15	126.50	75.69	-55.99
18B (CH201)	9.4141	11.152	1.7379	58.39	101.48	134.00	73.01	-70.48
25B (CH202)	19.375	22.207	2.832	57.1	161.71	67.10	148.96	62.94
28B (CH203)	8.125	10.879	2.754	57.45	158.22	67.50	146.17	60.56
31B (CH204)	12.168	12.168	0	43.81	0.00	8.00	-	-
							<b>SUM</b>	<b>456.36</b>
								<b>-23.28</b>

\*NOTE: 50 lbs for each end bin

Tension is positive

TABLE 11. BOEING BIN STATIC CALIBRATION: ANALYSIS 5

ATTACHMENT ID	SENSOR READING @ 0 LBS (mV)	SENSOR READING @ 621 LBS* (mV)	SENSOR READING DELTA (mV)	CALIBRATION FACTOR (Reference 7)	RESULTANT LOAD (LBS)	BETA ANGLE (DEGREES)	VERTICAL (Z) LOAD COMPONENT LBS	LATERAL (Y) LOAD COMPONENT LBS
7B (CH113)	11.055	11.113	0.058	45.13	2.62	145.00	1.50	-2.14
8B (CH114)	0.48828	0.87891	0.39063	38.98	15.23	150.00	7.62	-13.19
17B (CH115)	5.5859	7.8906	2.3047	45.05	103.83	126.50	83.47	-61.74
18B (CH201)	9.4141	11.406	1.9919	58.39	116.31	134.00	83.68	-80.78
25B (CH202)	19.375	22.578	3.203	57.1	182.89	67.10	168.47	71.18
28B (CH203)	8.125	11.406	3.281	57.45	188.49	67.50	174.14	72.15
31B (CH204)	12.168	12.168	0	43.81	0.00	8.00	-	-
							<b>SUM</b>	<b>518.88</b>
								<b>-14.52</b>

\*NOTE: 100 lbs in each end bin  
Tension is positive

TABLE 12. BOEING BIN STATIC CALIBRATION: ANALYSIS 6

ATTACHMENT ID	SENSOR READING @ 0 LBS (mV)	SENSOR READING @ 0 LBS (mV)	SENSOR READING DELTA (mV)	CALIBRATION FACTOR (Reference 7)	RESULTANT LOAD (LBS)	BETA ANGLE (DEGREES)	VERTICAL (Z) LOAD COMPONENT LBS	LATERAL (Y) LOAD COMPONENT LBS
7B (CH113)	11.055	11.035	-0.02	45.13	-0.90	145.00	-0.52	0.74
8B (CH114)	0.48828	0.527344	0.039064	38.98	1.52	150.00	0.76	-1.32
17B (CH115)	5.5859	5.605	0.0191	45.05	0.86	126.50	0.69	-0.51
18B (CH201)	9.4141	9.394531	-0.019569	58.39	-1.14	134.00	-0.82	0.79
25B (CH202)	19.375	19.316	-0.059	57.1	-3.37	67.10	-3.10	-1.31
28B (CH203)	8.125	8.203125	0.078125	57.45	4.49	67.50	4.15	1.72
31B (CH204)	12.168	12.168	0	43.81	0.00	8.00	0.00	0.00
							<b>SUM</b>	<b>1.16</b>
								<b>0.11</b>

Tension is positive

TABLE 13. INFLUENCE COEFFICIENTS OF BOEING BIN LINKS

LINK ID	CHANNEL NUMBER	VERTICAL INFLUENCE COEFFICIENT OF CENTER COMPARTMENT 1/m <sub>c</sub> (mV/lb)	VERTICAL INFLUENCE COEFFICIENT OF SMALL END COMPARTMENT 1/m <sub>e</sub> (mV/lb)	LONGITUDINAL INFLUENCE COEFFICIENT 1/m <sub>l</sub> (lbs/lbs)
7B	113	0.0004	-0.00044	0.1149
8B	114	0.00093	-2.5E-5	-0.1728
17B	115	0.00484	0.00224	-0.0900
18B	201	0.00377	0.00241	-0.0919
25B	202	0.00624	0.00303	-0.02218
28B	203	0.00615	0.00399	0.0718
31B	204	0.0000	0.0000	0.7580

C&D STOWAGE BIN STATIC LOAD COMPUTATIONS.

Upper Brackets - The reaction force  $P_u$  (figures 17 and 18) of each upper bracket may be computed from the output of either the axial or the bending strain gages. In this calibration exercise, both gage configurations were used to compute the force  $P_u$  by multiplying the output of the gage by the calculated sensitivity coefficient. The following equations were used to convert the millivolts readings into reaction forces (in pounds),

$$P_u = K_a A \quad (9)$$

or

$$P_u = K_b B \quad (10)$$

where,

$K_a$  = Sensitivity coefficient of the axial gages (lbs/mV).

$A$  = Axial bridge, strain gage reading (mV)

$K_b$  = Sensitivity coefficient of the bending gages (lbs/mV).

$B$  = Bending bridge, strain gage reading (mV)

$K_a$  and  $K_b$  need to be determined for each upper bracket found on the C&D bin. These sensitivity coefficients may be computed from the following equations (reference 7),

a. For the forward upper bracket

$$K_a = -2.31L^2 + 18.56L - 304.21 \quad (11)$$

$$K_b = 1190L^2 - 96.11L + 24164 \quad (12)$$

b. For the middle upper bracket

$$K_a = -2.17L^2 + 15.43L - 367.36 \quad (13)$$

$$K_b = 3.30L^2 - 28.76L + 114.07 \quad (14)$$

c. For the rear upper bracket

$$K_a = -5.28L^2 + 16.01L - 309.93 \quad (15)$$

$$K_b = 2.60L^2 - 19.44L + 93.38 \quad (16)$$

where,

$L$  = location of the bolt in the 1" slot of the C&D upper bracket

After calculating the reacting forces, the forces were translated from the bracket's  $z_u$ -axis to the aircraft primary vertical (Z-axis) and lateral (Y-axis) axes, using the following equations:

Let  $\alpha = v + \phi$  ; (figure 18)

Then,

$$P_{u,vertical} = P_u \sin\alpha \quad (17)$$

$$P_{u,lateral} = P_u \cos\alpha \quad (18)$$

Lower Fittings. The forces acting on the lower fittings were calculated using a combination of axial and bending reactions. This combination was

TABLE 14. SENSITIVITY COEFFICIENTS OF THE C&D LOWER FITTINGS

ATTACHMENT IDENTIFICATION	CHANNEL NUMBER	SPECIAL TEST CONDITION	SENSITIVITY COEFFICIENT K (lbs/mV)	OFFSET (lbs)
CL1A (Axial Gage)	211	Z-Axis Test X-Axis Test	$K_3 = 58.05$ $K_1 = 458.40$	$c_3 = 8.65$ $c_1 = 11.73$
CL1A (Bending Gages)	212	Z-Axis Test X-Axis Test	$K_4 = 14.10$ $n_2 = 0$	$c_4 = 6.34$ -
CL3A (Axial Gage)	213	Z-Axis Test X-Axis Test	$K_3 = 57.32$ $K_1 = 457.14$	$c_3 = 3.32$ $c_1 = 4.96$
CL3A (Bending Gages)	214	Z-Axis Test X-Axis Test	$K_4 = 14.42$ $n_2 = 0$	$c_4 = 1.70$ -
CL1B (Axial Gage)	215	Z-Axis Test X-Axis Test	$K_3 = -58.49$ $K_1 = 434.96$	$c_3 = 8.72$ $c_1 = 13.28$
CL1B (Bending Gages)	216	Z-Axis Test X-Axis Test	$K_4 = -14.56$ $n_2 = 0$	$c_4 = -2.62$ -

necessary because during previous calibrations of these attachments there was crosstalk between these two bridges. Crosstalk is defined as an electrical interaction between the bending and axial bridges. For example, when the attachments were pulled axially, the bending bridge reacted to that load and vice versa. The following equations, in combination with the above table, were used to determine the reacting forces of each fitting .

If  $n_1 = \frac{1}{K_1}$ ,  $n_2 = \frac{1}{K_2}$ ,  $n_3 = \frac{1}{K_3}$ ,  $n_4 = \frac{1}{K_4}$ , (19)

and,  $M_1 = A + \frac{c_1}{K_1} + \frac{c_3}{K_3}$ , (20)

$$M_2 = B + \frac{c_2}{K_2} + \frac{c_4}{K_4}, \quad (21)$$

Then  $P_y = \frac{n_4 M_1 - n_3 M_2}{n_1 n_4 - n_2 n_3}$ , (22)

and,  $P_z = \frac{n_1 M_2 - n_2 M_1}{n_1 n_4 - n_2 n_3}$  (23)

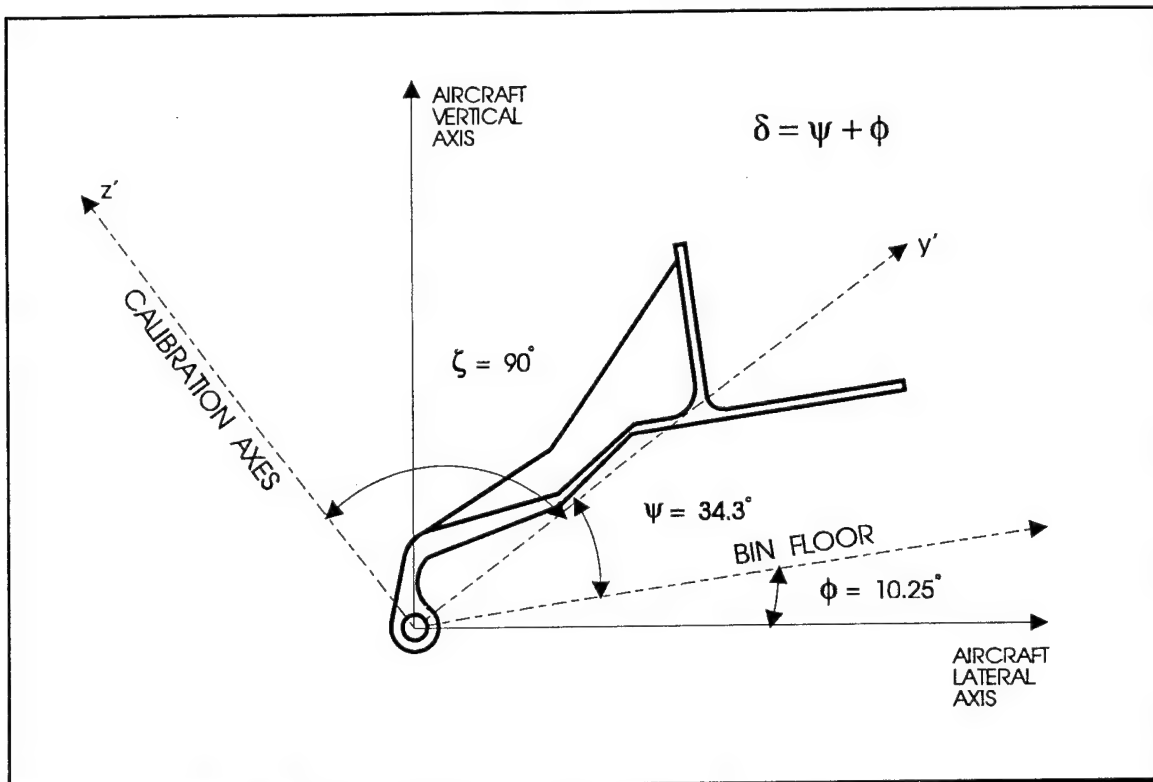


FIGURE 20. LOWER FITTING INSTALLATION ANGLES

where,

$K_i$  = Sensitivity Coefficient (Calibration Factor, lbs/mV); (table 14)

$A$  = Axial strain gage bridge output (mV)

$c_i$  = Offsets from the sensitivity equations (lbs); (table 14)

$B$  = Bending strain gage bridge output (mV)

$P_{y'}$  = Reaction force acting on the  $y'$  axis of the fitting (lbs); (figure 20)

$P_{z'}$  = Reaction force acting on the  $z'$  axis of the fitting (lbs); (figure 20)

After the reaction forces were calculated, each force vector was translated to the aircraft primary axes. Equations 21 through 24 were used for these translations.

$$P_{y',vertical} = P_{y'} \sin\delta \quad (24)$$

$$P_{y',lateral} = P_{y'} \cos\delta \quad (25)$$

$$P_{z',vertical} = P_{z'} \sin\beta \quad (26)$$

$$P_{z',lateral} = P_{z'} \cos\beta \quad (27)$$

where,

$$\delta = \psi + \phi; \text{ (figure 20)}$$

$$\beta = \delta + 90^\circ$$

The next step was to verify force equilibrium using equations 28 and 29, which sum all forces reacting on the brackets and fittings in a specified direction. The sum of the lateral forces should equal zero and the sum of the vertical forces should equal the applied load (W).

$$\sum P_{lateral} = \sum_{i=Location} P_{u,lateral,i} + \sum_{i=Location} P_{y',lateral,i} + \sum_{i=Location} P_{z',lateral,i} = 0 \quad (28)$$

$$\sum P_{vertical} = \sum_{i=Location} P_{u,vertical,i} + \sum_{i=Location} P_{y',vertical,i} + \sum_{i=Location} P_{z',vertical,i} = W \quad (29)$$

where

Location = 1,2, 3 (1= front, 2 = middle, 3 = rear)

The results of these calculations, tables 15 through 18, show that the strain gages were working properly and verified equilibrium.

A slight difference existed between the actual weight and the measured weight when utilizing the output of the axial strain gages of the upper brackets. This difference may be explained by the fact that the axial gages were much less sensitive to the applied load than the bending gages.

The vertical influence coefficients of each C&D attachment were computed from the data recorded during the static calibrations. Table 19 presents the vertical influence coefficients for these attachments during bin loading. The computation of these influence coefficients and the acquisition of the longitudinal ones from the manufacturer were required for the dynamic analysis of the drop test data. The longitudinal influence coefficients are reported in table 19.

TABLE 15. C&D STATIC CALIBRATION: ANALYSIS 1

A. MEASURED DATA					
CHANNEL NUMBER	DESCRIPTION	(a) MEASUREMENT (MV) @ 1017 LBS	(b) MEASUREMENT (MV) @ 0 LBS	(a-b) CORRECTED MEASUREMENT (MV)	
205	FWD UPPER BRACKET, BENDING	3.5160	0.0391	3.4769	
206	FWD UPPER BRACKET, AXIAL	-0.5460	-0.0049	-0.5811	
207	MIDDLE UPPER BRACKET, BENDING	6.4840	0.0391	6.4449	
208	MIDDLE UPPER BRACKET, AXIAL	-0.6390	0.0000	-0.6390	
209	REAR UPPER BRACKET, BENDING	2.5980	0.0000	2.5390	
210	REAR UPPER BRACKET, AXIAL	-0.5130	-0.0049	-0.5081	
211	FWD LOWER FITTING, AXIAL	1.9530	0.0000	1.9530	
212	FWD LOWER FITTING, BENDING	4.5810	-0.0195	4.5705	
213	REAR LOWER FITTING, AXIAL	1.0160	0.0000	1.0160	
214	REAR LOWER FITTING, BENDING	1.7770	-0.0391	1.8161	
215	MIDDLE LOWER FITTING, AXIAL	0.9875	0.0000	0.9875	
216	MIDDLE LOWER FITTING, BENDING	2.3240	-0.0195	2.3435	

B. INSTALLATION ANGLES					
DESCRIPTION	ANGLE	MEASURED ANGLE (DEGREES)	VARIATION ( )	TRANSLATION ANGLE	
UPPER BRACKET	✓	130.50	10.25	140.75	
LOWER FITTING	Ψ	34.30	10.25	44.55	
LOWER FITTING	Ψ + 90	124.30	10.25	134.55	

C. REACTING FORCES/FORCE BALANCE (USING BENDING DATA)					
ATTACHMENT ID	REACTING FORCES ON Y-AXIS (LBS) (Eqn. 22)	REACTING FORCES ON Z-AXIS (LBS) (Eqn. 10 for brackets) (Eqn. 23 for fittings)	VERTICAL COMPONENT (AIRCRAFT AXIS) (LBS) (Eqn. 17 for brackets) (Eqns. 24 & 26 for fittings)	LATERAL COMPONENT (AIRCRAFT AXIS) (LBS) (Eqn. 18 for brackets) (Eqns. 25 & 27 for fittings)	
FWD UPPER BRACKET	-	280.43	183.80	-224.87	
MIDDLE UPPER BRACKET	-	236.08	149.40	-182.79	
REAR UPPER BRACKET	-	154.98	98.08	-119.99	
FWD LOWER FITTING	416.33	70.78	342.50	247.06	
REAR LOWER FITTING	273.48	27.89	211.72	175.34	
MIDDLE LOWER FITTING	82.98	-36.74	32.02	84.91	
<b>SUMMATION</b>	<b>1017.52</b>				
BALLAST WEIGHT		(Equation 29)	1017.00	(Equation 28)	
FORCE RATIO			100.05%		

TABLE 16. C&D STATIC CALIBRATION: ANALYSIS 2

A. MEASURED DATA					
CHANNEL NUMBER	DESCRIPTION	MEASUREMENT (MV) @ 1017 LBS	MEASUREMENT (MV) @ 0 LBS	(a - b) CORRECTED MEASUREMENT (MV)	(a - b) CORRECTED MEASUREMENT (MV)
205	FWD UPPER BRACKET, BENDING	3.5160	0.0391	3.4769	
206	FWD UPPER BRACKET, AXIAL	-0.5860	-0.0449	-0.5811	
207	MIDDLE UPPER BRACKET, BENDING	6.4840	0.0391	6.4449	
208	MIDDLE UPPER BRACKET, AXIAL	-0.6590	0.0000	-0.6590	
209	REAR UPPER BRACKET, BENDING	2.5390	0.0000	2.5390	
210	REAR UPPER BRACKET, AXIAL	-0.5130	-0.0049	-0.5081	
211	FWD LOWER FITTING, AXIAL	1.9530	0.0000	1.9530	
212	FWD LOWER FITTING, BENDING	4.5610	-0.0195	4.5705	
213	REAR LOWER FITTING, AXIAL	1.0160	0.0000	1.0160	
214	REAR LOWER FITTING, BENDING	1.7770	-0.0391	1.8161	
215	MIDDLE LOWER FITTING, AXIAL	0.9375	0.0000	0.9375	
216	MIDDLE LOWER FITTING, BENDING	2.3240	-0.0195	2.3435	

B. INSTALLATION ANGLES					
DESCRIPTION	ANGLE	MEASURED ANGLE (DEGREES)	VARIATION ( )	TRANSLATION ANGLE (DEGREES)	TRANSLATION ANGLE (DEGREES)
UPPER BRACKET	$\checkmark$	130.50	10.25	140.75	
LOWER FITTING	$\Psi$	34.30	10.25	44.55	
LOWER FITTING	$\Psi + 90$	124.30	10.25	134.55	

C. REACTING FORCES / FORCE BALANCE (USING AXIAL DATA)					
ATTACHMENT ID	REACTING FORCES ON Y-AXIS (LBS) (Eqn. 22)	REACTING FORCES ON Z-AXIS (LBS) (Eqn. 9 for brackets) (Eqn. 23 for fittings)	VERTICAL COMPONENT (AIRCRAFT AXIS) (LBS) (Eqn. 17 for brackets) (Eqns. 24 & 26 for fittings)	LATERAL COMPONENT (AIRCRAFT AXIS) (LBS) (Eqn. 18 for brackets) (Eqns. 25 & 27 for fittings)	
FWD UPPER BRACKET	-	159.07	100.67	-123.16	
MIDDLE UPPER BRACKET	-	237.25	150.14	-163.70	
REAR UPPER BRACKET	-	153.92	97.41	-119.18	
FWD LOWER FITTING	416.33	70.78	342.50	247.06	
REAR LOWER FITTING	273.48	27.89	211.72	175.34	
MIDDLE LOWER FITTING	82.98	-36.74	32.02	84.91	
		<b>SUMMATION</b>	<b>934.46</b>	<b>81.28</b>	
			(Equation 29)		(Equation 28)
			1017.00		
			FORCE RATIO	91.68%	

TABLE 17. C&D STATIC CALIBRATION: ANALYSIS 3

A. MEASURED DATA					
CHANNEL NUMBER	DESCRIPTION	(a) MEASUREMENT (mV) @ 1018 LBS	(b) MEASUREMENT (mV) @ 0 LBS	(a - b) CORRECTED MEASUREMENT (mV)	
205	FWD UPPER BRACKET, BENDING	3.5160	0.0391	3.4769	
206	FWD UPPER BRACKET, AXIAL	-0.5860	-0.0049	-0.5811	
207	MIDDLE UPPER BRACKET, BENDING	6.4840	0.0391	6.4449	
208	MIDDLE UPPER BRACKET, AXIAL	-0.6592	0.0000	-0.6592	
209	REAR UPPER BRACKET, BENDING	2.5390	0.0000	2.5390	
210	REAR UPPER BRACKET, AXIAL	-0.5126	-0.0049	-0.5077	
211	FWD LOWER FITTING, AXIAL	1.9530	0.0000	1.9530	
212	FWD LOWER FITTING, BENDING	4.5510	-0.0195	4.5105	
213	REAR LOWER FITTING, AXIAL	1.0156	0.0000	1.0156	
214	REAR LOWER FITTING, BENDING	1.7770	-0.0391	1.8161	
215	MIDDLE LOWER FITTING, AXIAL	0.9375	0.0000	0.9375	
216	MIDDLE LOWER FITTING, BENDING	2.3240	-0.0195	2.3435	
B. INSTALLATION ANGLES					
DESCRIPTION	ANGLE	MEASURED ANGLE (DEGREES)	VARIATION ( $\Delta$ )	TRANSLATION ANGLE (DEGREES)	
UPPER BRACKET	$\Delta$	130.50	10.25	140.75	
LOWER FITTING	$\Psi$	34.30	10.25	44.55	
LOWER FITTING	$\Psi + 90$	124.30	10.25	134.55	
C. REACTING FORCES / FORCE BALANCE (USING BENDING DATA)					
ATTACHMENT ID	REACTING FORCES ON Y-AXIS (LBS) (Equation 22)	REACTING FORCES ON Z-AXIS (LBS) (Eqn. 10 for brackets) (Eqn 23 for fittings)	VERTICAL COMPONENT (AIRCRAFT AXIS) (LBS) (Eqn 17 for brackets) (Eqns 24 & 26 for fittings)	LATERAL COMPONENT (AIRCRAFT AXIS) (LBS) (Eqn 18 for brackets) (Eqns 25 & 27 for fittings)	
FWD UPPER BRACKET	-	290.43	183.80	224.87	
MIDDLE UPPER BRACKET	-	236.08	149.40	-182.79	
REAR UPPER BRACKET	-	154.98	98.08	-120.00	
FWD LOWER FITTING	416.33	70.78	342.50	247.06	
REAR LOWER FITTING	273.30	27.89	211.59	175.21	
MIDDLE LOWER FITTING	82.98	-36.74	32.02	84.91	
			<b>SUMMATION</b>	<b>1017.39</b>	<b>-20.48</b>
				(Equation 29) 1018.00	(Equation 28)
				FORCE RATIO 99.94%	

TABLE 18. C&D STATIC CALIBRATION: ANALYSIS 4

A. MEASURED DATA					
CHANNEL NUMBER	DESCRIPTION	(a) MEASUREMENT (MV) @ 1018 LBS	(b) MEASUREMENT (MV) @ 0 LBS	(a-b) CORRECTED MEASUREMENT (MV)	
205	FWD UPPER BRACKET, BENDING	3.5160	0.0391	3.4769	
206	FWD UPPER BRACKET, AXIAL	-0.5860	-0.0049	-0.5811	
207	MIDDLE UPPER BRACKET, BENDING	6.4840	0.0391	6.4449	
208	MIDDLE UPPER BRACKET, AXIAL	-0.6582	0.0000	-0.6582	
209	REAR UPPER BRACKET, BENDING	2.5590	0.0000	2.5590	
210	REAR UPPER BRACKET, AXIAL	-0.5126	-0.0049	-0.5077	
211	FWD LOWER FITTING, AXIAL	1.8530	0.0000	1.9530	
212	FWD LOWER FITTING, BENDING	4.5510	-0.0195	4.5705	
213	REAR LOWER FITTING, AXIAL	1.0556	0.0000	1.0156	
214	REAR LOWER FITTING, BENDING	1.7770	-0.0391	1.8161	
215	MIDDLE LOWER FITTING, AXIAL	0.9575	0.0000	0.9875	
216	MIDDLE LOWER FITTING, BENDING	2.3240	-0.0195	2.3435	

B. INSTALLATION ANGLES					
DESCRIPTION	ANGLE	MEASURED ANGLE (DEGREES)	VARIATION ( $\_$ )	TRANSLATION ANGLE (DEGREES)	
UPPER BRACKET	$\checkmark$	130.50	10.25	140.75	
LOWER FITTING	$\Psi$	34.30	10.25	44.55	
LOWER FITTING	$\Psi + 90$	124.30	10.25	134.55	

C. REACTING FORCES / FORCE BALANCE (USING AXIAL DATA)					
ATTACHMENT ID	REACTING FORCES ON Y'-AXIS (LBS) (Eqn. 22)	REACTING FORCES ON Z-AXIS (LBS) (Eqn. 9 for brackets) (Eqn. 23 for fittings)	VERTICAL COMPONENT (AIRCRAFT AXIS) (LBS) (Eqn. 17 for brackets) (Eqns. 24 & 26 for fittings)	LATERAL COMPONENT (AIRCRAFT AXIS) (LBS) (Eqn. 18 for brackets) (Eqns. 25 & 27 for fittings)	
FWD UPPER BRACKET		159.08	100.67	-123.17	
MIDDLE UPPER BRACKET		237.33	150.19	-183.76	
REAR UPPER BRACKET		153.80	97.33	-119.06	
FWD LOWER FITTING	416.33	70.78	342.50	247.06	
REAR LOWER FITTING	273.30	27.89	211.59	175.21	
MIDDLE LOWER FITTING	82.98	-35.74	32.02	84.91	
			<b>SUMMATION</b>	<b>934.32</b>	<b>81.17</b>
				(Equation 28)	
			BALLAST WEIGHT	1018.00	(Equation 28)
			FORCE RATIO	91.78%	

TABLE 19. INFLUENCE COEFFICIENTS OF C&D OVERHEAD STOWAGE BIN ATTACHMENTS

ATTACHMENT IDENTIFICATION	CHANNEL NUMBER	VERTICAL INFLUENCE COEFFICIENT (mV/lb)	LONGITUDINAL INFLUENCE COEFFICIENT (lbs/lb)
UF2A3 (BENDING)	205	0.0038	- 0.1816
UF2A3 (AXIAL)	206	-0.0007	-0.1816
UM3 (BENDING)	207	0.0058	0.0296
UM3 (AXIAL)	208	-0.0006	0.0296
UR1A3 (BENDING)	209	0.0040	-0.1538
UR1A3 (AXIAL)	210	-0.0007	-0.1538
CL1A (AXIAL)	211	0.0018	-
CL1A (BENDING)	212	0.0042	-
CL3A (AXIAL)	213	0.0012	-
CL3A (BENDING)	214	0.0030	-
CL1B (AXIAL)	215	0.0005	-
CL1B (BENDING)	216	0.0036	-

Posttest overhead stowage-calibration inspection revealed that the aft compartment of the C&D bin had a 16-inch crack on the top lamina of the composite sandwich panel's back wall. Specifically, there was a crack around the perimeter (semicircular shape) of the two aft lower fittings (CL1B and CL3A). This crack might have been attributed to the fact that, when the bin was loaded during calibration, these fittings imparted an out-of-plane loading on the surface of the back wall structure.

#### TEST INITIATION

Prior to the test, the airframe test section was leveled by adjusting the supporting turnbuckles. It was then raised to the desired height of 14 feet. Four guide ropes, manned by members of the drop test team, steadied the test article while it hung above the platform. At this point the high-speed and video cameras began filming. The aircraft was then released and accelerated to an approximate velocity of 30 ft/sec at impact.

## RESULTS AND DISCUSSION

### FUSELAGE STRUCTURE.

The test section experienced static deformation of the lower section as a result of the platform impact. The left side experienced 19.6 inches of crush in the front and an 8.4-inch crush in the aft end. The right side crushed 13.6 inches in the front end and 4.4 inches in the rear. See table 20 for the pretest and posttest measurements and the corresponding crush measurements.

Measurements were taken from the four corners of the fuselage floor to the platform.

TABLE 20. LOWER FUSELAGE CRUSH MEASUREMENTS

MEASUREMENT	LEFT HAND		RIGHT HAND	
	FRONT	AFT	FRONT	AFT
PRETEST (inches)	66.7	50.1	66.1	49.5
POSTTEST (inches)	47.1	41.7	52.5	45.1
CRUSH (inches)	19.6	8.4	13.6	4.4

No significant deformation was experienced on the aircraft cabin floor or the upper section of the fuselage. The seat tracks stayed intact and connected to the floor beams. All of the 9G seats, used primarily to add weight and hold the test dummies, collapsed during the test.

### BOEING STOWAGE BIN.

The Boeing stowage bin maintained its structural integrity and remained attached to the aircraft structure throughout the dynamic test sequence, even though four of the fifteen support links broke. Inspection of the bin after the test and high-speed film revealed the following:

- a. The personal service units (PSUs) detached from the bin prior to the primary impact pulse.
- b. Both door hinges fractured. The contents in the center compartment did not spill due to the plastic strap, which was added for this test, placed around the door and bin.
- c. Five support links, out of a total of 15 links, were damaged after the primary impact pulse. Four links were broken, two instrumented (17B and 28B) and two noninstrumented (one placed on the bottom of the bin at BS1145 and

the other was on the top of the bin at BS1140). Link 31B (drag link) buckled approximately one inch.

d. The high-speed film revealed a crack that partially opened the joint of the center compartment's upper and front walls interface during fuselage section pitching which occurred after primary impact.

#### C&D STOWAGE BIN.

The C&D stowage bin did not maintain its structural integrity during the dynamic test sequence; consequently, its contents spilled out of the compartments. The C&D stowage bin compartments were designed to withstand an ultimate downward static force of 7.3 G.

Posttest inspection revealed the following:

a. The bin remained partially attached to the aircraft structure. The upper rear bracket separated from the rear stowage compartment 84 milliseconds after the primary impact. Adhesive and cohesive failures of the bonded and bolted sections, which join the bin to the bracket, were the first failure modes of this bin.

b. The middle bracket remained attached to the bin; however, it fractured a 10-inch piece of the 120-inch support rail (second failure mode) 87 milliseconds after the primary impact. The upper forward bracket and all three lower fittings were still attached to the bin and fuselage after the crash.

c. The third failure mode, occurring 92 milliseconds after the primary impact, was the complete opening of the floor/front wall intersection of both compartments and the floor/rear wall intersection of the forward compartment.

d. The forward and aft door latches were broken.

#### AUXILIARY FUEL TANK SYSTEM.

The following was noted during the posttest inspection of the auxiliary fuel tank:

a. The auxiliary fuel tank sustained approximately 4" of crush in its center lower surface due to the protrusion of the discharge fuel line hardware.

b. The inner and outer walls of the tank cracked around the welding of the discharge fuel line hardware allowing the fluid to leak out of the double-wall tank.

- c. The ribs inside the tank fractured at each welded joint.
- d. The self-sealing fuel valves were not separated and remained open.
- e. The tank remained attached to its mounting cradle and did not penetrate the cabin floor, although some floor beams cracked.

## DATA ANALYSIS

### FILM ANALYSIS.

Besides recording test data, the test events were also recorded by 12 high-speed cameras, as described in the Instrumentation section. The speed for each camera was mechanically set within an error of approximately 30 frames per second. Since there was no temporal correlation between the film sequences and the data collection system, precise film speeds had to be determined to accurately analyze the data. The film speeds were calculated based upon the free fall time which is determined by equation 30

$$t = \sqrt{2h/g} \quad (30)$$

where  $h$  is the height and  $g$  is the acceleration due to gravity ( $32.174 \text{ ft/s}^2$ ). Table 21 presents the calculated film speeds.

TABLE 21. CAMERA SPEEDS

Camera	Speed (frames/sec)	Description
1	1000	front auxiliary tank
2	471	front overall
3	321	Boeing bin
4	447	front quarter
5	419	starboard/lower fuselage
6	failed	aft quarter
7	failed	aft overall
8	478	C&D bin
9	failed	aft auxiliary tank
10	406	forward upper Boeing link
11	failed	center aisle
12	461	C&D center upper bracket

These film speeds were used to correlate the test pictorial events with the test data. They also helped to determine the sequence of events, loads, and accelerations at significant times. The sequence of the significant events is shown in table 22.

TABLE 22. TIME REFERENCE EVENTS

Event	Time (seconds)
Platform light is on	-1.165
Hook release	-0.933
Impact	0.000
C&D bin support rail bends	0.019
Fuselage completely touches platform	0.048
C&D bin support rail cracks	0.087
C&D forward floor cracks	0.092
Fuselage section rolling motion	0.095
C&D bin support rail is fracturing	0.102
Maximum structural displacement	0.102
C&D bin support rail fractures	0.124
Fuselage rolling & pitching motion	0.150
Boeing bin moves forward	0.223
Boeing forward link fractures	0.279

## DATA REDUCTION.

The original data was first filtered with a 1000Hz analog filter and then recorded at a sampling rate 10K samples/second to save as much information as possible. However, at this point, the data contained high frequency noise. To remove the noise, the data was filtered with SAE J211 class 600Hz digital filter for the anthropomorphic dummy load cell data channels and class 60Hz digital filter for the acceleration, strain gage, displacement, and platform load cell data channels. The acceleration data was also validated by filtering with class 180Hz filter and then integrating the results to check the measured velocities. The data is valid if the measured velocities are compatible with the drop test velocity, which was 30ft/sec. The test data showed that the test article impacted 933 milliseconds after hook release. This matches the free fall time, which was calculated by equation 30 where  $h=14$  ft. Although the test data was recorded during free fall, this section only presents the data from the impact (at  $t=0$  second) to 900 milliseconds for the displacements and to 450 milliseconds for the other data.

## FUSELAGE STRUCTURE.

Due to the tapered shape of the bottom of the test airplane section (figure 2), the test data showed two distinct events during the impact: the initial impact and the primary impact. The initial impact occurred from impact ( $t=0$  sec) to approximately 53 milliseconds. The primary impact took place right after the initial impact. The airframe accelerations were calculated for both impact periods. The peak G values were read directly from the filtered data, which are shown in appendix A. The maximum G values were computed based on an idealized triangular pulse assumption (equation 31).

$$G_{\max} = \frac{2\Delta V}{\Delta t} \quad (31)$$

where  $\Delta t$  is the difference between the start and stop times of the integration interval, and  $\Delta V$  is the velocity change determined by integrating the acceleration data during  $\Delta t$ . Tables 23 and 24 present the airframe accelerations during the initial impact and the primary impact, respectively.

TABLE 23. FUSELAGE ACCELERATIONS DURING INITIAL IMPACT

		Idealized Triangular Pulse		
Body Station	Measured G peak	G <sub>max</sub>	Velocity Change (ft/s)	Duration (msec)
BS1120P	14.9	9.2	5.46	37
BS1120S	17.0	8.0	6.02	47
BS1170P	3.8	4.1	0.79	12
BS1170S	5.8	5.2	1.24	15
BS1180P flr	7.5	5.3	3.89	46
BS1180S flr	9.3	7.6	6.22	51
BS1180P up	8.3	7.0	5.17	46
BS1180S up	11.5	8.7	6.46	46
BS1240P	5.5	2.1	0.30	9
BS1240S	no data	no data	no data	no data

NOTE: P = port side, S = starboard side, flr = floor, up = upper

TABLE 24. FUSELAGE ACCELERATIONS DURING PRIMARY IMPACT

		Idealized Triangular Pulse		
Body Station	Measured G peak	G <sub>max</sub>	Velocity Change (ft/s)	Duration (msec)
BS1120P	31.7	40.5	31.24	47
BS1120S	32.1	36.2	28.50	49
BS1170P	39.2	31.0	33.43	67
BS1170S	41.5	32.8	35.86	68
BS1180P flr	39.3	37.5	28.34	47
BS1180S flr	30.1	36.5	31.14	53
BS1180P up	38.9	33.4	30.09	56
BS1180S up	47.1	40.3	33.74	52
BS1240P	44.6	26.6	33.30	78
BS1240S	no data	no data	no data	no data

NOTE: P = port side, S = starboard side, flr = floor, up = upper

The measured fuselage accelerations decreased from BS1120 to BS1240. The fuselage accelerations were approximately 7G<sub>max</sub> during the initial impact and 36G<sub>max</sub> during the primary impact.

Two displacement transducers were used to measure the floor deformations and two other transducers were used to measure the deformations of the bottom of the test article. The displacement data for the floor was lost due to the cables breaking during the impact. The displacement data for the aircraft test section showed that the forward bottom was initially crushed 19.5 inches, rebounded 4.5 inches, and the final static deformation was 18 inches. The flat section of the BS1140 curve shown in figure 21 indicates that the displacement data at the BS1140 location might exceed the full-scale limit. The aft bottom was initially crushed 14.3 inches, rebounded 3 inches, and the final static deformation was 11.4 inches deformation. These data are presented in figure 21 which shows close correlation to the posttest measurements which are shown in table 20.

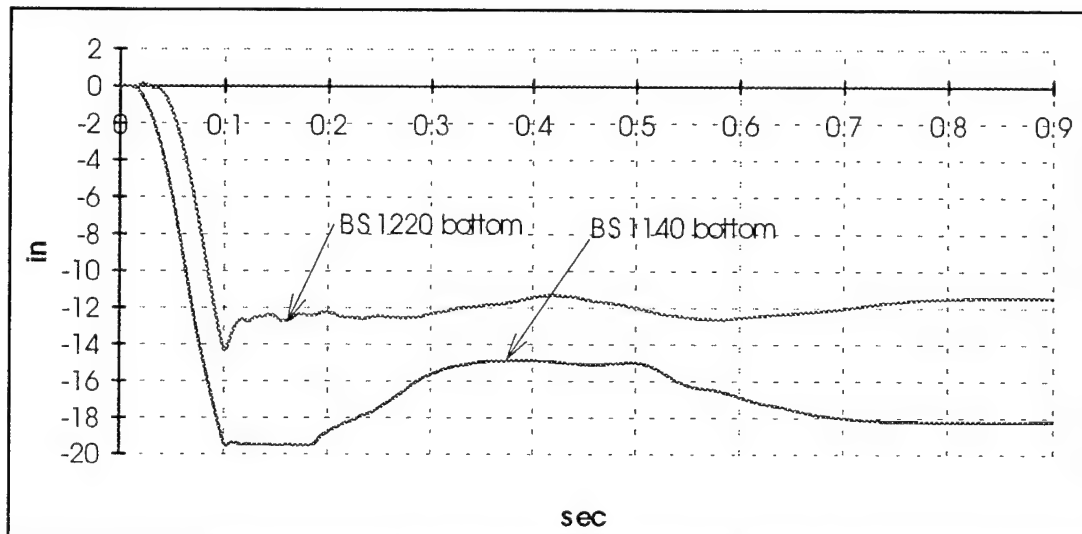


FIGURE 21. FUSELAGE DEFORMATIONS

#### AUXILIARY FUEL TANK.

Ten accelerometers, eight accelerometers in the Z-direction and two in the X-direction, were used to measure accelerations at different locations on the tank and the cradle. Three accelerometers fell off at some point during the impact due to an old adhesive bond. The accelerations of the tank in the Z-direction are shown in table 25.

TABLE 25. TANK ACCELERATIONS

		Idealized Triangular Pulse		
Body Station	Measured G peak	G <sub>max</sub>	Velocity Change (ft/s)	Duration (msec)
BS1198P	36.3	32.3	36.88	71
BS1198S	39.3	32.8	38.54	73
BS1200P	36.1	31.5	34.99	69
BS1200S	34.9	27.2	31.51	72
BS1160P	invalid	invalid	invalid	invalid
BS1160S	invalid	invalid	invalid	invalid
BS1150P	37.5	29.1	34.12	73
BS1150S	invalid	invalid	invalid	invalid

NOTE: P = port side, S = starboard side

The average G<sub>max</sub> tank acceleration was about 31G. The force applied on the tank was distributed to the tank supports, i.e., the cradles and the straps. Strain gages were mounted on the cradles and straps to determine the load distribution. The maximum tension and compression strains for each location on the tank supports are identified in table 26.

TABLE 26. MAXIMUM STRAINS ON THE TANK SUPPORTS

Location	Tension Microstrain	Time (msec)	Compression Microstrain	Time (msec)
Aft port strap	117.28	34	-9.13	75
Aft starboard strap	76.61	34	-29.05	62
Forward port strap	392.03	46	-277.78	77
Forward starboard strap	124.27	31	-41.76	48
Aft port cradle	156.75	34	-1885.7 *	71
Aft starboard cradle	172.77	34	-1890.4 *	70
Forward port cradle	525.36	41	-1894.5 *	66
Forward starboard cradle	452.54	31	-1896.5 *	66
Aft port rib	no data	-	no data	-
Aft starboard rib	252.01	73	-30.06	23
Forward port rib	307.20	67	-451.29	94
Forward starboard rib	1875.2 *	75	-	-

\* indicates the full scale value

The strains on the straps were not significant. However, all the strains on the cradles exceeded the full-scale value of the data acquisition system, which was

$\pm 20\text{mV}$  ( $\pm 1887$  microstrain). These high values of strains were the result of the fuselage bottom hitting the auxiliary fuel tank.

#### PLATFORM.

The platform was supported by 12 load cells to measure the impact load. One platform load cell located at the mid-aft left side exceeded the full-scale load limit (33,500 lbs) at 57 milliseconds after impact. One load cell located at the mid-forward right side failed. Comparing the measured loads based on locations and sides, which are symmetric, it is reasonable to assume that a load cell on the left side measured the equivalent load as one on the opposite side (right side) at a same longitudinal location, i.e., forward or aft. In this case, the maximum platform total load during the primary impact was approximately 107,000 lbs. The platform load data is presented in figure 22.

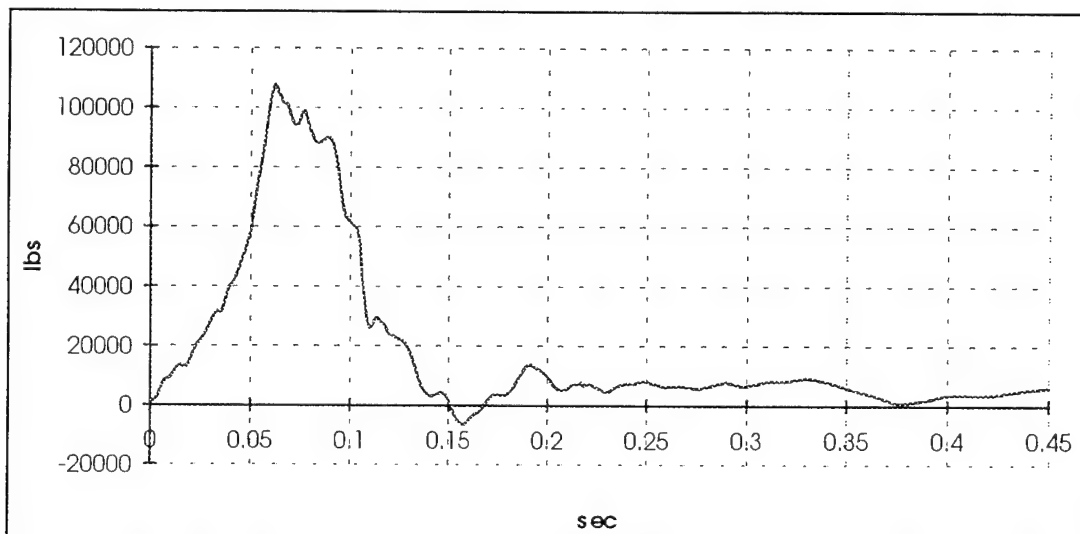


FIGURE 22. PLATFORM TOTAL LOAD

### ANTHROPOMORPHIC DUMMIES.

Two instrumented anthropomorphic dummies were located in seats 8 and 11 (figure 3) on the test section. The maximum load on the pelvis of the anthropomorphic dummy (ATD) on the right side was 1461 pounds and the highest acceleration at this location was 26G. Using the idealized triangular pulse with a duration 52 milliseconds, the maximum acceleration was calculated to be 21G. The maximum pelvic load of the ATD on the left side was 1404 pounds; however, the acceleration data for this ATD was lost.

### OVERHEAD STOWAGE BINS.

As described previously, two overhead stowage bins were used in this test, a Boeing bin and a C&D bin.

BOEING BIN. The Boeing bin and links remained in good condition during both initial and primary impacts. The bin accelerations are shown in table 27.

TABLE 27. BOEING BIN ACCELERATIONS

			Idealized Triangular Pulse		
Impact Period	Accelerometer Location	Measured G Peak	Gmax	Velocity Change (ft/s)	Duration (msec)
Initial	BS1120	13.8	12.2	8.22	42
Primary	BS1120	24.1	29.7	29.59	62
Initial + Primary	BS1180	31.1	21.5	43.85	127

The measured time histories of the Boeing bin support link dynamic loads were compared to the analytical estimates of bin support link loads that were determined using the results of the bin installation static load calibration tests and measured acceleration data.

The measured load is defined as:

$$P_m = e_o \times K \quad (32)$$

where

$e_o$  = The strain gage output voltage during the test.

$K$  = The sensitivity coefficient (calibration factor) of the individual strain gages.

The calculated load is defined by:

$$P_c = G \times K \times [(W_e \times (1/m_e)) + (W_c \times (1/m_c))] \quad (33)$$

where

$G$  = Acceleration measured by an accelerometer located on the bin.

$K$  = Sensitivity coefficient of the individual strain gages.

$W_e$  = Weight of the two end bins.

$W_c$  = Weight of the center bin.

$m_e$  = Influence coefficient when the static calibration tests were performed with weight in the end bin alone.

$m_c$  = Influence coefficient when the static calibration tests were performed with weight in the center bin alone.

The coefficients for the Boeing links were shown in table 13.

The two load functions were plotted for 0.45 second, beginning with the test article's impact with the platform.

The plots of measured versus calculated loads for links 17B, 18B, 25B, and 28B were virtually the same in shape, magnitude, and phasing as shown in figures 23-26.

Links 7B and 8B were not similar in shape or magnitude, only phasing. The correlation differences in these two channels can be explained by the orientation of the links. The two links in question are only 30° above horizontal in the Y-direction, therefore the links are not loaded consistently during a vertical test. Link 31B experienced a similar response as links 7B and 8B as it was mounted only 8.5 degrees above horizontal in the X-direction. Link 31B also exceeded the elastic limit of the strain gage at approximately 165 milliseconds causing the data to be unusable after that point. The comparison plots of measured and calculated loads for these three links are not shown in this report since they are meaningless.

The maximum measured loads on each link during the initial impact, the primary impact, and after the primary impact are shown in table 28. These loads were not the cause of the link fractures. Some links failed due to bending and shearing forces which occurred when the bins shifted fore and aft after the impact, due to fuselage section pitching, as evidenced from film analysis.

TABLE 28. BOEING LINKS' MAXIMUM MEASURED LOADS

Boeing Link	Initial Impact Maximum Load (lbs)	Primary Impact Maximum Load (lbs)	After Primary Impact Max. Load (lbs)	After Impact Link Condition
7B	175	522	-485	Intact
8B	-453	603	-676	Fractured:186ms
17B	391	467	No data	Fractured:279ms
18B	566	1318	-457	Intact
25B	916	1015	-753	Intact
28B	555	1254	-1177	Fractured:284ms
31B	1051	-	-1838	Buckled:165ms

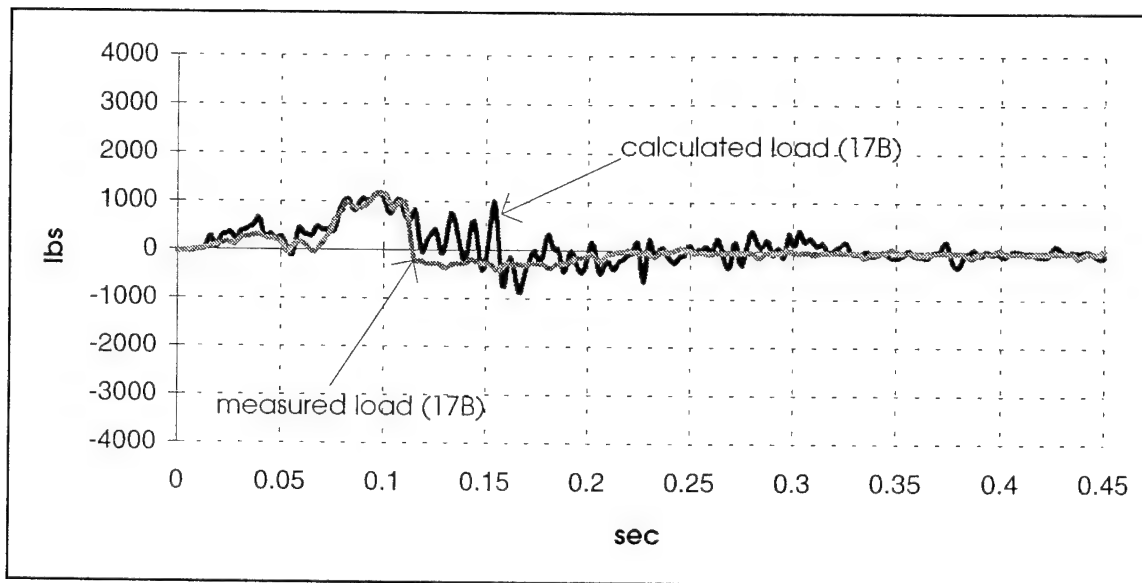


FIGURE 23: BOEING LINK 17B LOAD COMPARISON

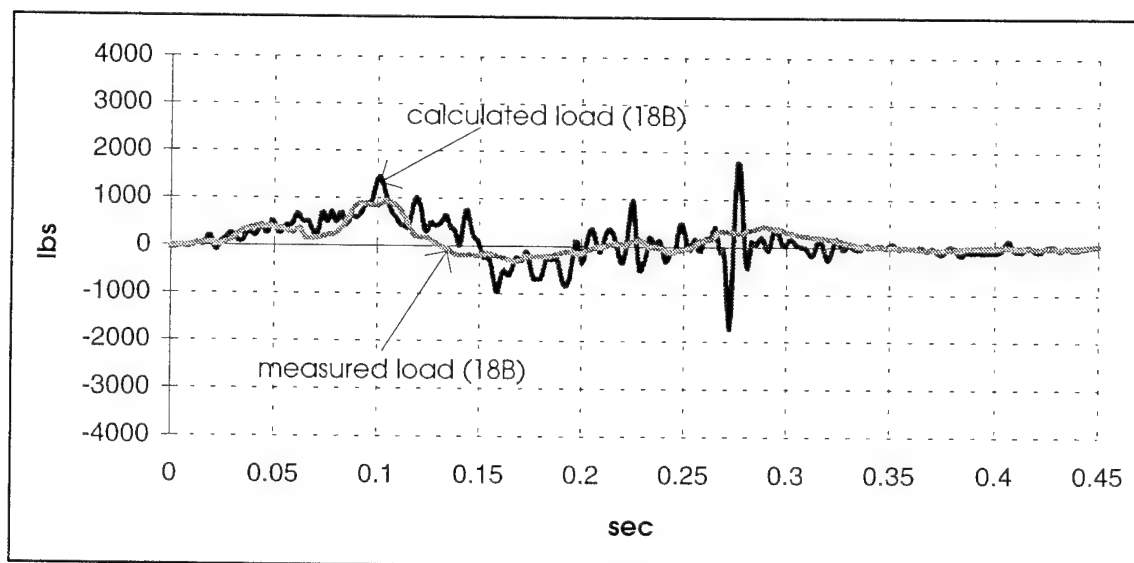


FIGURE 24: BOEING LINK 18B LOAD COMPARISON

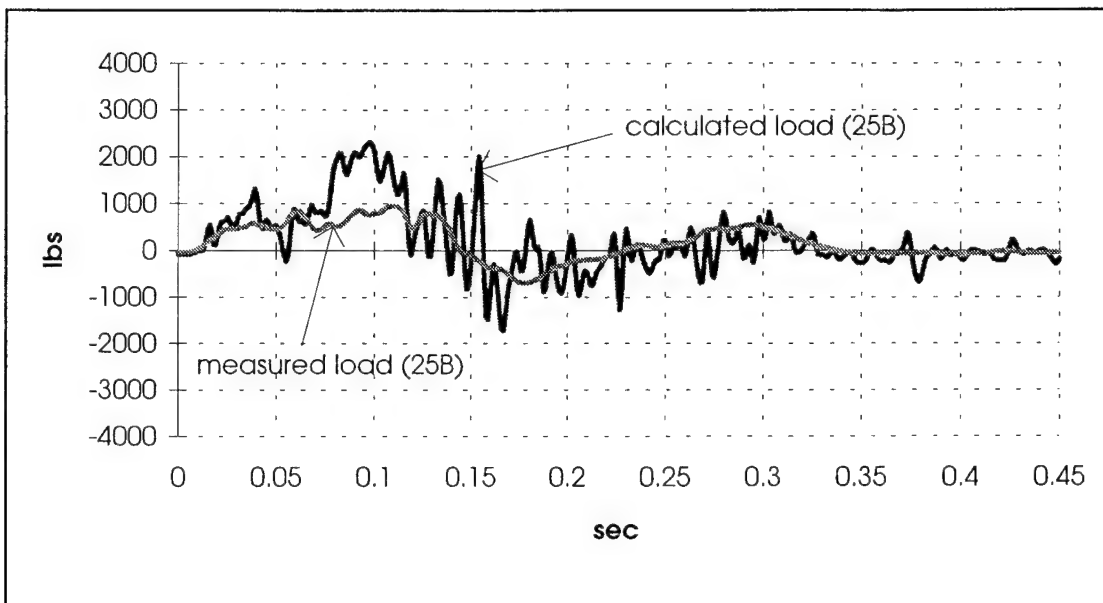


FIGURE 25: BOEING LINK 25B LOAD COMPARISON

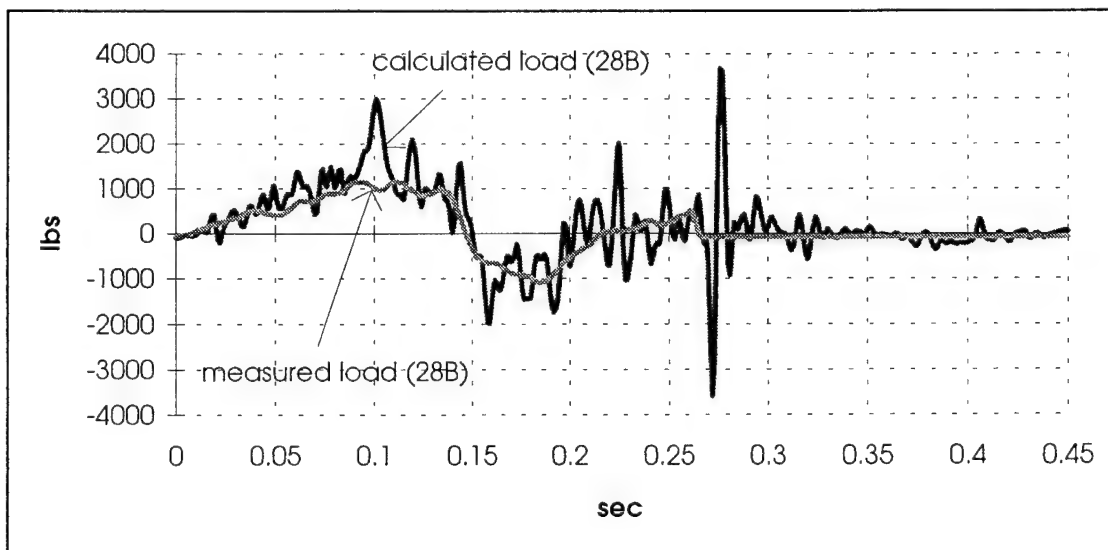


FIGURE 26: BOEING LINK 28B LOAD COMPARISON

**C&D BIN.** The C&D bin remained intact during the initial impact period, but experienced a variety of fracture modes during the primary impact period. Table 29 shows the C&D bin accelerations for both initial and primary impact periods.

TABLE 29. C&D BIN ACCELERATIONS

Impact Period	Accelerometer Location	Measured G peak	Idealized Triangular Pulse		
			G <sub>max</sub>	Velocity Change (ft/s)	Duration (msec)
Initial	BS1120	12.2	11.8	8.94	47
Primary	BS1120	54.2	47.2	34.93	46
Initial	BS1180	9.76	10.8	10.60	61
Primary	BS1180	24.2	22.3	14.34	40
Primary	BS1240	17.6 *	-	-	-

\* Note: The cable connected to the end bin accelerometer at BS1240 broke 92 milliseconds after impact. Before the cable failure, the highest acceleration at this location was 17.6G at 71 milliseconds.

Similar to what was done for the Boeing bin, the loads applied on the C&D bin were also correlated by comparing the measured loads to the calculated loads. The measured loads were determined in the same way as they were during the static calibrations, as shown in Equations 17, 24 and 26. The calculated loads, on the other hand, were computed by using the following expression:

$$P_C = \frac{G W K}{m} \quad (34)$$

where

$P_C$  = Calculated load  
 $m$  = Influence coefficient  
 $G$  = Accelerometer output  
 $W$  = Total weight on bin  
 $K$  = Sensitivity coefficient

The total bin weight was 279 lbs. The influence coefficients can be found in table 19. The sensitivity coefficients of the upper brackets were calculated with equations 11-16. The sensitivity coefficients of the lower fittings can be found in table 14. Since the axial data for the upper brackets at BS1120 and BS1180 were invalid, the bending data were used to determine the measured loads. However, the axial data were used to determine the loads for the upper bracket at BS1240, since the bending data were not available due to the fact the bending gage cable had broken before the bin was separated from the bracket. The maximum measured loads on the upper brackets and the lower fittings during the initial

impact period and during the primary impact period or until the failure occurred are presented in tables 30 and 31.

TABLE 30. C&D BIN UPPER BRACKETS MAXIMUM MEASURED LOADS

Bracket	Initial Impact Maximum Load (lbs)	Primary Impact or Fracture Max. Load (lbs)	Note on Bracket/Fitting
UF2A3	630	892	Intact
UM3	942	1487	Fracture at 87ms
UR1A3	758	1544	Fracture at 84ms

TABLE 31. C&D LOWER FITTINGS MAXIMUM MEASURED LOADS

	Initial Impact Maximum Loads (lbs)			Primary Impact Maximum Loads (lbs)		
Fitting	Px	Pz	Resultant P	Px	Pz	Resultant P
CL1A	987	-195	1000	1486	-433	1494
CL1B	489	-115	489	850	-283	919
CL3A	589	-107	587	1751	-403	1775

Figures 27-29 illustrate the comparison between measured and calculated loads for the brackets. Figure 30 shows the total vertical load of the C&D bin.

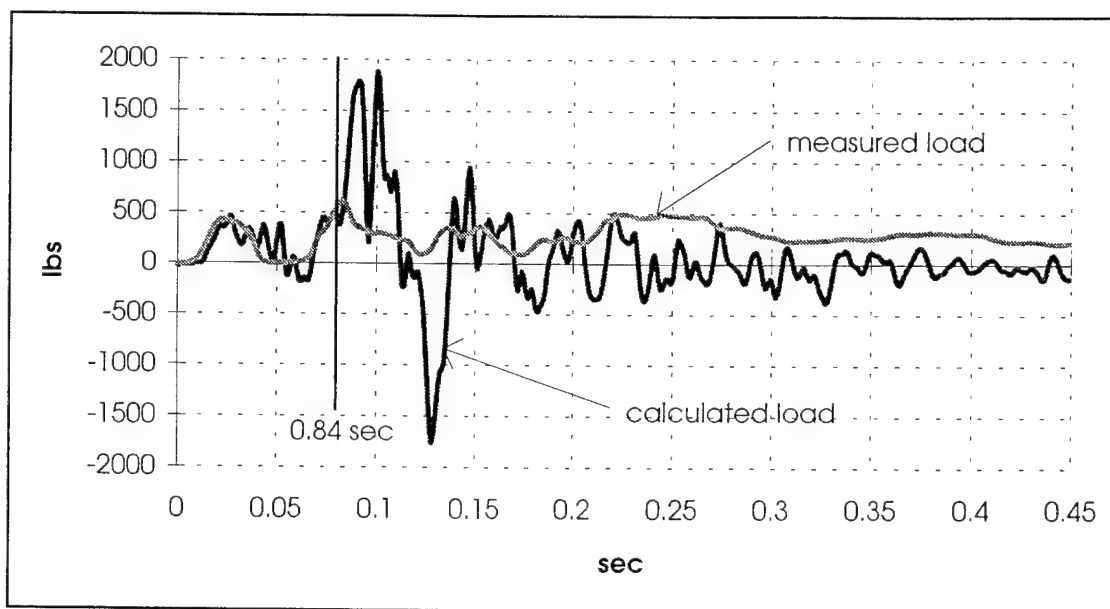


FIGURE 27: FORWARD UPPER BRACKET LOAD COMPARISON

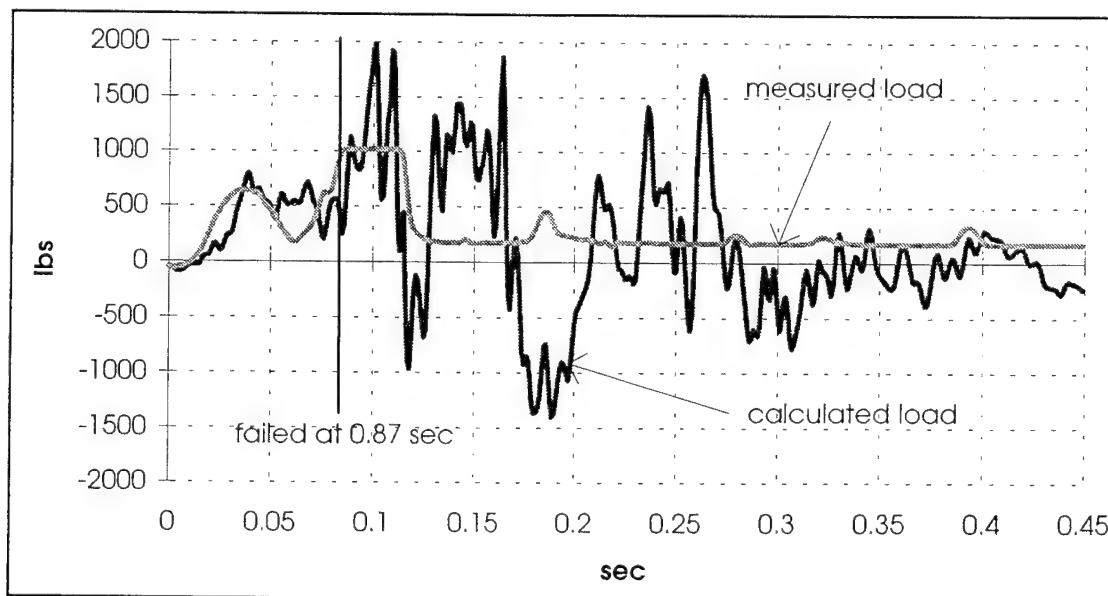


FIGURE 28: MIDDLE UPPER BRACKET LOAD COMPARISON

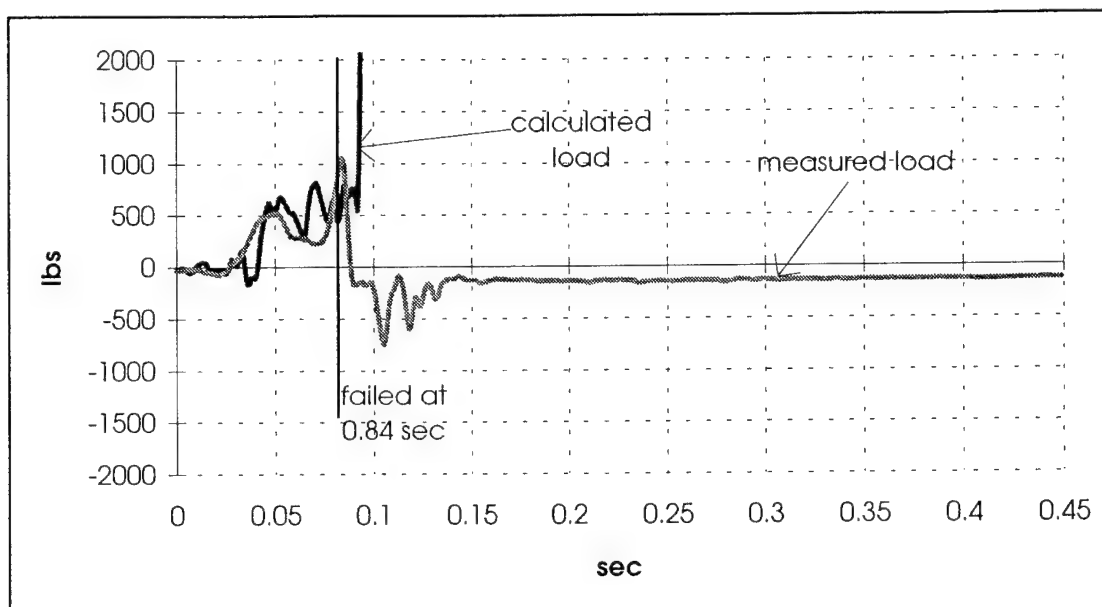


FIGURE 29: REAR UPPER BRACKET LOAD COMPARISON

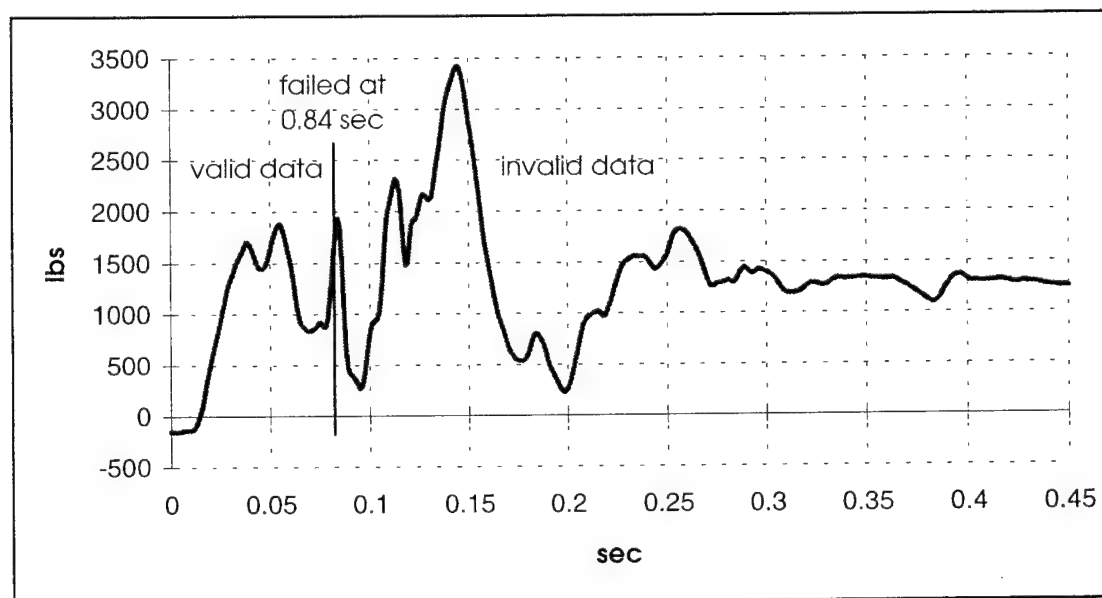


FIGURE 30: C&D BIN TOTAL VERTICAL LOAD

Comparisons of the measured loads and the calculated loads are only valid for the first 0.084 second, because at that time the aft upper bracket disbanded from the bin.

### SUMMARY OF ACCELERATIONS

For better readability and understanding of the deceleration level of the test, the overall diagrams of the accelerometer locations and their associated  $G_{max}$  values are shown in figures 31 and 32.

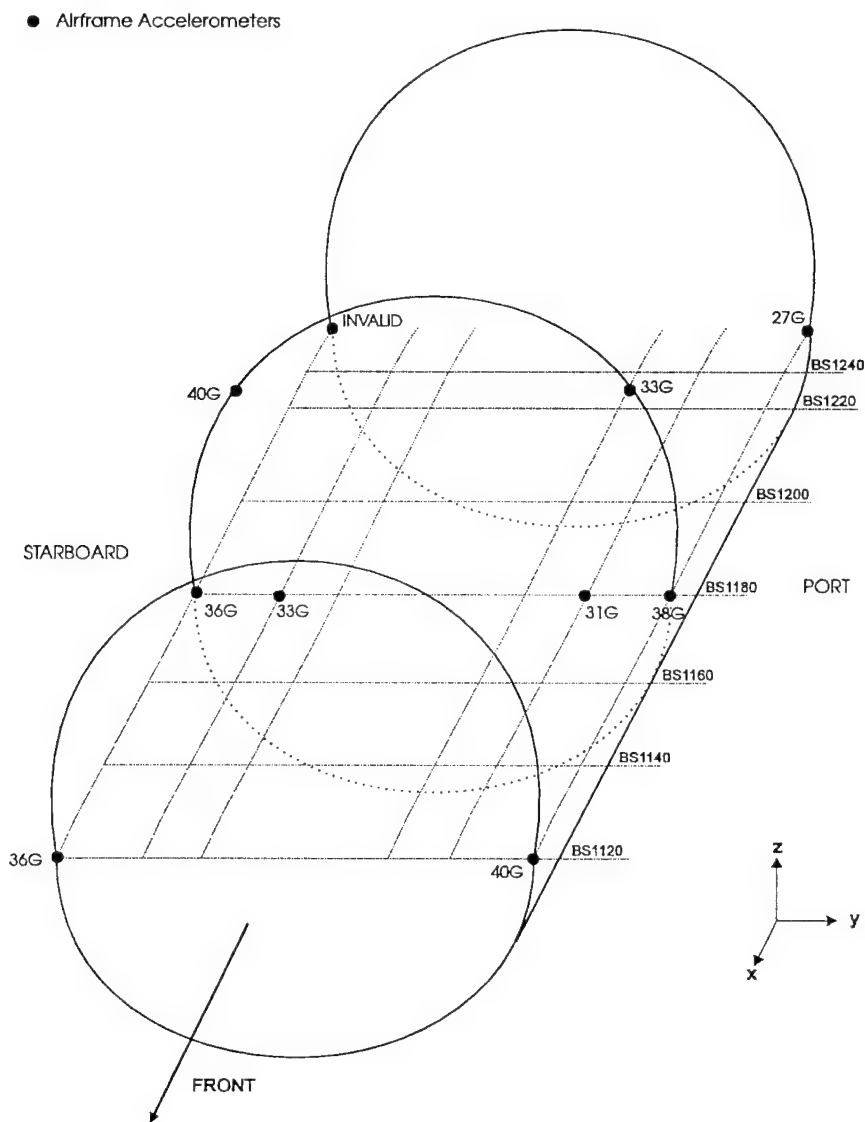


FIGURE 31. ACCELEROMETER LOCATIONS AND  $G_{max}$  VALUES OF THE FUSELAGE

- Bin Accelerometers
- ◆ Tank Accelerometers

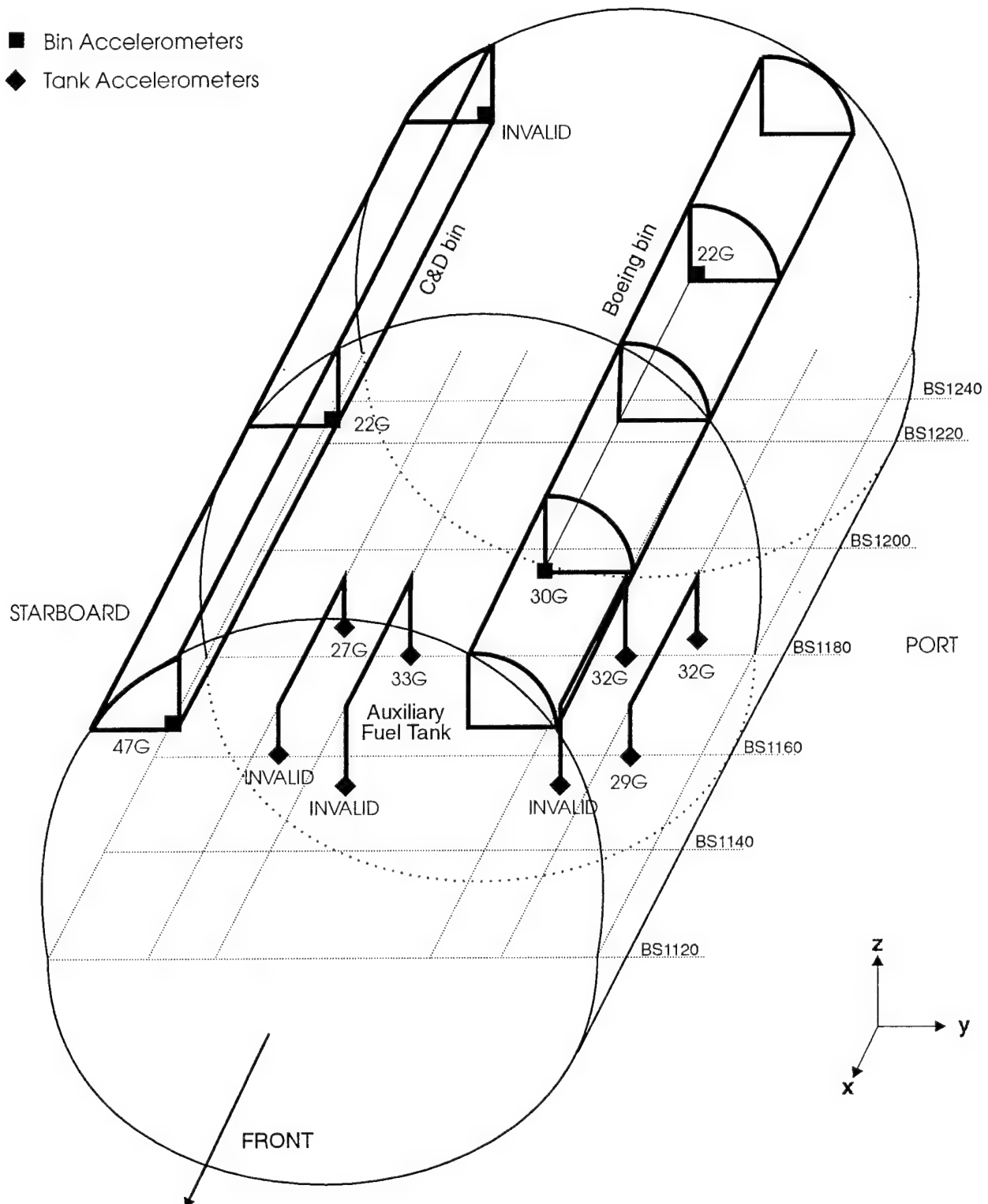


FIGURE 32. ACCELEROMETER LOCATIONS AND  $G_{max}$  VALUES OF THE OVERHEAD STOWAGE BIN COMPARTMENTS AND THE AUXILIARY FUEL TANK

## PHOTOGRAPHIC DOCUMENTATION

The still photographs in this report were taken with a 35-mm camera both prior to and following the drop test. Figures 33 through 35 show overall pictures of the test facility and test article, both prior to and following the test.

Figures 36 through 45 are pictures of the Boeing bin. Included in these photographs are an overall view and a close-up view of some of the support links. There are also views of the door hinges where the door separated and the PSU after it broke free from its supports. Figures 46 through 53 are views of the C&D bin. There are pretest and posttest overall views of the bin, followed by close-ups of various brackets and fittings to show the damage to the bin.

Figures 54 through 62 include overall photographs of the auxiliary fuel tank before and after the test. There are also pictures of the underside of the tank, as well as the tank interior, and close ups of the discharge hose fittings and fuel discharge area where the leaking occurred.

Figures 63 through 69 show the structural damage to the fuselage at various locations. The photos include fuselage crush to the exterior and interior as well as some minor damage to the underside of the floor. The final views are figures 70 through 73 which show overall views of the cabin interior after the test.

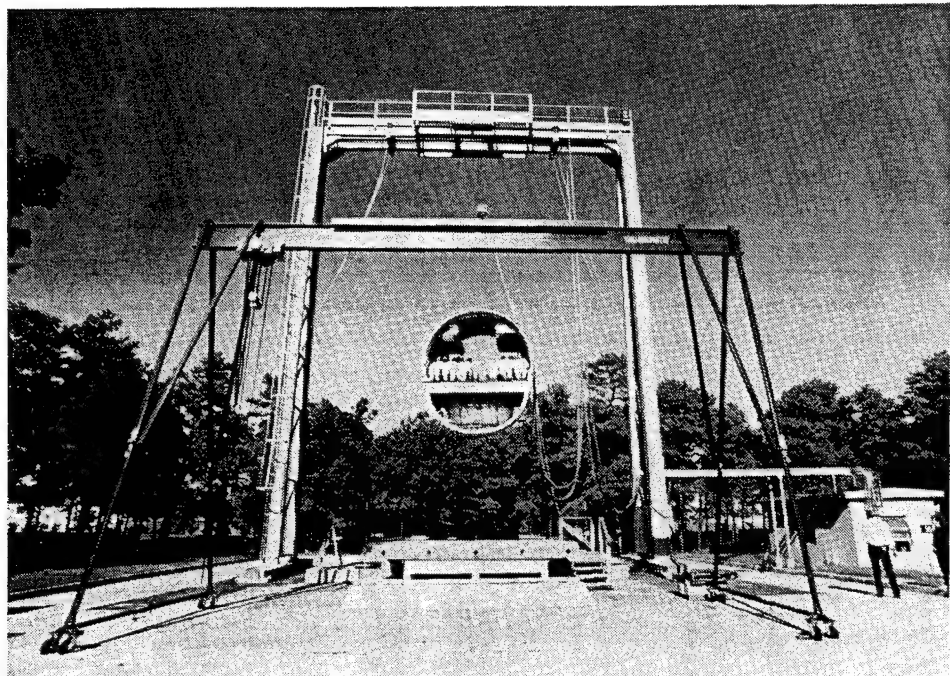


FIGURE 33. FRONT VIEW OF DROP TEST FACILITY

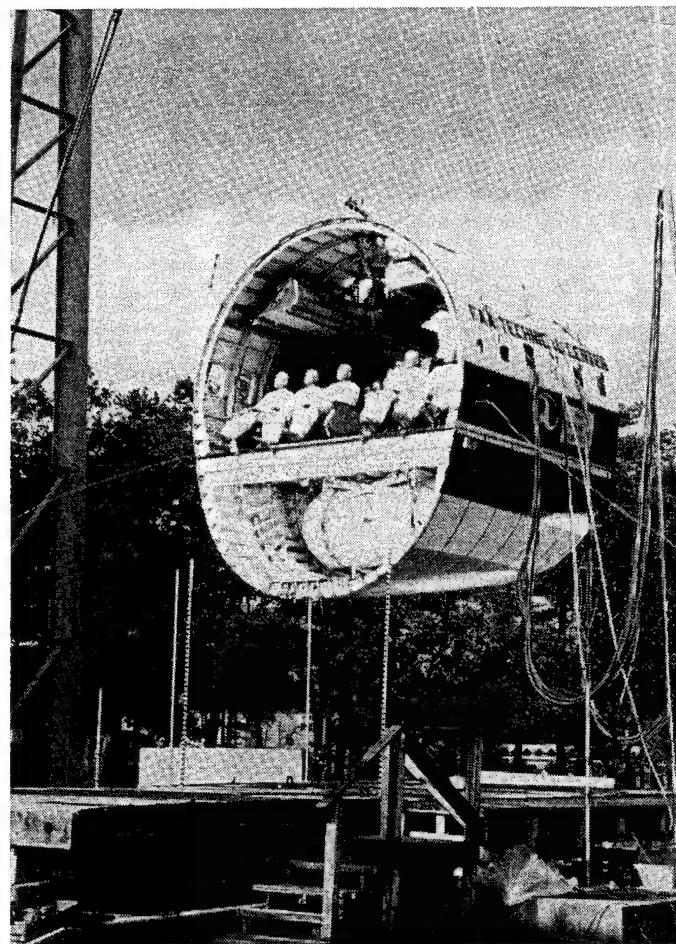


FIGURE 34. SIDE VIEW OF TEST ARTICLE, PRIOR TO IMPACT

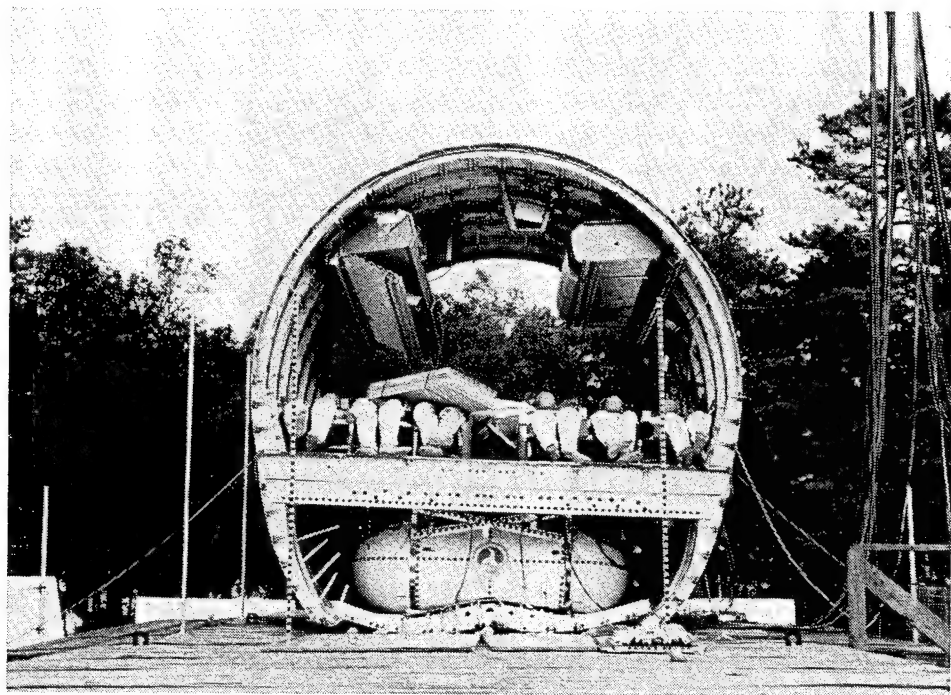


FIGURE 35. FRONT VIEW OF TEST ARTICLE AFTER IMPACT

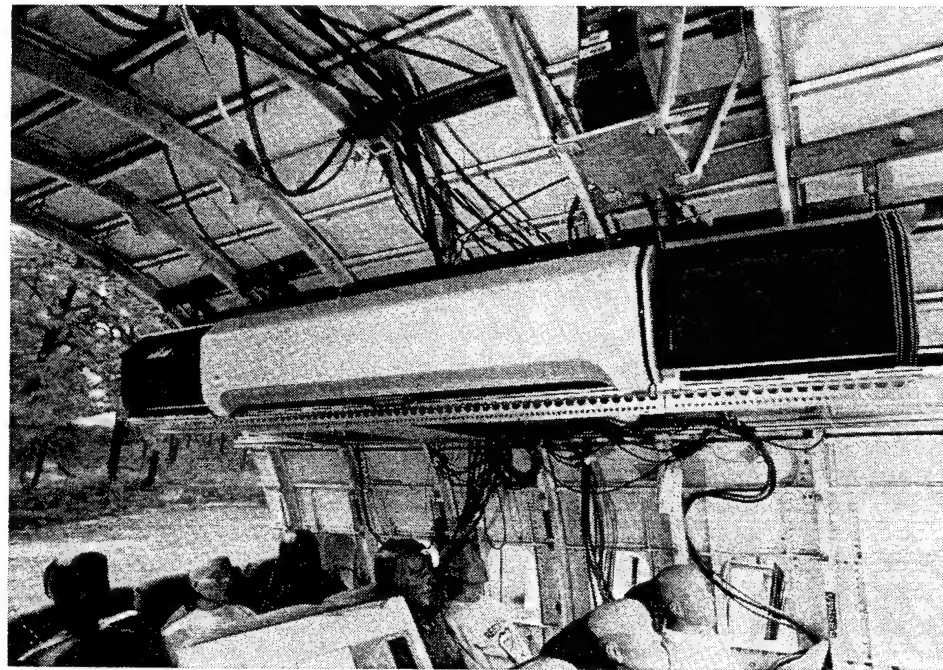


FIGURE 36. OVERALL VIEW OF BOEING BIN

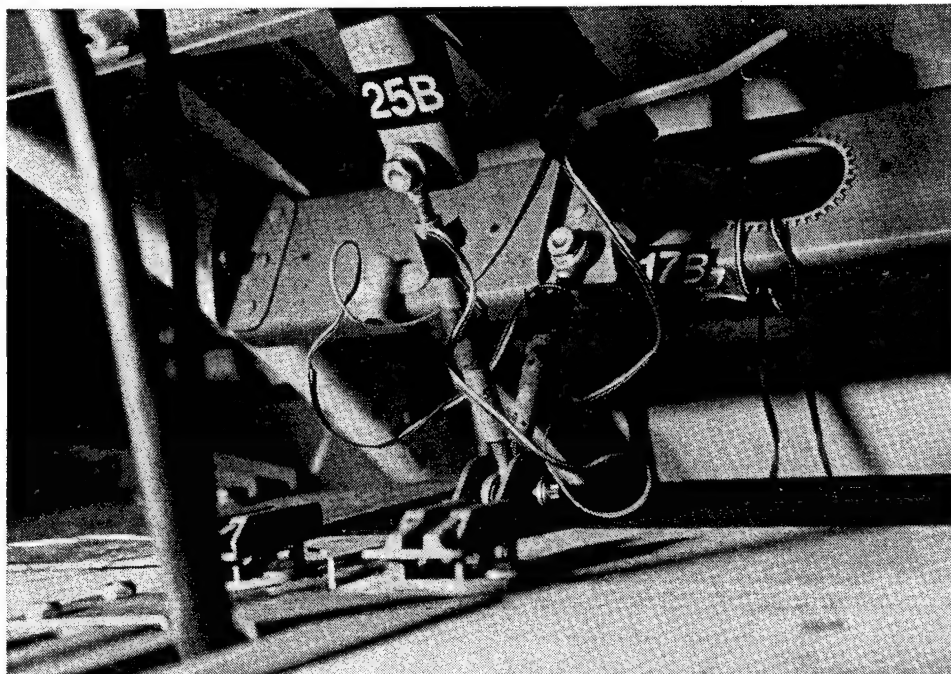


FIGURE 37. BOEING LINKS 25B AND 17B, PRETEST

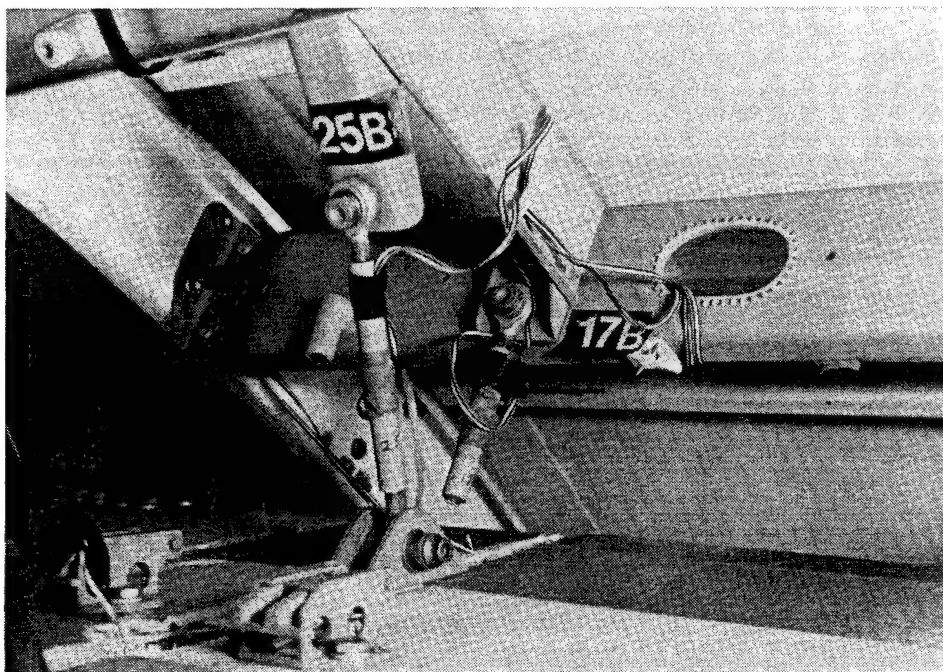


FIGURE 38. BOEING LINKS 25B AND 17B, POSTTEST

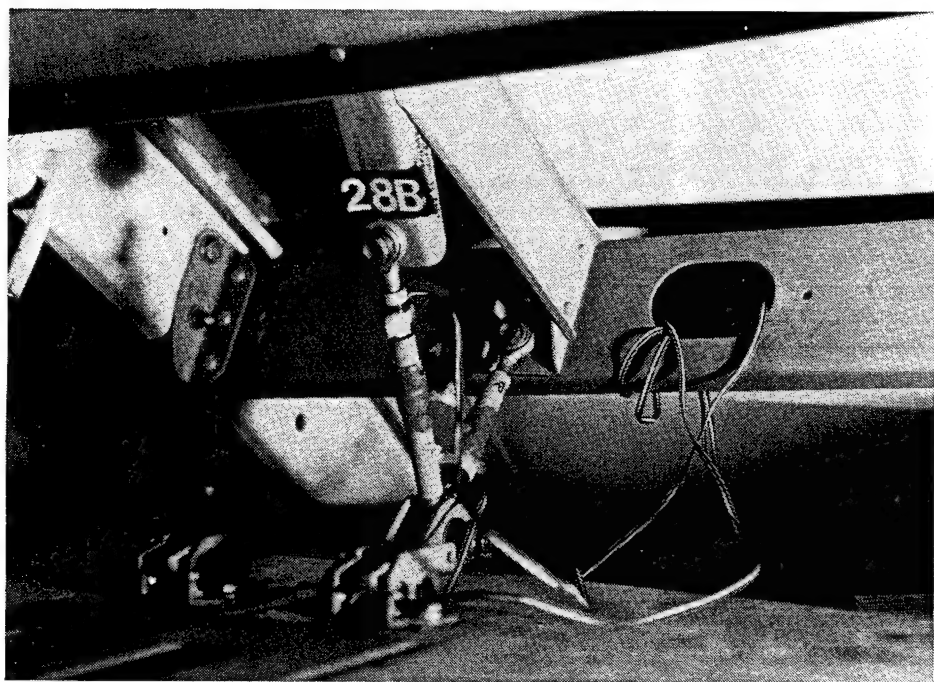


FIGURE 39. BOEING LINKS 28B AND 18B, PRETEST

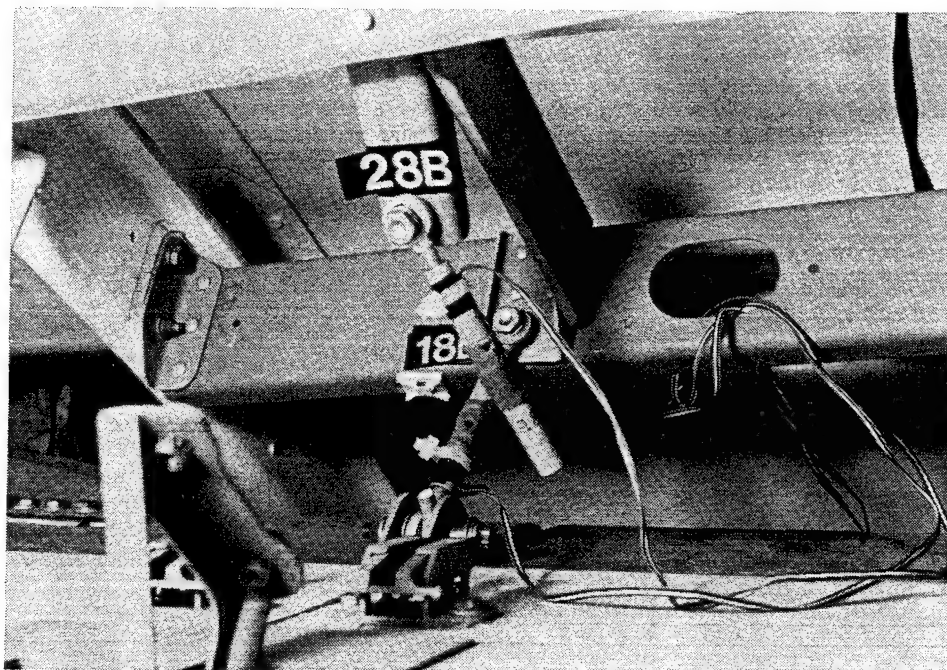


FIGURE 40. BOEING LINKS 28B AND 18B, POSTTEST

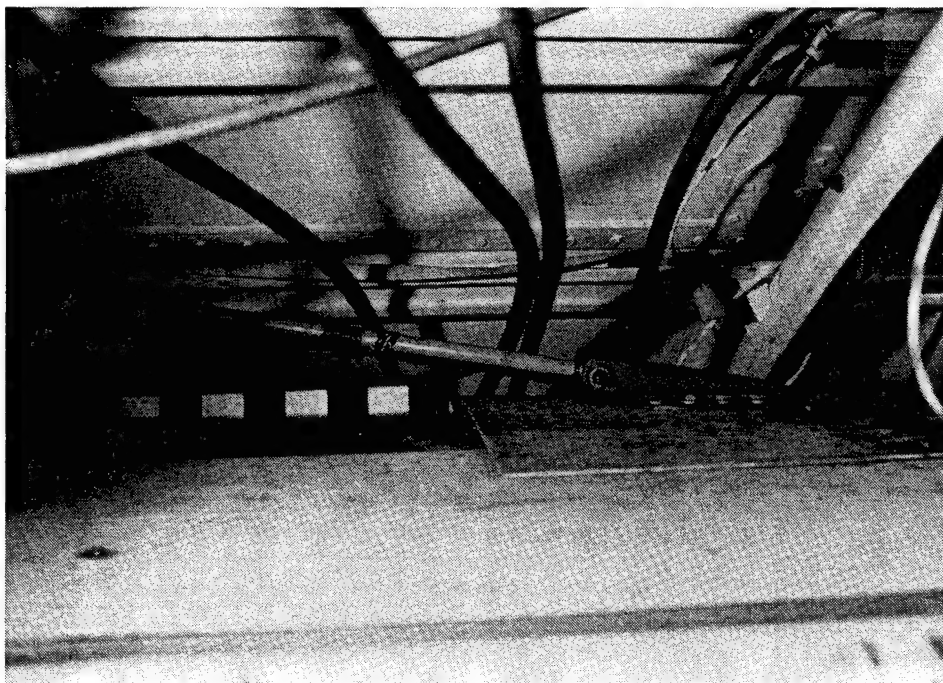


FIGURE 41. BOEING LINK 31B, PRETEST

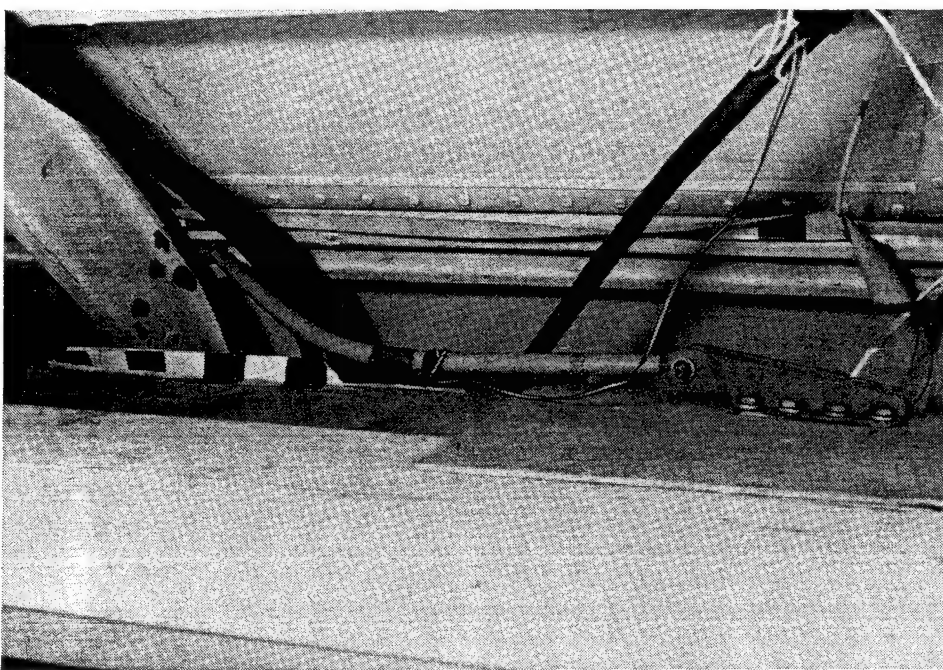


FIGURE 42. BOEING LINK 31B, POSTTEST



FIGURE 43. BOEING BIN BROKEN FORWARD HINGE, POSTTEST



FIGURE 44. BOEING BIN BROKEN AFT HINGE, POSTTEST

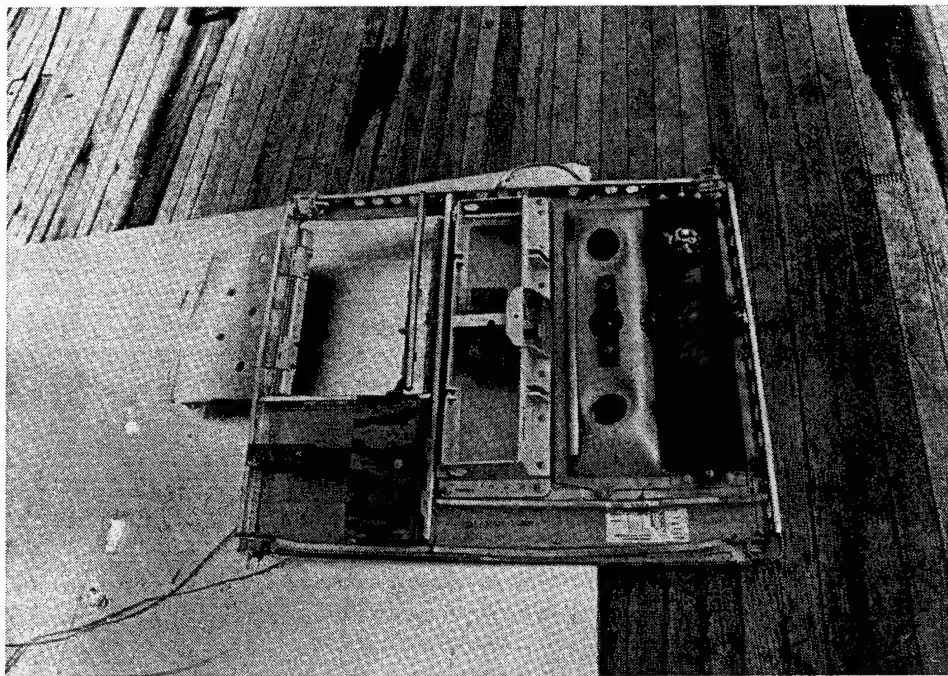


FIGURE 45. PSU UNIT AFTER SEPARATION, POSTTEST

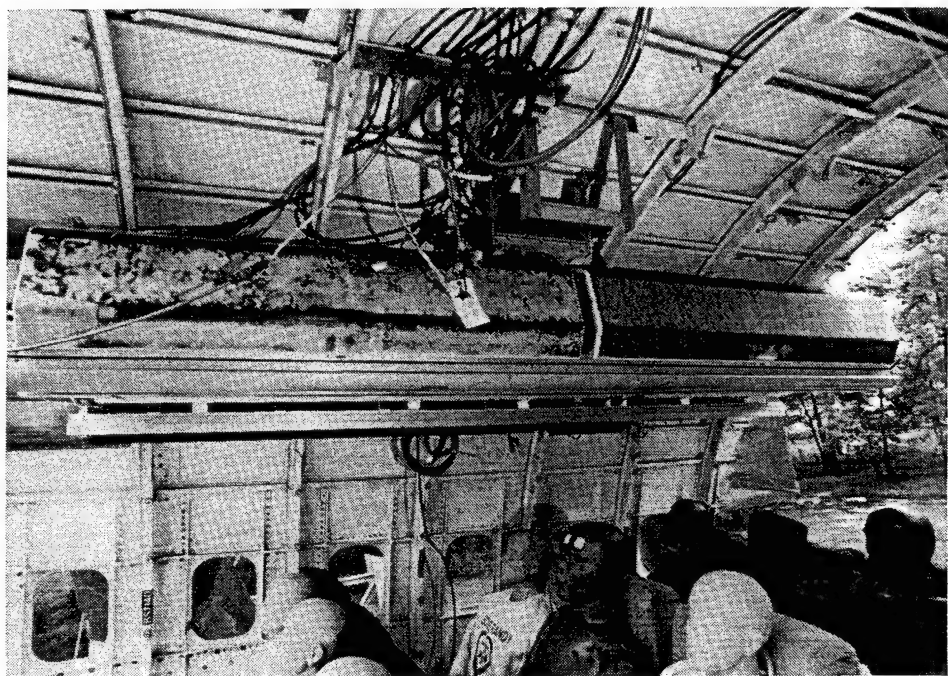


FIGURE 46. C&D BIN OVERALL VIEW, PRETEST

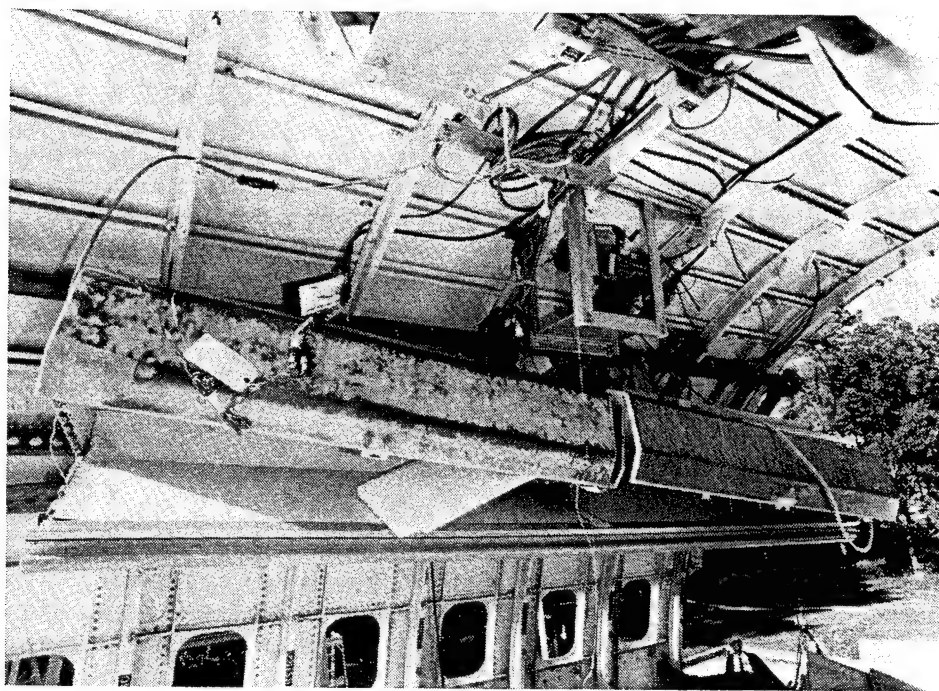


FIGURE 47. C&D BIN OVERALL VIEW, POSTTEST

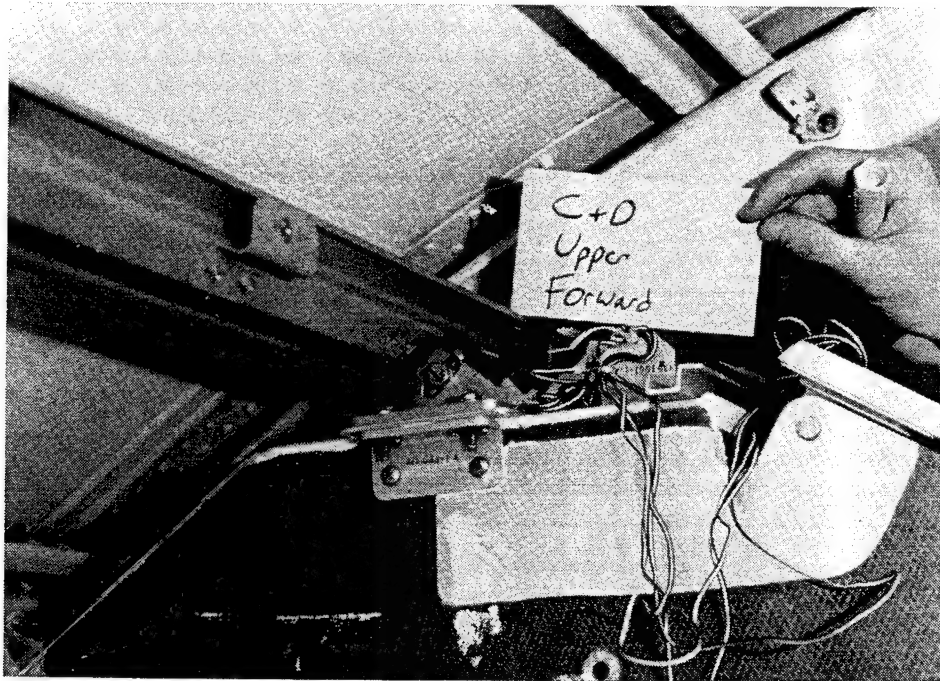


FIGURE 48. C&D BIN UPPER FORWARD BRACKET, POSTTEST

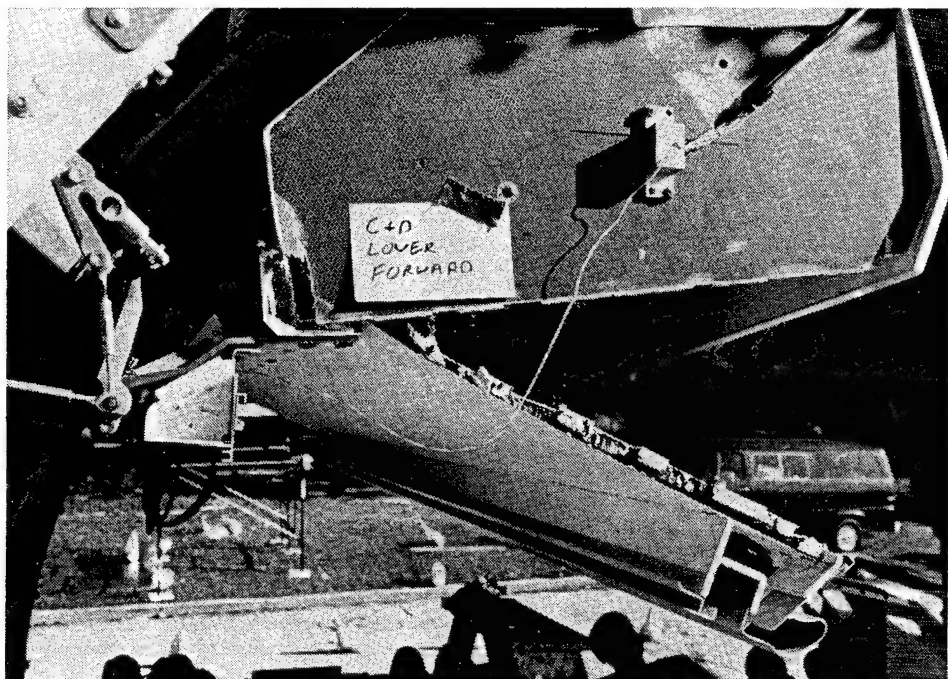


FIGURE 49. C&D BIN LOWER FORWARD AREA, POSTTEST

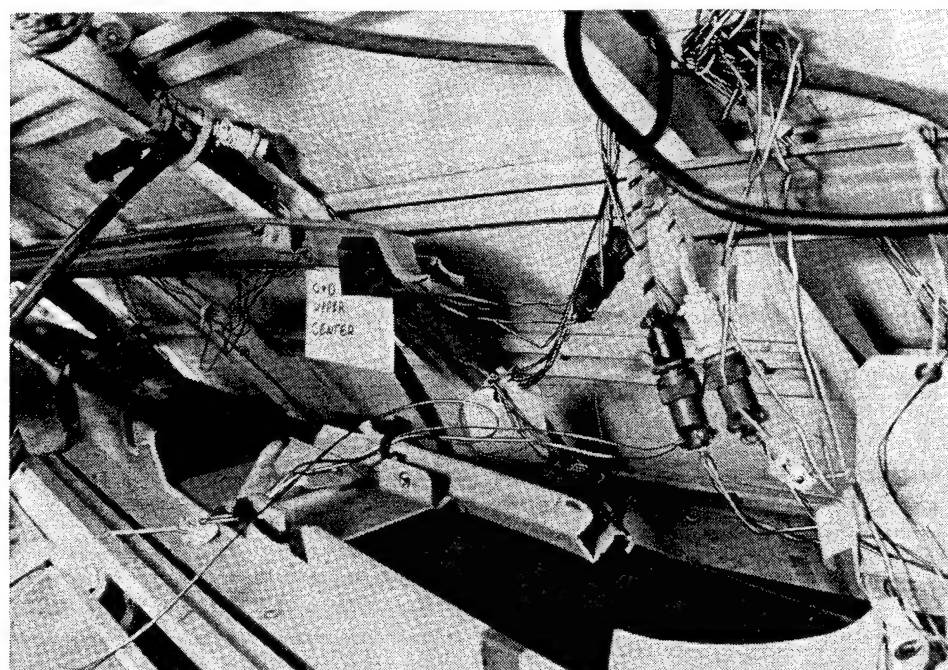


FIGURE 50. C&D BIN UPPER CENTER SECTION, POSTTEST

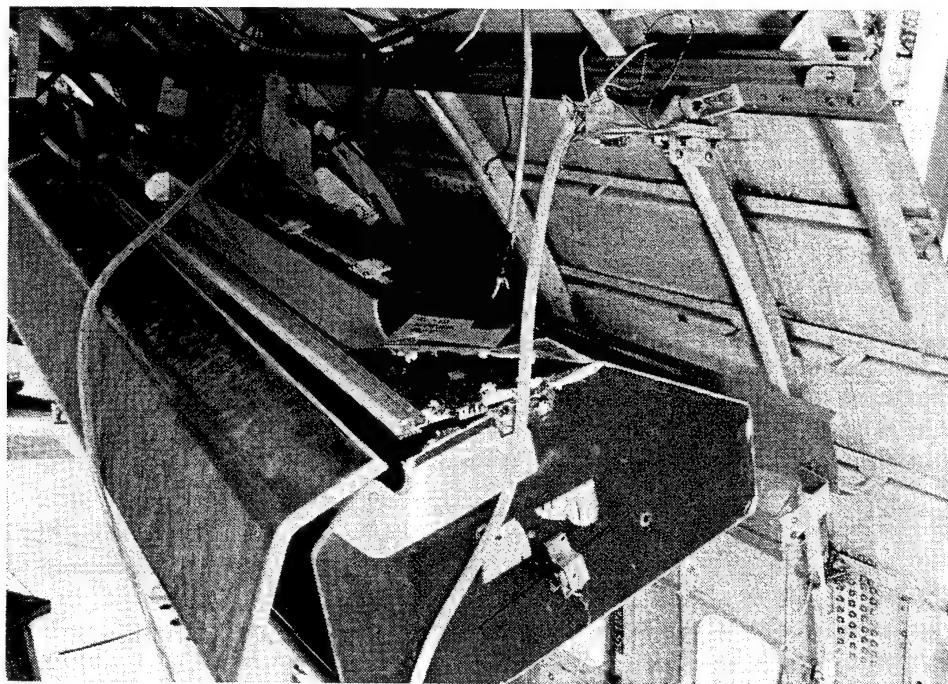


FIGURE 51. C&D BIN AFT OVERALL VIEW, POSTTEST

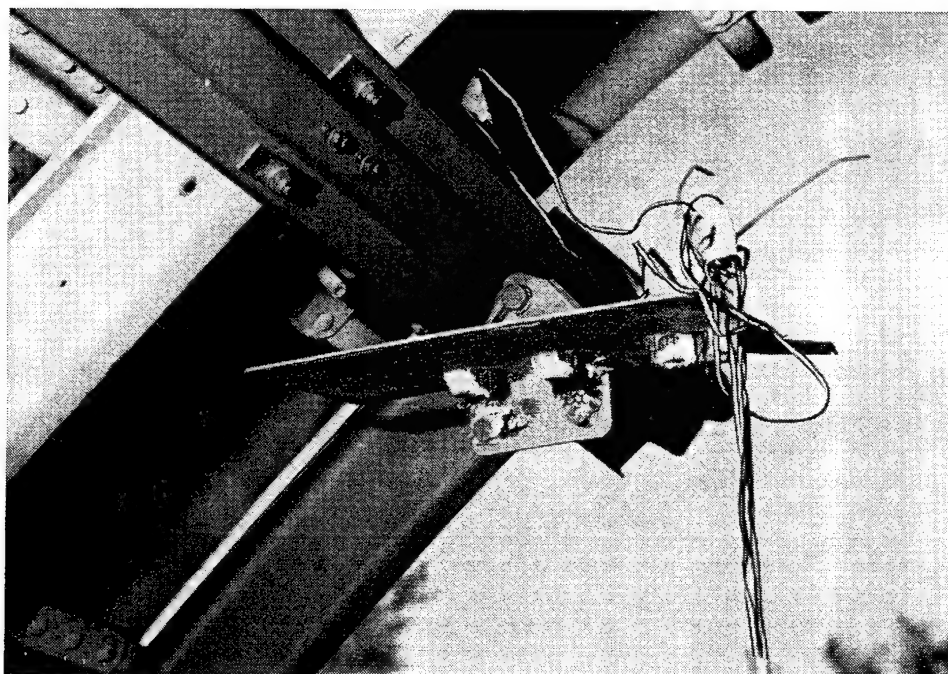


FIGURE 52. C&D BIN AFT UPPER BRACKET, POSTTEST

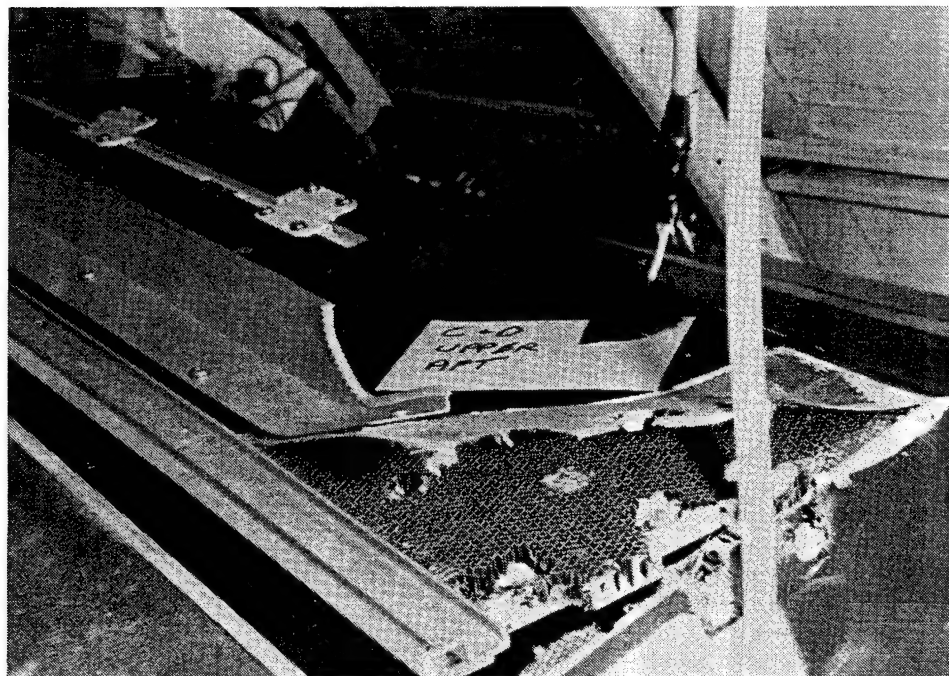


FIGURE 53. C&D BIN UPPER AFT BIN, POSTTEST

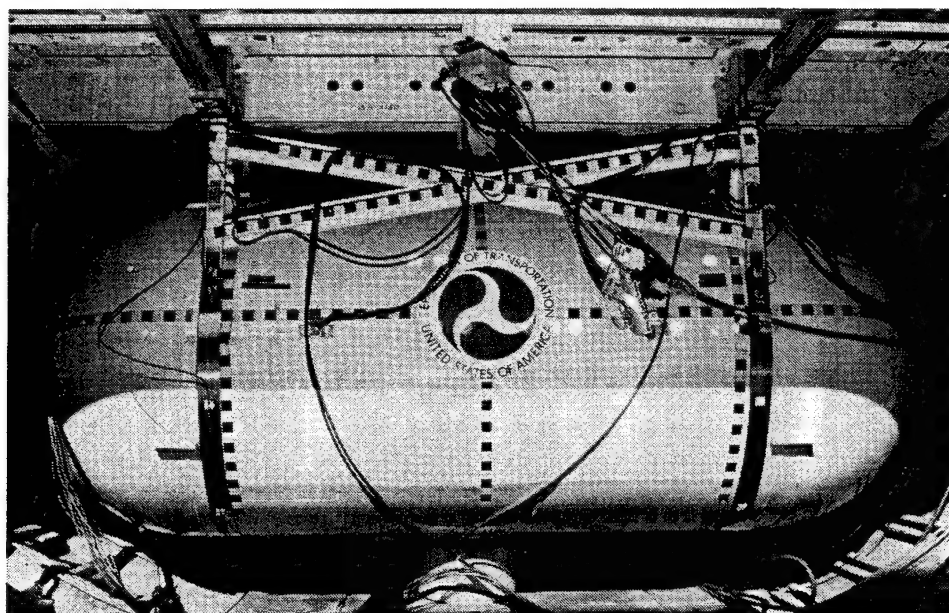


FIGURE 54. AUXILIARY FUEL TANK FRONT OVERALL VIEW, PRETEST

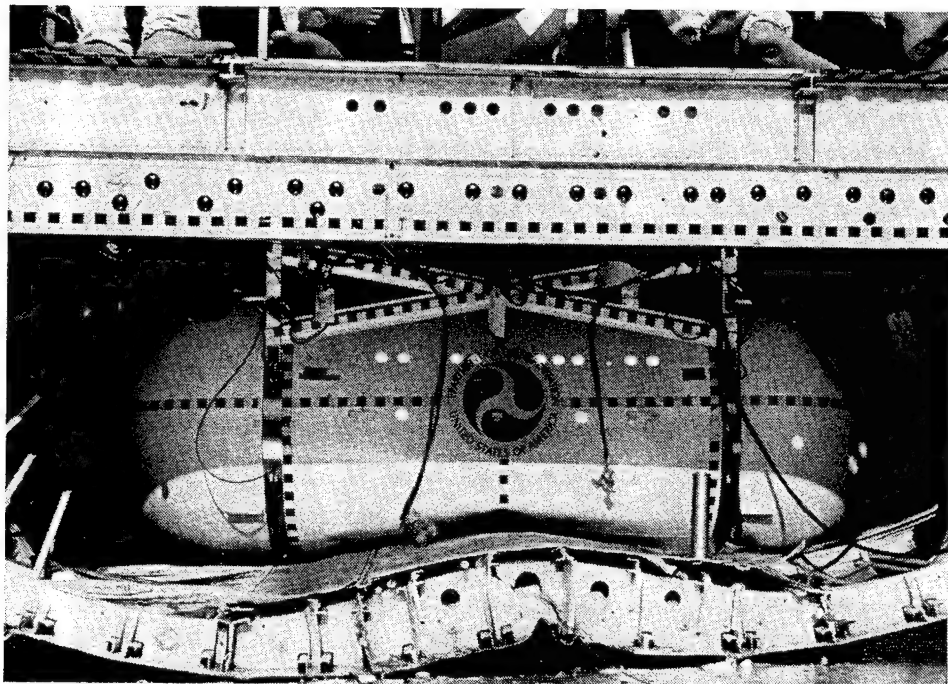


FIGURE 55. AUXILIARY FUEL TANK FRONT OVERALL VIEW, POSTTEST

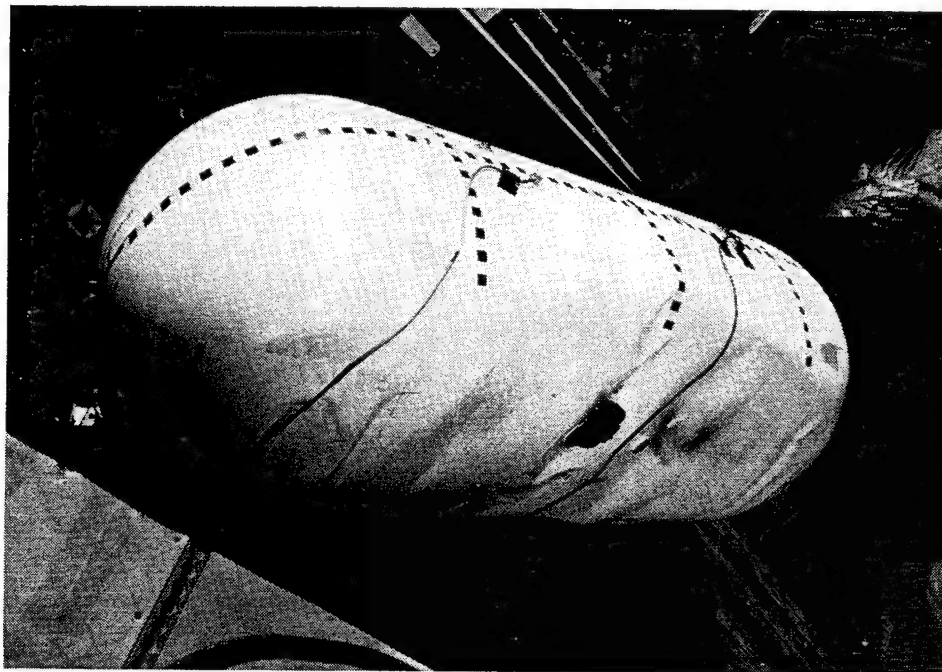


FIGURE 56. AUXILIARY FUEL TANK UNDERSIDE VIEW, POSTTEST

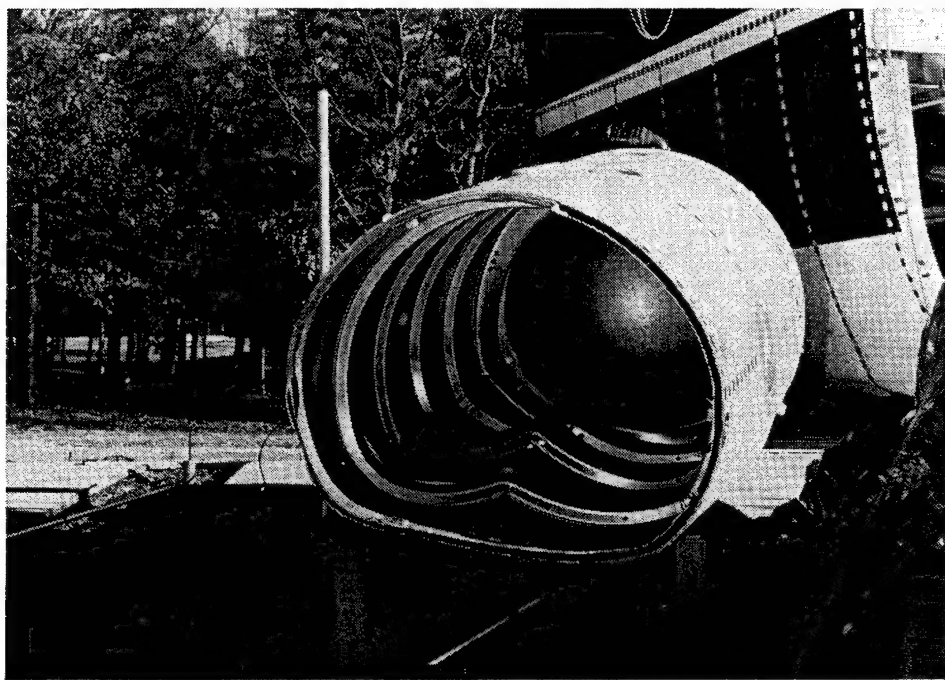


FIGURE 57. AUXILIARY FUEL TANK INSIDE, POSTTEST

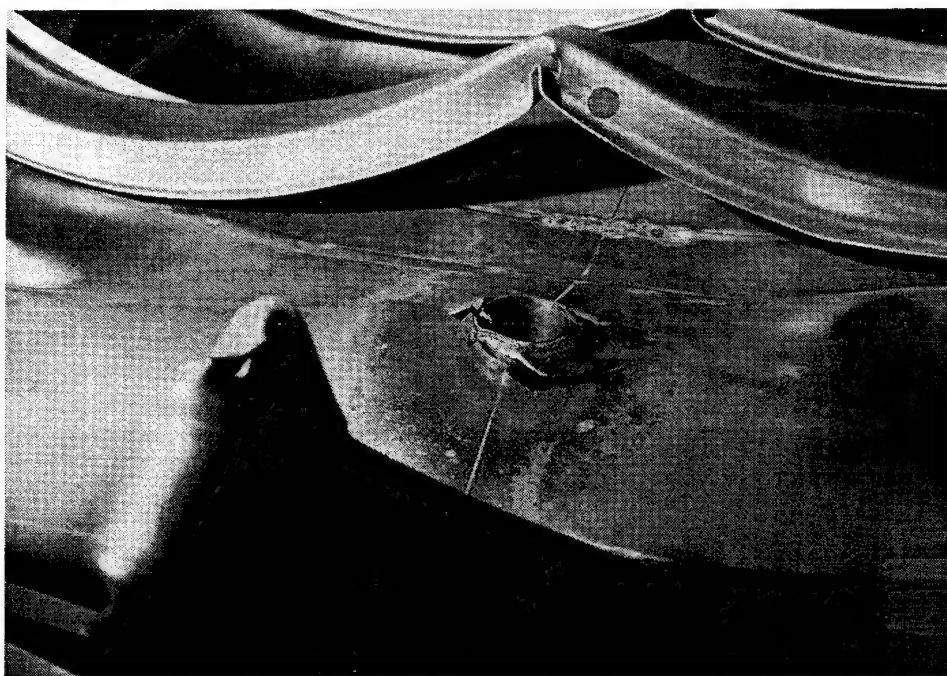


FIGURE 58. AUXILIARY FUEL TANK DRAINAGE HOLE, POSTTEST



FIGURE 59. AUXILIARY FUEL TANK DRAINAGE HOLE CLOSE UP,  
POSTTEST

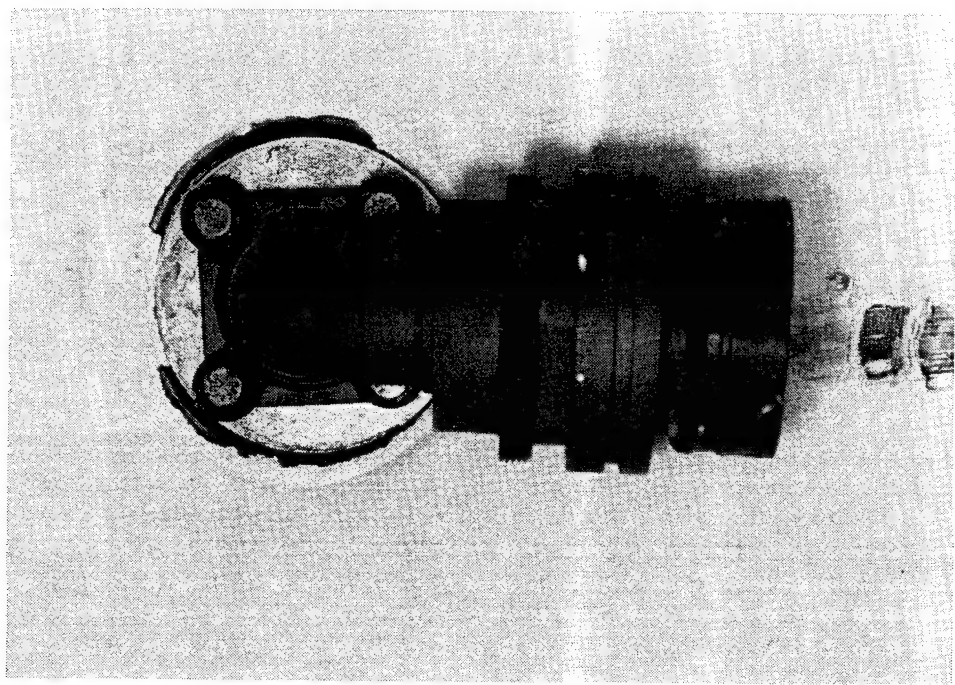


FIGURE 60. AUXILIARY FUEL TANK DRAINAGE HOLE CONNECTOR,  
POSTTEST

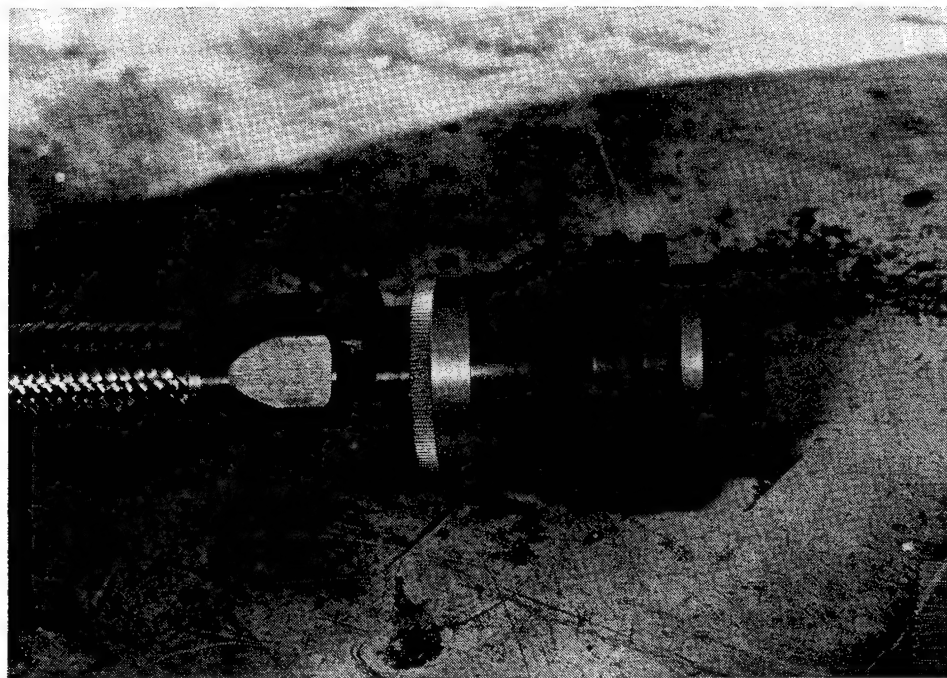


FIGURE 61. AUXILIARY FUEL TANK DRAINAGE HOSE CONNECTOR,  
POSTTEST

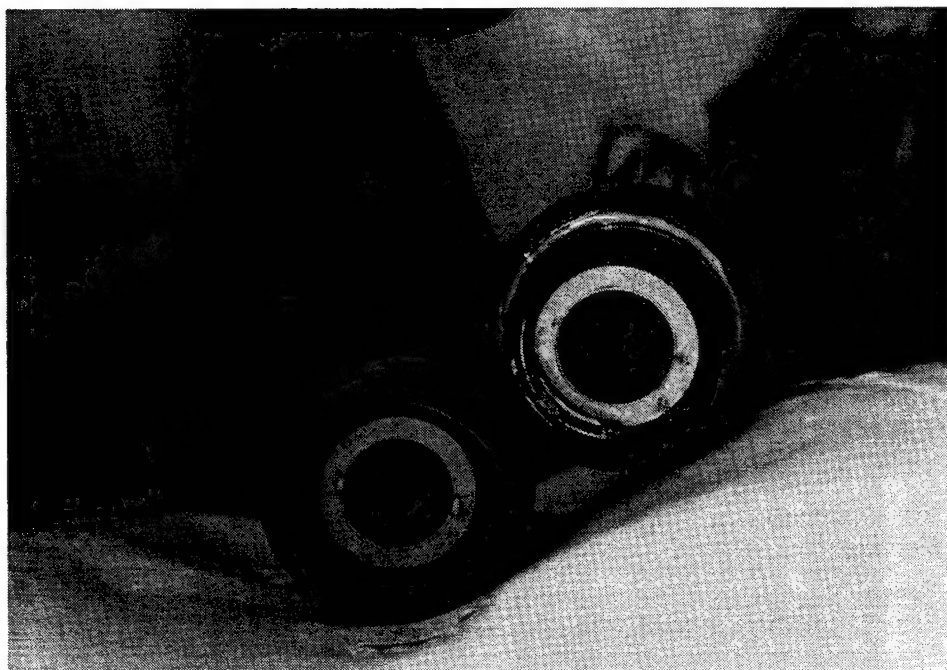


FIGURE 62. AUXILIARY FUEL TANK DRAINAGE HOLE CONNECTORS  
INSIDE VIEW, POSTTEST

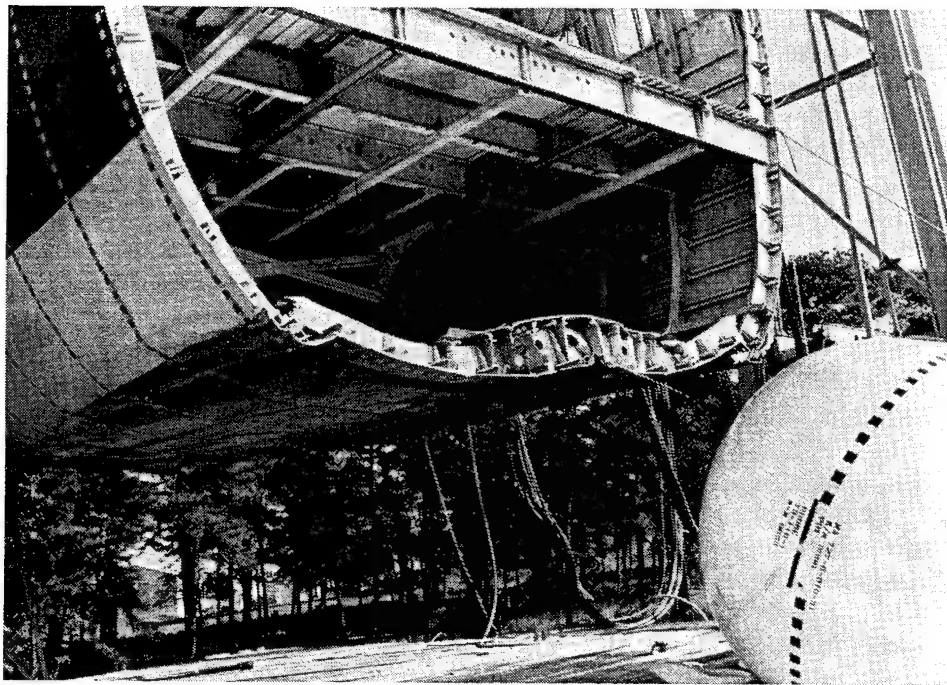


FIGURE 63. FRONT QUARTER VIEW OF LOWER FUSELAGE SECTION,  
POSTTEST

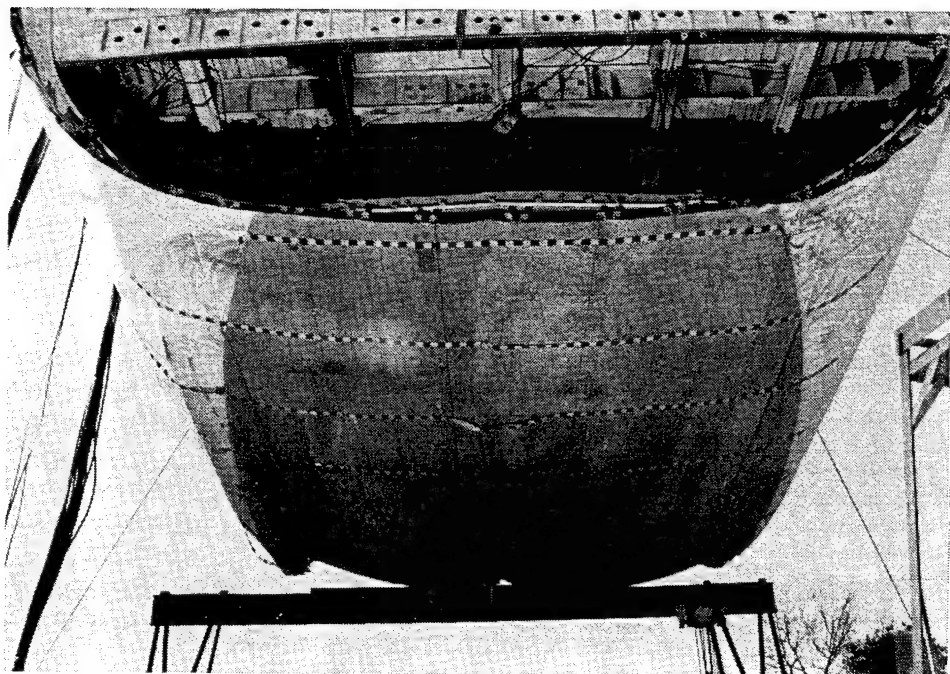


FIGURE 64. UNDERSIDE OF FUSELAGE SECTION, AFT TO FORWARD,  
POSTTEST

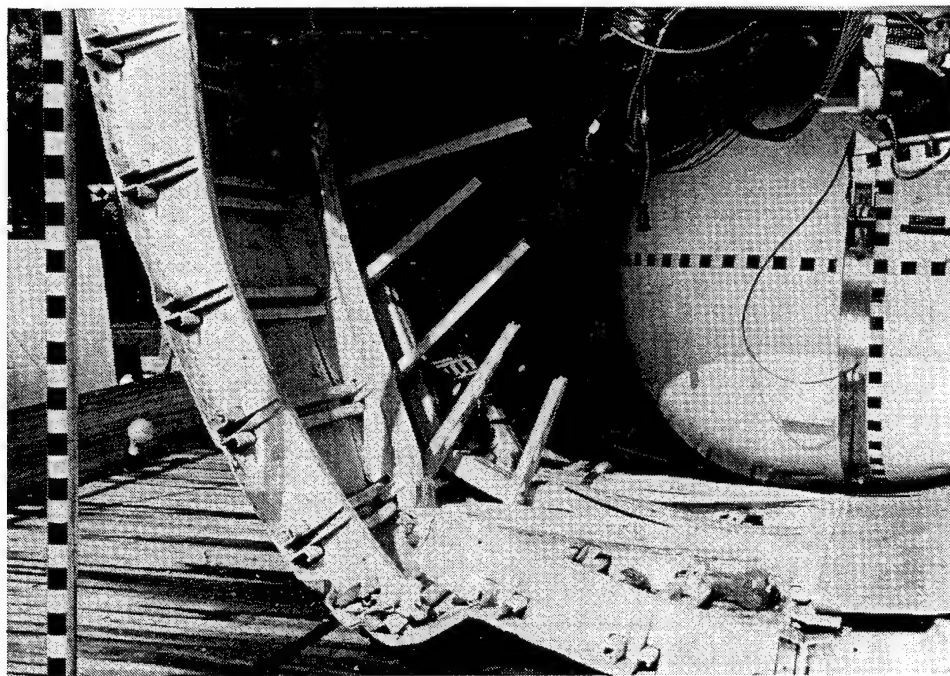


FIGURE 65. FORWARD RIGHT SIDE LOWER FUSELAGE SECTION,  
POSTTEST

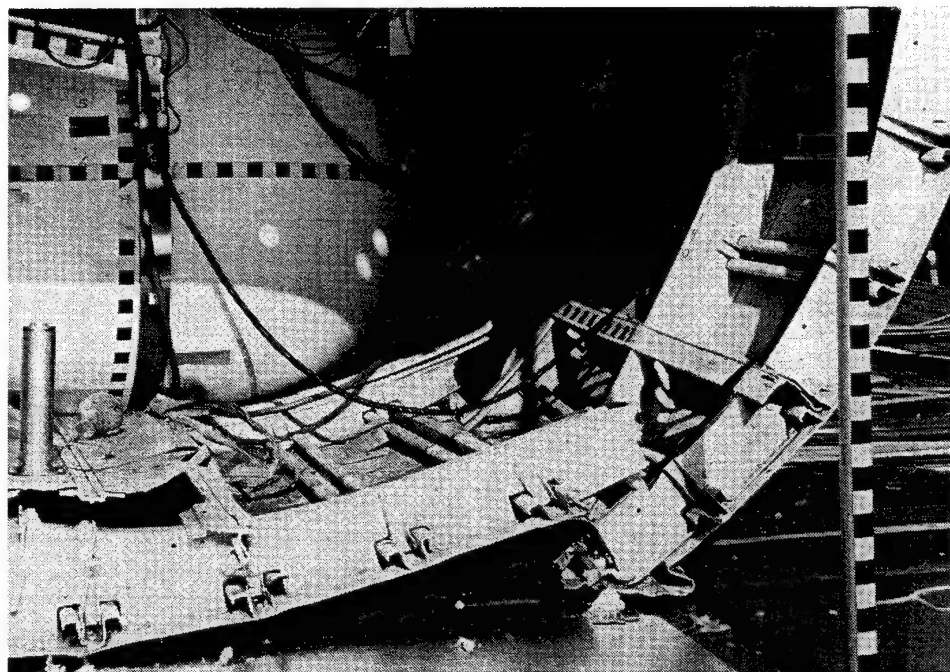


FIGURE 66. FORWARD LEFT SIDE LOWER FUSELAGE SECTION,  
POSTTEST

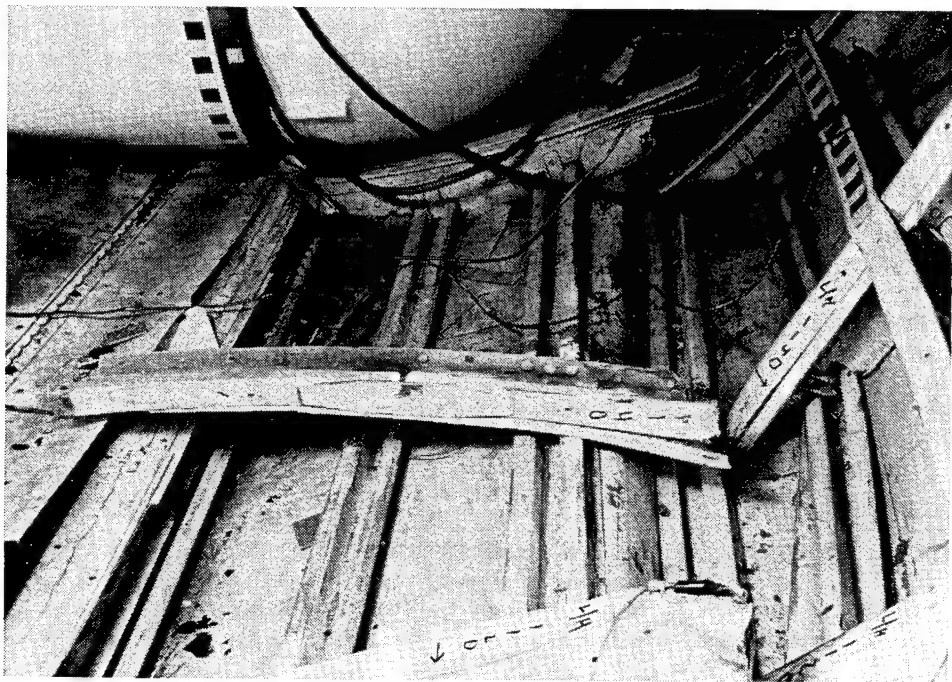


FIGURE 67. LOWER FUSELAGE SECTION, LEFT SIDE BS 1140, POSTTEST

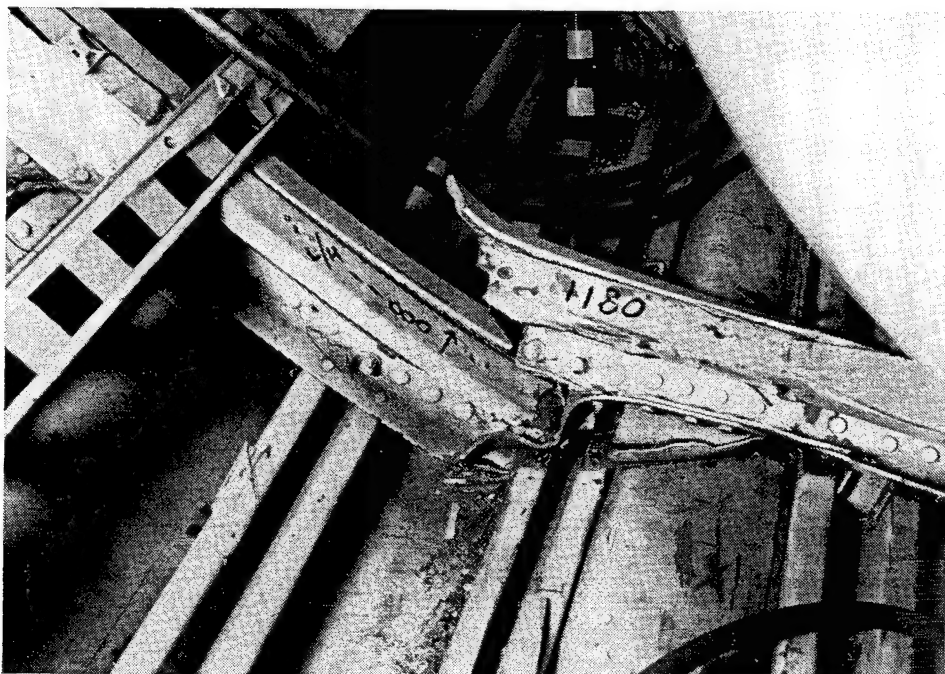


FIGURE 68. LOWER FUSELAGE SECTION, LEFT SIDE BS 1180, POSTTEST

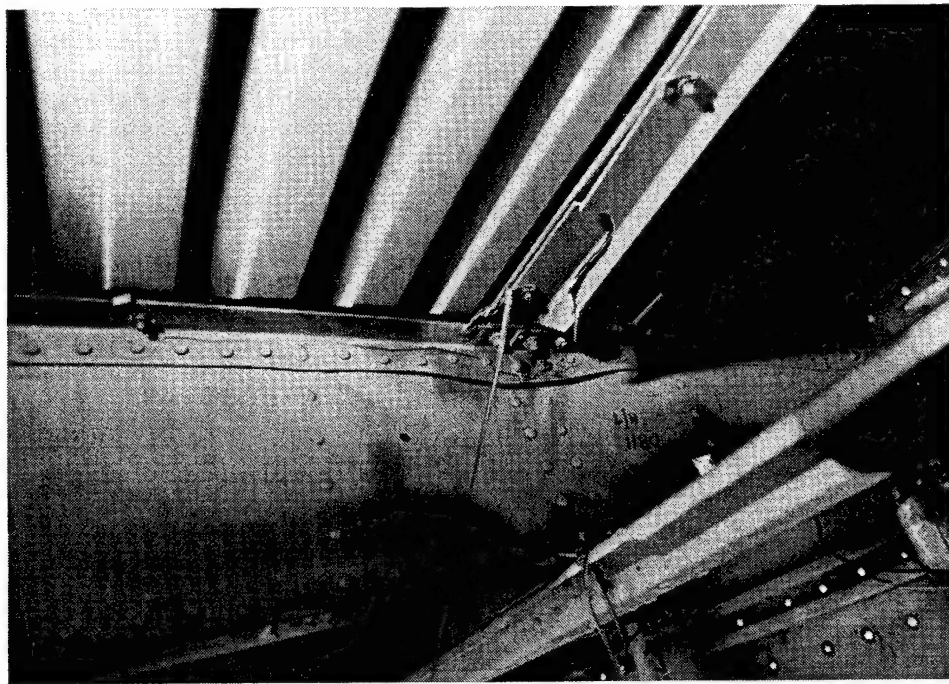


FIGURE 69. UNDERSIDE FUSELAGE FLOOR SECTION LEFT SIDE BS 1180,  
POSTTEST

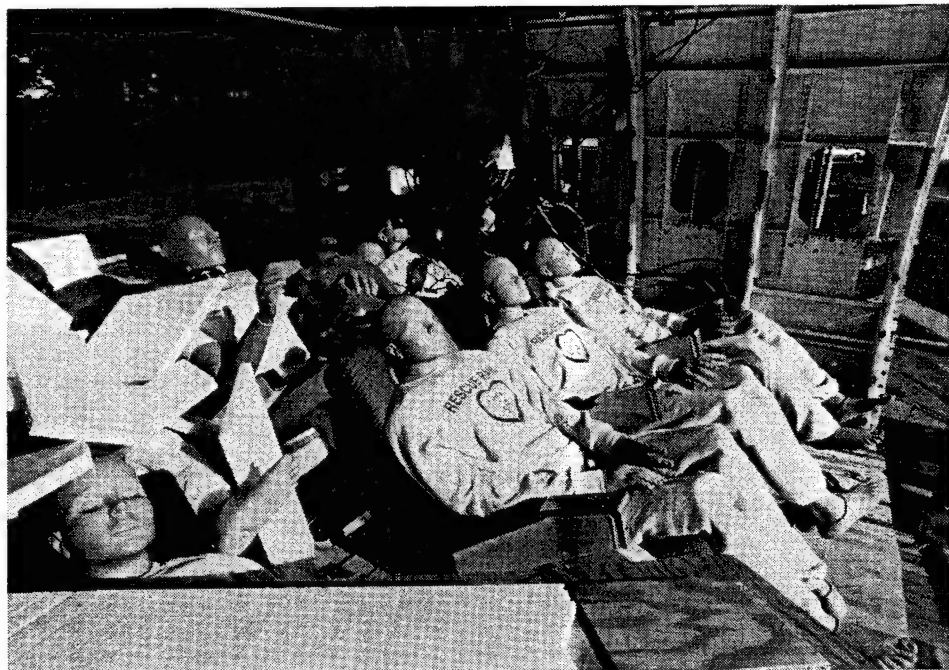


FIGURE 70. FUSELAGE INTERIOR RIGHT QUARTER VIEW, POSTTEST

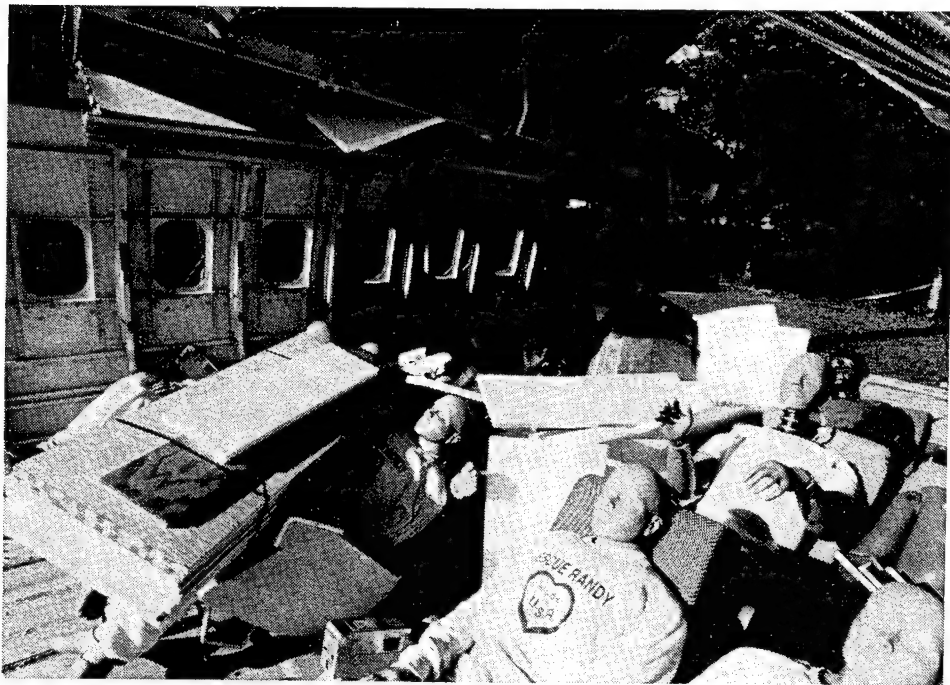


FIGURE 71. FUSELAGE INTERIOR LEFT QUARTER VIEW, POSTTEST



FIGURE 72. FUSELAGE INTERIOR SEATS 16-18, POSTTEST

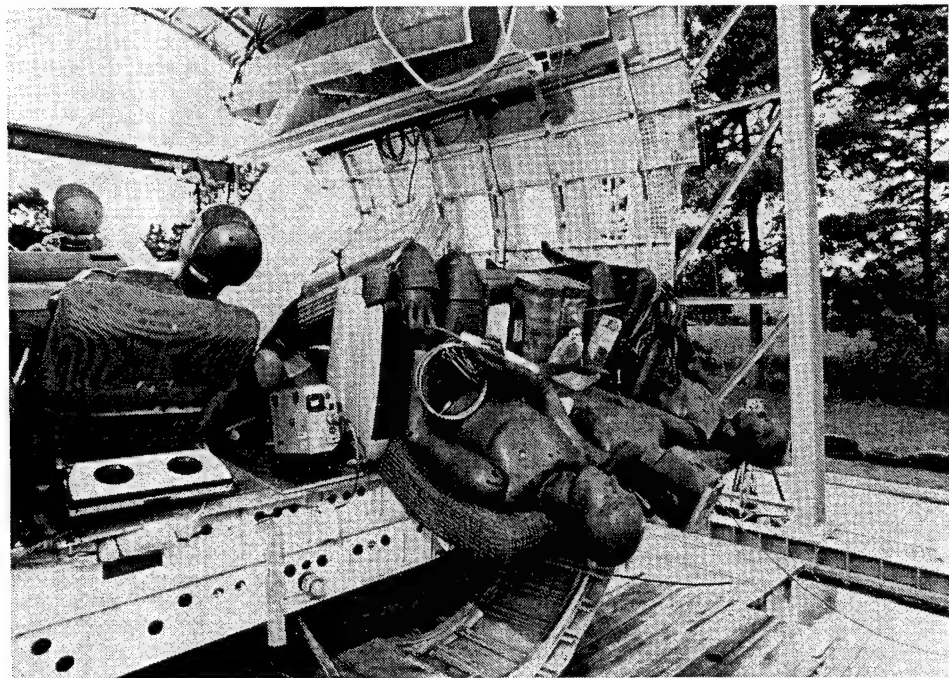


FIGURE 73. FUSELAGE INTERIOR REAR VIEW, POSTTEST

## CONCLUSIONS

At a 30-feet-per-second vertical impact velocity, this drop test of a narrow-body fuselage section resulted in a severe but survivable test which could be expected to inflict moderate injury to occupants. The average idealized triangular pulse deceleration for the fuselage was 36 G<sub>max</sub>, with an approximate duration of 57 milliseconds.

The cabin area maintained its structural integrity and provided a habitable environment. Due to the tapered nature of the fuselage, the measured fuselage accelerations decreased from BS1120 (front) to BS1240 (rear).

Compared to similar tests conducted previously, the measured accelerations on this aircraft structure and bins were higher than expected. This was due to the auxiliary fuel tank installation which prevented additional fuselage crushing, thereby, not allowing the fuselage to absorb additional impact energy. In other words, the same aircraft section without a tank, under the same conditions, should have experienced lesser G forces.

The auxiliary fuel tank crushed approximately four inches at the center lower surface due to the penetration of the fuel discharge hardware. The tank remained connected to its mounting and did not penetrate the cabin area. A redesign of the auxiliary fuel tank discharge plumbing might prevent a rupture of the lower tank and thereby prevent fuel leakage.

The Boeing bin maintained its structural integrity and remained attached to the fuselage after the test, although four links of a total of fifteen, fractured after the primary impact. The door of this bin was strapped closed for test purposes otherwise its contents would have spilled out due to the fracture of its door hinges and latching mechanism.

A comparison of the calculated loads and the measured loads for the upper attachment links of the Boeing bin showed good correlation with minimal dynamic amplification. The measured and analytical data may be used to evaluate current regulatory requirements and analytical load predictive methodologies.

The passenger service units (PSU) attached to the Boeing bin came lose primarily due to the relative motion between the bin and the fuselage. The PSUs were attached to both the bin and the fuselage side wall.

Two of six C&D bin attachments separated. The bin exhibited an additional structural fracture, resulting in the bin breaking up and remaining only partially attached to the fuselage structure. This resulted in the spilling of the bin contents.

A comparison of the calculated loads and the measured loads, up to the point of failure, for the upper brackets of the C&D bin showed good correlation with minimal dynamic amplification. Again, the measured and analytical data may be used to evaluate current regulatory requirements and analytical load predictive methodologies.

## REFERENCES

1. Aircraft Safety Research Plan, November 1991, Federal Aviation Administration Technical Center, Atlantic City International Airport, NJ 08405.
2. Impact Data From a Transport Aircraft During a Controlled Impact Demonstration, NASA Technical Paper 2589, September 1986.
3. Galley and Overhead Compartment Experiment Results - Full-Scale Transport Controlled Impact Demonstration, DOT/FAA/CT-85/33, December 1985, Federal Aviation Administration Technical Center, Atlantic City International Airport, NJ 08405.
4. Longitudinal Impact Test of a Transport Airframe Section, DOT/FAA/CT-87/26, July 1988, Federal Aviation Administration Technical Center, Atlantic City International Airport, NJ 08405.
5. Investigation of Transport Airplane Fuselage Fuel Tank Installations Under Crash Conditions, DOT/FAA/CT-88/24, July 1989, Federal Aviation Administration Technical Center, Atlantic City International Airport, NJ 08405.
6. Longitudinal Acceleration Test of Overhead Luggage Bins in a Transport Airframe Section, DOT/FAA/CT-92/9, November 1992, Federal Aviation Administration Technical Center, Atlantic City International Airport, NJ 08405.
7. Characterization of the Strain Gage Bonded on the Overhead Bin Attachments, DOT/FAA/CT-TN94/24, (Draft), Federal Aviation Administration Technical Center, Atlantic City International Airport, NJ 08405.
8. Society of Automotive Engineers, SAE Recommended Practice: SAE J211, "Instrumentation for Impact Test," October 1988.

## APPENDIX A

### DYNAMIC TEST DATA

FUSELAGE DATA (A-1)

OVERHEAD STOWAGE BIN DATA (A-11)

TANK DATA (A-27)

PLATFORM AND ANTHROPOMORPHIC DUMMIES DATA (A-35)

## FUSELAGE DATA

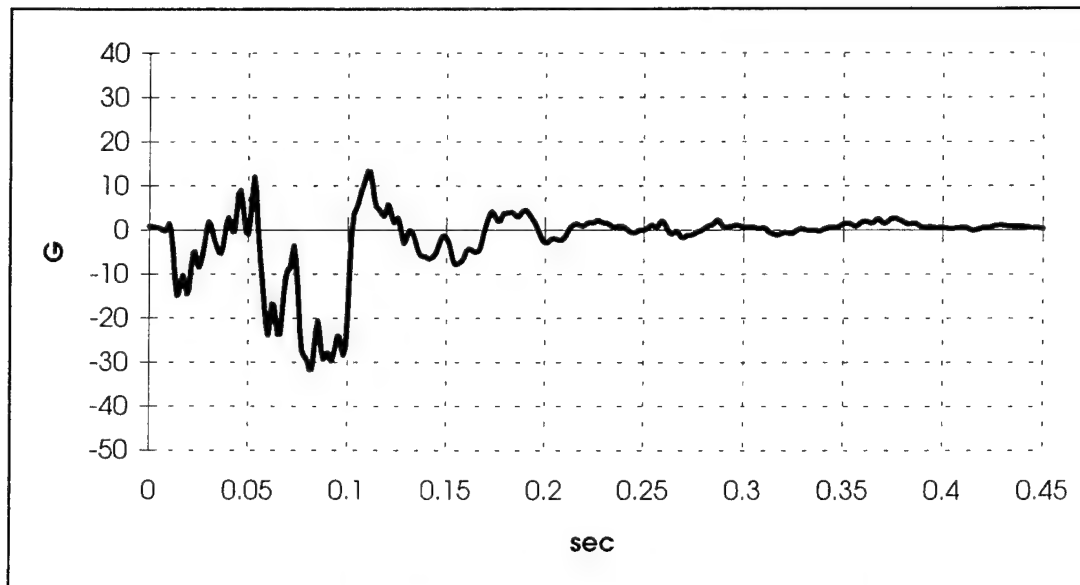


FIGURE A-1: BS1120 FLOOR PORT VERTICAL ACCELERATION

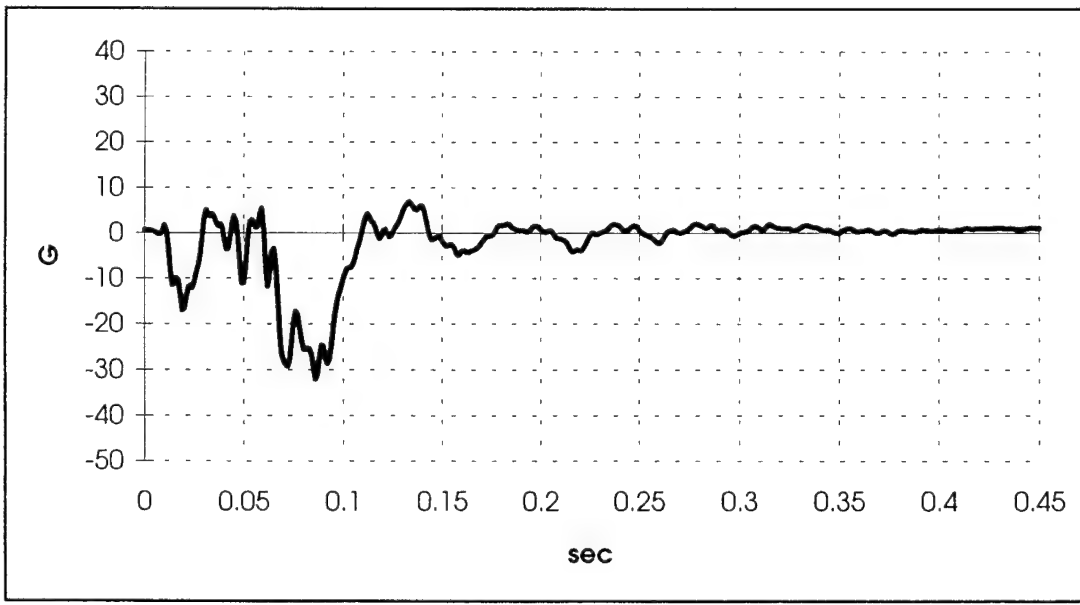


FIGURE A-2: BS1120 FLOOR STARBOARD VERTICAL ACCELERATION

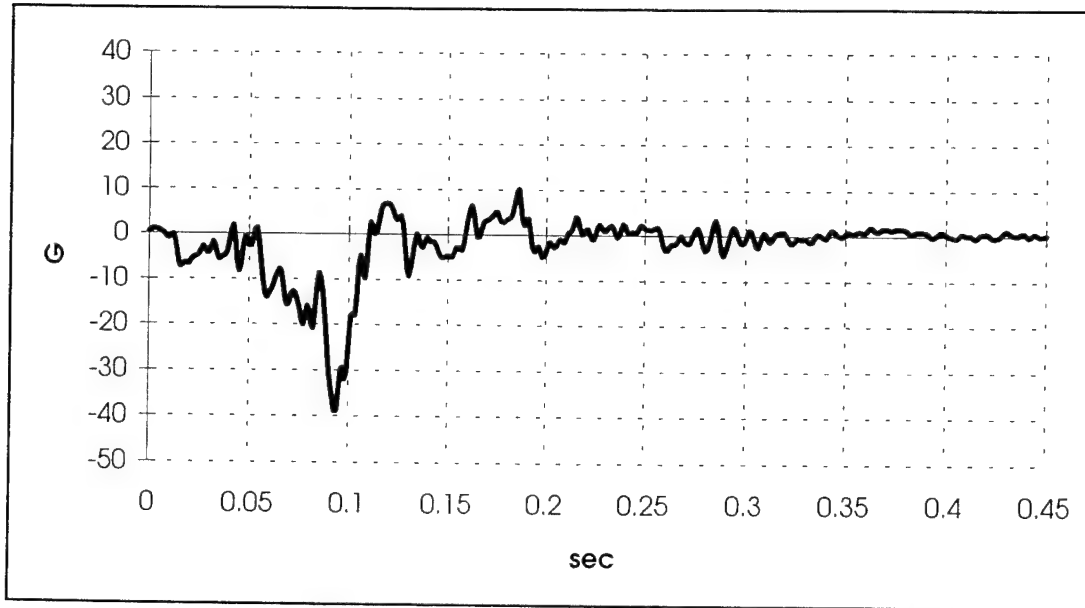


FIGURE A-3: BS1180 TOP PORT VERTICAL ACCELERATION

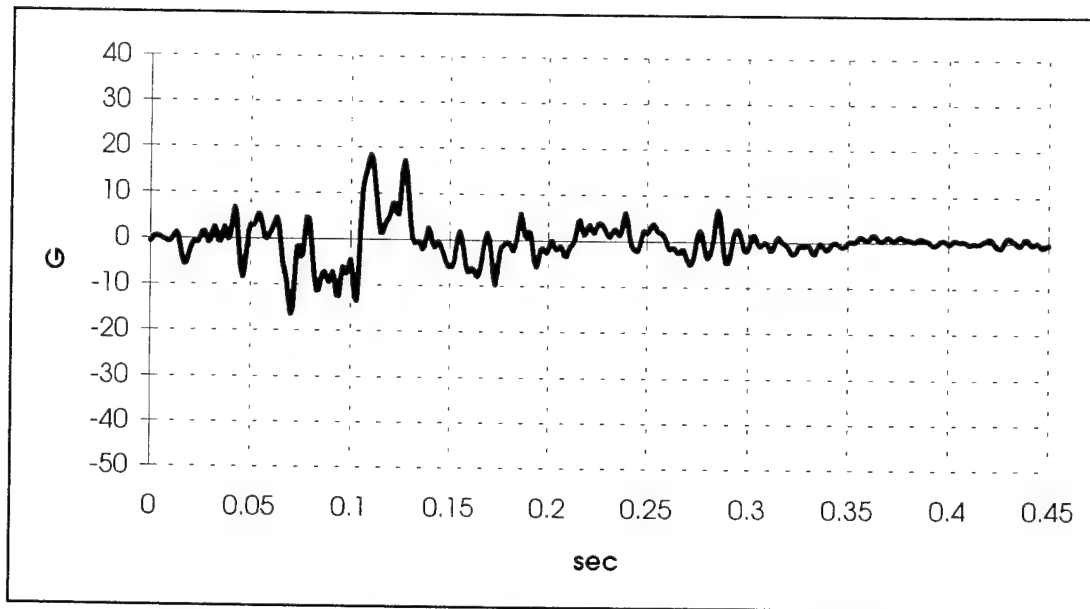


FIGURE A-4: BS1180 TOP PORT LATERAL ACCELERATION

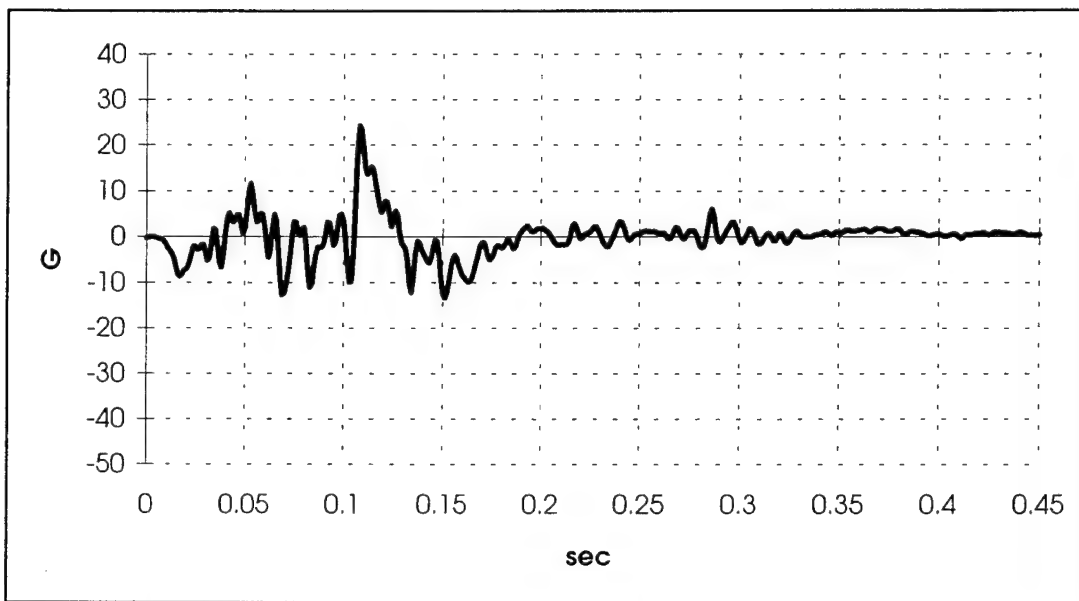


FIGURE A-5: BS1180 TOP PORT LONGITUDINAL ACCELERATION

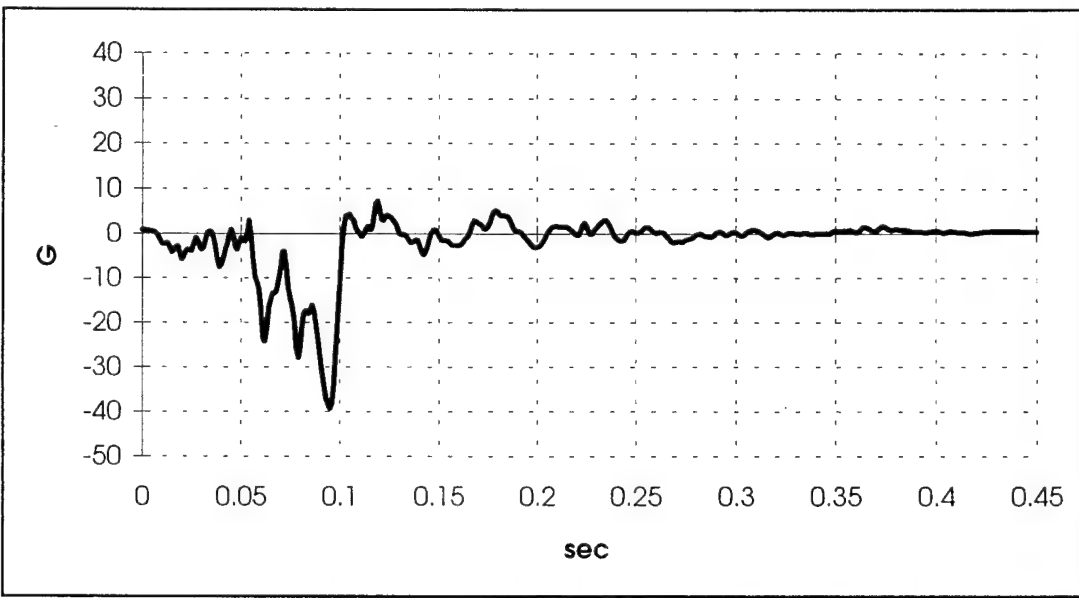


FIGURE A-6: BS1180 FLOOR PORT VERTICAL ACCELERATION

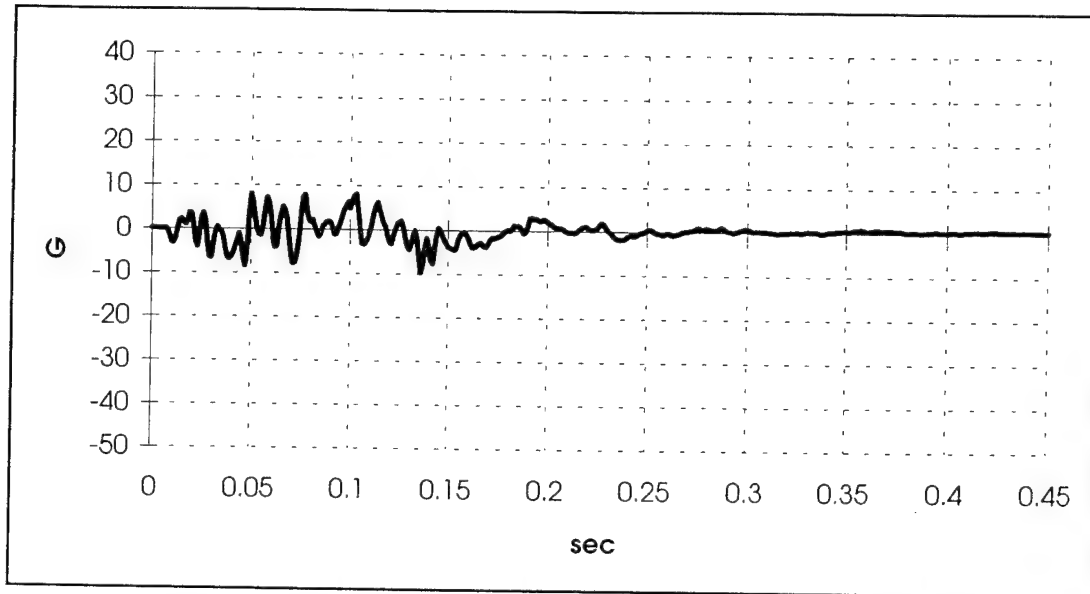


FIGURE A-7: BS1180 FLOOR PORT LATERAL ACCELERATION

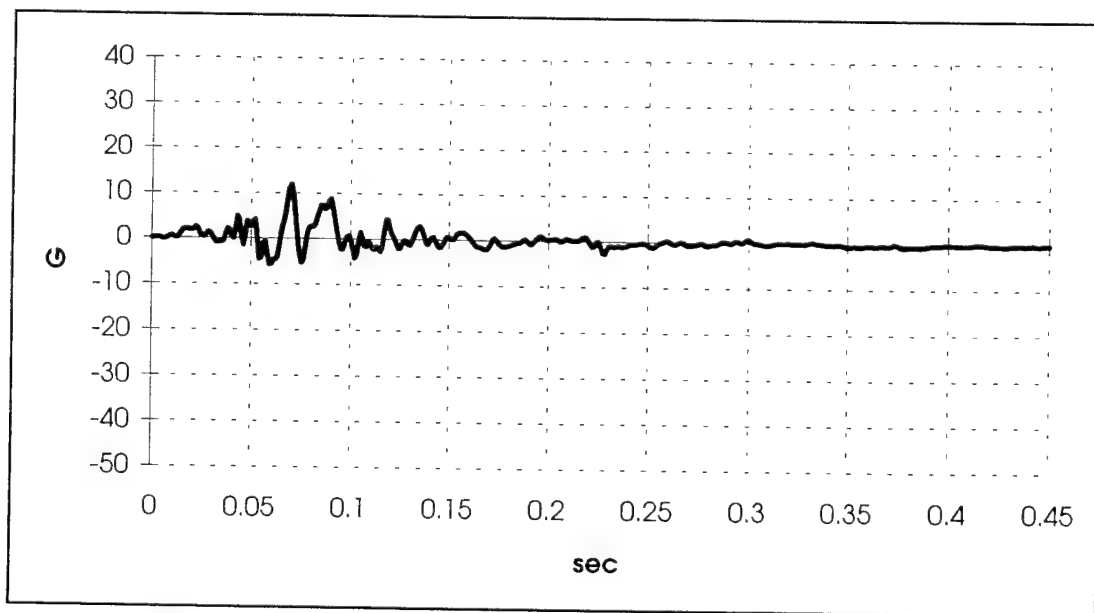


FIGURE A-8: BS1180 FLOOR PORT LONGITUDINAL ACCELERATION

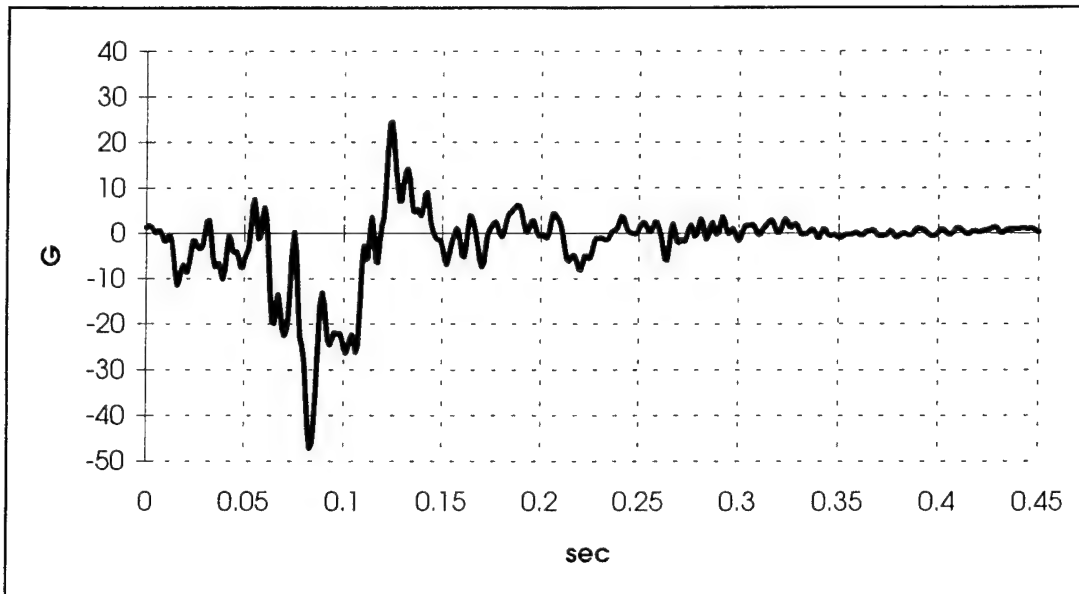


FIGURE A-9: BS1180 TOP STARBOARD VERTICAL ACCELERATION

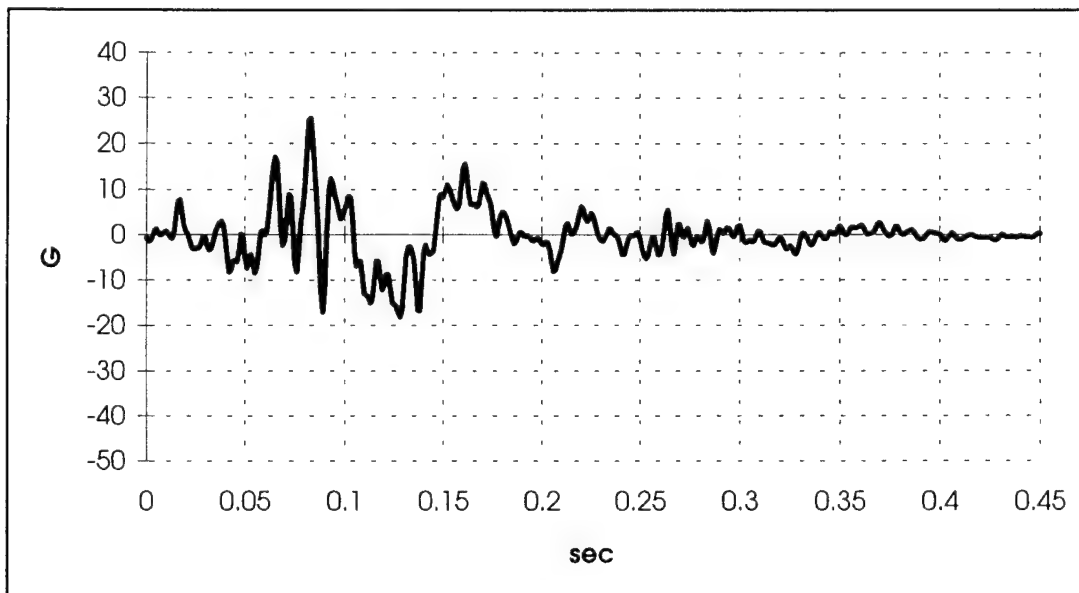


FIGURE A-10: BS1180 TOP STARBOARD LATERAL ACCELERATION

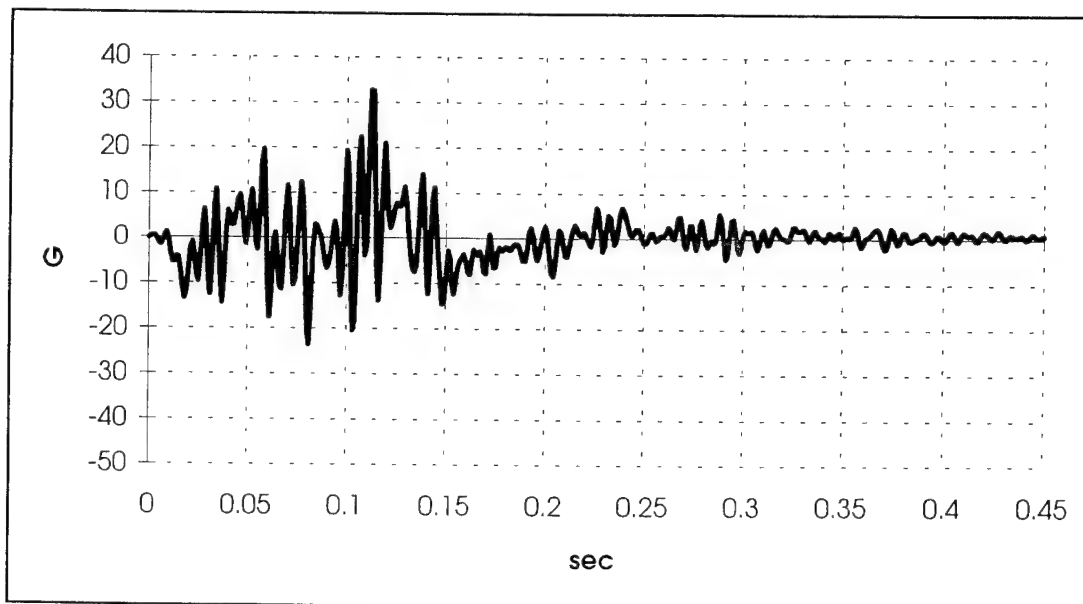


FIGURE A-11: BS1180 TOP STARBOARD LONGITUDINAL ACCELERATION

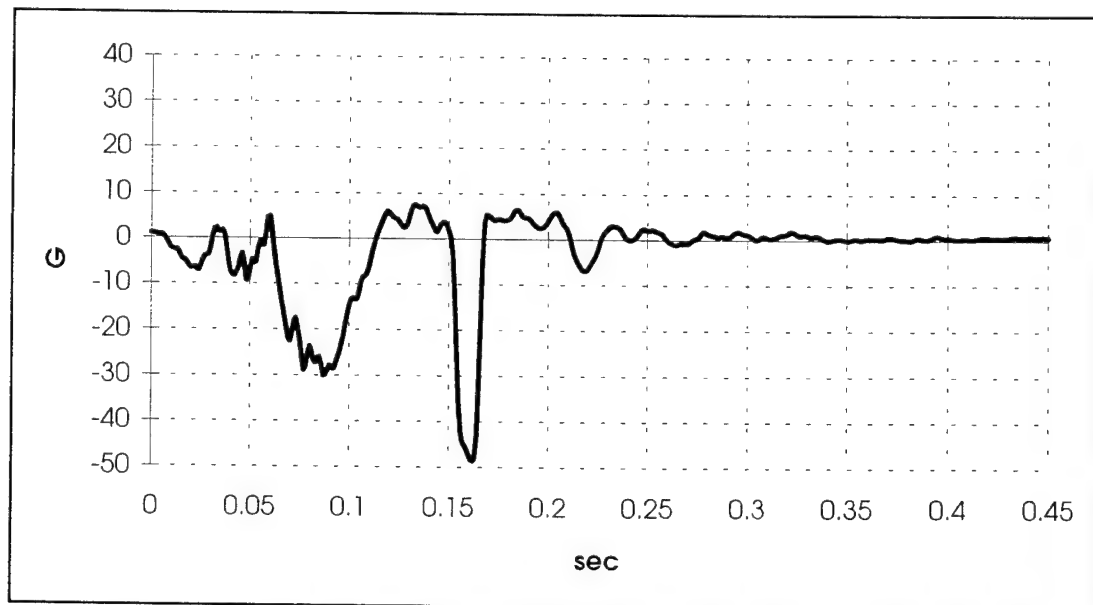


FIGURE A-12: BS1180 FLOOR STARBOARD VERTICAL ACCELERATION

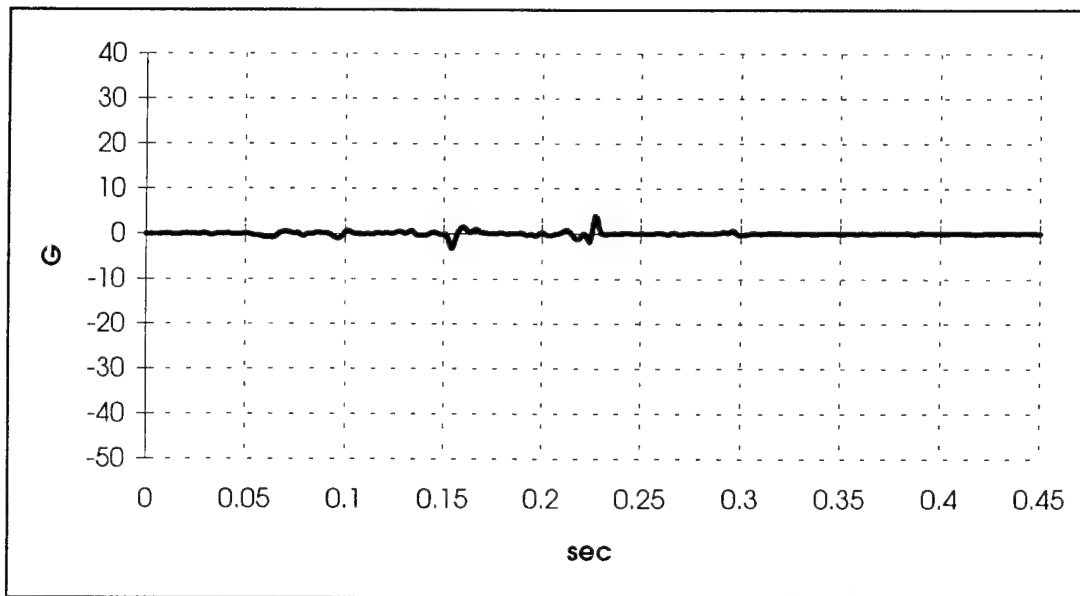


FIGURE A-13: BS1180 FLOOR STARBOARD LATERAL ACCELERATION

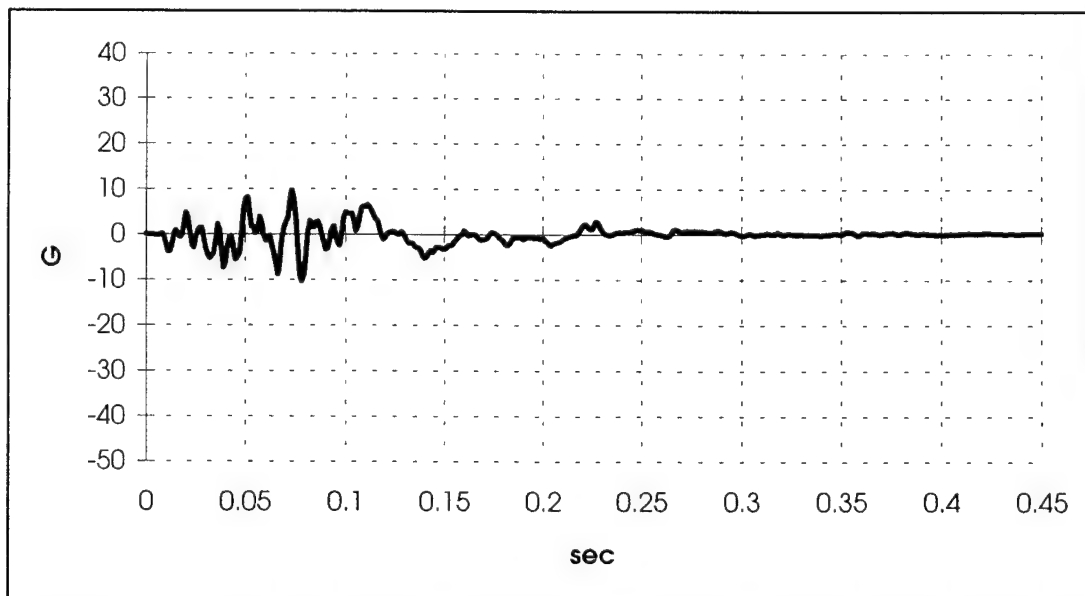


FIGURE A-14: BS1180 FLOOR STARBOARD LONGITUDINAL ACCELERATION

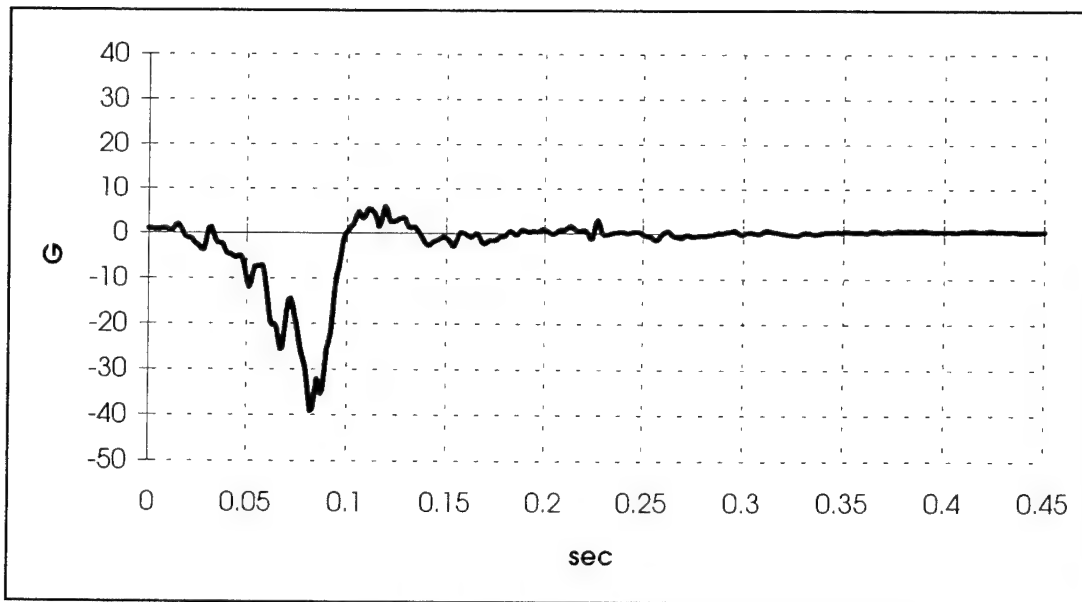


FIGURE A-15: BS1170 PORT SEAT TRACK ACCELERATION

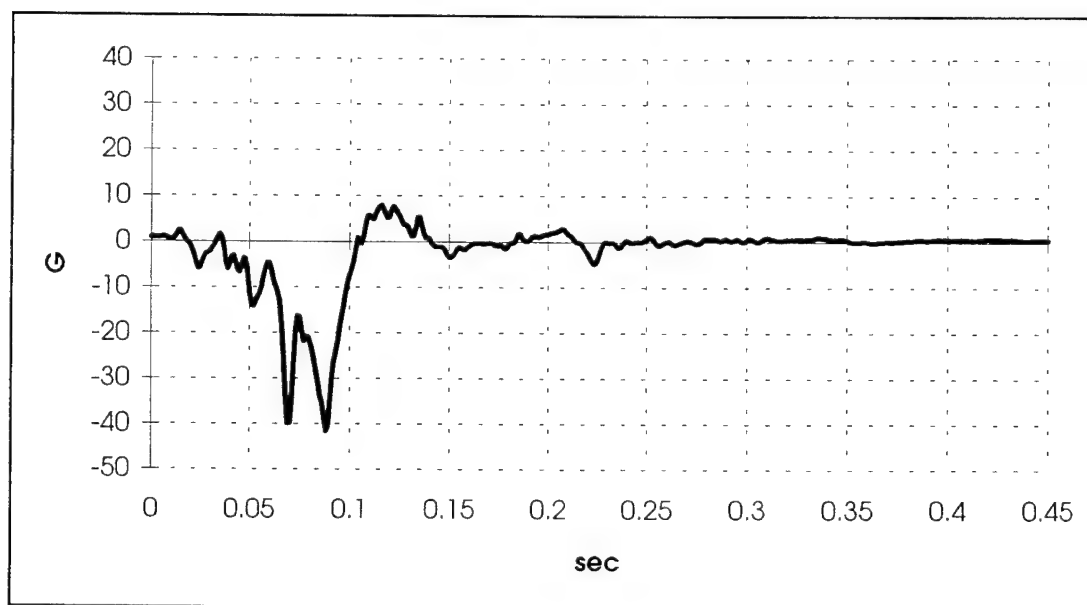


FIGURE A-16: BS1170 STARBOARD SEAT TRACK ACCELERATION

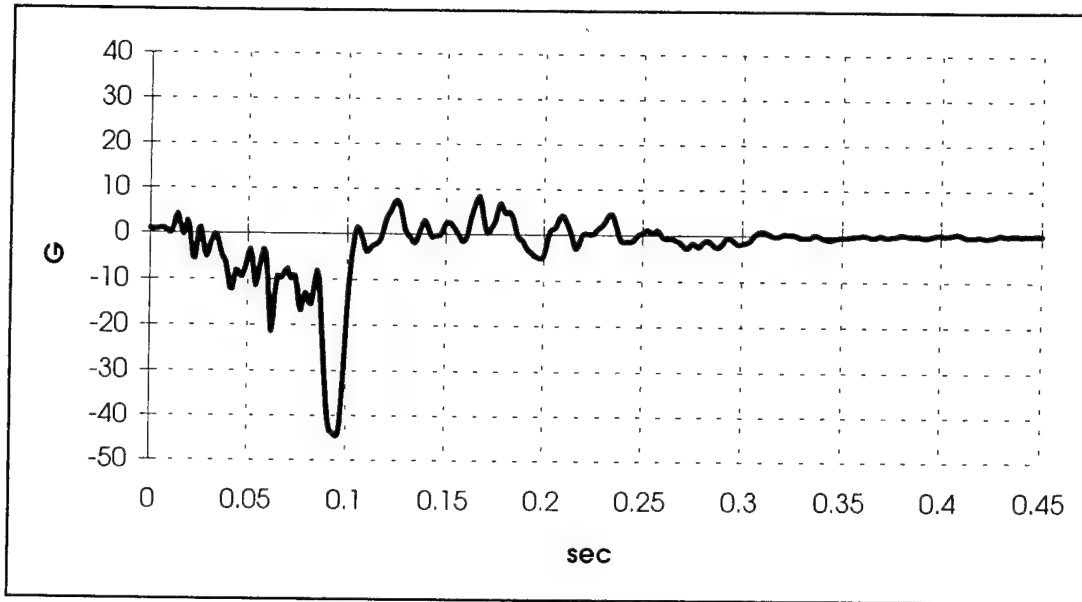


FIGURE A-17: BS1240 FLOOR PORT VERTICAL ACCELERATION

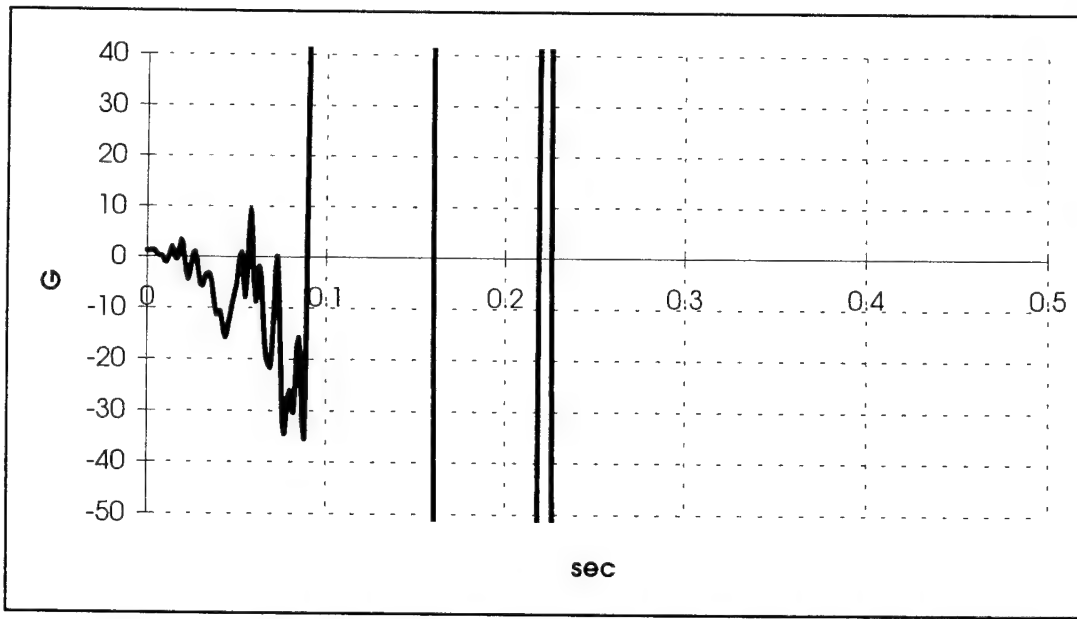


FIGURE A-18: BS1240 FLOOR STARBOARD VERTICAL ACCELERATION

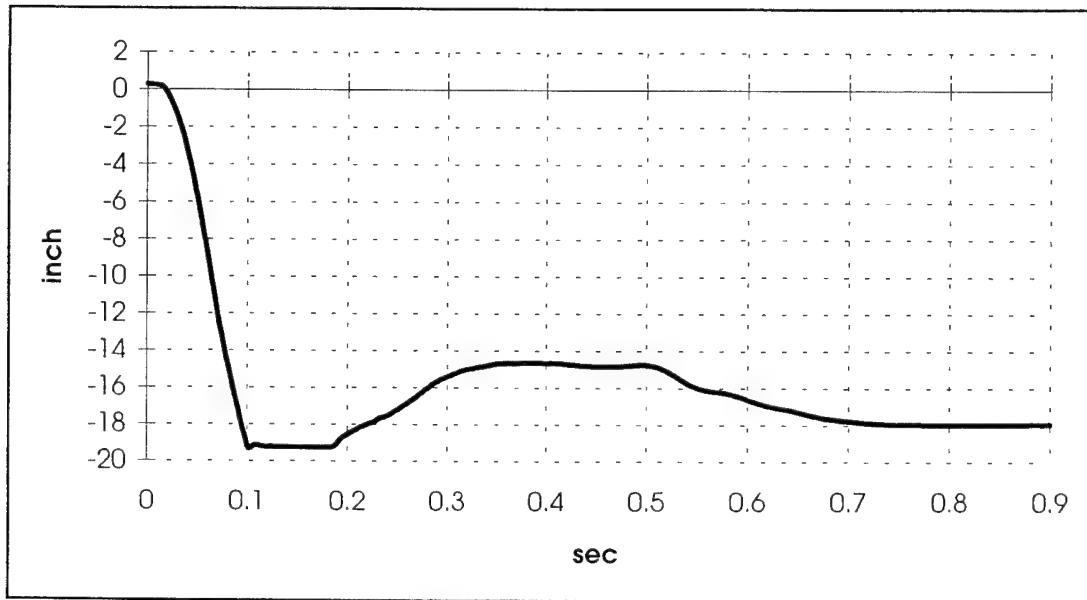


FIGURE A-19: BS1140 BOTTOM DEFORMATION

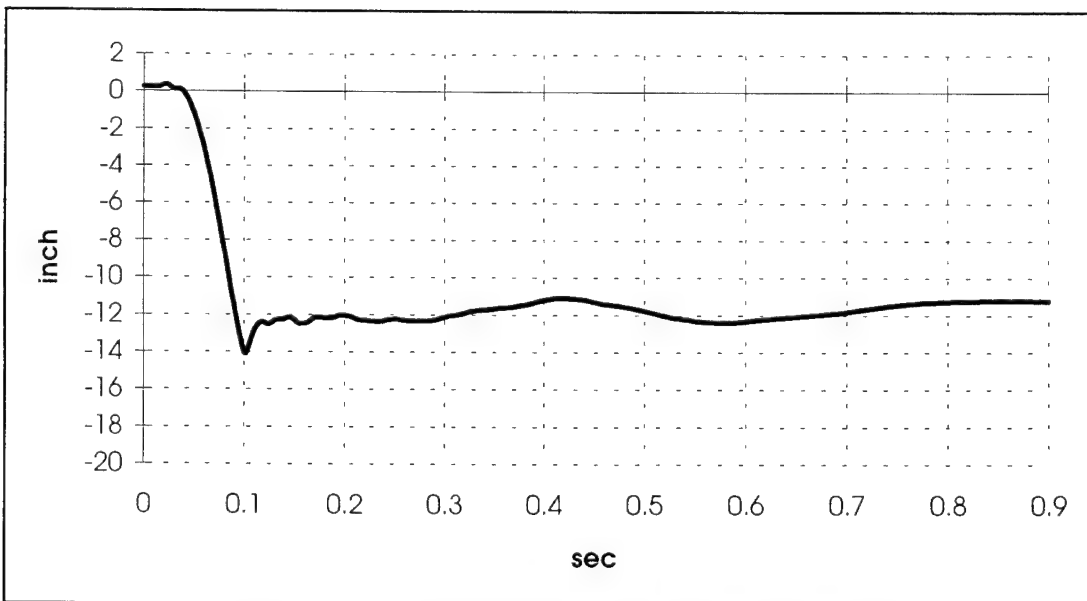


FIGURE A-20: BS1220 BOTTOM DEFORMATION

## OVERHEAD STOWAGE BIN DATA

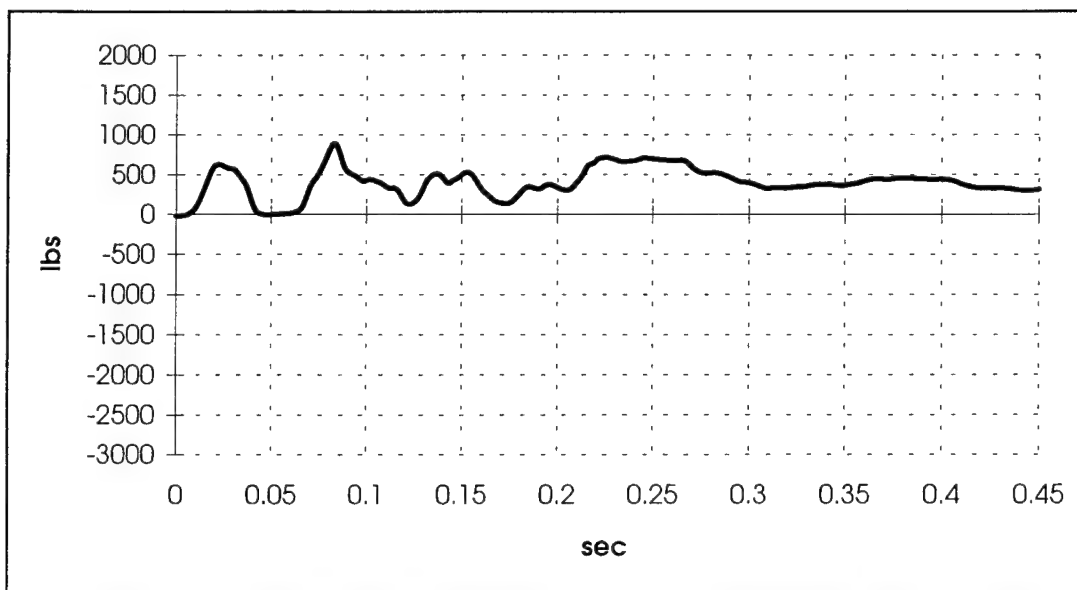


FIGURE A-21: C&D UF2A3 FORWARD BRACKET BENDING GAGE LOAD

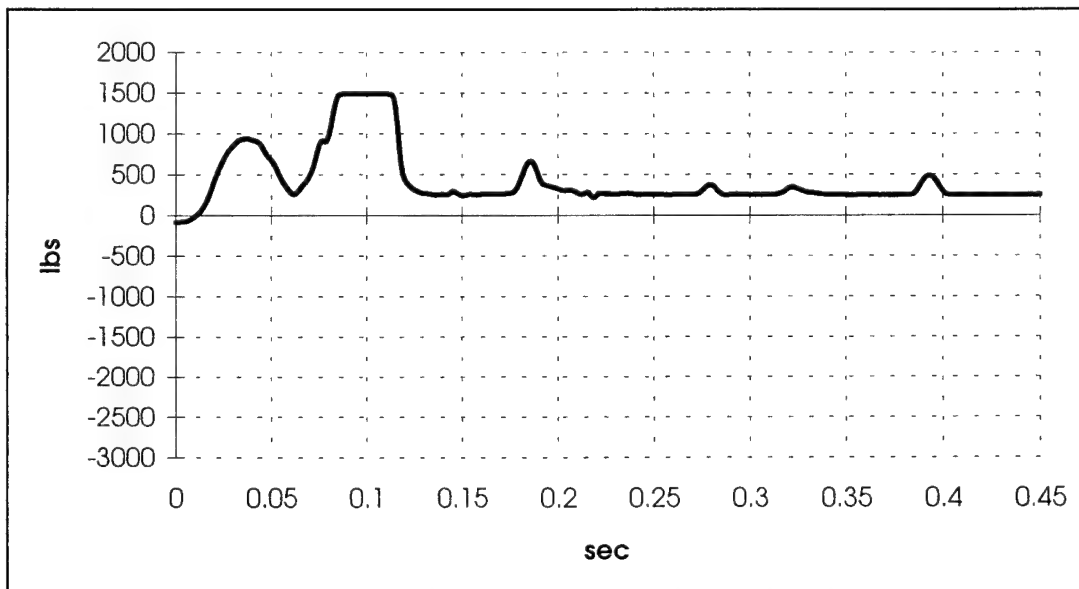


FIGURE A-22: C&D UM3 MIDDLE BRACKET BENDING GAGE LOAD

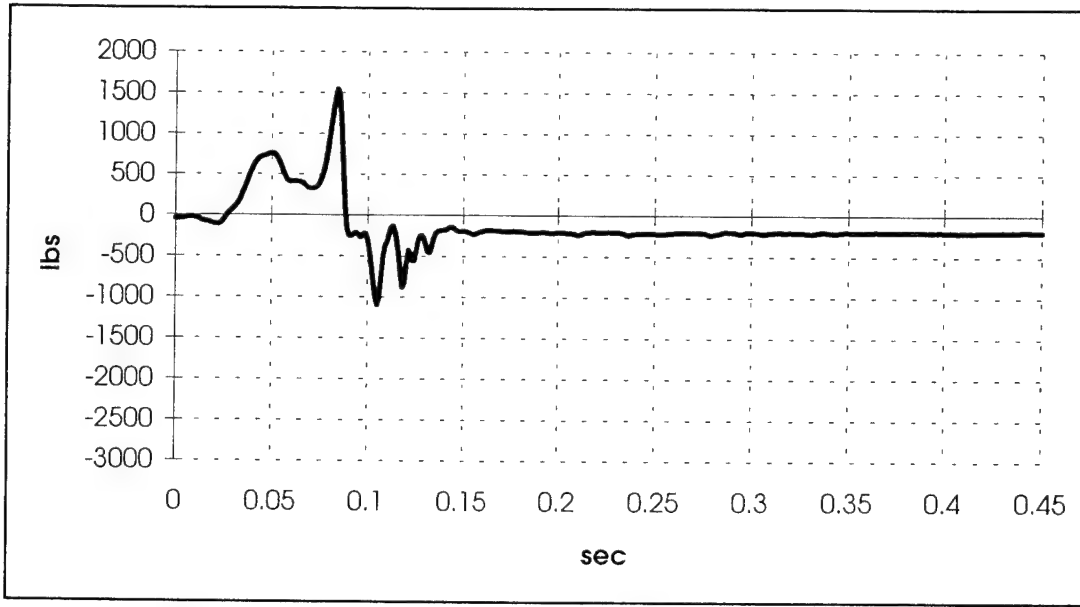


FIGURE A-23: C&D UR1A3 AFT BRACKET AXIAL GAGE LOAD

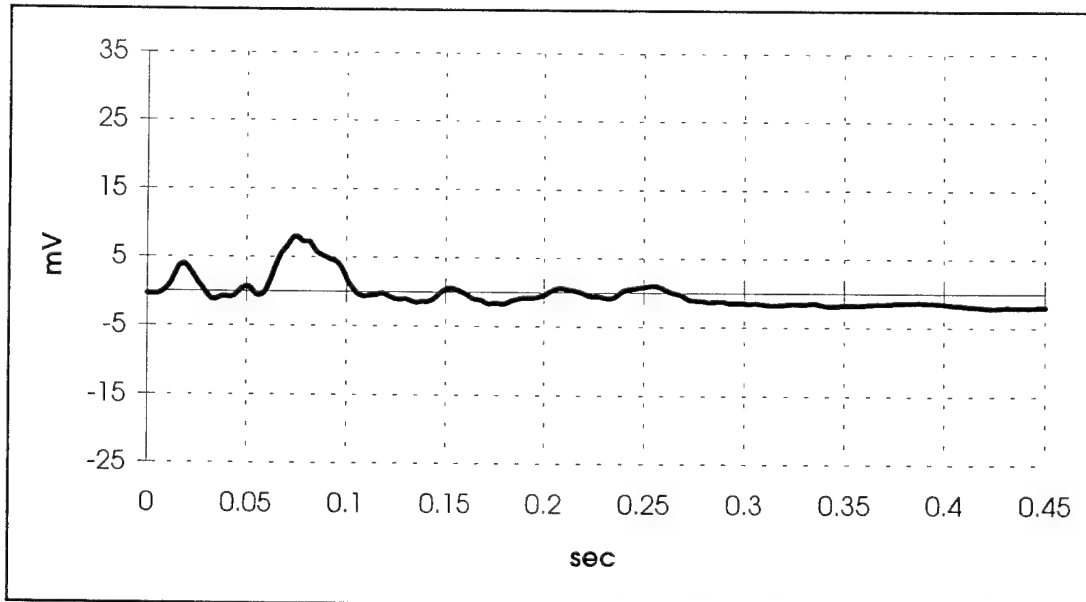


FIGURE A-24: C&D CL1A FORWARD FITTING AXIAL GAGE ELECTRICAL OUTPUT

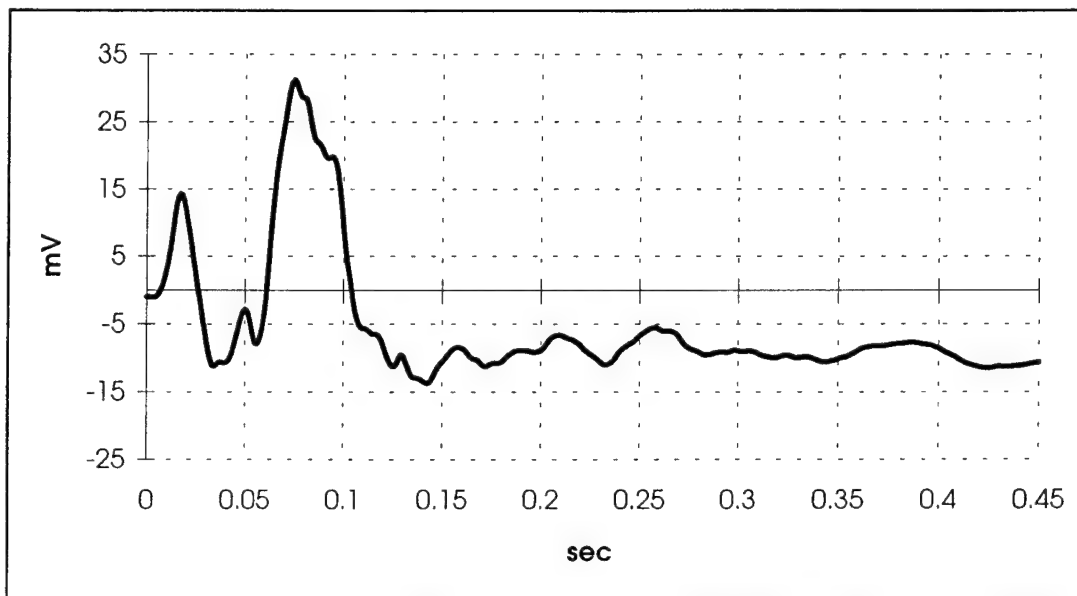


FIGURE A-25: C&D CL1A FORWARD FITTING BENDING GAGE ELECTRICAL OUTPUT

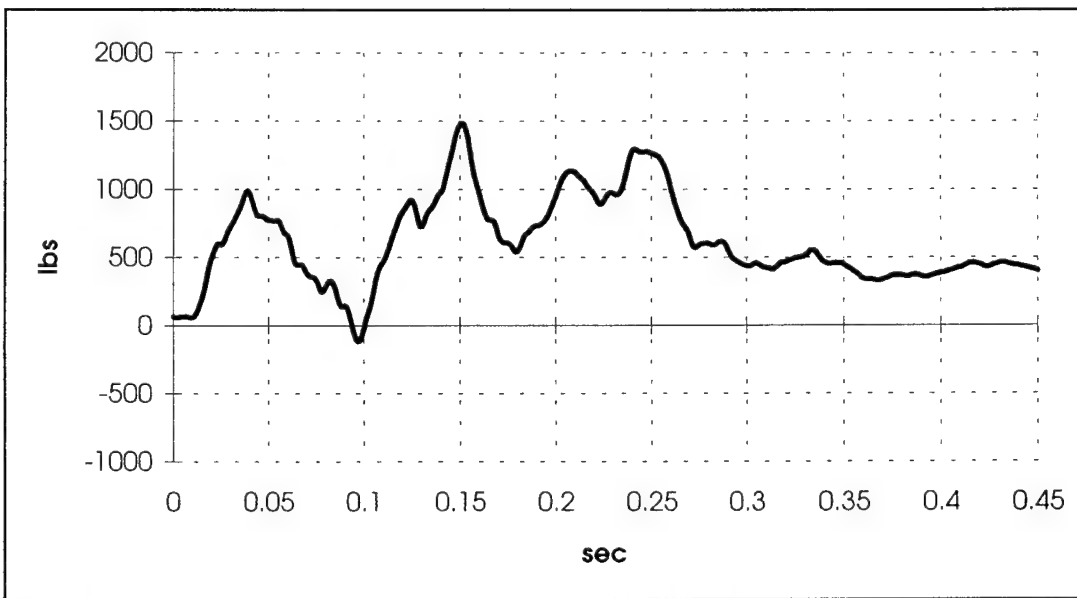


FIGURE A-26: C&D CL1A FORWARD FITTING LOAD IN THE Y' DIRECTION

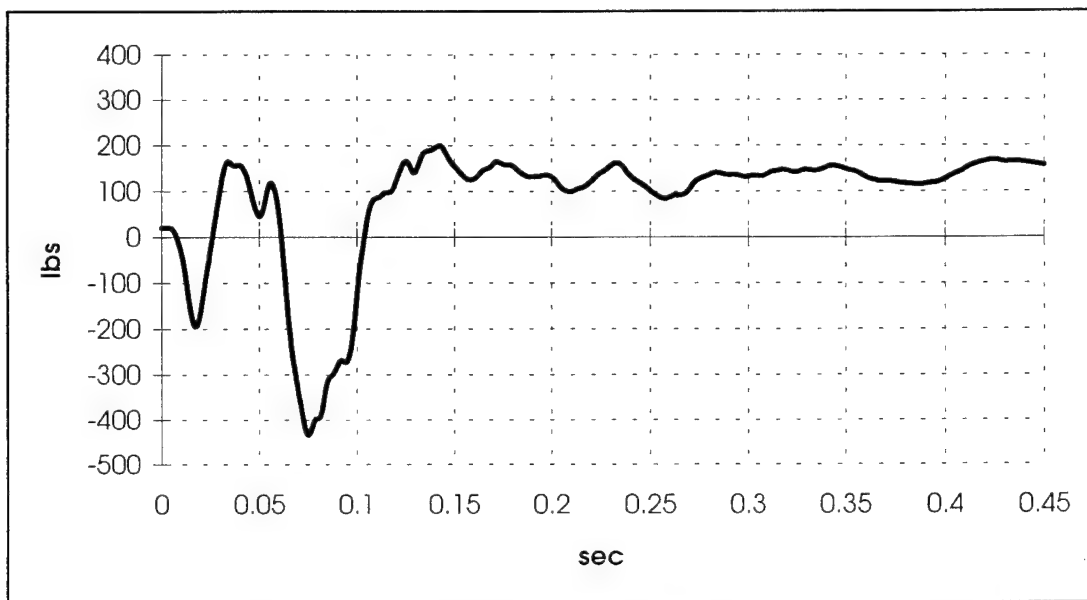


FIGURE A-27: C&D CL1A FORWARD FITTING LOAD IN THE  $Z'$  DIRECTION

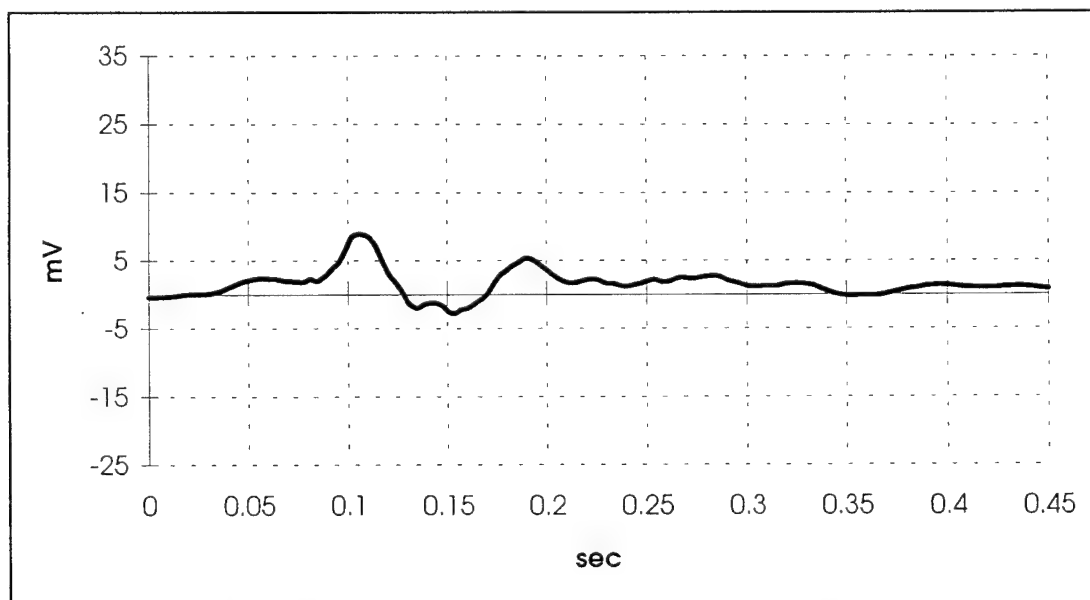


FIGURE A-28: C&D CL3A AFT FITTING AXIAL GAGE ELECTRICAL OUTPUT

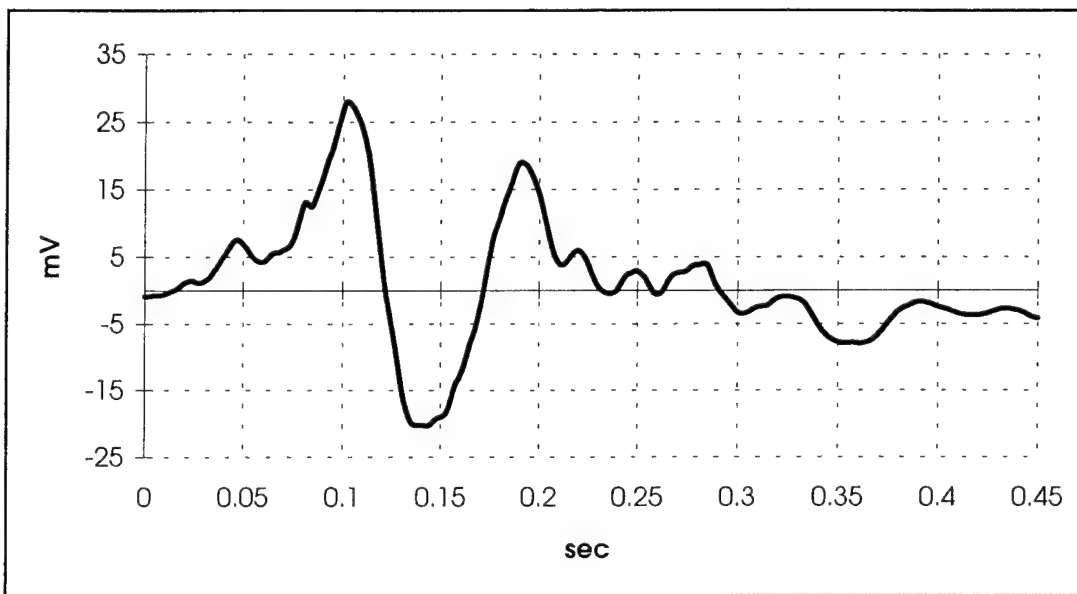


FIGURE A-29: C&D CL3A AFT FITTING BENDING GAGE ELECTRICAL OUTPUT

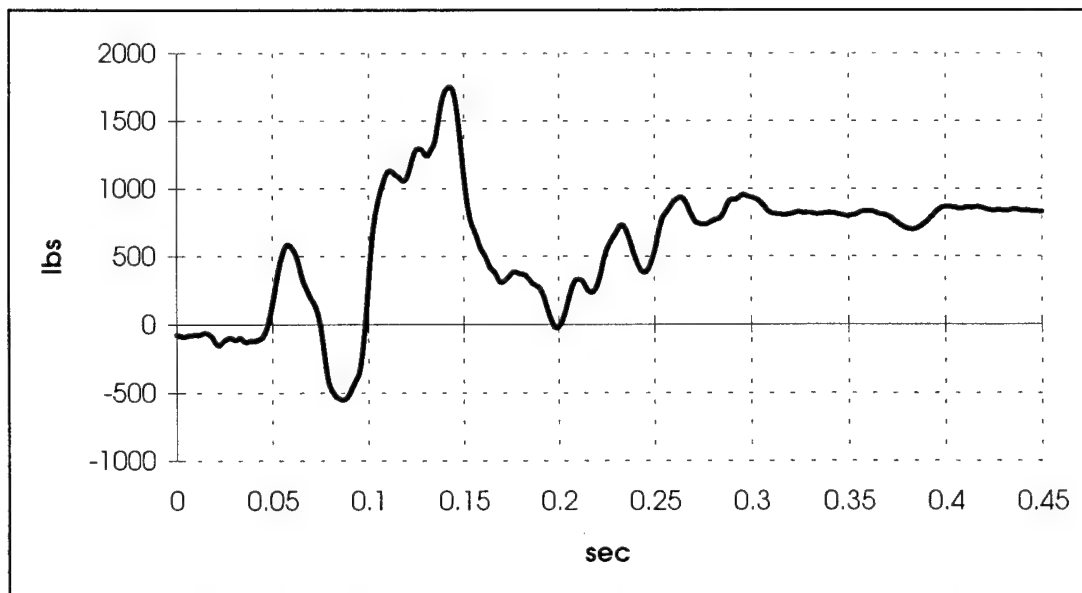


FIGURE A-30: C&D CL3A AFT FITTING LOAD IN THE Y' DIRECTION

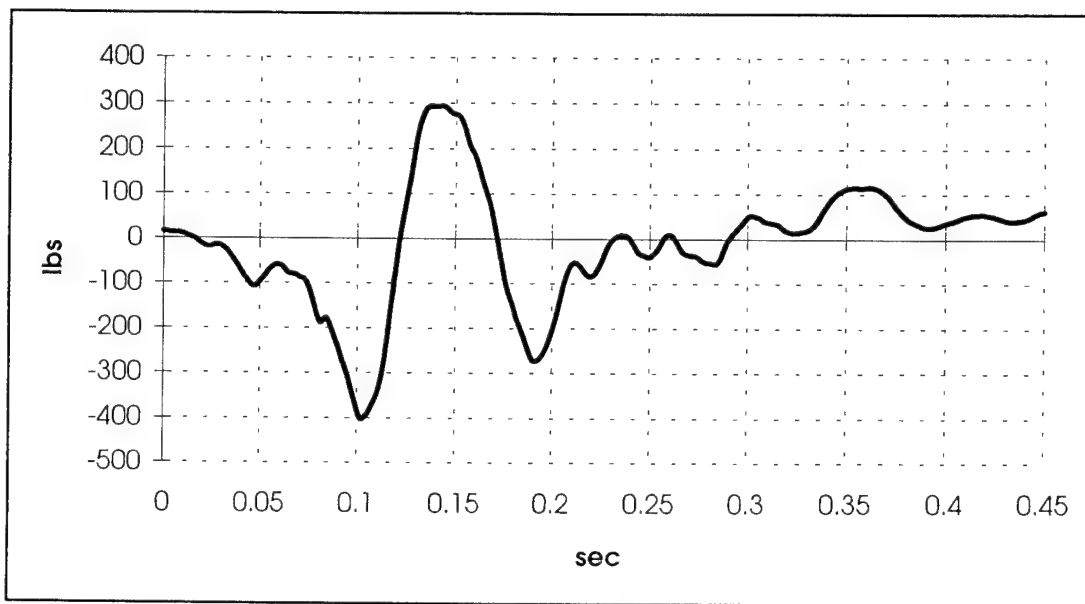


FIGURE A-31: C&D CL3A AFT FITTING LOAD IN THE Z' DIRECTION

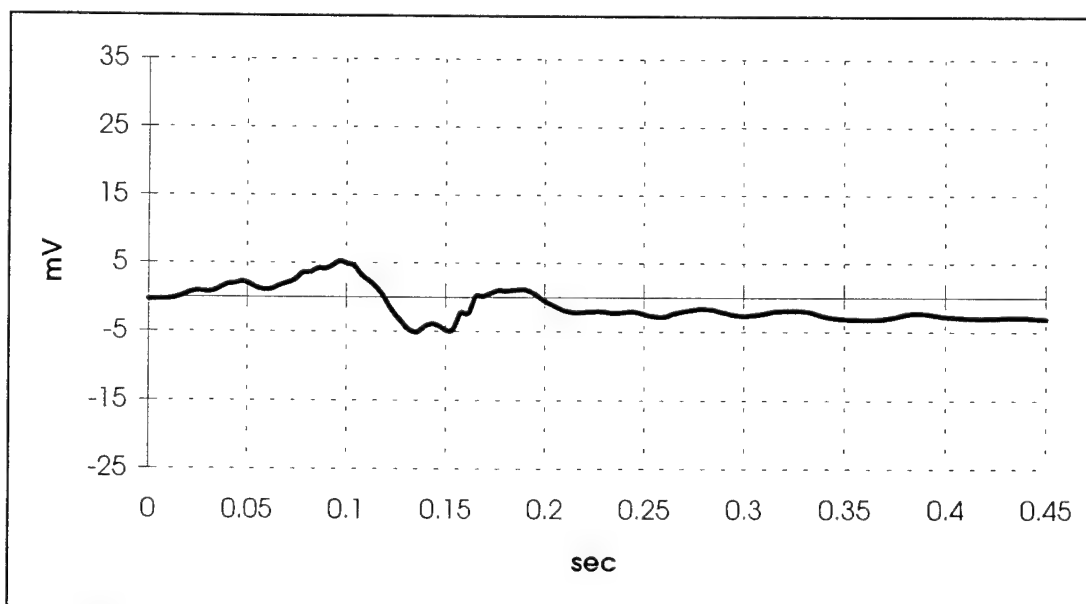


FIGURE A-32: C&D CL1B MIDDLE FITTING AXIAL GAGE ELECTRICAL OUTPUT

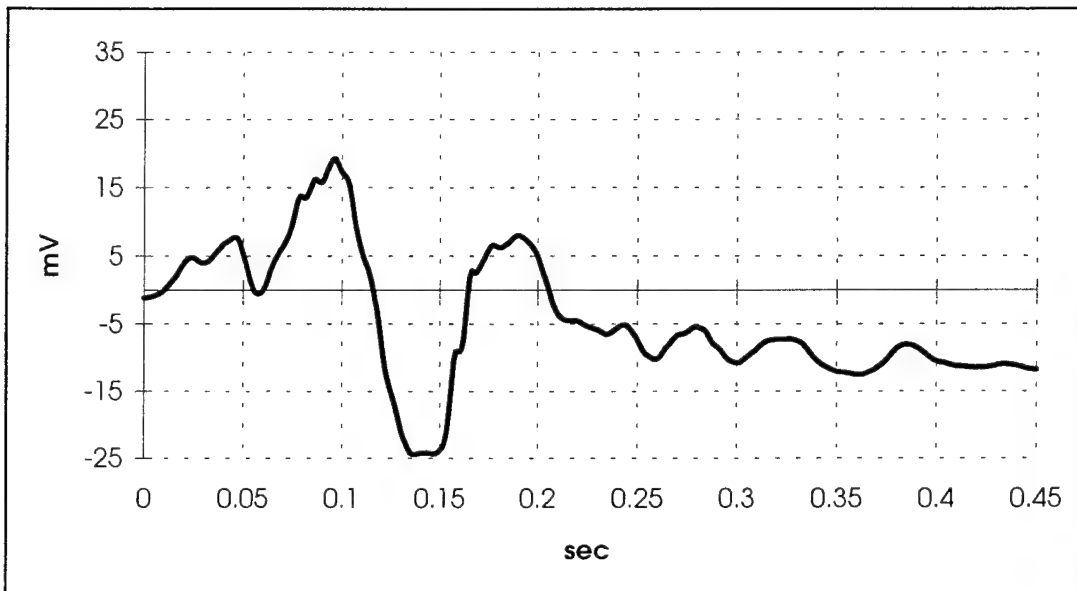


FIGURE A-33: C&D CL1B MIDDLE FITTING BENDING GAGE ELECTRICAL OUTPUT

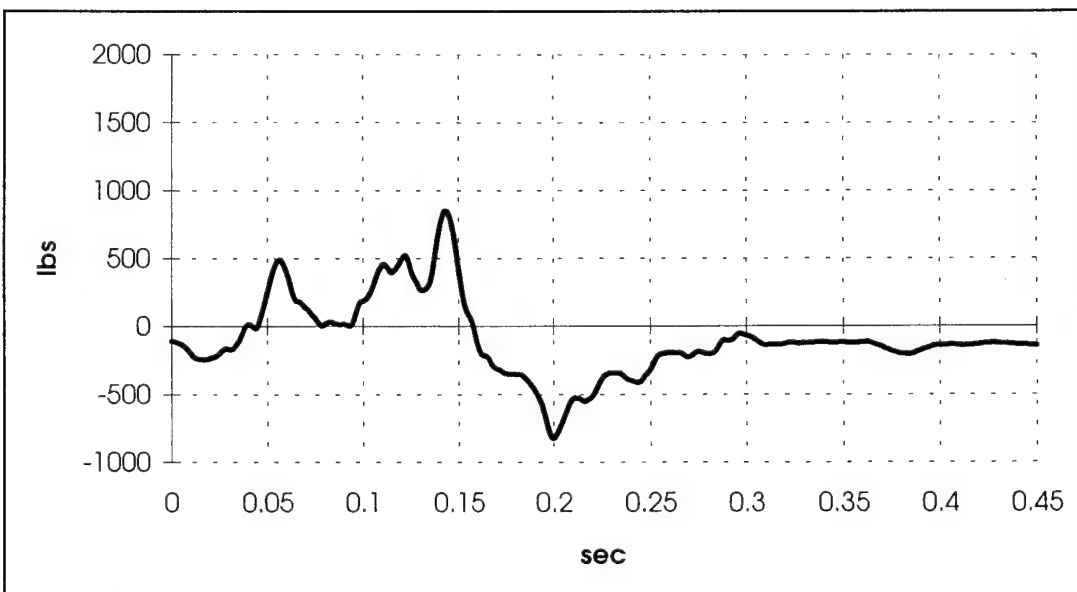


FIGURE A-34: C&D CL1B MIDDLE FITTING LOAD IN THE Y' DIRECTION

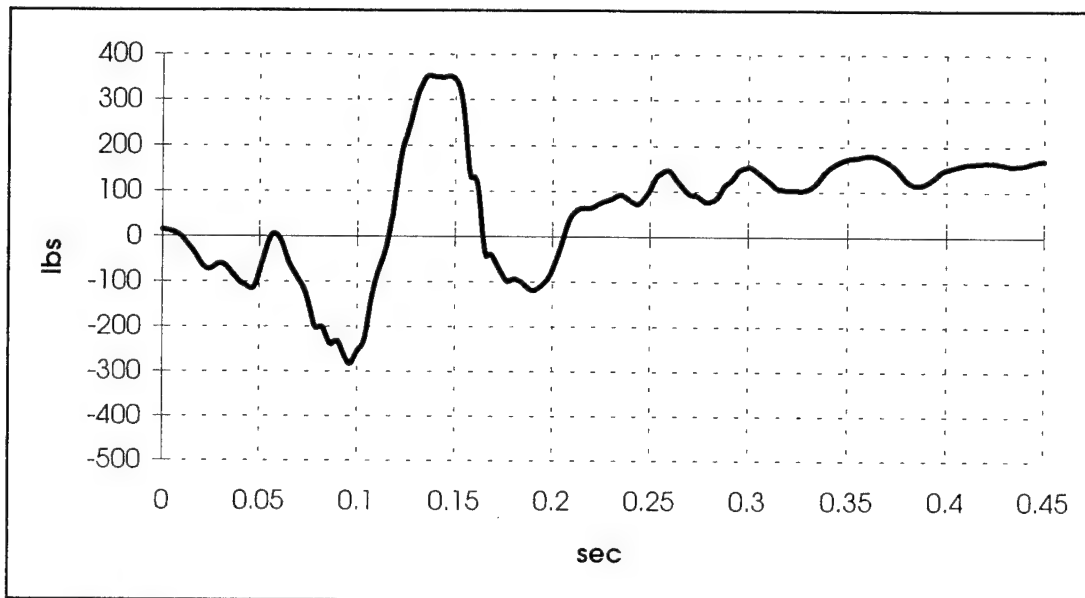


FIGURE A-35: C&D CL1B MIDDLE FITTING LOAD IN THE Z' DIRECTION

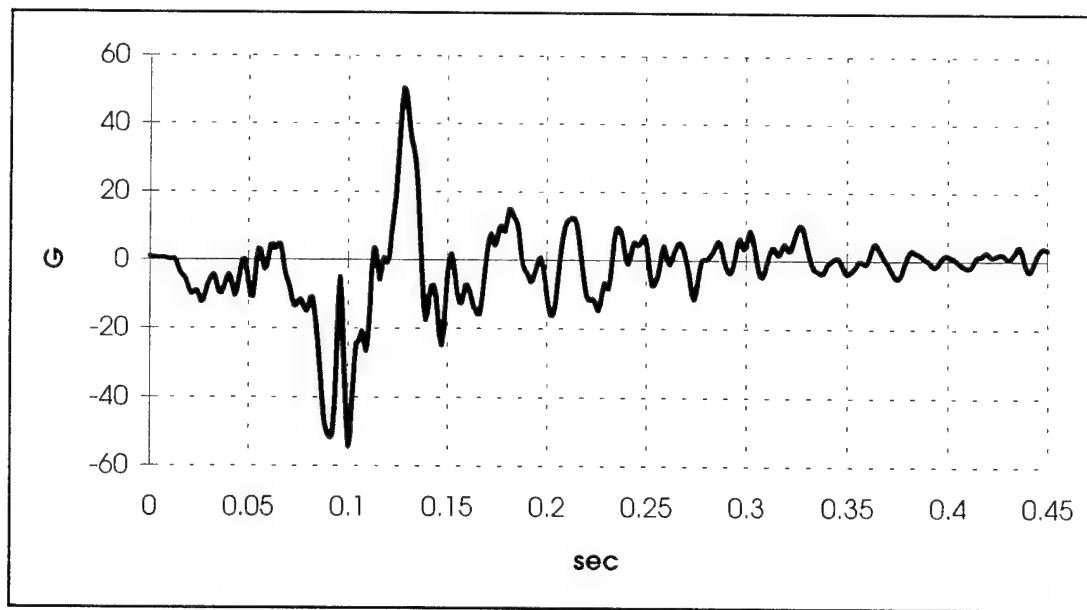


FIGURE A-36: BS1120 C&D VERTICAL ACCELERATION

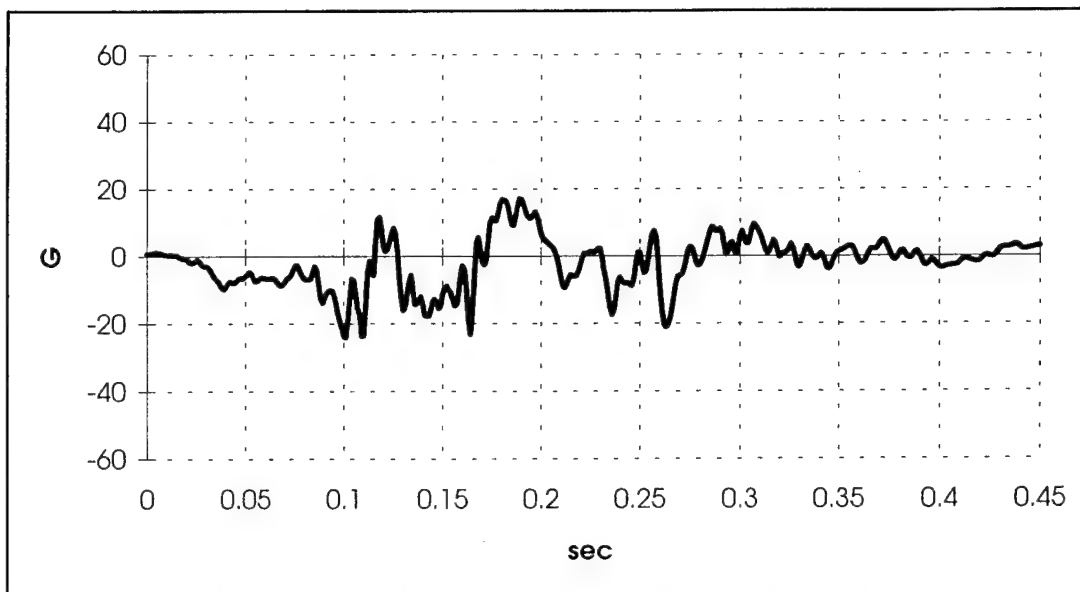


FIGURE A-37: BS1180 C&D VERTICAL ACCELERATION

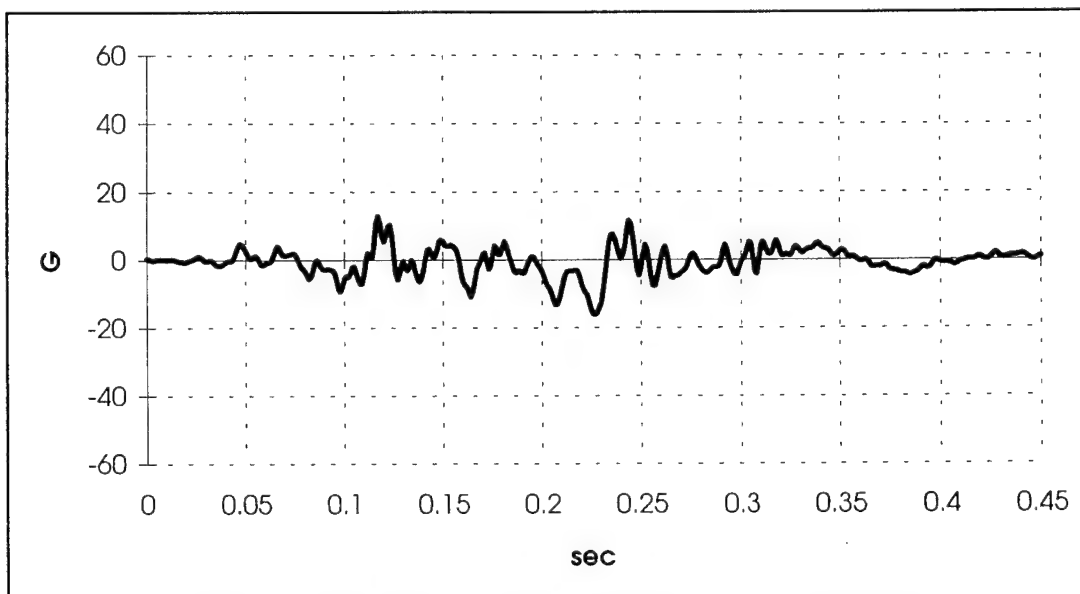


FIGURE A-38: BS1180 C&D LATERAL ACCELERATION

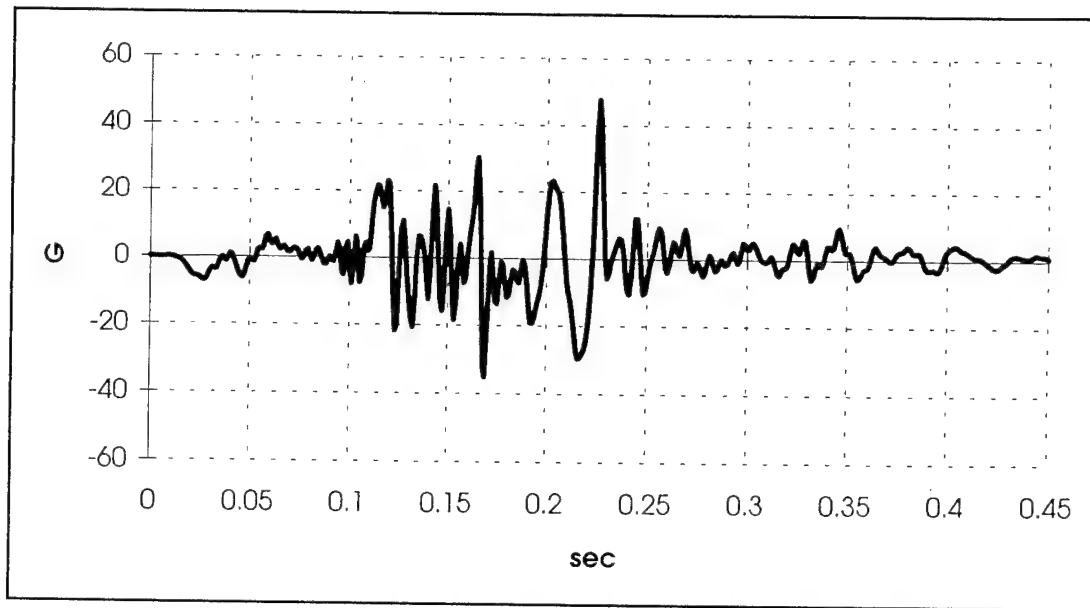


FIGURE A-39: BS1180 C&D LONGITUDINAL ACCELERATION

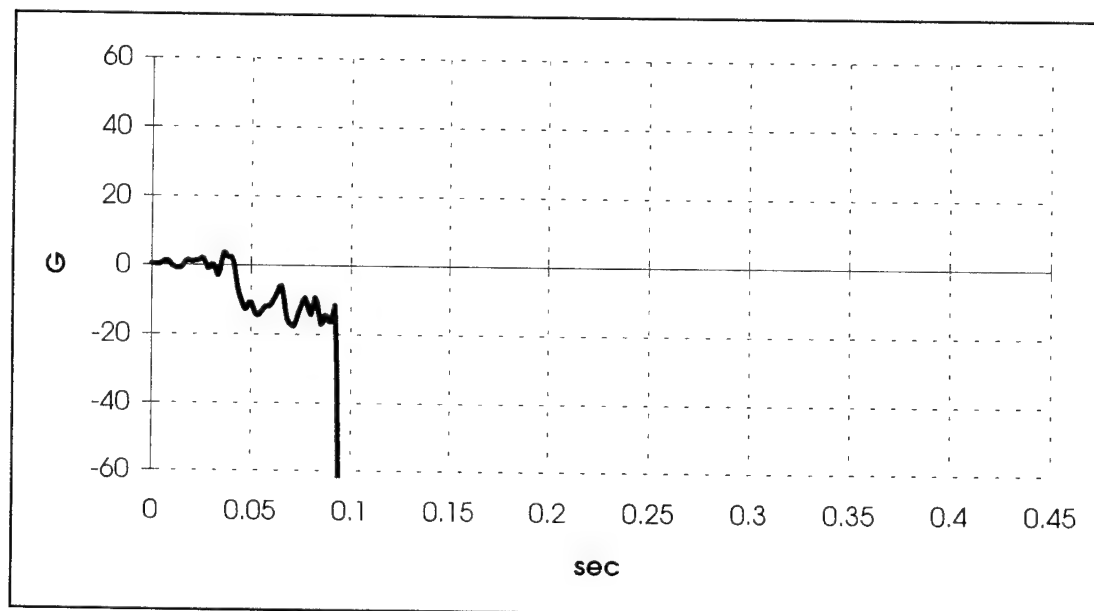


FIGURE A-40: BS1240 C&D VERTICAL ACCELERATION

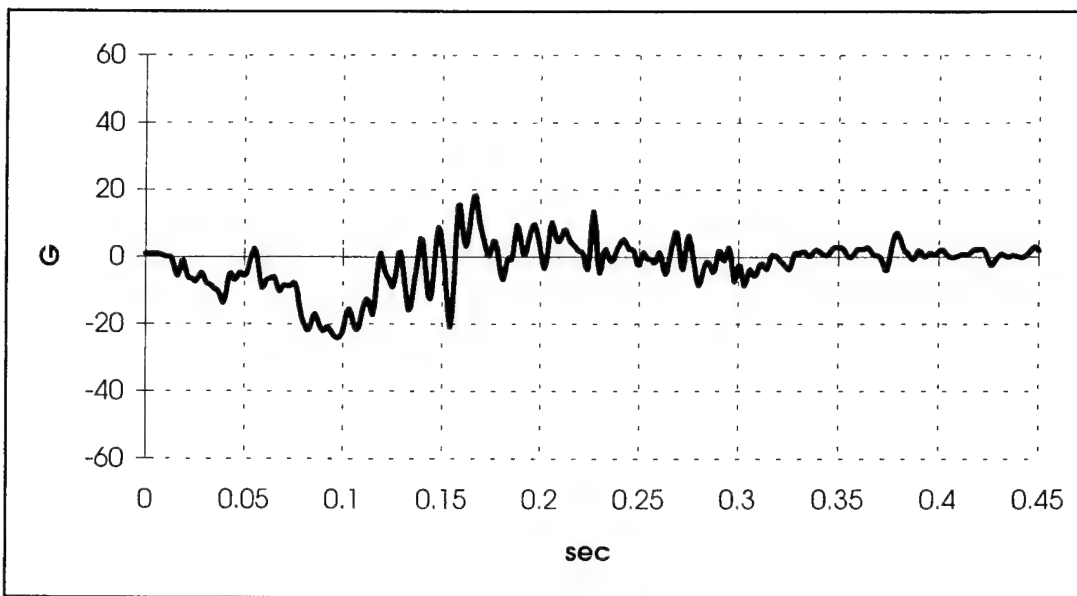


FIGURE A-41: BS1145 BOEING VERTICAL ACCELERATION

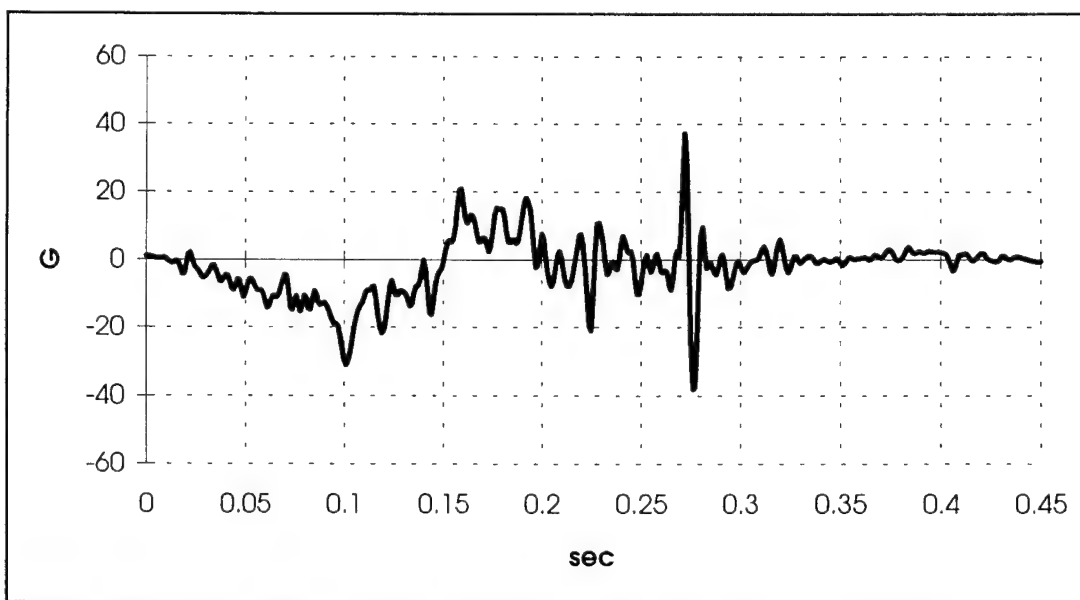


FIGURE A-42: BS1210 BOEING VERTICAL ACCELERATION

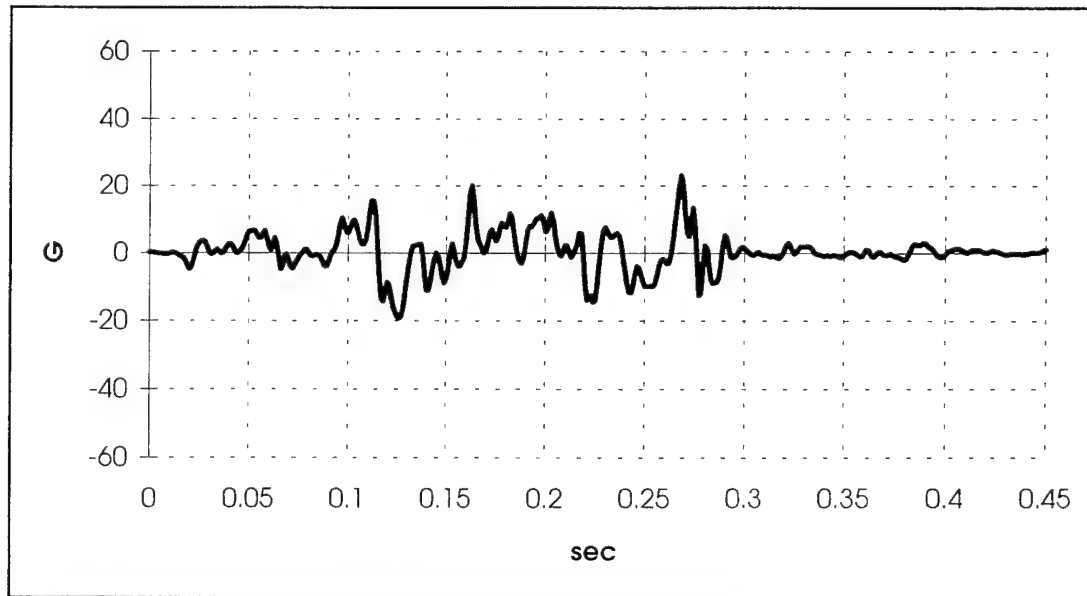


FIGURE A-43: BS1210 BOEING LATERAL ACCELERATION

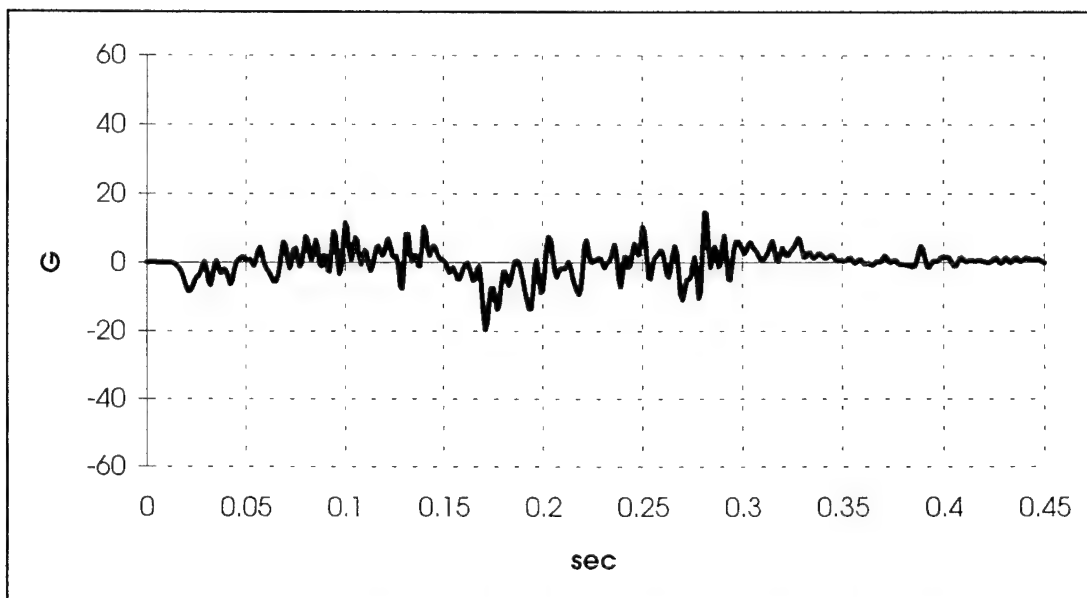


FIGURE A-44: BS1210 BOEING LONGITUDINAL ACCELERATION



FIGURE A-45: BOEING LINK 7B LOAD

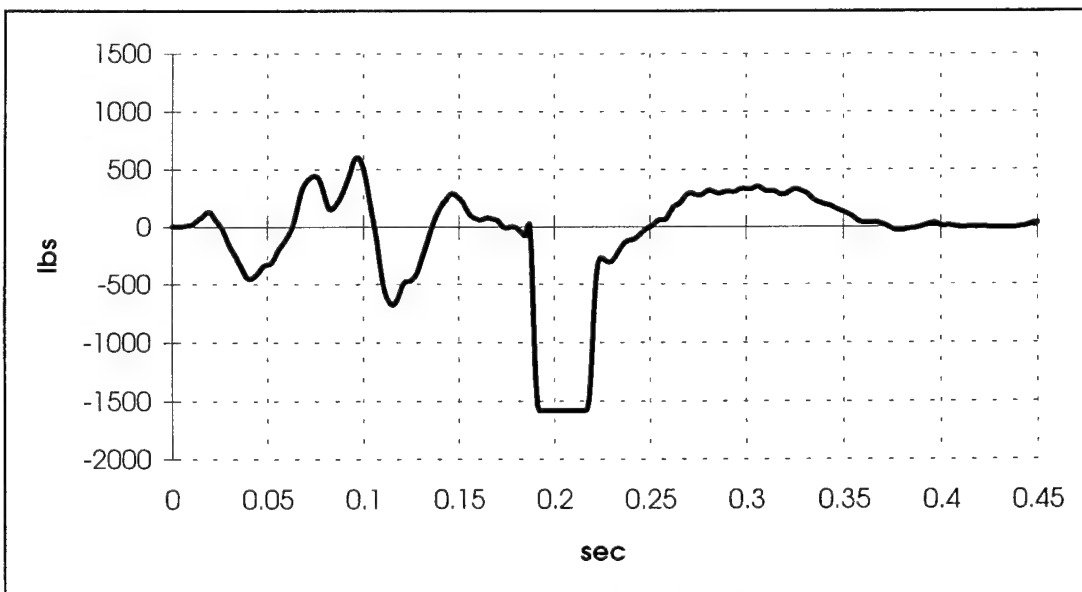


FIGURE A-46: BOEING LINK 8B LOAD

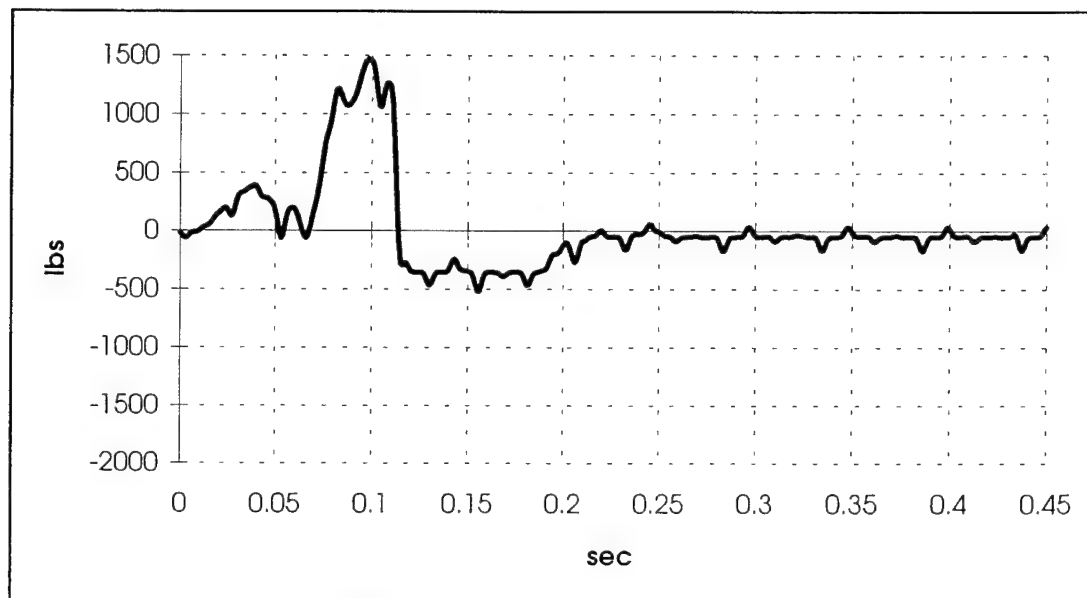


FIGURE A-47: BOEING LINK 17B LOAD

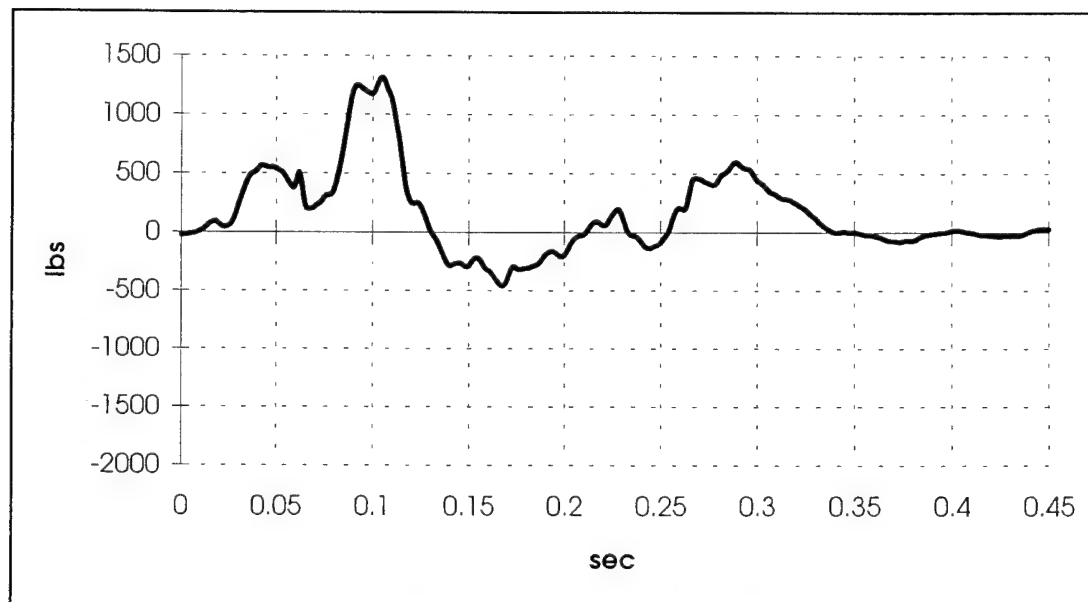


FIGURE A-48: BOEING LINK 18B LOAD

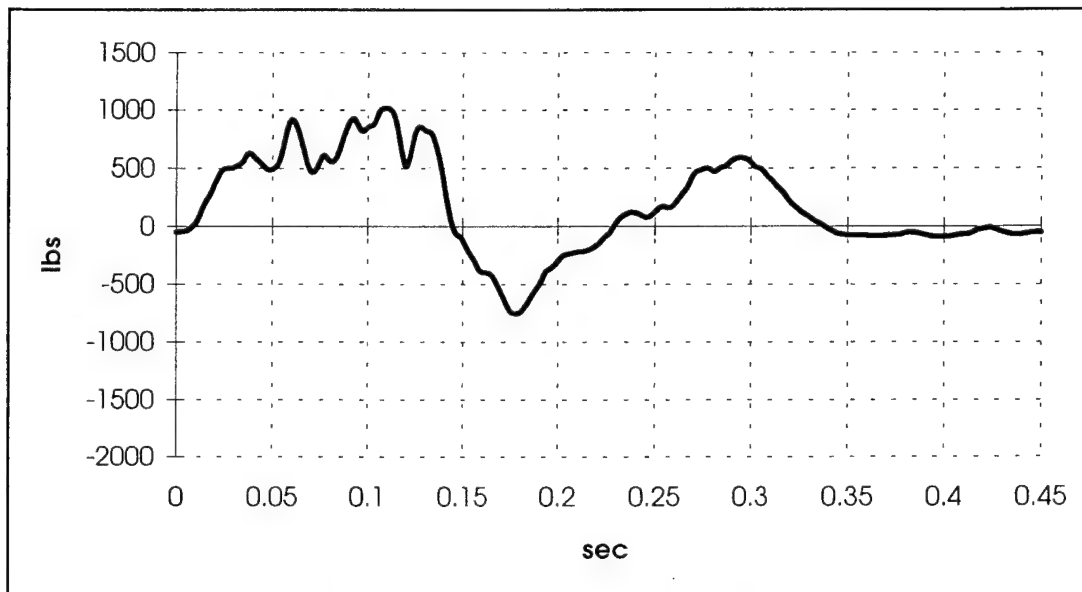


FIGURE A-49: BOEING LINK 25B LOAD



FIGURE A-50: BOEING LINK 28B LOAD

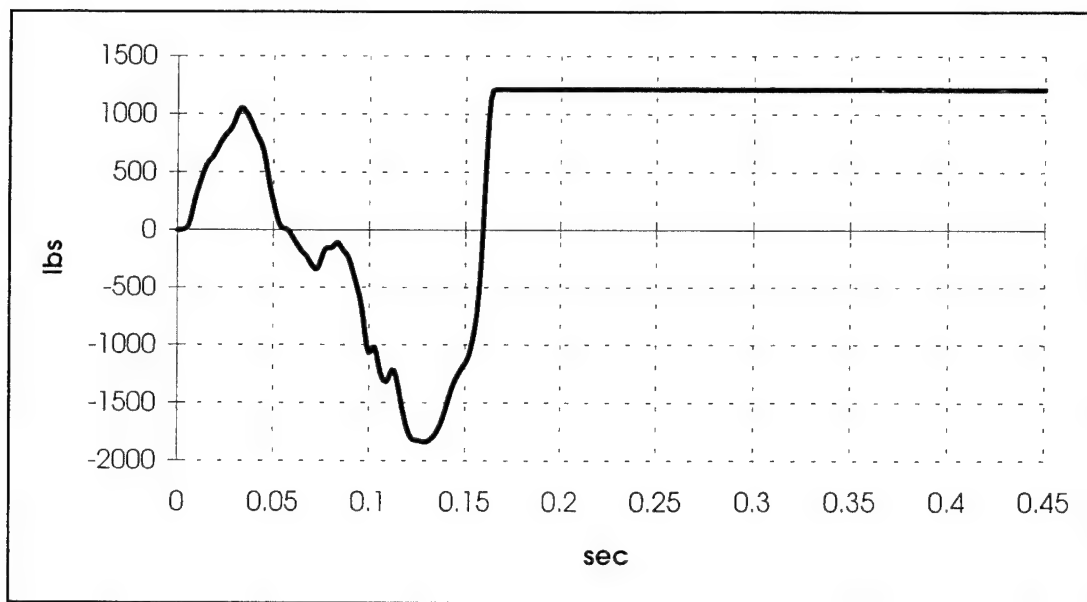


FIGURE A-51: BOEING LINK 31B LOAD

TANK DATA

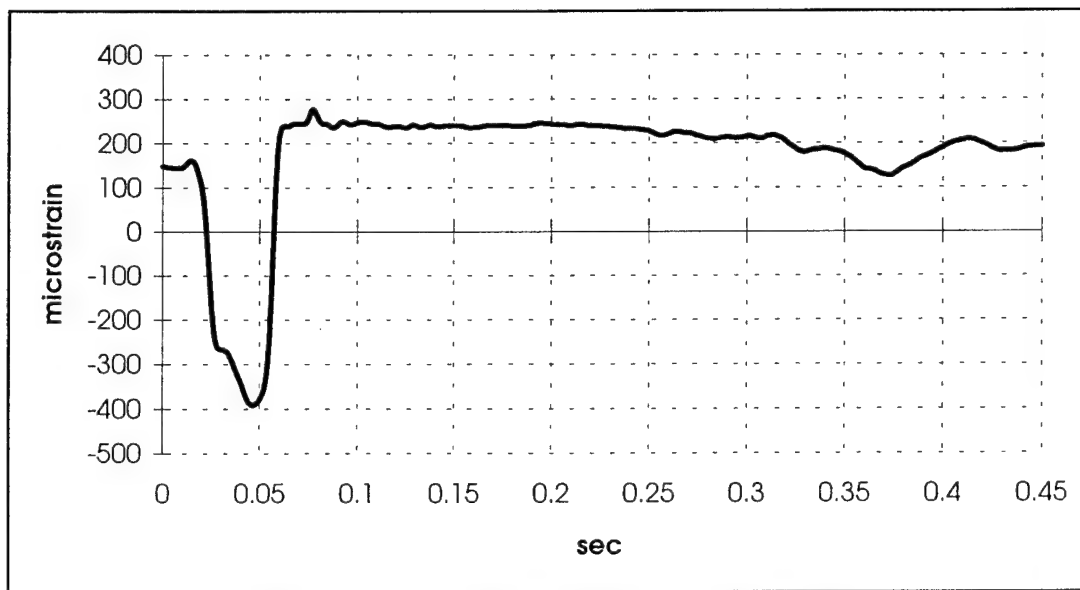
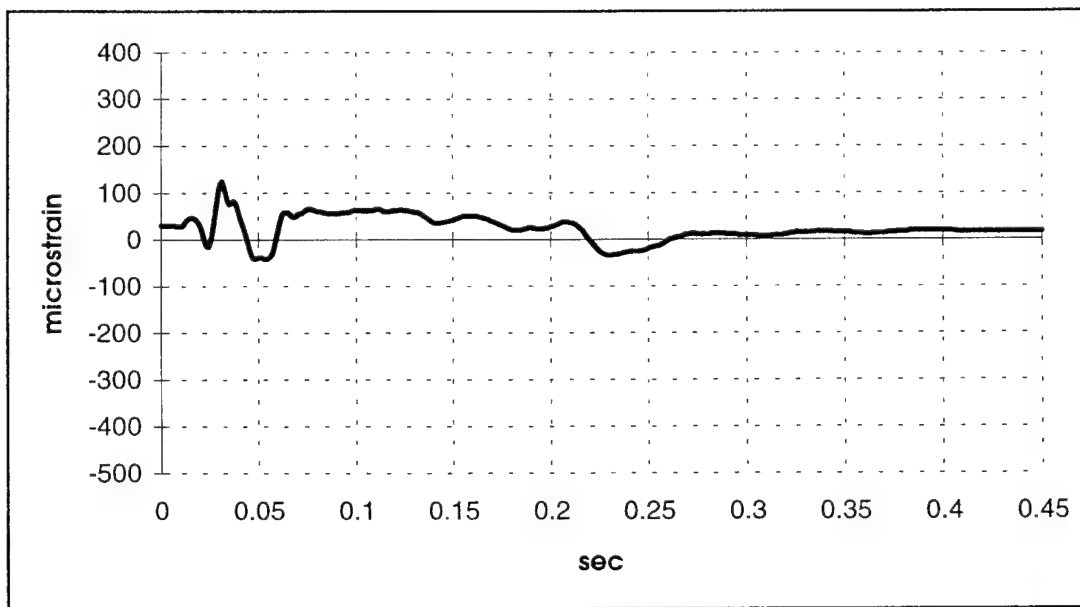


FIGURE A-52: STRAP FORWARD PORT LOAD



A-53: STRAP FORWARD STARBOARD LOAD

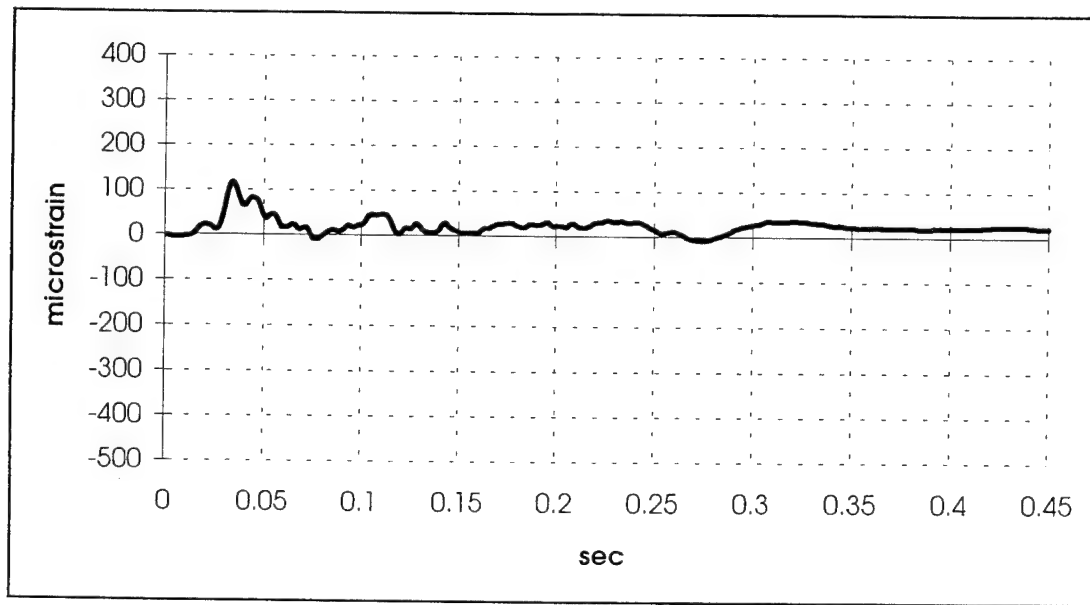


FIGURE A-54: STRAP AFT PORT LOAD

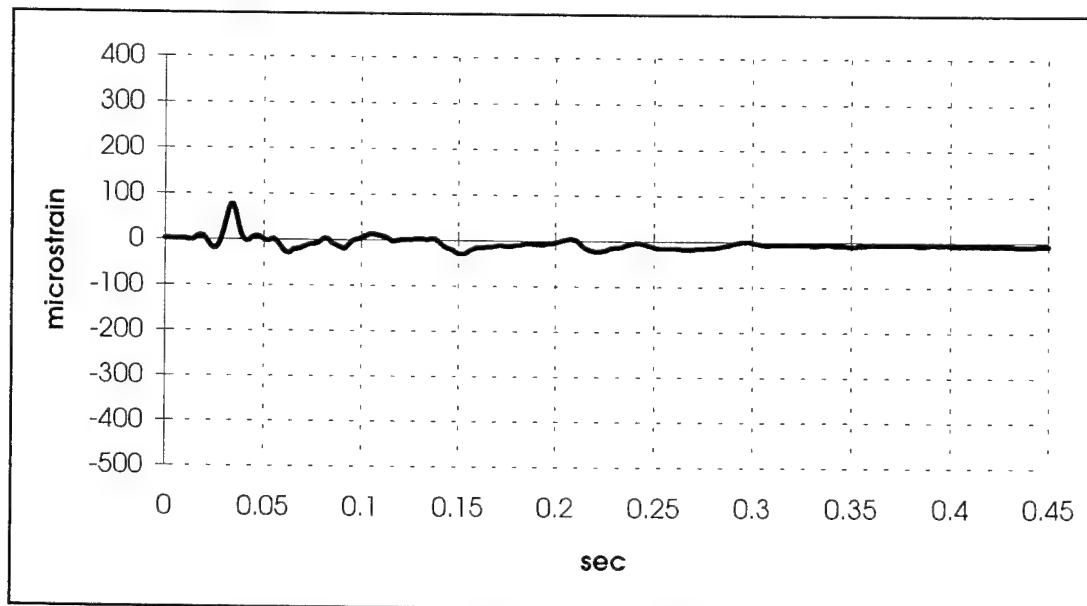


FIGURE A-55: STRAP AFT STARBOARD LOAD

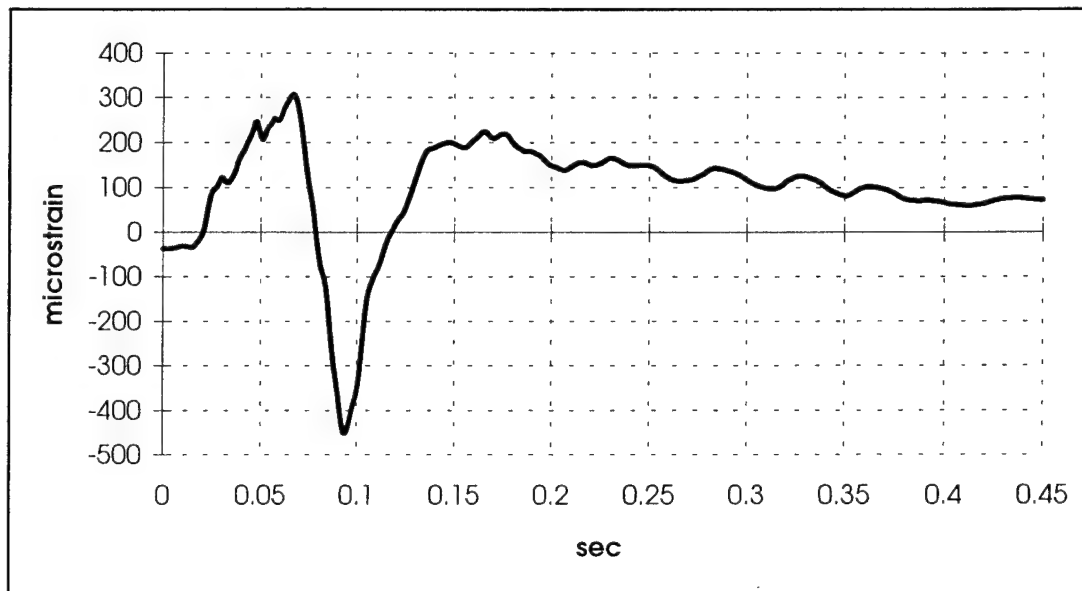


FIGURE A-56: RIB FORWARD PORT LOAD

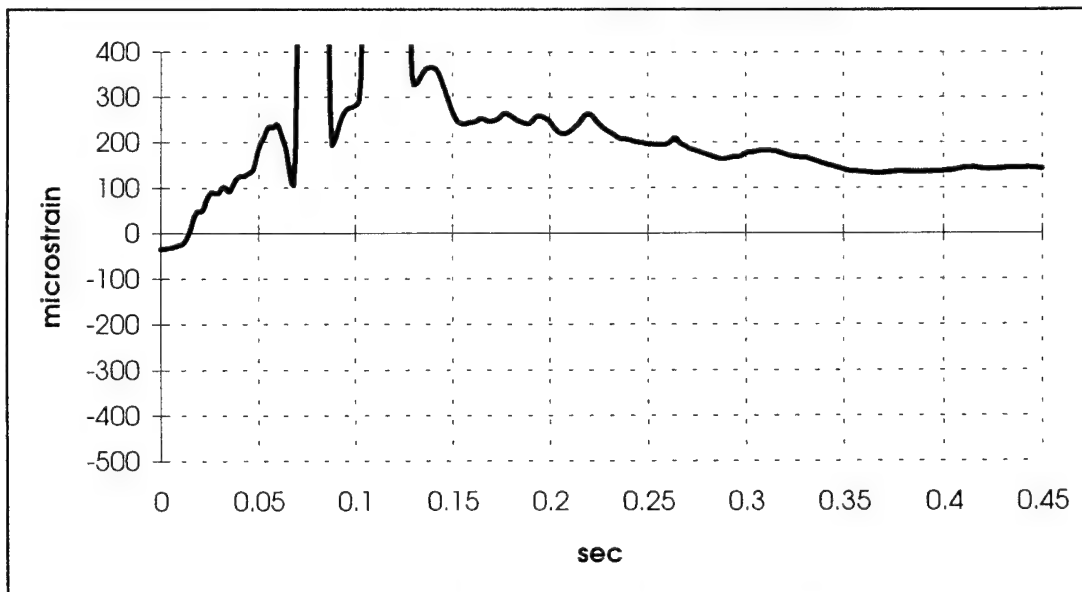


FIGURE A-57: RIB FORWARD STARBOARD LOAD

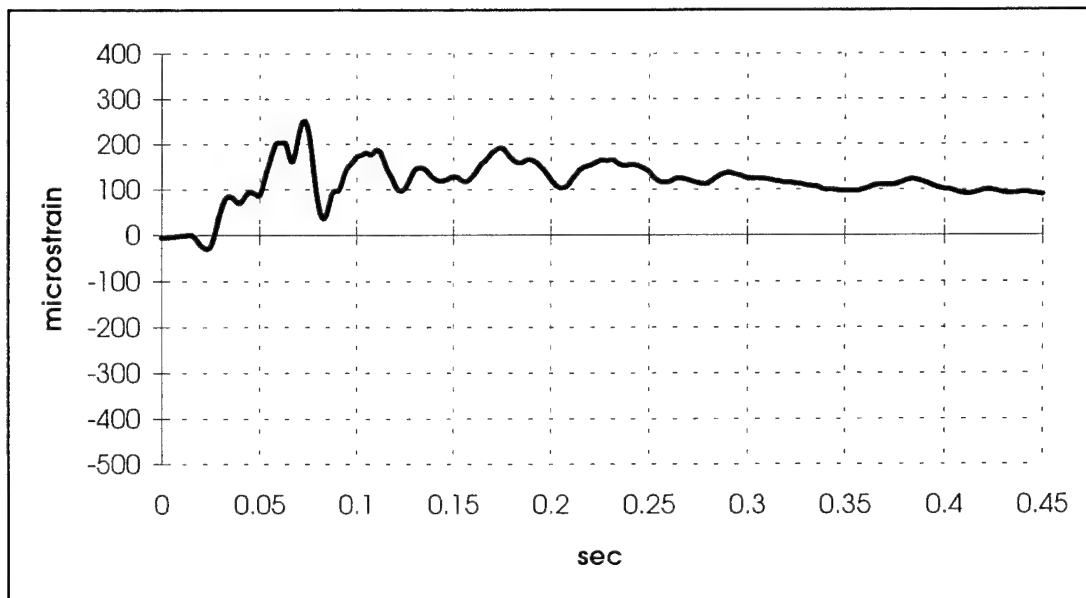


FIGURE A-58: RIB AFT STARBOARD LOAD

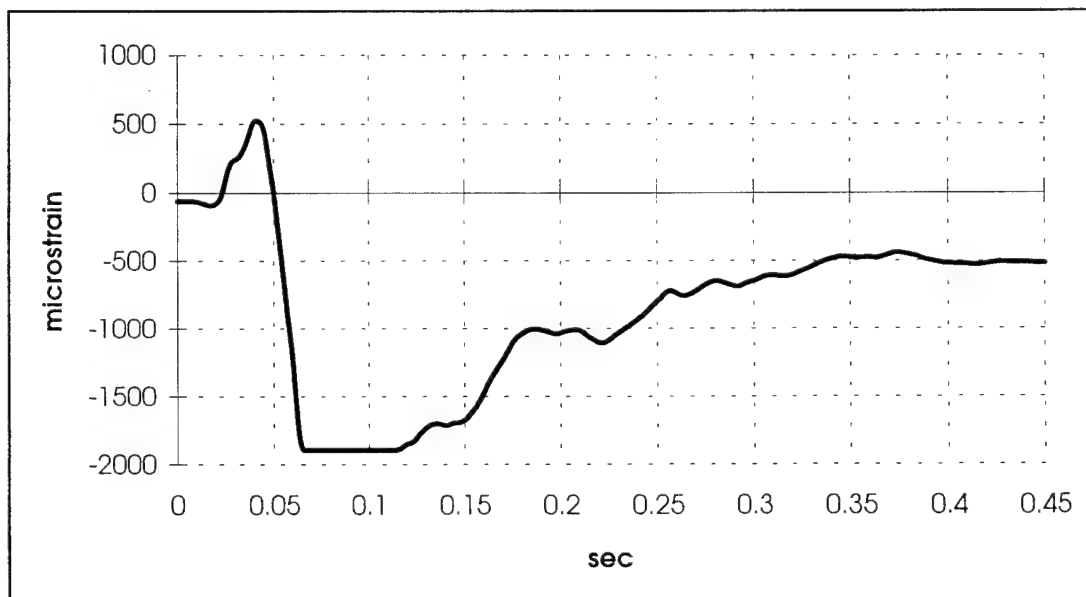


FIGURE A-59: CRADLE FORWARD PORT LOAD

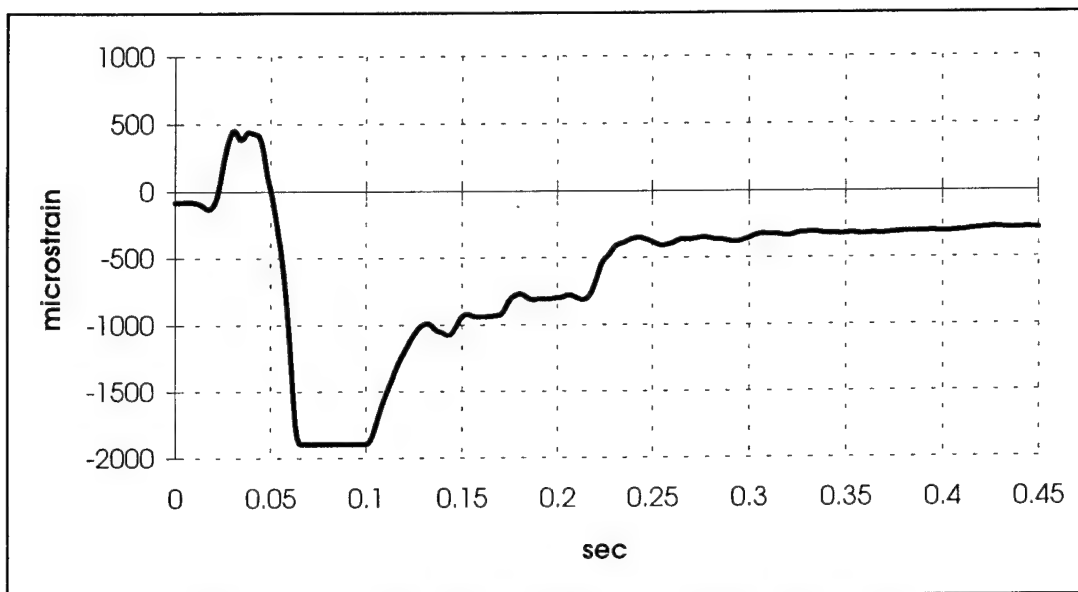


FIGURE A-60: CRADLE FORWARD STARBOARD LOAD

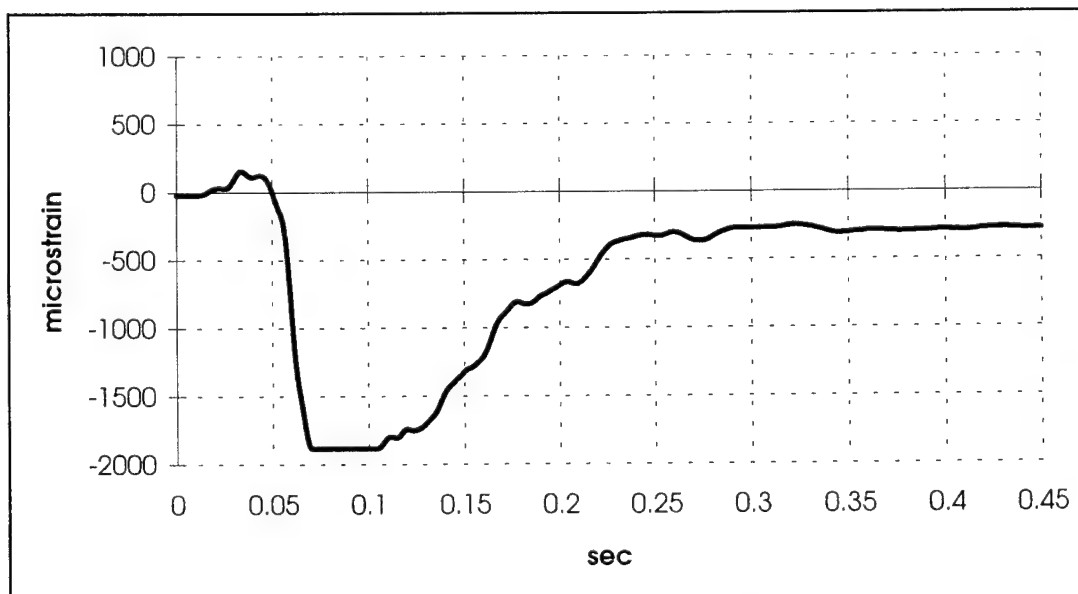


FIGURE A-61: CRADLE AFT PORT LOAD

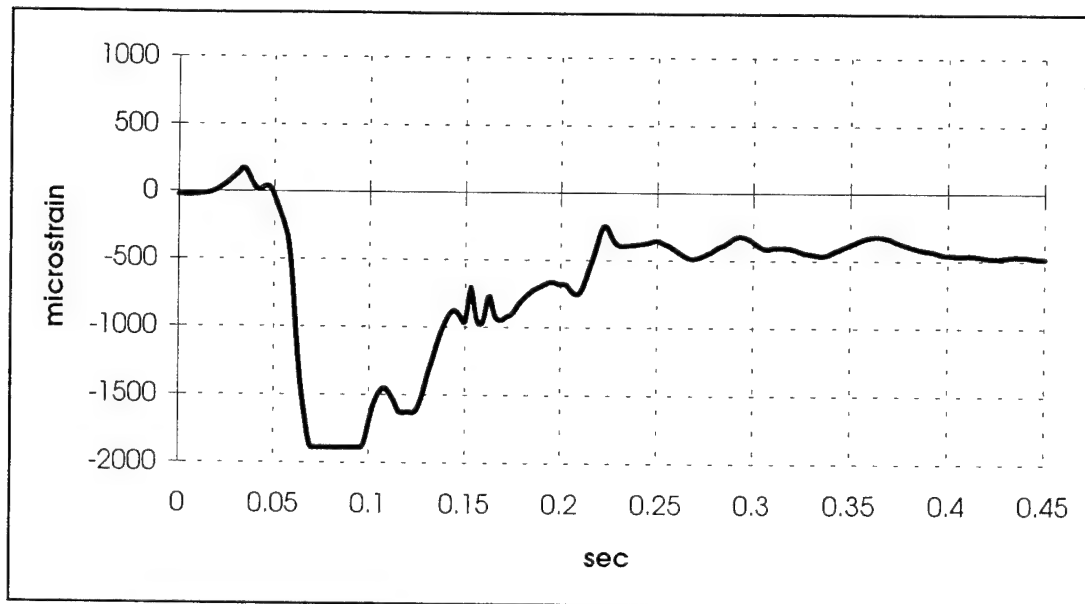


FIGURE A-62: CRADLE AFT STARBOARD LOAD

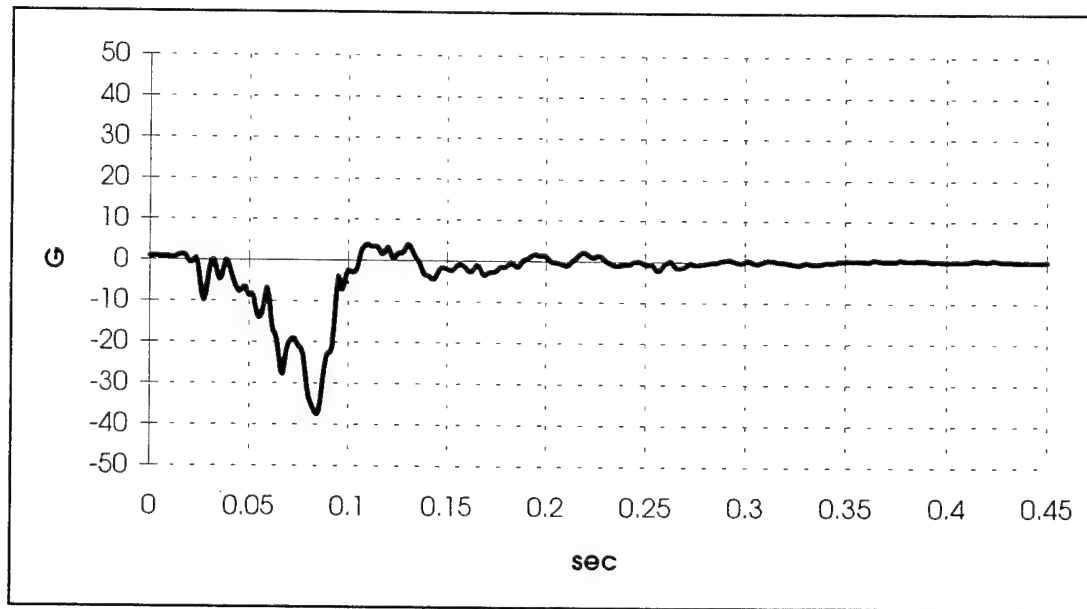


FIGURE A-63: CRADLE FORWARD PORT VERTICAL ACCELERATION

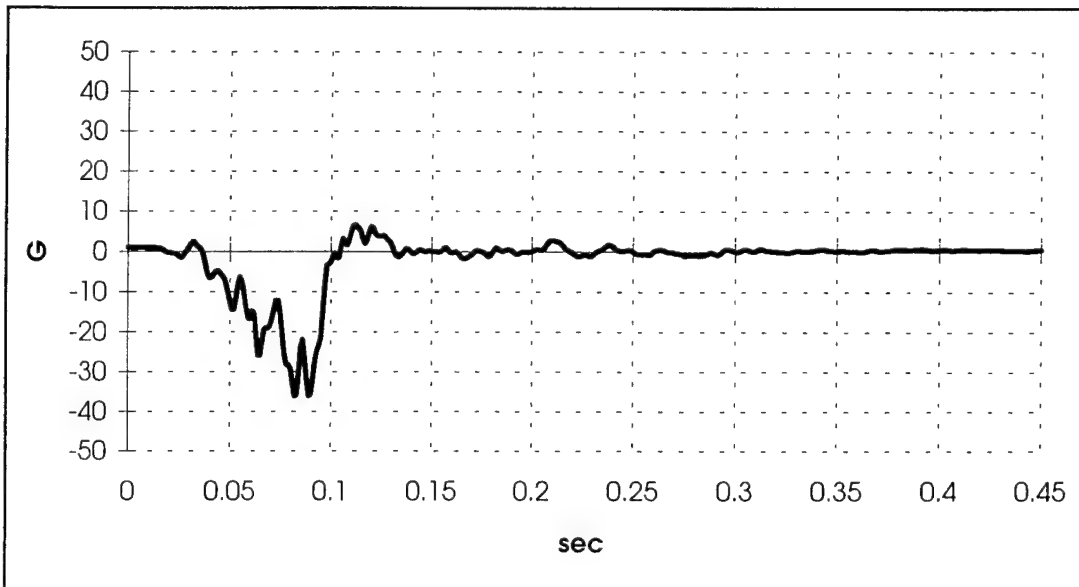


FIGURE A-64: CRADLE REAR PORT VERTICAL ACCELERATION

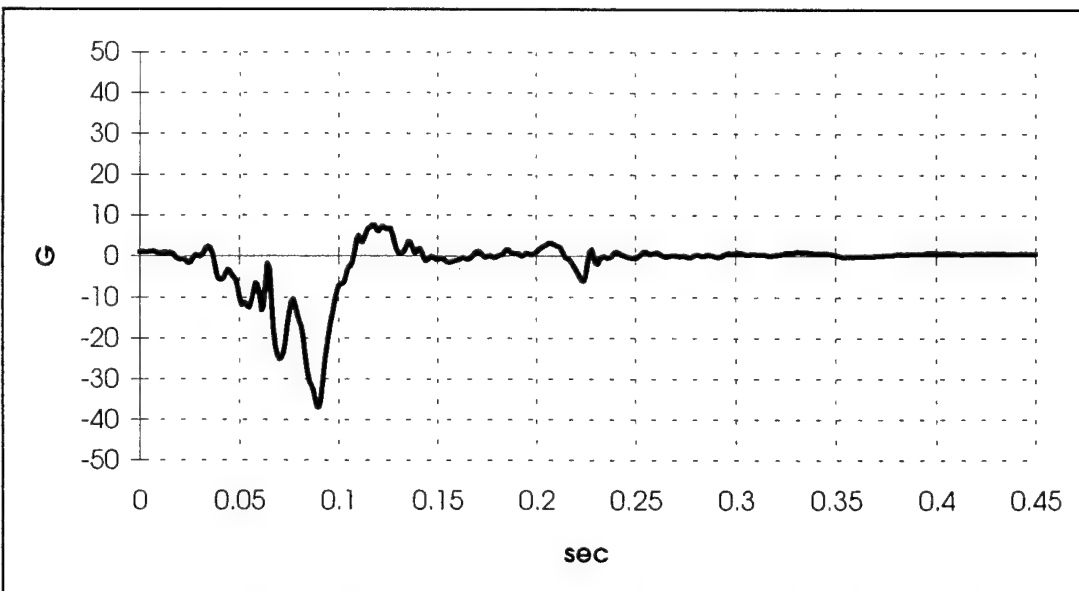


FIGURE A-65: CRADLE REAR STARBOARD VERTICAL ACCELERATION

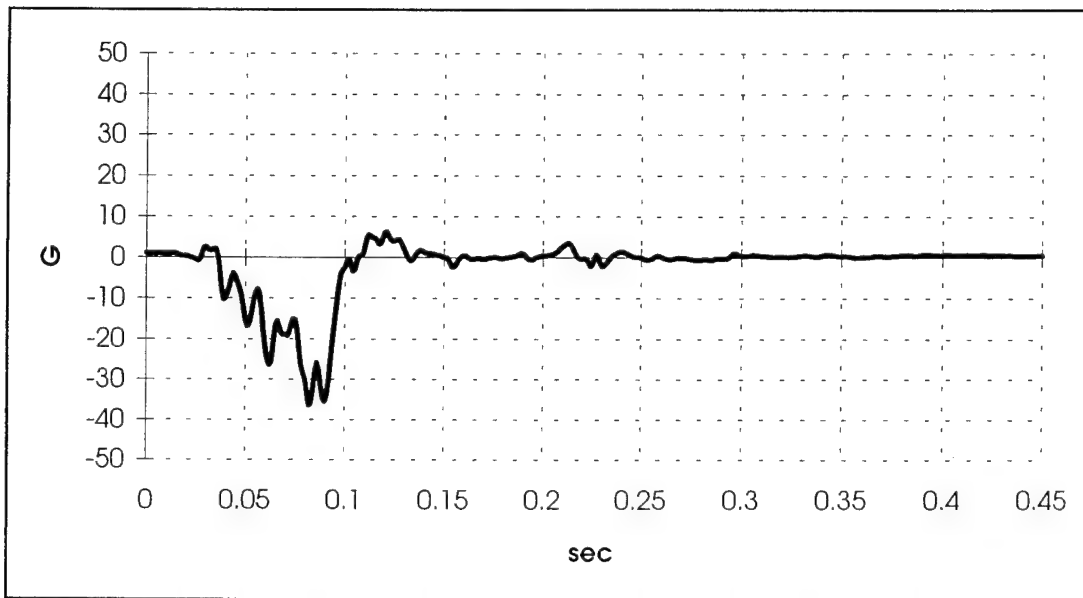


FIGURE A-66: TANK REAR PORT VERTICAL ACCELERATION

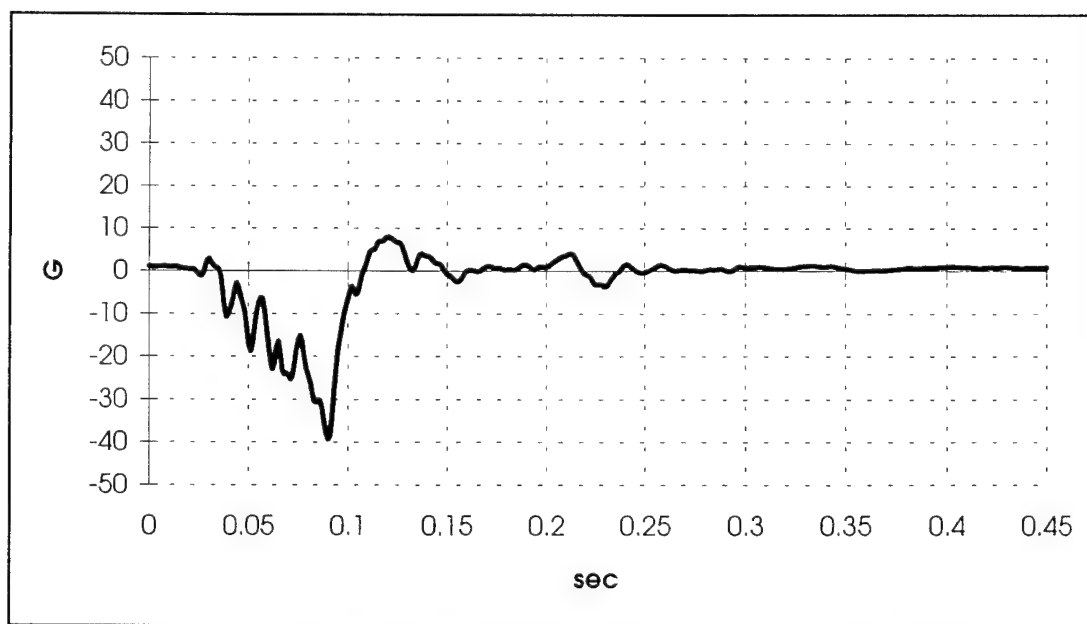


FIGURE A-67: TANK REAR STARBOARD VERTICAL ACCELERATION

PLATFORM AND ANTHROPOMORPHIC DUMMIES DATA

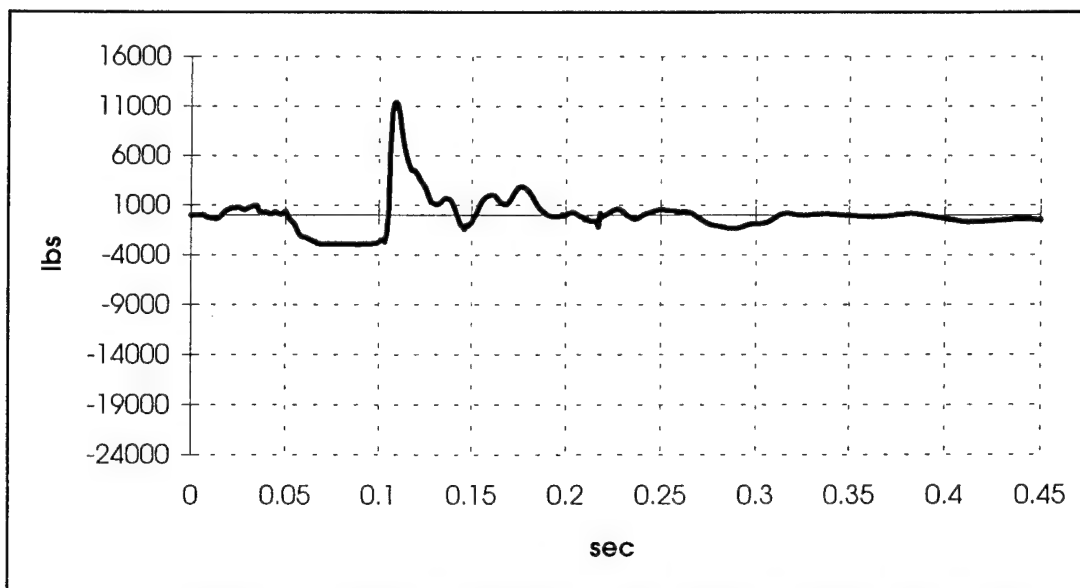


FIGURE A-68: PLATFORM FORWARD FIRST ROW STARBOARD LOAD

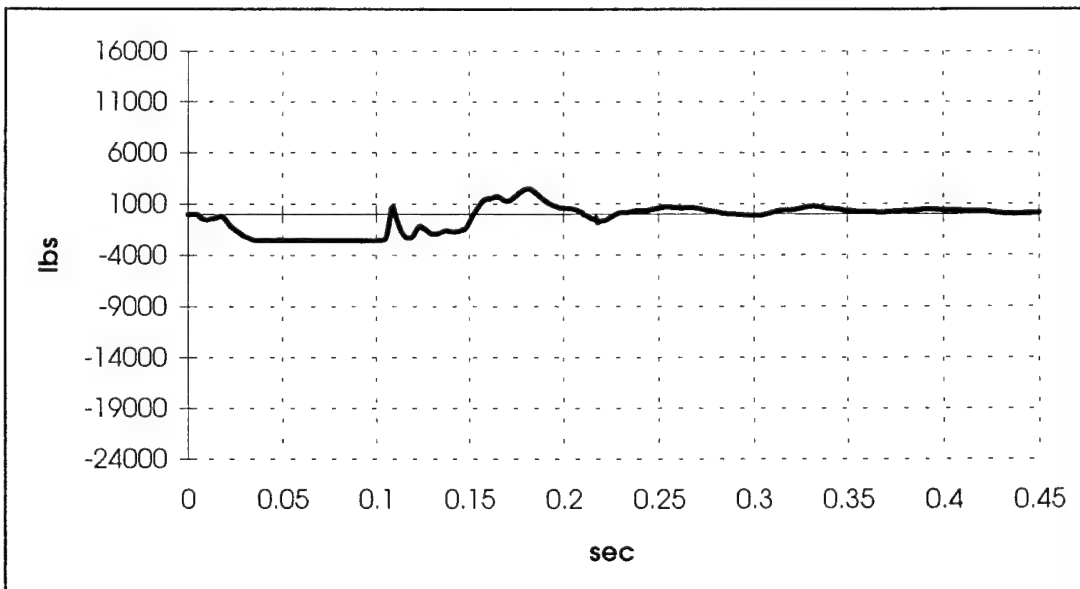


FIGURE A-69: PLATFORM FORWARD FIRST ROW CENTER LOAD

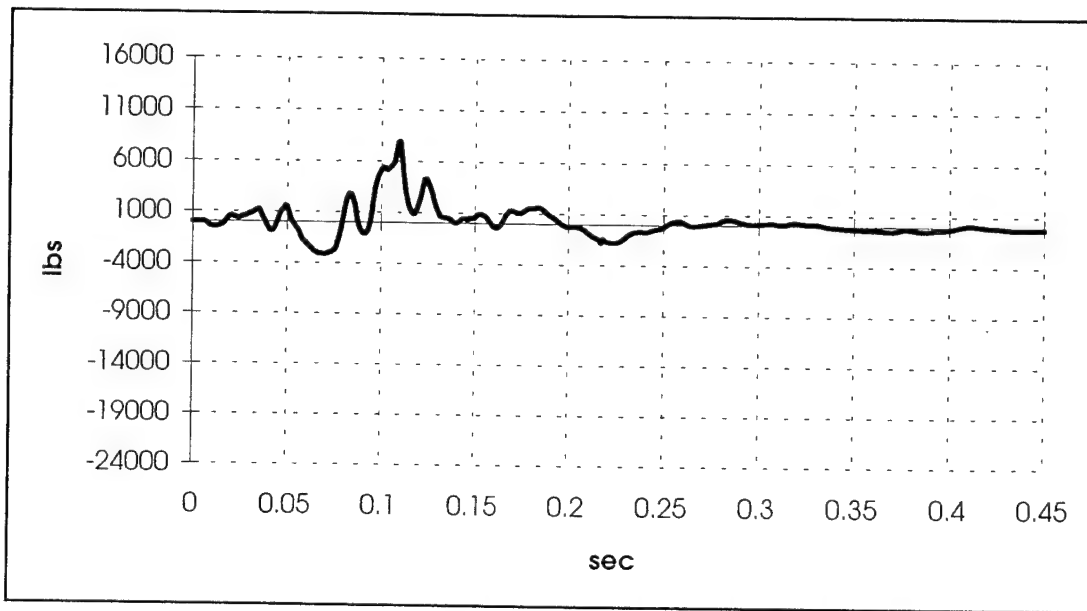


FIGURE A-70: PLATFORM FORWARD FIRST ROW PORT LOAD

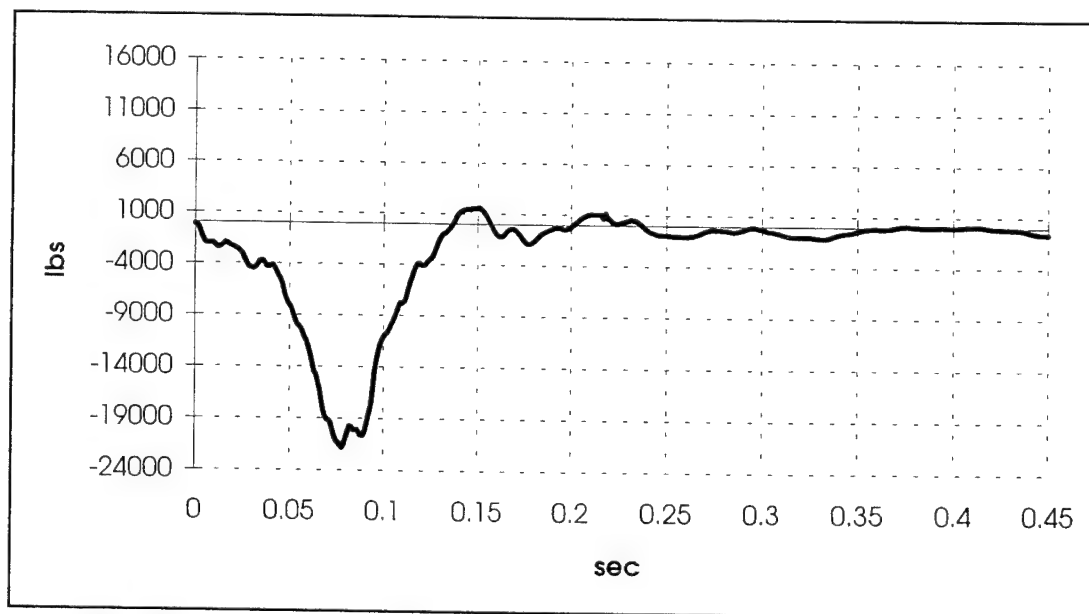


FIGURE A-71: PLATFORM FORWARD SECOND ROW CENTER LOAD

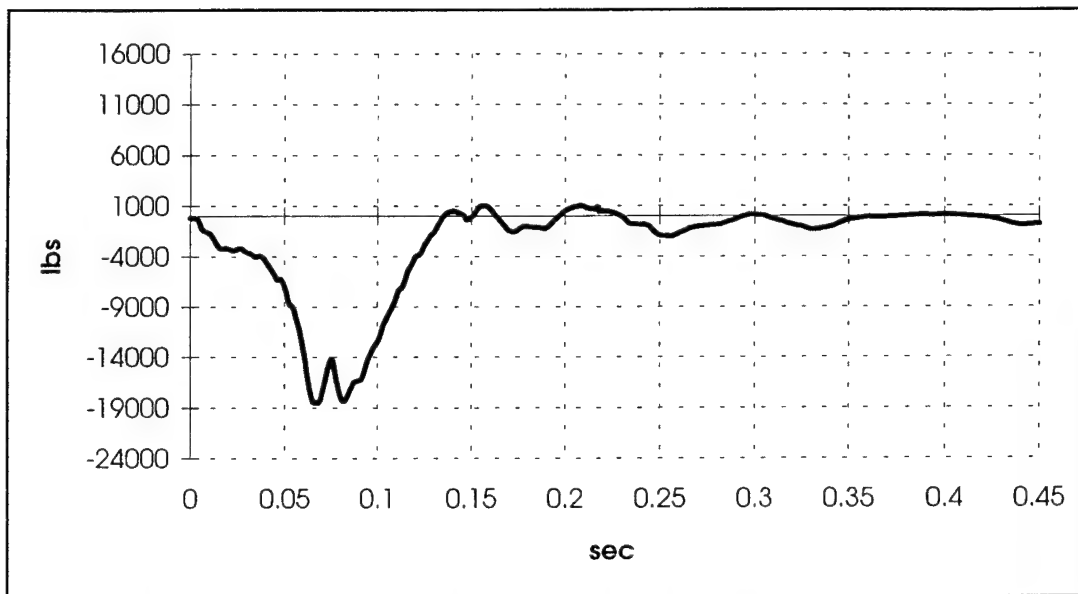


FIGURE A-72: PLATFORM FORWARD SECOND ROW PORT LOAD

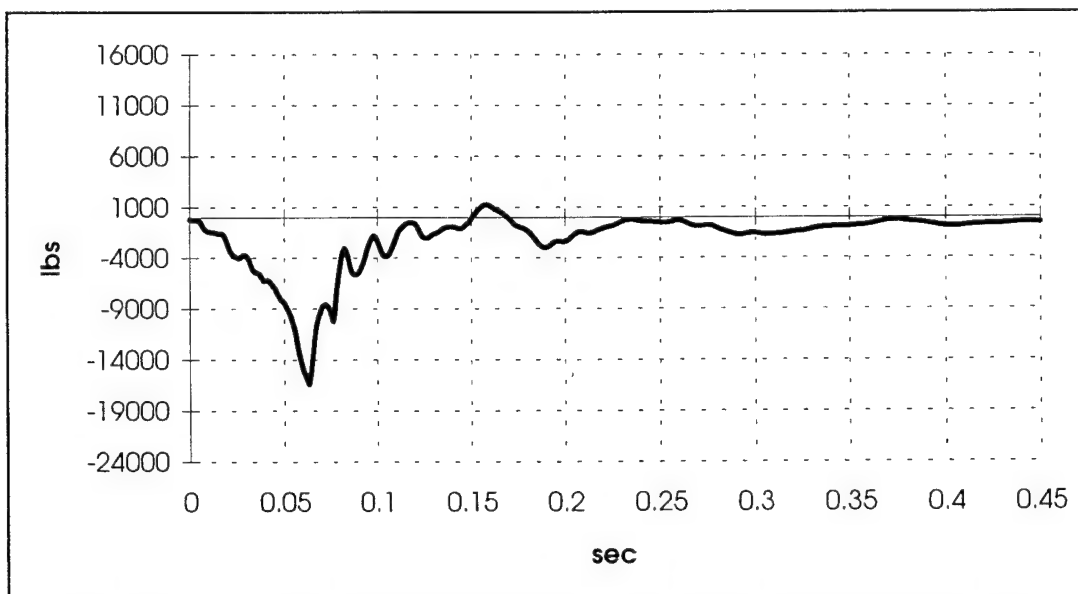


FIGURE A-73: PLATFORM FORWARD THIRD ROW STARBOARD LOAD

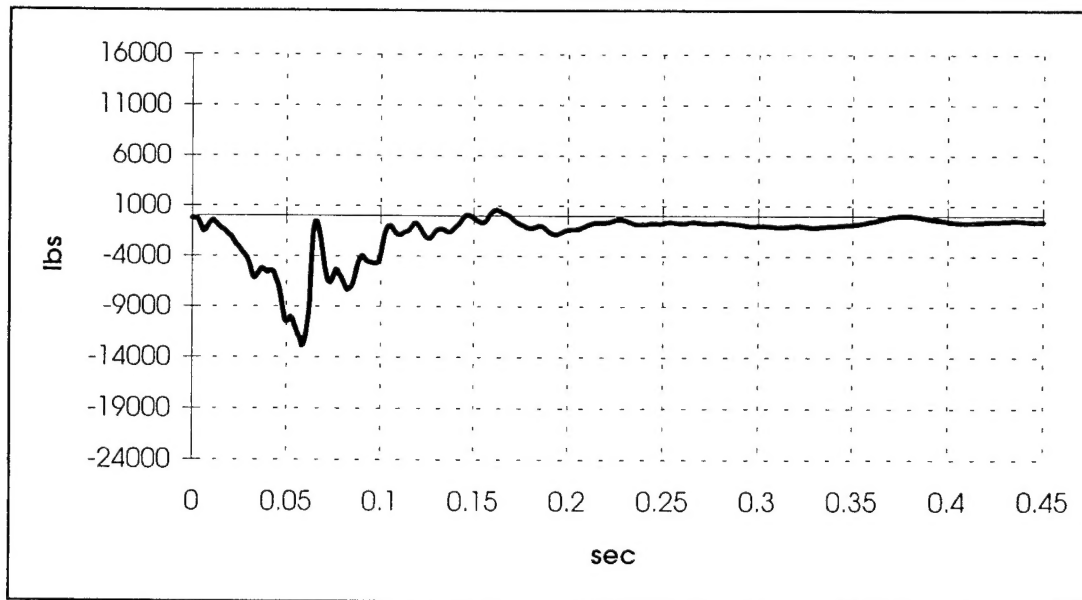


FIGURE A-74: PLATFORM FORWARD THIRD ROW CENTER LOAD

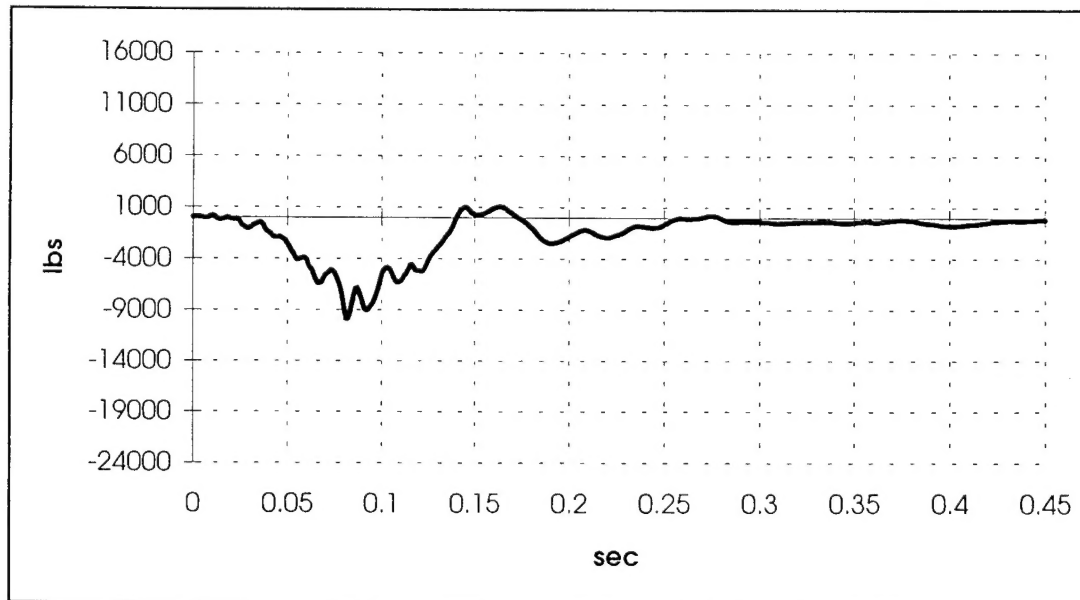


FIGURE A-75: PLATFORM AFT STARBOARD LOAD

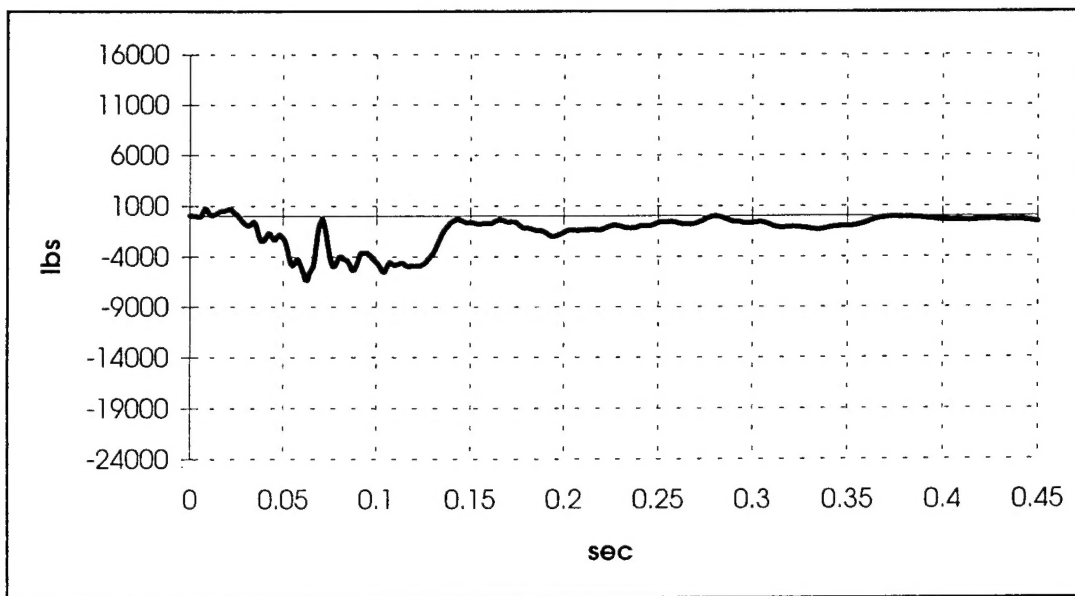


FIGURE A-76: PLATFORM AFT CENTER LOAD

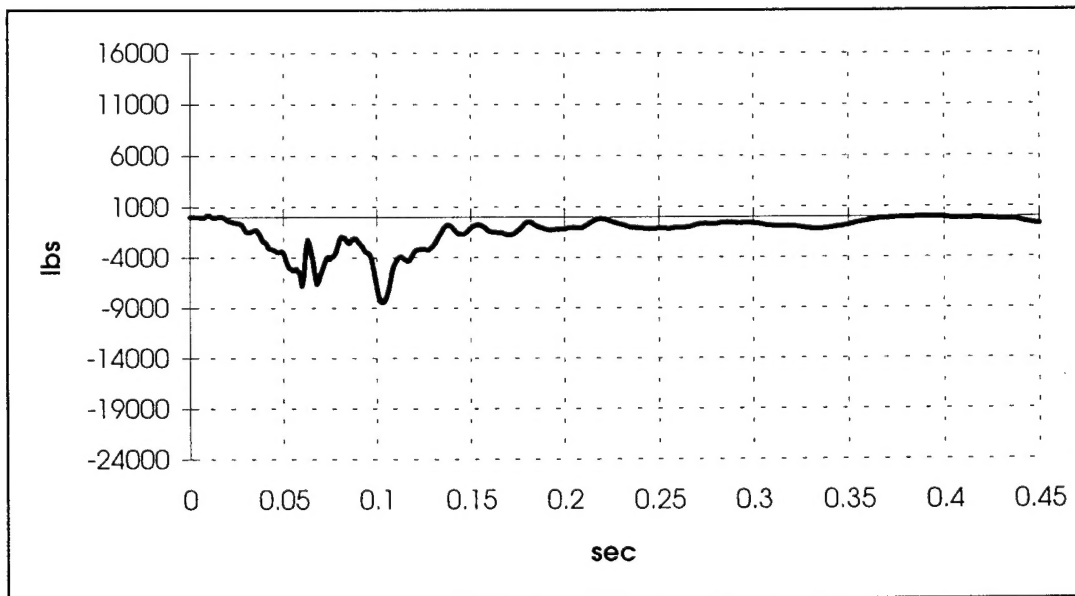


FIGURE A-77: PLATFORM AFT PORT LOAD

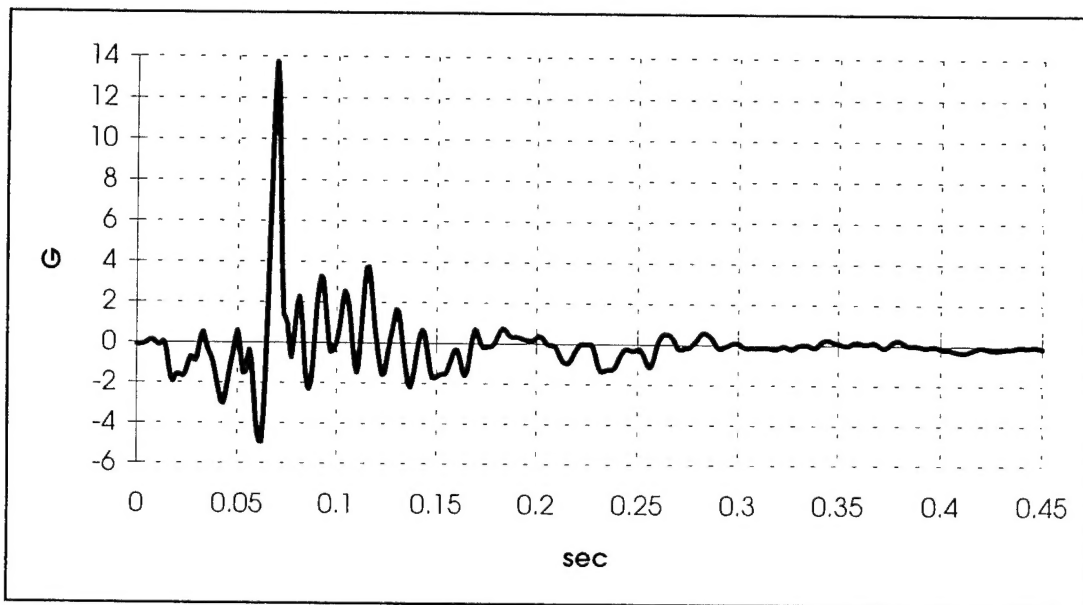


FIGURE A-78: PLATFORM VERTICAL ACCELERATION

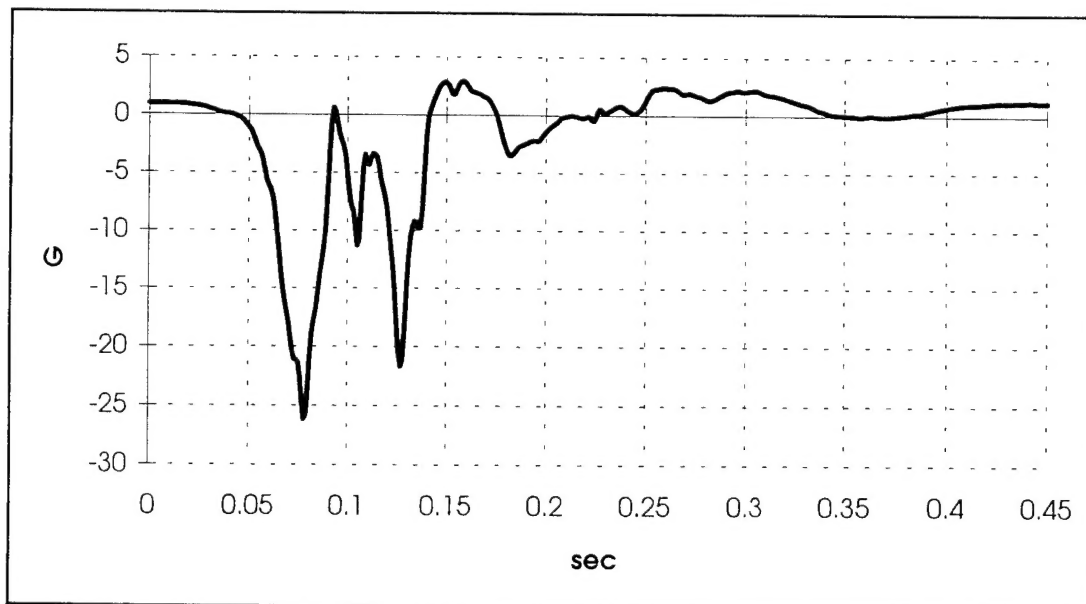


FIGURE A-79: STARBOARD DUMMY PELVIS VERTICAL ACCELERATION

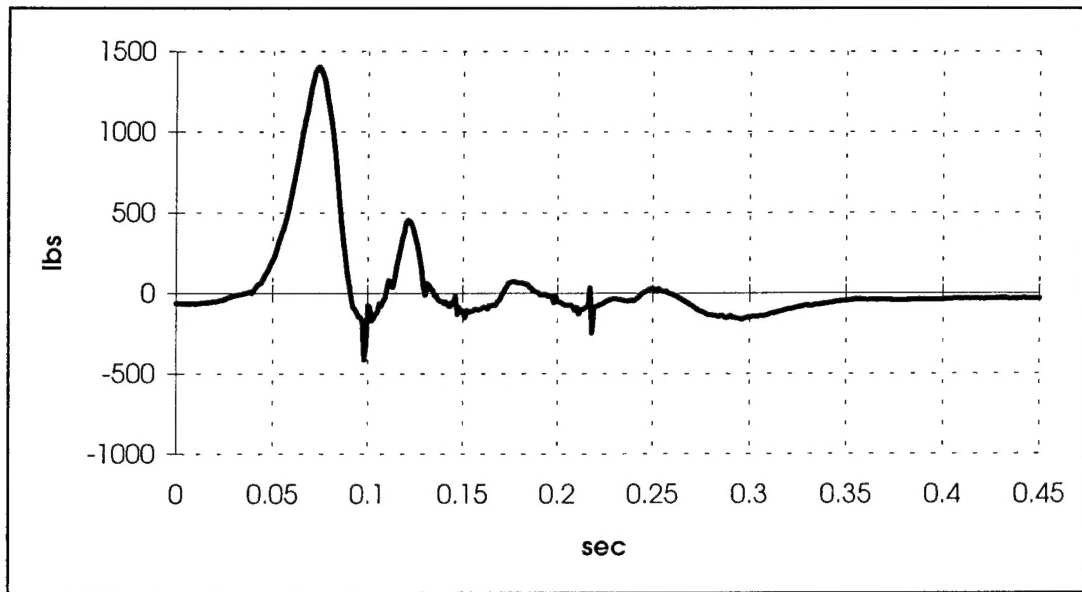


FIGURE A-80: PORT DUMMY PELVIS LOAD

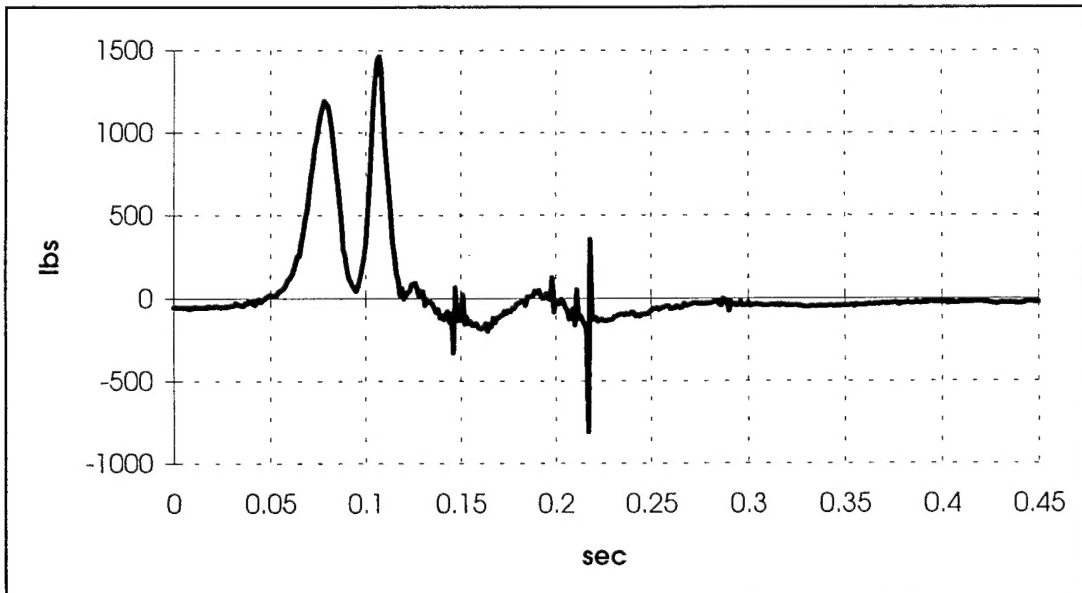


FIGURE A-81: STARBOARD DUMMY PELVIS LOAD